

## **INFORMATION TO USERS**

This manuscript has been reproduced from the microfilm master. UMI films the text directly from the original or copy submitted. Thus, some thesis and dissertation copies are in typewriter face, while others may be from any type of computer printer.

**The quality of this reproduction is dependent upon the quality of the copy submitted.** Broken or indistinct print, colored or poor quality illustrations and photographs, print bleedthrough, substandard margins, and improper alignment can adversely affect reproduction.

In the unlikely event that the author did not send UMI a complete manuscript and there are missing pages, these will be noted. Also, if unauthorized copyright material had to be removed, a note will indicate the deletion.

Oversize materials (e.g., maps, drawings, charts) are reproduced by sectioning the original, beginning at the upper left-hand corner and continuing from left to right in equal sections with small overlaps.

Photographs included in the original manuscript have been reproduced xerographically in this copy. Higher quality 6" x 9" black and white photographic prints are available for any photographs or illustrations appearing in this copy for an additional charge. Contact UMI directly to order.

Bell & Howell Information and Learning  
300 North Zeeb Road, Ann Arbor, MI 48106-1346 USA  
800-521-0600

**UMI<sup>®</sup>**



A Characterization and Performance Evaluation of Digitally  
Redesigned Control Systems

Camille Alain Rabbath

Department of Mechanical Engineering  
McGill University  
Montreal, Canada  
March 1999

A thesis submitted to the Faculty of Graduate Studies and Research in partial  
fulfillment of the requirements for the degree of  
Doctor of Philosophy  
in  
Mechanical Engineering

© C.A. Rabbath, 1999



National Library  
of Canada

Acquisitions and  
Bibliographic Services

395 Wellington Street  
Ottawa ON K1A 0N4  
Canada

Bibliothèque nationale  
du Canada

Acquisitions et  
services bibliographiques

395, rue Wellington  
Ottawa ON K1A 0N4  
Canada

*Your file* *Votre référence*

*Our file* *Notre référence*

The author has granted a non-exclusive licence allowing the National Library of Canada to reproduce, loan, distribute or sell copies of this thesis in microform, paper or electronic formats.

The author retains ownership of the copyright in this thesis. Neither the thesis nor substantial extracts from it may be printed or otherwise reproduced without the author's permission.

L'auteur a accordé une licence non exclusive permettant à la Bibliothèque nationale du Canada de reproduire, prêter, distribuer ou vendre des copies de cette thèse sous la forme de microfiche/film, de reproduction sur papier ou sur format électronique.

L'auteur conserve la propriété du droit d'auteur qui protège cette thèse. Ni la thèse ni des extraits substantiels de celle-ci ne doivent être imprimés ou autrement reproduits sans son autorisation.

0-612-55370-1

## Abstract

This thesis examines the characterization and performance evaluation of sampled-data control systems obtained with the digital redesign of continuous-time control systems.

The first part of the characterization is concerned with the Plant Input Mapping (PIM) method which is the only digital redesign technique guaranteeing closed-loop stability provided the sampling period is non-pathological. Three modified PIM methods are proposed to solve the issues of reducing the order and the number of controllers present in a PIM-based control system. Furthermore, alternatives to the regular PIM method which utilize classical discretization techniques on the systems relating the reference input to the control input and the controlled output are proposed. To solve the polynomial Diophantine equation involved in the PIM process, a set of guidelines is presented, rendering the approach more systematic.

The second part of the characterization investigates the behavior of sampled-data control systems in terms of (i) their responses to reference and disturbance inputs, (ii) their internal and input-output stability, (iii) the controller block transfer functions, (iv) their discrete-time sensitivity functions, (v) the induced norms of the closed-loop systems, and (vi) the transform representation of the control input and controlled output. The main objective of the characterization is to make clear the intuitive idea that a digitally redesigned control system should approach, in a certain sense, its continuous-time counterpart for sufficiently fast sampling frequencies. The time-domain characterization is partly accomplished by employing a continuous-time lifting reformulation of the control systems.

The performances of sampled-data control systems are evaluated via the  $L^\infty$ ,  $L^2$  norms and ITAE index of the control-input and controlled-output errors, and the  $L^\infty$ -,  $L^2$ -induced norms of the systems of interest. The variation of the performance measures with the sampling period is clarified and the superiority of the PIM methods over the local digital redesign techniques, for relatively large sampling intervals, is analytically

and quantitatively determined. Four simulation examples and one experiment illustrate the effectiveness of the PIM methods over other digital redesign techniques and validate the theorems developed on the characterization of sampled-data control systems.

## Sommaire

Cette thèse a pour but la caractérisation et l'évaluation de la performance des systèmes de commande à données échantillonnées tels qu'obtenus à partir de systèmes évoluant en temps continu en utilisant la méthode de reconception numérique.

La première partie de la caractérisation traite de la méthode globale de reconception numérique connue sous le nom de Correspondance d'Entrée du Système sous Contrôle (CESC ou *PIM* en anglais). Dans le but de solutionner les problèmes reliés au système de commande à données échantillonnées fonctionnant en boucle fermée et obtenu avec la méthode CESC, tels que le grand nombre de blocs présents et la possible augmentation de l'ordre de la fonction de transfert associée à chacun des blocs, trois méthodes CESC modifiées sont proposées. De plus, des alternatives à la méthode traditionnelle CESC sont présentées. Celles-ci utilisent les méthodes de l'équivalence du bloqueur et de l'intégration numérique pour digitaliser le système reliant le signal d'entrée de la boucle à l'entrée du système sous contrôle, et la méthode d'appareillage des pôles et zéros pour digitaliser le système reliant le signal d'entrée de la boucle au signal de sortie du système sous contrôle. La méthode d'élimination de matrice (*eliminant matrix* en anglais) et de factorisation de l'espace de l'état (*state-space* en anglais) sont étudiées en tant que moyens de solution de l'équation de Diophantine qui est associée à la méthode CESC. Particulièrement, les conditions qui permettent d'obtenir une solution unique à l'équation de Diophantine sont établies.

Les systèmes de commande à données échantillonnées obtenus en utilisant la méthode de reconception numérique sont analysés en ce qui a trait à leurs réponses aux signaux d'entrée de référence et de perturbation, à leur stabilité interne et stabilité d'entrée-sortie, au comportement des fonctions de transfert des blocs de commande, à leurs fonctions de sensibilité à temps discret, aux normes induites de systèmes à boucle fermée, et à la représentation de la transformée de Laplace des signaux d'entrée et de sortie du système sous contrôle. La caractérisation est partiellement accomplie au moyen d'une reformu-

lation des systèmes de commande à données échantillonnées basée sur la méthode dite *lifting*, traduite ici par méthode d'augmentation. Le résultat principal concerne les conditions suffisantes qui résultent en une convergence uniforme dans le temps des signaux d'entrée et de sortie du système sous contrôle, présent dans le système de commande à données échantillonnées, à leurs homologues du système de commande évoluant en temps continu, à mesure que la période d'échantillonnage est réduite. Un système de commande à données échantillonnées qui possède un tel comportement est appelé modèle à données échantillonnées d'un système à temps continu.

Lorsque les périodes d'échantillonnage sont relativement longues, l'évaluation de la performance des systèmes de commande à données échantillonnées est effectuée grâce aux normes  $L^\infty$  et  $L^2$  des signaux d'entrée et de sortie du système sous contrôle, aux normes induites de systèmes à boucle fermée, et à l'indice de performance ITAE tel qu'appliqué aux signaux d'erreurs. La quantification de la performance est accomplie pour quatre simulations et une expérience. Ces applications illustrent l'efficacité des méthodes CESC traditionnelle et modifiées en rapport avec d'autres méthodes de reconception numérique, et valident les théorèmes sur la caractérisation des systèmes de commande à données échantillonnées.

*À mon père, Georges*

*À ma soeur, Sophie*

*À la mémoire de ma mère, Thérèse*

## Acknowledgments

The author wishes to thank everyone who has aided in the preparation of this thesis. In particular, the author expresses his deepest gratitude to his thesis supervisor, Dr. N. Hori, for his guidance, encouragements and interest over the past three years. The assuring attitude of Dr. Hori, his challenging questions and his positive outlook on obstacles that came along the way of this research work really helped the author keep his focus on the goal at hand. It was an honor to have worked under the supervision of such a respectful and kind individual. In addition, the author is grateful to the members of the control group, most noticeably Dr. Markazi, Dr. Comeau, Mr. Ro, and Chuk Man Ng with whom exchanges about various topics on digital control contributed to the realization of this thesis, and to Dr. T. Chen, of the University of Alberta, for his enlightening reply to my questions concerning his sampled-data control book.

The author would like to acknowledge members of the personnel at McGill for providing interesting courses which resulted in a better understanding of the fields of systems and control by the author. Thanks also go to Mr. Oswald Harris, formerly of Pratt & Whitney Canada, and Mr. Rowland Evans of Pratt & Whitney Canada for their help in the development of the digitally redesigned gas-turbine engine control system. The author appreciates the fact that Pratt & Whitney Canada has allowed him to use their facilities. Thanks also to Mr. Santhosh Jogi of dSPACE Incorporated for his helpful e-mail responses about the setup of the experiment. As well, the author wishes to thank Integrated Systems Incorporated for providing, free of charge, the software used in the engine simulations. The author is also indebted to anonymous reviewers of the International Federation of Automatic Control for their constructive comments on the material of Section 3.2.2.

On a personal note, the author truly appreciates the support provided from his father, Georges, and sister, Sophie, over the past three years and thanks them dearly for that: *Merci à vous deux*. Above all, the author thanks his parents for the sacrifices they have

made over the years so that he could enjoy a solid education both at home and at school.

Finally, the author thanks the Natural Sciences and Engineering Research Council (NSERC) of Canada and the *Fonds pour la Formation de Chercheurs et l'Aide à la Recherche* (FCAR) of Quebec for their financial support, in the form of scholarships, over the three years of the program.

Montreal, March 1999

# Contents

<b>1</b>	<b>Introduction</b>	<b>1</b>
1.1	Motivation of the Research Work . . . . .	1
1.1.1	Local Digital Redesign Methods . . . . .	2
1.1.2	Global Digital Redesign Methods . . . . .	4
1.1.3	Rationale of the Plant Input Mapping Method . . . . .	5
1.1.4	Aspects of the Plant Input Mapping Method Requiring Investigation . . . . .	8
1.2	Modern Approaches to the Analysis of Sampled-Data Control Systems . . . . .	16
1.2.1	Continuous-Time and Sampled-Data Control Systems . . . . .	16
1.2.2	Continuous-Time Lifting . . . . .	18
1.2.3	Induced Norms of Systems, Norms of Signals and Performance Index . . . . .	20
1.3	Objective of the Thesis . . . . .	24
<b>2</b>	<b>Preliminaries</b>	<b>27</b>
2.1	Main Assumptions . . . . .	27
2.2	Time-Domain Concepts . . . . .	28
2.3	Stability of Continuous-Time and Sampled-Data Control Systems . . . . .	30
<b>3</b>	<b>Global Digital Redesign Methods</b>	<b>35</b>
3.1	Regular Plant Input Mapping Method . . . . .	36
3.1.1	Design Steps . . . . .	36

3.1.2	Solutions to Diophantine Equation . . . . .	39
3.2	Modified Plant Input Mapping Methods . . . . .	42
3.2.1	Truncated Plant Input Mapping Method . . . . .	42
3.2.2	Reduced-Order Plant Input Mapping Method . . . . .	43
3.2.3	Reduced-Order, Truncated Plant Input Mapping Method . . . . .	52
3.3	Alternative Digital Redesign Methods Based on the Classical Discretization of a Closed-Loop System . . . . .	53
<b>4</b>	<b>Analysis of Digitally Redesigned Control Systems</b>	<b>55</b>
4.1	Representation of Systems . . . . .	57
4.2	Stability of Systems . . . . .	59
4.3	Behavior of Control Input and Controlled Output as $T \rightarrow 0$ . . . . .	64
4.4	Convergence of the Controller Blocks and Loop Signals as $T \rightarrow 0$ . . . . .	68
4.4.1	Preliminary Definition . . . . .	69
4.4.2	Block Convergence . . . . .	70
4.4.3	Loop Signal Convergence . . . . .	77
4.5	Robustness Characteristics of PIM-Based Sampled-Data Control Systems as $T \rightarrow 0$ . . . . .	81
4.5.1	Sensitivity to Controller and Plant Uncertainties . . . . .	81
4.5.2	Responses to Disturbance Input . . . . .	83
4.6	Performance Evaluation of Sampled-Data Control Systems . . . . .	86
4.6.1	Norms of Control-Input and Controlled-Output Error Signals . . . . .	88
4.6.2	Induced Norm . . . . .	89
4.6.3	ITAE index . . . . .	93
4.6.4	Error System Responses to Inputs in $\mathcal{S}_2$ . . . . .	96
<b>5</b>	<b>Applications of Digitally Redesigned Control Systems</b>	<b>106</b>
5.1	Example Taken from the Optimal Digital Redesign Literature . . . . .	107

5.1.1	Simulations with Fixed-Point Arithmetic and Finite Number of Bits . . . . .	112
5.2	Digital Flight Control of T-2 Aircraft . . . . .	114
5.2.1	Responses to Reference Input . . . . .	118
5.2.2	Response to Disturbance Input . . . . .	126
5.3	Control of Voice-Coil-Driven Flexible Positioner . . . . .	129
5.3.1	Experimental Results . . . . .	132
5.4	Gas-Turbine Engine Speed Control <sup>1</sup> . . . . .	139
5.4.1	Control of Linearized System . . . . .	142
5.4.2	Gain-Scheduled Control of the Engine . . . . .	150
5.5	Example of a MIMO Control System . . . . .	154
5.6	Summary of the Performances Achieved with the Examples . . . . .	158
<b>6</b>	<b>Conclusions</b>	<b>159</b>
6.1	Contributions of the Research Work . . . . .	159
6.1.1	Solutions to Unresolved Issues of the Regular PIM Method . . . . .	159
6.1.2	Characterization and Performance Evaluation of Digitally Redesigned Control Systems . . . . .	160
6.1.3	Summary of Numerical Simulation and Experimental Results . . . . .	161
6.2	Future Research Work . . . . .	162
<b>A</b>	<b>Mathematical Details</b>	<b>174</b>
A.1	Proof of Proposition 4.2.1 . . . . .	174
A.2	Proof of Theorem 4.3.1 . . . . .	175
A.3	Proofs of Propositions 4.3.1, 4.3.2 and 4.3.3 . . . . .	186
A.4	Proof of Proposition 4.4.1 . . . . .	187
A.5	Proof of Proposition 4.4.2 . . . . .	188

---

<sup>1</sup>The material is based on a collaborative research work with Pratt & Whitney Canada, Inc., which has authorized the release of information contained in this section.

A.6	Proof of Proposition 4.4.3 . . . . .	191
A.7	Proof of Proposition 4.4.4 . . . . .	193
A.8	Proof of Theorem 4.6.2 . . . . .	195
A.9	Proof of Theorem 4.6.3 . . . . .	198
<b>B</b>	<b>Matched Pole-Zero Discrete-Time Model as a Hold-Equivalent Structure</b>	<b>205</b>
B.1	Determination of Hold Functions . . . . .	207
B.1.1	Discrete-time Vectors $B_{I,c,o}$ and $B_{II,c,o}$ . . . . .	209
B.1.2	Response Function of Generalized Hold of Type I . . . . .	210
B.1.3	Response Function of Generalized Hold of Type II . . . . .	212
B.2	Properties of the Matched Pole-Zero Discrete-Time Model . . . . .	213
B.2.1	Stability, Controllability and Observability . . . . .	213
B.2.2	Behavior as the Sampling Period Approaches Zero . . . . .	215
B.2.3	Similarities and Differences with the Invariant Models . . . . .	216
<b>C</b>	<b>Alternative Digital Redesign Methods Based on the Classical Discretization of a Closed-Loop System</b>	<b>218</b>
C.1	Digital Redesign Based on Discretization of System Relating Reference Input to Control Input Using Numerical Integration and Hold-Equivalent Techniques . . . . .	218
C.2	Digital Redesign Based on Discretization of System Relating Reference Input to Controlled Output . . . . .	220
<b>D</b>	<b>Laplace Transforms of Control Input and Controlled Output</b>	<b>223</b>
<b>E</b>	<b>Gas-Turbine Engine Speed Control</b>	<b>226</b>

# List of Figures

1.1	Conceptual flow of ideas in the PIM method . . . . .	6
1.2	Feedback control system . . . . .	8
1.3	Bounded continuous signal . . . . .	11
1.4	(a) Continuous-time and (b) sampled-data control systems . . . . .	18
1.5	Lifting of a continuous-time signal . . . . .	19
2.1	Discrete-time control system . . . . .	34
4.1	External connections for (a) the continuous-time and (b) the sampled-data control systems . . . . .	69
4.2	Disturbance input to sampled-data control system . . . . .	84
4.3	Disturbance as a staircase equivalent . . . . .	85
4.4	Control input responses for the example . . . . .	103
5.1	(a) Control inputs and (b) controlled outputs for $T = 0.1$ . . . . .	109
5.2	(a) Control inputs and (b) controlled outputs for $T = 0.4$ . . . . .	110
5.3	Step responses for $T = 0.1$ . . . . .	113
5.4	Step responses for $T = 0.4$ . . . . .	113
5.5	Continuous-time pitch control system . . . . .	114
5.6	Digitally redesigned pitch control system . . . . .	115
5.7	Maximum closed-loop pole relative errors with $T$ . . . . .	117
5.8	Maximum relative differences between corresponding coefficients of $\Omega_T(\varepsilon)$ and $\bar{\Omega}(s)$ . . . . .	118
5.9	(a) Pitch angle $\bar{\theta}(t)$ , (b) pitch rate $\bar{\omega}(t)$ , and (c) elevator deflection $\bar{\delta}_e(t)$ . . . . .	119

5.10	Control input and controlled output responses for $T = 0.3$ second . . . . .	120
5.11	Control input and controlled output responses for $T = 1$ second . . . . .	120
5.12	(a) $\ \Delta\theta_T(t)\ _{L^\infty}$ and (b) $\ \Delta\theta_T(t)\ _{L^2}$ with $T$ . . . . .	122
5.13	(a) $\ \Delta\omega_T(t)\ _{L^\infty}$ and (b) $\ \Delta\omega_T(t)\ _{L^2}$ against $T$ . . . . .	122
5.14	(a) $\ \Delta u_T(t)\ _{L^\infty}$ and (b) $\ \Delta u_T(t)\ _{L^2}$ with respect to $T$ . . . . .	123
5.15	ITAE index on (a) the control-input and (b) the controlled-output errors	124
5.16	Elevator deflections for (a) $T = t_r/40$ and (b) $T = t_r/2$ . . . . .	125
5.17	Pitch angles for (a) $T = t_r/40$ and (b) $T = t_r/2$ . . . . .	125
5.18	Pitch angles for (a) $T = t_r/40$ and (b) $T = t_r/2$ . . . . .	126
5.19	Disturbance to the plant input . . . . .	127
5.20	(a) $L^\infty$ and (b) $L^2$ norms on the controlled-output errors . . . . .	127
5.21	Controlled output responses to disturbance input ( $T = 0.55$ second) . . .	128
5.22	(a) $l^\infty$ - and (b) $l^2$ -induced norms with $T$ . . . . .	129
5.23	Sampled-data control system configuration . . . . .	133
5.24	Control input and controlled output responses ( $T = t_r/2$ ) . . . . .	134
5.25	Control input and controlled output responses ( $T = 1.7t_r$ ) . . . . .	134
5.26	$L^2$ error norms at (a) control input and (b) controlled output vs. $T$ . . .	135
5.27	$L^\infty$ error norms at (a) control input and (b) controlled output with respect to $T$ . . . . .	136
5.28	ITAE indices for (a) the control-input and (b) the controlled-output errors against $T$ . . . . .	136
5.29	Responses of sampled-data control systems . . . . .	137
5.30	Control inputs and controlled outputs ( $T = 2t_r/3$ ) . . . . .	138
5.31	Control inputs and controlled outputs ( $T = 1.7t_r$ ) . . . . .	139
5.32	Schematics of (a) turboshaft engine and (b) gas generator . . . . .	140
5.33	Block diagram of feedback control system . . . . .	141
5.34	(a) $L^2$ and (b) $L^\infty$ norms of the control-input errors . . . . .	145
5.35	(a) $L^2$ and (b) $L^\infty$ norms of the controlled-output errors . . . . .	146

5.36	ITAE index on (a) the control-input and (b) the controlled-output errors	147
5.37	(a) Control input and (b) controlled output responses for $T = 0.3$ second	148
5.38	Fixed-point simulation responses	149
5.39	Disturbance responses for (a) $T = 0.0208$ sec. and (b) $T = 0.3$ sec.	150
5.40	Block diagram of a gain-scheduled sampled-data control system	152
5.41	(a) Reference input, (b) control input and (c) controlled output	152
5.42	(a) $L^2$ and (b) $L^\infty$ norms of control-input errors with $T$	154
5.43	Control inputs (channel 1) for (a) MPZ method, (b) SIM, (c) Tustin, and (d) PIM	155
5.44	Control inputs (channel 2) for (a) MPZ method, (b) SIM, (c) Tustin, and (d) PIM	156
5.45	$L^\infty$ norms of control-input errors	157
5.46	$L^\infty$ norms of controlled-output errors	157
A.1	Lifted representation of a signal in $\mathcal{S}_1$	175
A.2	$ \Sigma_{\omega,T} $ versus $\omega T$	203
B.1	Matched pole-zero model as a hold-equivalent discrete-time system	205
B.2	Hold-equivalent structures	207
E.1	Control inputs for $T = 0.0208$ second	226
E.2	Control inputs for $T = 0.35$ second	227
E.3	Controlled outputs for $T = 0.35$ second	228

# List of Tables

5.1	Controller parameters for $T = 0.1$ . . . . .	108
5.2	Controller parameters for $T = 0.4$ . . . . .	109
5.3	Quantitative measures on the control-input errors for $T = 0.1$ (top of each entry) and $T = 0.4$ (bottom) . . . . .	111
5.4	Quantitative measures on the controlled-output errors for $T = 0.1$ (top of each entry) and $T = 0.4$ (bottom) . . . . .	112
5.5	Controllers obtained with PIM for $T = 0.05$ second . . . . .	115
5.6	Controller blocks obtained with the PIM methods for $T = 4.4$ seconds . . . . .	116
5.7	Plant parameters . . . . .	130
5.8	Performance parameters of continuous-time control system . . . . .	131
5.9	Controller transfer functions for $T = 1.5t_r$ . . . . .	132
5.10	Controller transfer functions obtained with the local digital redesign methods for $T = t_r/7$ . . . . .	143
5.11	Controller transfer functions obtained with the PIM methods for $T = t_r/7$ . . . . .	144
5.12	Observed performances of the digitally redesigned control systems . . . . .	158
E.1	Continuous-time controller parameters . . . . .	229

# Nomenclature

## Abbreviations

MIMO	Multi-Input, Multi-Output
SISO	Single-Input, Single-Output
PIM	Plant Input Mapping
PITF	Plant Input Transfer Function
ZOH	Zero-Order Hold
ITAE	Integral of Time-multiplied Absolute-value of Error

## Symbols

$R$	Set of real numbers.
$R^+$	Set of non-negative real numbers.
$Z^+$	Set of non-negative integers.
$t$	Time $\in R^+$ .
$T$	Sampling and lifting period.
$T^*$	Critical sampling period, see p. 62.
$\tau$	Time (real) in $[0, T)$ .
$k$	Step number $\in Z^+$ .
$L_{PC[0,\infty)}^\infty$	Linear space of piecewise-continuous functions over $t \in [0, \infty)$ having a finite supremum norm.
$l_R^\infty$	Linear space of functions from $k \in [0, \infty)$ to $R$ having a finite supremum norm.
$\widetilde{PC}[0, T)$	Set of piecewise-continuous functions over $[0, T)$ .
$l_{PC[0,T)}^\infty$	Linear space of functions from $k \in [0, \infty)$ to $\widetilde{PC}[0, T)$ having a finite supremum over $k$ of the supremum over $\tau \in [0, T)$ taking place for each step $k$ .

$S_0$	Space of bounded, continuous functions on the time set $[0, \infty)$ , and independent of $T$ .
$S_1$	Space of functions which are bounded, uniformly continuous over $[0, \infty)$ , and independent of $T$ .
$S_2$	Space of bounded functions which are constant in the intervals $[kT, (k+1)T)$ on $[0, \infty)$ , for $k = 0, 1, 2, \dots$ and $T \in (0, \infty)$ .
$L$	Lifting transformation.
$j$	$\sqrt{-1}$
$I$	Identity matrix except in proofs of Propositions A.2 and A.4 where it corresponds to the identity discrete-time system.
$I_{T_i}$	ITAE Index, defined on p. 23.
$\bar{G}(s)$	Transfer function of continuous-time plant $\bar{G}$ .
$[\bar{A}_{\bar{G}}, \bar{B}_{\bar{G}}, \bar{C}_{\bar{G}}, \bar{D}_{\bar{G}}]$	A realization of $\bar{G}(s)$ .
$\bar{H}(s)$	Transfer function from reference input to control input.
$[\bar{A}, \bar{B}, \bar{C}, \bar{D}]$	A realization of $\bar{H}(s)$ .
$\bar{\Pi}(s), \bar{\Omega}(s), \bar{\Gamma}(s)$	Controller block transfer functions.
$\bar{M}(s)$	Transfer function from reference input to controlled output.
$f$	Degree of polynomial $\bar{u}(s)$ in equation (3.26).
$h$	Degree of polynomial $\bar{v}(s)$ in equation (3.26).
$W$	Controllability Gramian of $\bar{G}$ .
$m$	Degree of numerator polynomial of $\bar{G}(s)$ .
$\bar{\phi}(s)$	Stable polynomial.
$\bar{\Sigma}(s)$	Stable, biproper, unity DC gain transfer function with identical sets of poles and zeros.
$c$	Degree of $\bar{\phi}(s)$ .
$\bar{A}\bar{X} = \bar{Y}$	Linear system of equations associated with characteristic polynomial of closed-loop system.
$s_0$	Real constant and $0 \leq s_0 \ll 1$ .

$\overline{S}_{\overline{G}}(s)$	Sensitivity of $\overline{M}(s)$ with respect to changes in $\overline{\Gamma}(s)$ .
$\overline{S}_{\overline{\Pi}}(s)$	Sensitivity of $\overline{M}(s)$ with respect to changes in $\overline{\Pi}(s)$ .
$\overline{S}_{\overline{\Gamma}}(s)$	Sensitivity of $\overline{M}(s)$ with respect to changes in $\overline{\Gamma}(s)$ .
$\overline{S}_{\overline{\Omega}}(s)$	Sensitivity of $\overline{M}(s)$ with respect to changes in $\overline{\Omega}(s)$ .
$z$	Variable of the $\mathcal{Z}$ -transform.
$q$	Shift operator.
$\varepsilon$	Variable of the $\mathcal{D}$ -transform, also Euler operator ( $= \frac{z-1}{T}$ ).
$\delta$	Delta operator ( $= \frac{q-1}{T}$ ).
$G_T(\varepsilon)$	Transfer function of hold-equivalent discrete-time plant model $G_T$ .
$[A_{G_T}, B_{G_T}, C_{G_T}, D_{G_T}]$	A realization of $G_T(\varepsilon)$ .
$H_T(\varepsilon)$	Transfer function from sampled reference input to discrete-time control input for control system obtained with regular PIM in Chapter 3, and for any sampled-data control system in Chapter 4.
$[A, B, C, D]$	A realization of $H_T(\varepsilon)$ .
$\Pi_T(\varepsilon), \Omega_T(\varepsilon), \Gamma_T(\varepsilon)$	Transfer functions of discrete-time controller blocks.
$M_T(\varepsilon)$	Transfer function from sampled reference input to sampled controlled output.
$H(\tau)$	Response function of hold at control input.
$S$	Ideal sampler.
$m$	Degree of numerator polynomial of $G_T(\varepsilon)$ .
$n$	Degree of denominator polynomials of $G_T(\varepsilon)$ and $\overline{G}(s)$ .
$l$	Degree of polynomial $u(\varepsilon)$ in equation (3.9).
$r$	Degree of polynomial $v(\varepsilon)$ in equation (3.9).
$p$	Degree of denominator polynomials of $H_T(\varepsilon), \overline{H}(s), M_T(\varepsilon), \overline{M}(s)$ .
$\ \cdot\ $	Matrix or vector norm, depending on the case.
$\ \cdot\ _{L^2}$	$L^2$ norm of continuous-time signal (see p. 22) or $L^2$ -induced norm of continuous-time system (see p. 21).

$\ \cdot\ _{L^\infty}$	$L^\infty$ norm of continuous-time signal (see p. 21) or $L^\infty$ -induced norm of continuous-time system (see p. 21).
$q$	Degree of numerator polynomial of $\bar{H}(s)$ , and of $H_T(\varepsilon)$ when the regular PIM method is performed.
$w$	Degree of numerator polynomial of $M_T(\varepsilon)$ .
$\hat{H}_T(\varepsilon)$	Transfer function from sampled reference input to discrete-time control input for control system obtained with reduced-order, truncated PIM.
$\widehat{H}_T(\varepsilon)$	Transfer function from sampled reference input to discrete-time control input for control system obtained with reduced-order PIM.
$A(\varepsilon), B(\varepsilon)$	Transfer functions used in the coprime factorization of $G_T(\varepsilon)$ .
$U(\varepsilon), V(\varepsilon)$	Transfer functions satisfying $A(\varepsilon)U(\varepsilon) + B(\varepsilon)V(\varepsilon) = 1$ .
$\lambda(\varepsilon), \lambda'(\varepsilon)$	Stable polynomials each of degree $n$ .
$f_T$	Constant row vector of length $n$ .
$h_T$	Constant column vector of length $n$ .
$\mathbf{A}X = Y$	Linear system of equations.
$\hat{X}$	Least-squares estimator of $X$ .
$\mathbf{A}X_{local} = Y_{local}$	Linear system of equations associated with the control system obtained with the local digital redesign method.
$\varepsilon_0$	Real constant given by $\varepsilon_0 = \frac{e^{*0T}-1}{T}$ .
$\lambda_i$	Eigenvalue of closed-loop system matrix, see p. 32.
$p_i$	Eigenvector associated with $\lambda_i$ , see p. 32.
$S_{G_T}^{M_T}(\varepsilon)$	Sensitivity of $M_T(\varepsilon)$ with respect to changes in $G_T(\varepsilon)$ .
$S_{\Pi_T}^{M_T}(\varepsilon)$	Sensitivity of $M_T(\varepsilon)$ with respect to changes in $\Pi_T(\varepsilon)$ .
$S_{\Gamma_T}^{M_T}(\varepsilon)$	Sensitivity of $M_T(\varepsilon)$ with respect to changes in $\Gamma_T(\varepsilon)$ .
$S_{\Omega_T}^{M_T}(\varepsilon)$	Sensitivity of $M_T(\varepsilon)$ with respect to changes in $\Omega_T(\varepsilon)$ .

$\|\cdot\|_{l^2}$

$l^2$  norm of discrete-time signal (see p. 22) or  
 $l^2$ -induced norm of discrete-time system (see p. 21).

$\|\cdot\|_{l^\infty}$

$l^\infty$  norm of discrete-time signal (see p. 22) or  
 $l^\infty$ -induced norm of discrete-time system (see p. 21).

## Claim of Originality

The work presented in this thesis has contributed to the fields of systems and control in the following regards:

1. A characterization of the plant input mapping (PIM) method is performed in Chapters 3 and 4. This is partly accomplished by a lifting reformulation of the sampled-data and continuous-time control systems; a method extensively used in the proofs of the propositions and theorems pertaining to the time-domain behavior of sampled-data systems. A state-space formulation of the matched pole-zero discretization is performed in Appendix B which provides a clear understanding of the PIM method and the behavior of PIM-based systems from a structural point of view.
2. Modified PIM techniques are proposed in Chapter 3. They provide solutions to some of the inherent problems associated with the regular PIM method; that is, increased complexity in terms of the number of controllers present in the loop and the orders of the controllers. Chapter 3 also presents the first set of guidelines in solving the Diophantine equations associated with the PIM methods.
3. From a time-domain perspective, the notion of sampled-data model, defined in Chapter 2 and applied to sampled-data control systems in Chapter 4, helps establish whether the control input and controlled output responses of digitally redesigned control systems to reference and disturbance inputs can be made arbitrarily close to those of the continuous-time control system. The first study of the behavior of the loop signals, as  $T \rightarrow 0$ , other than the control input and controlled output is carried out in this thesis. The convergence in the induced norms of sampled-data systems, as  $T \rightarrow 0$ , to their continuous-time counterpart is provided as well.

4. The  $L^\infty$ - and  $L^2$ -induced norms of the systems relating the reference and disturbance inputs to the control input, the  $L^\infty$  and  $L^2$  norms and the value of the ITAE index on the control-input and controlled-output errors between sampled-data and continuous-time control systems are presented in Chapter 4. These tools allow a control designer to compare quantitatively the performances of regular and modified PIM methods against that obtained with local methods for any finite sampling period. The advantages of the PIM methods over the local digital redesign techniques for relatively long sampling intervals are clarified via theorems and general observations are made on the basis of the system representation provided in Section 4.1.

# Chapter 1

## Introduction

### 1.1 Motivation of the Research Work

In the field of automatic control, there exist three approaches to the design of sampled-data control systems, which comprise discrete-time controllers in closed-loop with a continuous-time dynamic system or plant: (i) direct discrete-time design, (ii) sampled-data design, and (iii) digital redesign.

Direct discrete-time design consists of obtaining discrete-time controllers achieving closed-loop stability and a desired performance, at the sampling instants, based on the discrete-time plant model [1]. A well-known drawback associated with this method is the possibility that the sampled-data control system possesses intersample ripples at its plant input and output [2, 3]. In order to overcome the problem of intersample oscillations, the method known as sampled-data design has received considerable attention since the mid nineteen eighties. This method consists of designing discrete-time controllers while taking into account the intersample behavior of the continuous-time signals present in the sampled-data loop such as the disturbance and reference inputs, the control input, the controlled output, and the tracking error [4]. So far, the sampled-data design approach has concentrated on optimal controller design, leaving the classical control design methods, such as PID and pole-placement [5], untouched despite the fact they

are widely used in industry. For instance, in [6], the  $L^2$ -induced norm of sampled-data control systems is optimized, with the intersample information considered in the process. Researches on sampled-data design have also brought new control objectives. For example, the works found in [7] and [8] provide necessary and sufficient conditions to achieve ripple-free deadbeat control of sampled-data systems; that is, elimination of the ripples in the continuous-time responses past some finite time instant.

This thesis is concerned with the third approach to the design of sampled-data control systems: digital redesign. Digital redesign is the process of converting a continuous-time control system to a sampled-data control system. The continuous-time control system is composed of the plant and the controllers, which are all continuous-time systems, and is assumed to satisfy the design specifications. Digital redesign of a continuous-time control system has practical advantages over other methods such as the facts that the sampling time can be selected from the knowledge of the continuous-time closed-loop dynamics and that a large body of existing continuous-time methods can be put to use in the design. The success of the digital redesign relies on the closed-loop stability at the selected sampling rate, the relatively close performance, in terms of the signals of interest, with that of the continuous-time control system, and the controller implementations with few numerical problems.

### 1.1.1 Local Digital Redesign Methods

The digital redesign process involves two stages: (i) discretization of a system, and (ii) implementation of the system. Traditionally, the digital redesign has been accomplished in a local manner; that is, each controller block (i) is discretized using the conventional discretizations, which can be found in [2], and (ii) is implemented at the same location in the closed-loop as that of the continuous-time controller. This approach is named local digital redesign. In this thesis, the discretization methods considered are equi-order ones; that is, a continuous-time system is converted to a discrete-time system with a transfer function having the same order as that of the continuous-time transfer function.

Examples of such methods are the well-known hold-equivalent techniques [2], numerical integrations such as the backward difference and Tustin's method [1], and the matched pole-zero methods [9, 10, 11]. The discrete-time systems obtained with these discretizations are termed, respectively, the invariant, the mapping, and the matched pole-zero discrete-time models [12, 13]. The term discrete-time model refers to the fact that a discrete-time system has a continuous-time counterpart which does not depend on the sampling interval. Discretization methods not considered in this thesis are, for instance, the second order Adams-Bashforth [14] and first-order hold equivalent [15] methods, which result in discrete-time systems with orders higher than that of the continuous-time system. The work in [16] studies the higher-order discrete-time models.

The main disadvantage of a local digital redesign approach is that the resulting sampled-data control system usually requires relatively fast sampling frequencies for preserving closed-loop stability and achieving a close performance to that of the continuous-time control system [2]. This fact renders the design process an iterative one where the designer must be extra careful in the selection of a sampling rate in order to avoid highly oscillatory and unstable responses. In an age where digital processors are becoming cheaper and faster, the requirement of fast sampling frequencies may not be viewed, at first glance, as a negative factor. Yet, relatively slow sampling frequencies may be the only choice available to a control designer; for instance, (i) in chemical processes where the sampling times are typically slow and cannot be arbitrarily set for control purposes, (ii) in simple control algorithms for mass-production where one cent saved on the purchase of a slow chip can be the deciding factor on the choice of a control law, (iii) in a transportation system where the processor has limited computational power, the control update could be required to be slowed down in an emergency situation in order to make it possible for the processor to tackle the more important task at hand, or, as mentioned in [17], to perform additional functions, and (iv) in the case of a flight control system where a relatively slow microprocessor is chosen for proven reliability [18].

### 1.1.2 Global Digital Redesign Methods

With the digital redesign objective as stated previously, intuition suggests that the better approach would be to perform an approximation to the closed-loop continuous-time control system, as pointed out in [19]. Among the new methods subscribing to this philosophy, which are named global digital redesign techniques, the one proposed in [20] consists in obtaining a discrete-time controller such that the  $l^2$ -induced norm of a discrete-time multirate approximation to the weighted discretization error operator is minimized. For sufficiently small sampling periods, closed-loop stability is guaranteed, yet the local continuous-time control block must be stable in order to apply the method and the resulting discrete-time control block may have order higher than that of the continuous-time controller; for instance, the example in [20] presents a continuous-time control system with controller block of order one whereas the discrete-time controller resulting from the digital redesign is of third order. In [21], the technique proposed is to minimize the error between the frequency response of the discrete-time control system and that of the continuous-time control system by adjusting the parameters of the discrete-time controller block, which may be required to possess an order much higher than that of the continuous-time control block for satisfactory steady-state performance. The same type of process is carried out in [22] using the continuous frequency response of the digital control system instead of the discrete-time frequency response. Again, controller complexity can be high with this method. Another global digital redesign method is that of [23], where the transfer function of a fixed-structure discrete-time control system is inexactly matched to the step invariant model of the closed-loop system. The major drawback of this approach is the requirement of minimum-phase plant model and controller. An optimal digital redesign method, found in [24], consists in the following: Given a continuous-time plant and a well-designed continuous-time controller, design a discrete-time control system such that its continuous-time, closed-loop step responses, at control input and controlled output, optimally match those of the continuous-time system in the sense that a weighted sum of the energy of the associated error signals is mini-

mized. Two disadvantages of this method are the fact the discrete-time controller can be of order higher than that of the continuous-time controller, hence an order reduction technique should be employed as well, and the dependency on the reference input.

The global digital redesign approaches presented above suffer from three problems: (1) the complexity of the continuous-time controllers can be increased in the discrete-time domain; (2) most digital redesign processes require complicated mathematics, where some closed-loop parameter of the sampled-data control system is optimized; and, (3) the conditions of applications are quite stringent. As pointed out in [25], with simple controllers, there are fewer problems or bugs in the software, their effects are easier to understand, and the requirements on the computations are lessened with respect to more complex controllers. As for the optimization, a simpler approach would be to use classical discretization methods on the closed-loop control system, as is done with the digital redesign method in [23] but with the controller implementations and discrete-time plant model recovering the exact closed-loop discrete-time system transfer function. A consequence of the third problem is that some continuous-time control systems are excluded from the digital redesign process. As far as the author is aware, only the Plant Input Mapping (PIM) method, introduced in [26], is based on the discretization of a closed-loop system and can be applied to the most general situation, as explained next.

### 1.1.3 Rationale of the Plant Input Mapping Method

Although restricted to linear, time-invariant systems, the PIM method is the only known global digital redesign approach which can be utilized in the case of unstable, non-minimum phase and multi-input, multi-output (MIMO) controllers and plants [27]. Figure 1.1 illustrates the flow of ideas involved in carrying out the PIM method. The four steps yielding the PIM-based control system are: (1) calculation of the transfer function relating the reference input to the control input, which is defined as the Plant Input Transfer Function (PITF) of the continuous-time control system; (2) discretization of the PITF with the matched pole-zero method to obtain the discrete-time PITF; (3) dis-

cretization of the continuous-time plant to a discrete-time model; (4) determination of the discrete-time controller blocks from the knowledge of the discrete-time PITF and plant model. The process of the PIM method is explained in more details in Section 3.1.

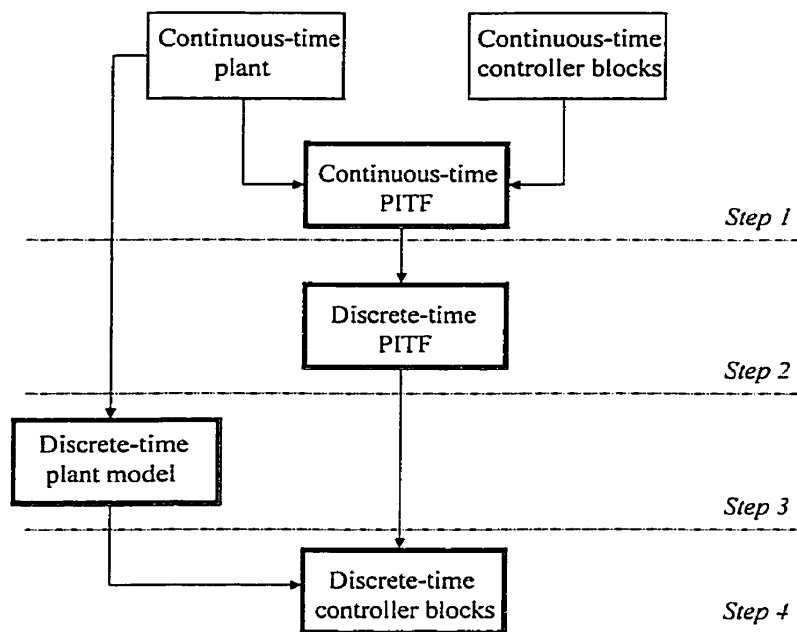


Figure 1.1: Conceptual flow of ideas in the PIM method

The PIM method relies on two characteristics of linear, time-invariant, single-input, single-output (SISO) single-loop feedback control systems: (1) closed-loop stability of the system relating the reference input to the controlled output is necessary and sufficient to guarantee the stability of the system relating the reference input to the control input [14]; and, (2) the equi-order matched pole-zero discretization can be performed on the continuous-time PITF and the resulting discrete-time system can be implemented as a single-loop, internally stable discrete-time control system by solving a Diophantine equation [28]. Point (1) can be seen as a cancellation of the plant poles by the zeros of the stable PITF, so that unstable poles of the plant, if any, do not appear in the transfer function relating the reference input to the controlled output. For instance, consider the linear, time-invariant continuous-time control system of Figure 1.2, where

$\bar{G}(s) = \bar{b}(s)/\bar{a}(s)$  and  $\bar{C}(s) = \bar{n}(s)/\bar{d}(s)$ . The closed-loop transfer function is given by

$$\bar{M}(s) \triangleq \frac{\bar{Y}(s)}{\bar{R}(s)} = \frac{\bar{G}(s)\bar{C}(s)}{1 + \bar{G}(s)\bar{C}(s)} = \frac{\bar{b}(s)\bar{n}(s)}{\bar{a}(s)\bar{d}(s) + \bar{b}(s)\bar{n}(s)} \quad (1.1)$$

and the continuous-time PITF, by

$$\bar{H}(s) \triangleq \frac{\bar{U}(s)}{\bar{R}(s)} = \frac{\bar{C}(s)}{1 + \bar{G}(s)\bar{C}(s)} = \frac{\bar{a}(s)\bar{n}(s)}{\bar{a}(s)\bar{d}(s) + \bar{b}(s)\bar{n}(s)}. \quad (1.2)$$

It then follows that

$$\bar{M}(s) = \bar{H}(s)\bar{G}(s) \quad (1.3)$$

and the poles of the plant model are cancelled by the zeros of the continuous-time PITF. This pole-zero cancellation is a consequence of the feedback and occurs with all linear, time-invariant feedback control systems. With PIM, the stability of the continuous-time PITF is carried over to the discrete-time PITF. Point (2) implies that by discretizing the PITF with the matched pole-zero method, there exists an implementation structure for which the discrete-time closed-loop system is internally stable. The key in finding such structure for the SISO case is to solve a polynomial Diophantine equation [29] of the form

$$a(\rho)u(\rho) + b(\rho)v(\rho) = d(\rho) \quad (1.4)$$

where  $\rho$  is the complex variable,  $a(\rho)$  and  $b(\rho)$  are the denominator and numerator polynomials, respectively, of the discrete-time plant model, and  $d(\rho)$  is the denominator polynomial of the discrete-time PITF. The polynomials  $u(\rho)$  and  $v(\rho)$  are used in the determination of the discrete-time controller transfer functions according to a procedure found in [30].

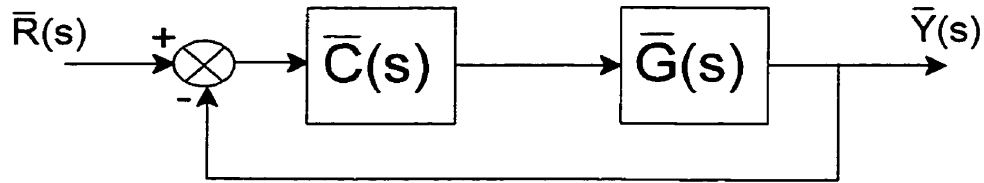


Figure 1.2: Feedback control system

### 1.1.4 Aspects of the Plant Input Mapping Method Requiring Investigation

The literature on the PIM method reveals that its characterization has not been exhausted and that there remain several questions to be answered. This subsection reviews the issues that the author considers as important. It should be pointed out that some of them apply to the other digital redesign methods as well.

#### Discrete-Time Control System

The currently available works on PIM examine the sampled-data control systems at the sampling instants only. For instance, in [31], the stability of the discrete-time control system is considered, leaving out the input-output stability over all times and its connection with the internal stability of the discrete-time closed-loop system. Input-output stability of a general sampled-data control system has been studied in [32] and [33], where the important aspect of sampling period pathologicity is discussed, yet for the 1-block sampled-data control system only. Of course, a discrete-time analysis has some merits. The most obvious being the study of the limiting behavior of the discrete-time control system as the sampling period is reduced. That is, with the knowledge that a discrete-time system has a continuous-time counterpart, a pointwise-in-time connection can be established between the continuous- and discrete-time systems, as the sampling period is shortened [34]. As an example, consider continuous- and discrete-time systems subjected to the same continuous-time input, which is sampled before entering the

discrete-time system. Suppose that, for a given sampling period, one takes any fixed time instant over the continuous time set and takes the norm on the difference between the value of the output of the continuous-time system at that time instant with that of the discrete-time system at the closest sampling time. The process is repeated for several different sampling periods. Then, as the sampling period is reduced, the norm of the difference in amplitudes will tend to zero. This relation exists between the continuous- and discrete-time PITFs when the PIM method is employed [27]. However, the very nature of a sampled-data control system prevents having to compare the outputs of discrete- and continuous-time systems; that is, both sampled-data and continuous-time control systems generate continuous-time outputs.

Another drawback of the current discrete-time characterization of PIM is that it does not address the issue of convergence of the discrete-time controller blocks to their continuous-time counterparts as the sampling period is reduced, instead only the discrete-time PITF convergence is studied [35]. The convergence, in some sense, of the discrete-time controller block representations to their continuous-time counterparts for relatively fast sampling frequencies arises from the desire to have the discrete-time loop signals, connected to the exterior world with a digital-to-analog converter, behaving as closely as possible to the corresponding signals of the continuous-time control system; that is, if each block is relatively close to its continuous-time counterpart, so will be the loop signals. Why would one want arbitrarily close signals, in the time domain, between the continuous-time and sampled-data systems? This is because the loop signals of a control system may be required to lie within prescribed limits for reasons which may be related to the actuators or any other device that restricts the amplitude of the signals.

The discrete-time treatment of sampled-data systems is not akin solely to the current works on PIM. In [36], discrete-time and continuous-time systems are compared as to their input-output behaviors at the sampling instants. This type of analysis ignores the intersample information associated with sampled-data control systems. For example, if a sampled-data system matches the response of a continuous-time system at the sampling

instants, for a given input, it does not mean that it offers a satisfactory performance over the continuous-time set. On the other hand, even if a sampled-data system has a response different from that of a continuous-time system, at the sampling instants, it can still offer a relatively close response to that of the continuous-time system over the continuous time. Clearly, the intersample information has to be taken into account in the analysis of sampled-data systems.

### **Control Input and Controlled Output**

The works on PIM study the system relating the sampled reference input to the discrete-time control input, disregarding what happens in between the sampling instants at the control input. Two factors motivate the study of the control input over all time instants: (i) with the PIM method, the difference between the continuous-time and sampled-data control systems, as perceived by the plant, occurs at the continuous-time control input, hence any means of keeping the size of this error small involves investigation of all time instants; and (ii) from a practical point of view, the physical limits of the actuators require that the amplitude of the control input lies within achievable values. Control input studies do not abound in the literature which is concerned with the digital redesign of continuous-time control systems, despite the issues of practicality and stability associated with such signal. At least, in [2], the importance of the control input is acknowledged in the sense that it could be the cause of ripples at the controlled output. By selecting a non-pathological sampling period, ripples can take place when the control input has an oscillatory behavior. The obvious way then to understand the occurrence of intersample ripples at controlled output is to investigate the control input behavior and the source of its unwanted oscillations.

At the controlled, or plant, output, a time domain analysis which treats the continuous-time signal, and not just its sampled version, has been carried out in [27]. There, the uniform-in-time convergence of the controlled output of the PIM-based sampled-data control system to its counterpart in the continuous-time control system has been stated.

However, the class of reference inputs considered in [27] is too vast for the study of the uniform-in-time convergence of the control input. The reason is that the bounded continuous signals may have ever-increasing derivatives over some time intervals. Reducing  $T$  to any positive value cannot change the fact that the, possibly, biproper discrete-time PITF is unaffected by the peaks reached by the reference input over portions of the time line. This point is illustrated for one particular continuous signal  $\bar{f}(t)$  shown in Figure 1.3, where  $\beta < \infty$  and  $T \in (0, \infty)$ . For a given  $T$ , it is seen that in the interval  $[3T, 4T)$ , the information is lost when sampled. Then one could sample at a faster rate. However, since the signal is made up of triangles of ever-increasing slopes, there exists at least one time interval, such as  $[\kappa T, (\kappa + 1)T)$  in the figure, where the spike-like behavior is not transmitted by the sampler, for any  $T \in (0, \infty)$ . For the continuous-time control system, a biproper continuous-time PITF transmits the spike occurring in the interval  $[\kappa T, (\kappa + 1)T)$ .

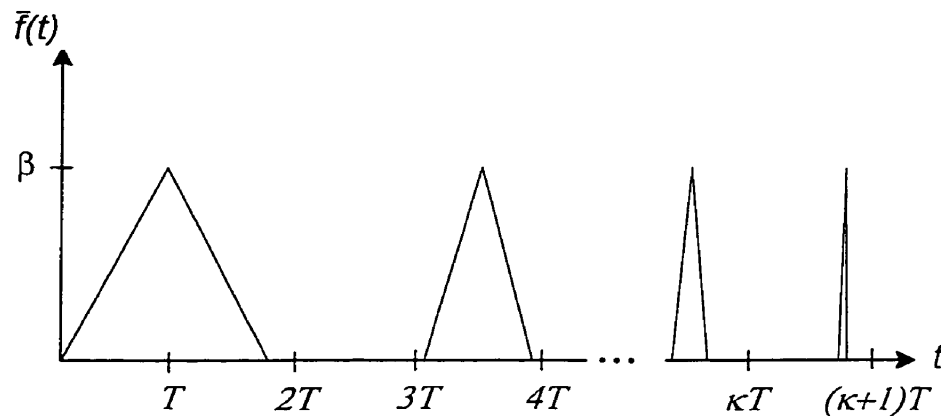


Figure 1.3: Bounded continuous signal

Intuition suggests that, even if the finite- $T$  performance of a sampled-data control system cannot be easily characterized, at least as the uniform sampling period  $T$  is reduced, the time domain performance, at the control input and controlled output, is expected to approach that of the continuous-time control system. However, to achieve such behavior, what conditions should be imposed on the sampled-data control system, and in what sense does the rapprochement take place? As far as the author is aware,

no work has looked into this aspect from a perspective applicable to all digital redesign methods, especially for the control input signal.

### **Performance of PIM-Based Sampled-Data Control Systems for Relatively Large Sampling Periods**

The study of PIM-based sampled-data control systems for relatively large sampling periods has been confined to a sensitivity analysis of the so called discretization error [27]. There is no quantitative comparison of the performance of PIM-based control systems with systems based on some other global or local digital redesign methods. Furthermore, there is no explanation to the responses obtained with PIM-based control systems for relatively long sampling intervals. As of now, only simulation response plots are provided to show how PIM fares against other discretization methods, both local and global, and this is done for a finite set of sampling periods, on simple low-order plants and for the unit step reference input. For instance, the performances of digital model-reference flight control systems of a VTOL aircraft obtained with PIM and the local digital redesign using the Tustin's mapping method are compared for five different sampling periods in [30]. The PIM- and Tustin-based digital flight controls of the T-2 aircraft are simulated for three sampling periods in [35]. In all those simulations, PIM has performed in a superior manner to the local digital redesign methods for these relatively long sampling intervals. This is in the sense that the control input and controlled output of PIM-based control systems are close to their counterpart of the continuous-time system, as assessed qualitatively with the response plots. Still, validating the hypothesis that PIM is superior to the other known digital redesign methods with only a few step responses is inconclusive.

### **Disturbance Rejection**

So far, researchers have emphasized the behavior of PIM-based control systems with respect to a reference input, and only the work in [26] discusses briefly the disturbance-rejection behavior of a PIM-based control system via a parameterization technique. How-

ever, only step-type disturbances are considered. Since the plant evolves in continuous-time and disturbances can represent physical phenomena, it is natural to enquire about the behavior of sampled-data control systems subjected to a wider class of disturbance inputs than the step. This lack of work in the disturbance-rejection area can be attributed to the limitations of the conventional analytical tools, such as the transfer functions in  $s$  or  $z$  and the state-space form [37], which consider either the continuous-time or the discrete-time domain. A topic related to the disturbance response of a control system is the sensitivity of the closed-loop system with respect to variations in plant and controller parameters. Still, the behavior of the sensitivity functions of the closed-loop discrete-time systems with the sampling period has not been investigated for the PIM-based systems.

### Diophantine Equation Solution

The theoretical basis of the Diophantine equation has been studied in numerous papers. In [38], a review of the use of Diophantine equations in control is provided. A fractional representation approach to the analysis and synthesis of continuous-time control systems, in which a parameterization of the stabilizing controllers is obtained, is reported in [39]. A polynomial Diophantine equation is used in [5], where the structure of a continuous-time feedback control system is fixed and the transfer function of a controller block is obtained based on the desired closed-loop poles. A similar process is carried out in [2], although for a discrete-time control system design.

The PIM method requires the solution to a discrete-time Diophantine equation. However, the PIM literature lacks the steps and algorithms allowing one to numerically solve the Diophantine equation involved in the process. Of course, there exist several methods such as that based on matrix algebra in [29]. Yet, the effect of using the different solution methods on the performance of a PIM-based control system is unknown. In addition, the requirements on the orders of the different transfer functions involved is not addressed in any work on PIM. Until these points are clarified, the behavior of the solution to the discrete-time Diophantine equation as the sampling interval is shortened cannot be

compared against that of the Diophantine equation associated with the continuous-time control system.

### Implementation Considerations

By implementation considerations it is meant the complexity of the controllers, the number of controllers present in the loop, the magnitudes of the transfer function coefficients, the realization structure [40] of each discrete-time block and the discrete-time operator used in the transfer functions. These considerations become especially critical when the discrete-time controllers are implemented with fixed-point arithmetic and a restricted number of bits. The main reason for using fixed-point processors is that they are generally cheaper than their floating-point counterparts [41]. Another reason which may justify the use of fixed-point processors is that, generally, a fixed-point hardware has a less complicated logic circuit, and consequently a smaller chip size, than that of a floating-point processor [42].

Depending on the manner in which the Diophantine equation is solved, the discrete-time controllers could be of higher order than the blocks of the continuous-time control system [43]. Furthermore, the number of controllers present in the sampled-data control system could be greater than that in the continuous-time control system [14]. For example, if a continuous-time control system consisting of one controller in closed-loop with the plant is digitally redesigned with the regular PIM method, there will result up to two additional controller blocks in the discrete-time implementation. The problem of increased number of controllers has been investigated in [44]. There it is shown that the number of controllers in the continuous-time control system can be preserved in the sampled-data control system by performing a minimization of the  $H^\infty$  norm of the error transfer function between the reference input and the control input. However, the controller orders are not taken into account with such an approach, and consequently the discrete-time controller orders can still be high relative to the orders of the continuous-time controllers.

An increase in complexity, from the points of view of controller order and controller number, is not appealing for practicing engineers. This is so mainly for reasons of practicality in the handling of the controllers, i.e. high-order controllers necessitate long off-line computational processes when modified, increased burden on the processor in real-time, more pronounced finite wordlength effects [45], and costs. It is also known that a relatively fast sampling rate cannot be selected when the computation time associated with a general complex discrete-time control scheme is long [46]. Furthermore, from the viewpoint of performance comparison of the local digital redesign and the PIM methods, the differences in controller block orders and numbers may be perceived as making the evaluation an unfair one.

When implementing a control algorithm, the discrete-time operator  $\varepsilon = (z - 1)/T$  in the complex plane, or  $\delta = (q - 1)/T$  [47] in the time domain, where  $q$  is the shift operator, should be the preferred choice since it provides superior coefficient representation and computational properties than the conventional shift, or  $z$  operator, in the presence of finite number of bits and fixed-point arithmetic, especially in the case of relatively fast sampling [48, 49, 50]. Moreover, the  $\varepsilon$  operator should be used when solving the Diophantine equation, as mentioned in [26], [29] and [51], as opposed to the  $z$  operator.

There has not been any experiment using the PIM method reported in the literature. Until the PIM technique is applied to an actual experimental setup, where the aforementioned considerations should come into play, it will remain a theoretical idea only.

### **Alternatives to the PIM Method Based on the Same Rationale**

The main idea of PIM is to discretize a closed-loop system rather than a local controller block. However, only the matched pole-zero discretization and an *ad hoc* method proposed in [52], which restricts the reference input to be piecewise-constant, have been used to discretize the continuous-time PITF. The possibility of having other digital redesign methods based on the same rationale as that of PIM has not been investigated.

The questions still remain as to the use of classical discretization techniques, other than the matched pole-zero method, on the continuous-time PITF. Furthermore, discretizing a closed-loop system different from the one relating the reference input to the control input is still an open issue.

## 1.2 Modern Approaches to the Analysis of Sampled-Data Control Systems

During the recent years, the study of sampled-data control systems has shifted from one directed toward a discrete-time domain analysis to one which considers the continuous-time signals present in the loop. To do so, the lifting of continuous-time signals and systems is performed on the sampled-data and continuous-time control systems so that all elements involved in the analysis can be characterized under a unified framework. The induced norms of systems and norms of signals are evaluated in order to quantitatively determine the performance of a sampled-data control system. Before clarifying these modern approaches, the systems studied in this thesis are explained.

### 1.2.1 Continuous-Time and Sampled-Data Control Systems

The continuous-time feedback control system is shown in Figure 1.4(a). The linear, time-invariant, continuous-time plant has transfer function  $\bar{G}(s)$ . The system relating the reference input to the control input is denoted as  $\bar{H}$ . The reference input  $\bar{r}(t)$  is assumed to lie in the following normed linear space

$$L_{PC}^{\infty}[0, \infty) = \{\bar{f}(t) \in \widetilde{PC}[0, \infty) : \sup_{0 \leq t < \infty} |\bar{f}(t)| < \infty\} \quad (1.5)$$

where  $\widetilde{PC}[0, \infty)$  denotes the set of real piecewise-continuous time functions over  $[0, \infty)$ , and  $|\cdot|$ , the absolute value. In the figure, the Laplace transform of a signal such as  $\bar{r}(t)$  is written as  $\bar{R}(s)$ .

The digital redesign process is performed on the continuous-time control system and results in a sampled-data control system with a general structure shown in Figure 1.4(b), where the system relating the reference input to the control input is  $HH_T S$ .  $H_T$  represents the discrete-time system relating the sampled reference input to the discrete-time control input. In the figure, the discrete-time transfer functions are written in terms of the  $\varepsilon$  operator. For instance, the Delta transform [29] of the sampled reference input signal  $r_{k,T}$ ,  $k \geq 0$ , is given by

$$\mathcal{D}\{r_{k,T}\} \triangleq \sum_{k=0}^{\infty} r_{k,T} (T\varepsilon + 1)^{-kT} \quad (1.6)$$

and is denoted as  $R_T(\varepsilon)$  in Figure 1.4(b). In addition,  $U_T(s)$  represents the Laplace transform of the continuous-time control input of the sampled-data control system, i.e.  $u_T(t)$ , where the subscript  $T$  refers to the dependence on the sampling period. The ideal sampler  $S$  maps a signal in  $L_{PC[0,\infty)}^{\infty}$  to one in  $l_R^{\infty}$ , where  $l_R^{\infty}$  denotes the linear space of functions from the set of integers to  $R$  having finite supremum norm, such that  $y_{k,T} = y(t)|_{t=kT}$ ,  $k \geq 0$ .  $H$  is a one-interval hold which is assumed to comprise finitely many points of discontinuity, is synchronized with  $S$ , and transforms real sequences in  $l_R^{\infty}$  to signals in  $L_{PC[0,\infty)}^{\infty}$  such that  $u_T(t) = H(t - kT)u_{k,T}$ ,  $kT \leq t < (k + 1)T$ ,  $k \geq 0$ , where  $H(t - kT)$  is the response function of the hold [53].

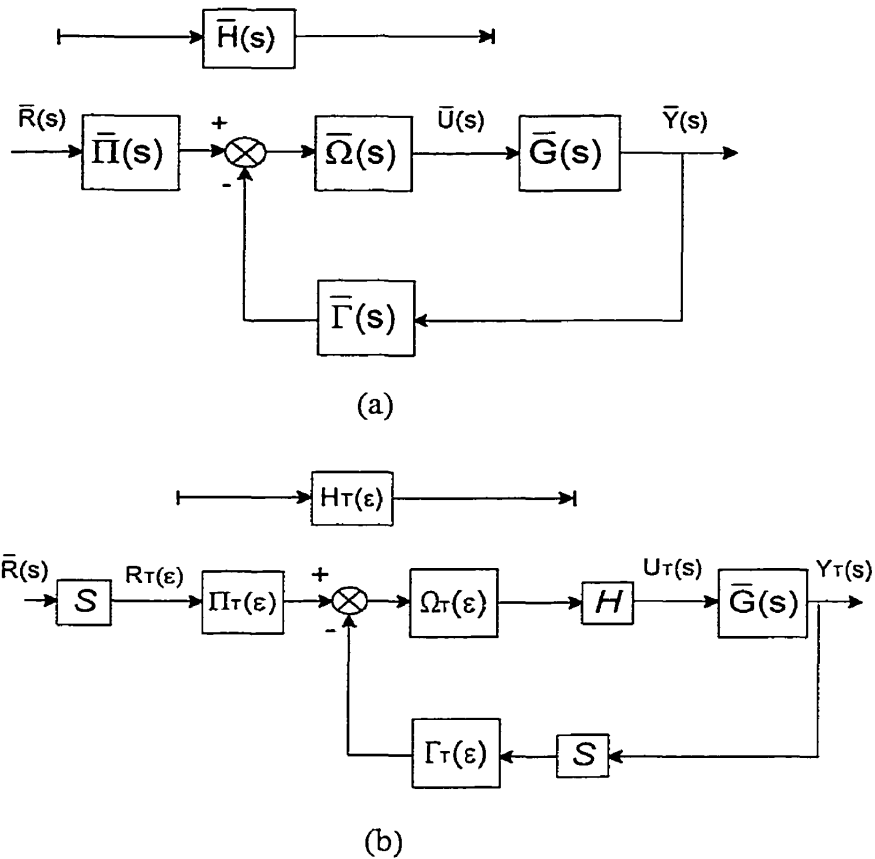


Figure 1.4: (a) Continuous-time and (b) sampled-data control systems

With the knowledge of the continuous-time and sampled-data control systems involved, the characterization of the systems can be more clearly understood.

## 1.2.2 Continuous-Time Lifting

This subsection reviews the process of continuous-time lifting. The continuous-time lifting method, introduced in [54], conceptually reformulates a linear, periodic system into a linear, time-invariant one [4]. Contrary to the perspective on sampled-data systems where signals are considered only at the sampling instants, lifting allows to keep track of the intersample information and to preserve algebraic and topological properties of signals and systems [55].

The lifting of a function  $f(t) \in L_{PC}^{\infty}(0, \infty)$  can be visualized as a partitioning of its time

trajectory into an infinite number of piecewise-continuous functions, each of which being a copy of  $f(t)$  within the time interval  $[kT, (k+1)T)$  for  $k \geq 0$ , as shown graphically on Figure 1.5. The lifted signal is represented as a sequence  $\{\widehat{f}_{k,T}(\tau)\}_{k=0}^{\infty}$ . The step  $k$  lies in  $Z^+$ , which is the set of non-negative integers. Each element of the sequence, such as the  $k$ th element  $\widehat{f}_{k,T}(\tau)$ , is a function in  $\widetilde{PC}[0, T)$ , where  $\widetilde{PC}[0, T)$  is the set of piecewise-continuous functions over  $[0, T)$ . Let the set of such sequences as  $\{\widehat{f}_{k,T}(\tau)\}_{k=0}^{\infty}$  be denoted as  $l_{\widetilde{PC}[0, T)}^{\infty}$  and the normed, linear space  $l_{\widetilde{PC}[0, T)}^{\infty}$  be defined as

$$l_{\widetilde{PC}[0, T)}^{\infty} = \left\{ \{\widehat{f}_{k,T}(\tau)\}_{k=0}^{\infty} \in l_{\widetilde{PC}[0, T)}^{\infty} : \sup_{0 \leq k < \infty} \left( \sup_{0 \leq \tau < T} |\widehat{f}_{k,T}(\tau)| \right) < \infty \right\}. \quad (1.7)$$

The lifting is therefore a transformation between functions in  $L_{\widetilde{PC}[0, \infty)}^{\infty}$  and  $l_{\widetilde{PC}[0, T)}^{\infty}$ ; that is, the lifting represented as  $L$  is a linear mapping denoted as  $L : L_{\widetilde{PC}[0, \infty)}^{\infty} \rightarrow l_{\widetilde{PC}[0, T)}^{\infty}$ . On the other hand, the inverse lifting operation is expressed as  $L^{-1} : l_{\widetilde{PC}[0, T)}^{\infty} \rightarrow L_{\widetilde{PC}[0, \infty)}^{\infty}$ . One important characteristic of the lifting of signals is the fact it is norm-preserving [56].

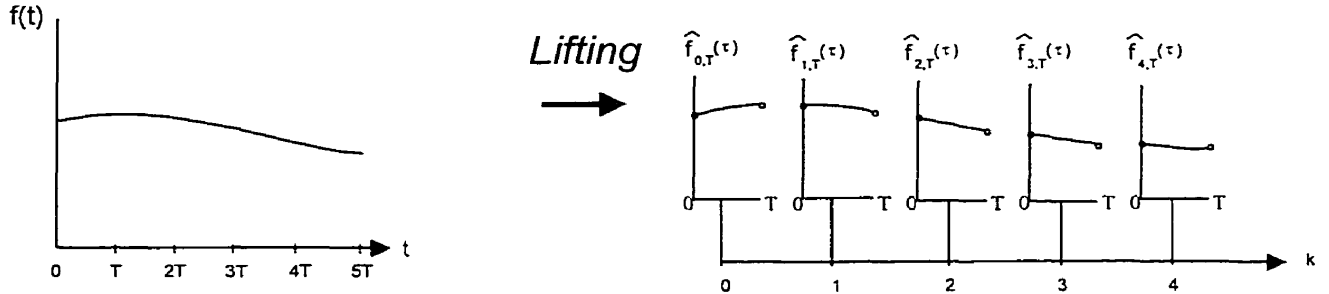


Figure 1.5: Lifting of a continuous-time signal

In this work, when  $f(t)$  is lifted to the sequence  $\{\widehat{f}_{k,T}(\tau)\}_{k=0}^{\infty}$ ,  $\{\widehat{f}_{k,T}(\tau)\}_{k=0}^{\infty}$  is called the lifted equivalent of  $f(t)$ .

Systems dealing with signals in  $l_{\widetilde{PC}[0, T)}^{\infty}$  at their input and output are called lifted systems. The lifted equivalent of  $\overline{H}$ , in Figure 1.4(a), is  $\widehat{H} \triangleq L\overline{H}L^{-1}$  and that of  $HH_T S$ , in Figure 1.4(b),  $\widehat{HH_T S} \triangleq LHH_T SL^{-1}$ . The lifted output of the hold can be expressed as  $\widehat{u}_{k,T}(\tau) = H(\tau)u_{k,T}$ ,  $0 \leq \tau < T$ , and the discrete-time output of  $SL^{-1}$  subjected to  $\widehat{r}_{k,T}(\tau)$  is  $r_{k,T} = \widehat{r}_{k,T}(0)$ ,  $k \geq 0$ . Lifted sampled-data systems such as  $\widehat{HH_T S}$  are time-

invariant in the sense that a unit shift of the input sequence results in a unit shift of the output sequence.

The continuous-time lifting used in this thesis is that developed in [56], where a system's input and output are lifted and the state of the system is perceived at the sampling instants. Other works, such as [54] and [57], provide a lifting method which considers the trajectory of the state over the continuous time. Both types of lifting perform the same transformation on signals in  $L_{PC}^\infty[0, \infty)$  and result in the same input-output expression for lifted systems. However, the former is better suited for a description of continuous-time and sampled-data systems in which the states of the continuous- and discrete-time systems lie in a common space.

In this thesis, the continuous-time lifting is used extensively in the proofs of propositions and theorems concerned with the characterization of the sampled-data control systems in the time domain.

### 1.2.3 Induced Norms of Systems, Norms of Signals and Performance Index

The quantification of the performance of a sampled-data control system can be accomplished in three ways. First, the gain, or induced norm, of the system can be evaluated for a given sampling period. Two, the signals which are of interest can be measured with norms appropriate to the space in which they exist. Third, a performance index can be employed on the relevant continuous-time signals.

In operator notation, let  $F : X \rightarrow Y$  be a linear, bounded transformation from  $X$  to  $Y$ , which are both normed, linear spaces. The smallest number  $\lambda$  for which  $\|Fx\|_Y \leq \lambda \|x\|_X$  holds for all  $x \in X$  is called the induced norm of  $F$ ,  $\|F\|_{X \rightarrow Y}$ ; that is,

$$\|F\|_{X \rightarrow Y} = \inf_{\lambda} \{ \lambda : \|Fx\|_Y \leq \lambda \|x\|_X, \forall x \in X, \lambda \geq 0 \}. \quad (1.8)$$

An equivalent form is the least upper bound on the norm of the output given an input

of unit norm [58]:

$$\|F\|_{X \rightarrow Y} = \sup_{\|x\|_X=1} \{\|Fx\|_Y, \forall x \in X\}. \quad (1.9)$$

In this thesis, when the operator maps signals from  $X$  to itself, the induced norm is denoted simply as  $\|F\|_X$ . The  $L^\infty$ - and  $L^2$ -induced norms of a linear, time-invariant continuous-time system  $\bar{H}$  are given by (1.10) and (1.11) [59], respectively, where  $\omega$  represents the frequency,  $\bar{g}(t)$  is the impulse response of  $\bar{H}$ , and  $j = \sqrt{-1}$ .

$$\|\bar{H}\|_{L^\infty} = \int_{t=0}^{\infty} |\bar{g}(t)| dt \quad (1.10)$$

$$\|\bar{H}\|_{L^2} = \sup_{-\infty < \omega < \infty} |\bar{H}(j\omega)| \quad (1.11)$$

For a linear, time-invariant discrete-time system  $H_T$ , its  $l^\infty$ -induced norm [60], with  $T$  weighting, and  $l^2$ -induced norm [4, 61] are defined as follows:

$$\|H_T\|_{l^\infty} = \sum_{k=0}^{\infty} |g_{k,T}| \cdot T \quad (1.12)$$

$$\|H_T\|_{l^2} = \sup_{-\pi/T \leq \omega \leq \pi/T} \left| H_T\left(\frac{e^{j\omega T} - 1}{T}\right) \right| \quad (1.13)$$

where  $g_{k,T}$  is the response of the system  $H_T$  to the discrete-time impulse input  $\delta_{k,T}$  given by

$$\delta_{k,T} = \begin{cases} \frac{1}{T}, & k = 0 \\ 0, & k \geq 1. \end{cases} \quad (1.14)$$

The  $L^\infty$ - and  $L^2$ -induced norms of sampled-data systems can be found in [62] and [63], respectively.

For a continuous-time signal, such as  $e(t)$ , the  $L^\infty$  and  $L^2$  norms are respectively given by (1.15) and (1.16).

$$\|e(t)\|_{L^\infty} = \sup_{0 \leq t < \infty} |e(t)| \quad (1.15)$$

$$\|e(t)\|_{L^2} = \left( \int_{t=0}^{\infty} |e(t)|^2 dt \right)^{1/2} \quad (1.16)$$

The  $L^2$  norm can represent the square root of the energy of a signal [59]. For a discrete-time signal  $e_{k,T}$ , the  $l^\infty$  and  $l^2$  norms are defined as follows:

$$\|e_{k,T}\|_{l^\infty} = \sup_{k \geq 0} |e_{k,T}| \quad (1.17)$$

$$\|e_{k,T}\|_{l^2} = \sqrt{\sum_{k=0}^{\infty} |e_{k,T}|^2 \cdot T}. \quad (1.18)$$

The  $L^\infty$  and  $L^2$  norms could be applied to the continuous-time signals of a sampled-data control system or to the difference between the control inputs of the sampled-data and continuous-time control systems, also known as control-input error, and similarly for the controlled outputs, also named controlled-output error. The signal norms complement the conventional step response design specifications and facilitate the performance evaluation over a wide range of sampling frequencies; that is, relying on a scalar quantity to determine the performance of a sampled-data system is a simpler task than having to go through the long process of generating response plots over a wide range of sampling rates. Furthermore, the norms serve as criteria in the selection of the sampling period at which to perform the digital redesign process. Generally, a digital redesign method resulting in the smallest error signal norms among the digital redesign methods, for a given  $T$ , would be the preferred choice. Still, the norms should be used in conjunction with other system parameters, such as the location of the closed-loop poles, in order to clarify the shapes of the responses of a sampled-data system for a given sampling interval.

The literature on sampled-data systems encompasses several works using the concepts of induced norms of systems and norms of signals for performance evaluation. As stated in [60], the magnitude of a signal is best controlled by using a time-domain specification, and thus norms of signals are useful in this sense. In [64], the degradations of two sampled-data control systems obtained with the local digital redesign are quantified as a function

of the sampling period. There they emphasize the norm of the sensitivity functions of the given sampled-data control systems, which is shown to grow in magnitude as the sampling period is increased whereas it approaches that of the continuous-time system when the sampling interval is reduced. They come to the important conclusion that with the local digital redesign, the choice of  $T$  should not be solely based on the achievement of closed-loop stability; in fact, it should include consideration of the desired performance, in terms of the value of the sensitivity norm. In [65], a sampled-data design is performed by minimizing an approximation to the  $L^\infty$ -induced norm of the system relating an exogenous input such as the reference, or disturbance, to the tracking error. A similar process is carried out in [62] and in [66], where the  $L^\infty$  norm of the signals of interest are considered. For example, a sampled-data system should reject disturbances while tracking reference inputs, both having finite  $L^\infty$  norm. In [67], the  $L^2$ -induced norm of the system relating the disturbance input to the plant output is considered. A sampled-data controller is designed such that the  $L^2$ -induced norm of the closed-loop system from the continuous-time disturbance to the continuous-time plant output is less than a specified bound. Formulas for the  $L^2$ -induced norms of sampled-data systems are given in [68].

The performance evaluation based on norms and induced norms has been extensively studied for the sampled-data design of control systems. However, it has been absent with the digital redesign approach.

A simplified approach to the analysis of the response of a system is to use a single, positive real quantity which tells a designer about the performance of the system subjected to a known input. The  $L^2$  and  $L^\infty$  norms are such quantities. The so called Integral of Time-multiplied Absolute-value of Error (ITAE) index is another. The ITAE index, or criterion, denoted as  $I_{T_i}$  in this thesis, is given by (1.19) for the continuous-time signal  $e(t)$  :

$$I_{T_i} = \int_{t=0}^{T_i} t |e(t)| dt, \quad 0 < T_i < \infty \quad (1.19)$$

where  $T_i$  is a fixed time instant. In [69] this index is used to measure the error between

a linear, time-invariant continuous-time system's step response and the step input; the control design yielding the smallest value of the ITAE index is proclaimed as the best design. The relevance of this index can be seen as follows. In assessing the step response performance of a second order system given by

$$\bar{G}(s) = \frac{1}{s^2 + 2\zeta s + 1} \quad (1.20)$$

the work in [70] found that the smallest value of the ITAE index occurs for a damping ratio  $\zeta$  of 0.7, which offers a relatively good compromise between speed of response and overshoot. It is not the only performance index available, yet it is known to offer a clear distinction between the optimum value and the others in the context of the evaluation of the step response behavior, as explained in [69].

As far as the author is aware, the ITAE index has never been used in the performance assessment of sampled-data control systems. It could serve, for instance, to evaluate the control-input and controlled-output errors between sampled-data and continuous-time control systems as functions of the sampling period.

### 1.3 Objective of the Thesis

The objective of the thesis is threefold: (1) provide solutions to the unresolved issues associated with the regular PIM method; (2) characterize digitally redesigned sampled-data control systems with emphasis placed on the systems obtained with the PIM methods; and (3) quantitatively compare the performances of sampled-data control systems against that of the continuous-time control system upon which the digital redesign originates.

In order to solve the issues concerned with the complexity of the controllers obtained with the PIM method and their possible great number in the sampled-data loop, three global digital redesign methods are introduced in Chapter 3 based on the same rationale as that of PIM. These methods are the truncated, reduced-order and reduced-order plus truncated PIM methods. In this thesis, the three methods are also known as the modified

PIM methods. Alternatives to the PIM approach which use a different technique than the matched pole-zero method to discretize the PITF and rely on the discretization of the closed-loop system relating the reference input to the controlled output are succinctly presented in Chapter 3; their details can be found in Appendix C. Furthermore, two ways of solving the Diophantine equation associated with the current PIM method are presented in Chapter 3. These are the eliminant matrix method and the state-space factorization. Emphasis is placed on assessing the degree requirements and the conditions yielding a unique solution to the Diophantine equation.

In Chapter 4, the digitally redesigned sampled-data control systems are characterized in terms of the time-domain behavior of the loop signals, the transfer functions of the discrete-time blocks and the robustness characteristics. The continuous-time lifting is used to represent the behavior of the sampled-data systems for any sampling frequency selected in the digital redesign. The lifting method, which was first employed in the characterization of digitally redesigned control systems in [71], allows one to explicitly formulate the errors between the corresponding continuous-time signals of the sampled-data and continuous-time control systems, and to understand the mechanisms of the digital redesigns, in particular what makes the PIM method work well for relatively large sampling periods. Conditions are provided such that the control input and controlled output of a sampled-data control system converge uniformly in time, as the sampling interval is reduced, to those respective signals of the continuous-time control system upon which the digital redesign is based. A sampled-data system satisfying such elementary requirement is called a sampled-data model of a continuous-time system, a notion defined in Chapter 2. The convergence of the transfer functions of the discrete-time controller blocks to their continuous-time counterpart, in a sense explained in Chapter 4, is established. The by-product of this discrete-time investigation is the characterization of the behavior of the loop signals other than the control input and controlled output when  $T$  is relatively small. The convergence in the induced norms of the sampled-data systems, as the sampling period is decreased, is also studied. Concerning the performance evaluation

of a sampled-data control system for any non-pathological sampling period, the quantification is obtained via the  $L^\infty$  and  $L^2$  norms of the control-input and controlled-output errors, the  $L^\infty$ - and  $L^2$ -induced norms of the systems of interest, and the ITAE index on the error signals. The behavior of the performance measures with increasing sampling interval and the influence of the discrete-time closed-loop poles on the responses is explained in Chapter 4.

Chapter 5 provides five applications of digitally redesigned control systems. Comparative and quantitative assessments of the performances attained with some of the most widely used local digital redesign methods, the optimal global digital redesign method reported in [24], and the PIM methods are conducted. The tools used to evaluate the performance of the sampled-data control systems, as explained in Chapters 3 and 4, enable an explicit demonstration of the effectiveness of the regular and modified PIM methods over the local and other modern global digital redesign techniques through four simulation examples and one experiment. In addition, the control applications validate the theorems presented in the previous chapters.

# Chapter 2

## Preliminaries

In order to clarify the concepts and terminology involved in the chapters that follow, the main assumptions, the definitions pertaining to the signals and systems, and the notion of stability as understood in this thesis are given. In particular, restrictions on the choice of the sampling period and hold at control input are established in Section 2.1, the class of exogenous inputs admitted in the analysis and the novel concept of sampled-data model of a continuous-time system are defined in Section 2.2, and the internal stability at the sampling instants and its relation with the individual blocks present in the sampled-data loop are given in Section 2.3.

### 2.1 Main Assumptions

Throughout this thesis, the following are assumed to hold unless explicitly stated otherwise:

1. The systems are linear, SISO and have zero initial conditions.
2. The continuous-time control systems, on which digital redesign is carried out, are performing in a satisfactory fashion when they satisfy the requirements of stability, disturbance rejection and reference input tracking.

3.  $T$  represents the period of sampling and lifting which is chosen to be non-pathological with respect to the plant under control. The sampling period  $T$  is non-pathological with respect to  $\bar{G}(s)$ , which has a realization given by  $[\bar{A}_{\bar{G}}, \bar{B}_{\bar{G}}, \bar{C}_{\bar{G}}, \bar{D}_{\bar{G}}]$ , provided that  $\bar{A}_{\bar{G}}$  has no two eigenvalues with equal real parts and imaginary parts that differ by an integral multiple of  $2\pi/T$  [4]. When the PIM method is carried out,  $T$  is also chosen to be non-pathological with respect to the continuous-time PITF. The non-pathologicity of  $T$  with respect to the plant is needed, for instance, to prevent extra pole-zero cancellations in the discrete-time plant model. On the other hand,  $T$  is chosen as non-pathological to the continuous-time PITF when the PIM method is performed in order to preserve the order of the transfer function.
4. The hold, which is located at the control input of the sampled-data control system, is assumed to have a bounded response function and not to introduce discrete zeros in the hold-equivalent model of the plant which cancel poles of the model at non-pathological  $T$  values. The reader is referred to [72] for more details on the subject.

## 2.2 Time-Domain Concepts

The following definitions present the basic concepts used in the time-domain analysis of sampled-data control systems. Definitions 2.2.1 to 2.2.3 introduce the possible spaces in which the exogenous inputs to the sampled-data and continuous-time control systems may lie.

**Definition 2.2.1**  $S_0$  is defined as the space of functions which have a finite supremum norm and are continuous on the time set  $[0, \infty)$ , and independent of  $T$ . $\bowtie$

**Definition 2.2.2**  $S_1$  is defined as the space of functions which have a finite supremum norm and are uniformly continuous over  $[0, \infty)$ , and independent of  $T$ . $\bowtie$

**Definition 2.2.3**  $S_2$  is the space of functions which have a finite supremum norm and

are constant in each of the intervals  $[kT, (k+1)T)$  on  $[0, \infty)$ , for  $k = 0, 1, 2, \dots$  and  $T \in (0, \infty)$ .  $\bowtie$

Note that  $\mathcal{S}_0$ ,  $\mathcal{S}_1$  and  $\mathcal{S}_2$  are subspaces of  $L_{PC}^\infty[0, \infty)$ . Definition 2.2.4 applies specifically to sampled-data control systems, whereas Definition 2.2.5 could be applied to a piecewise-constant approximation of a reference input sent to the continuous-time and sampled-data control systems.

**Definition 2.2.4** A bounded *reconstructed signal* is defined as the output of a hold and therefore is in  $L_{PC}^\infty[0, \infty)$ .  $\bowtie$

**Definition 2.2.5** A *staircase equivalent* of a signal in  $\mathcal{S}_0$  or  $\mathcal{S}_1$  is obtained by passing the signal which lies in  $\mathcal{S}_0$  or  $\mathcal{S}_1$  through an ideal sampler followed by a zero-order hold (ZOH), both of which have period  $T$ . Staircase equivalents are in  $\mathcal{S}_2$ .  $\bowtie$

The following definition considers the metric between two signals in  $L_{PC}^\infty[0, T)$ .

**Definition 2.2.6** A signal expressed in lifted form as  $\{\widehat{y}_{k,T}(\tau)\}_{k=0}^\infty$  is said to *converge uniformly in time as  $T \rightarrow 0$*  to a continuous-time signal given by  $\{\widehat{y}_{k,T}(\tau)\}_{k=0}^\infty$  in the lifted form if

$$\lim_{T \rightarrow 0} \left[ \sup_{k \in [0, \infty)} \left\{ \sup_{\tau \in [0, T)} \left| \widehat{y}_{k,T}(\tau) - \widehat{y}_{k,T}(\tau) \right| \right\} \right] = 0. \quad \bowtie \quad (2.1)$$

With the knowledge of the metric between two lifted signals, a sampled-data system can be characterized in terms of its input-output behavior with respect to a continuous-time system, as presented in the following definition.

**Definition 2.2.7** A sampled-data system is said to be a *sampled-data model of a continuous-time system* if its output is converging uniformly in time to that of the continuous-time system, as  $T \rightarrow 0$ , when its input is converging uniformly in time to that of the continuous-time system.  $\bowtie$

Obviously, a particular case of the above definition is when the sampled-data and continuous-time systems are subjected to the same input.

## 2.3 Stability of Continuous-Time and Sampled-Data Control Systems

Before giving the meaning of stability as understood in this thesis, the notion of composite state is introduced.

**Definition 2.3.1** The *composite state* of a closed-loop system is obtained by stacking the state of each dynamic block present in the loop into one state.  $\blacktriangleright$

For instance, consider the system of Figure 1.4(b). Let the state of a realization of  $\Omega_T(\varepsilon)$  be  $x_{\Omega_T,k,T}$ , that of  $\Pi_T(\varepsilon)$  be  $x_{\Pi_T,k,T}$ , that of  $\Gamma_T(\varepsilon)$ ,  $x_{\Gamma_T,k,T}$  and the state of the hold-equivalent plant model,  $x_{G_T,k,T}$ . Then a discrete-time composite state of the sampled-data control system is

$$x_{k,T} = [x_{\Omega_T,k,T}^T, x_{\Pi_T,k,T}^T, x_{\Gamma_T,k,T}^T, x_{G_T,k,T}^T]^T \quad (2.2)$$

for each  $k \geq 0$  and  $T$ . With the knowledge of the realization of each block present in the sampled-data control system, the state equation of the discrete-time closed-loop system can be expressed as

$$\delta x_{k,T} = Ax_{k,T} + Br_{k,T} \quad (2.3)$$

where  $\delta x_{k,T} = (x_{k+1,T} - x_{k,T})/T$  [29] and  $r_{k,T}$  is the sampled reference input. When the reference input is set to zero and the initial composite state  $x_{0,T}$  is finite, then the zero-input composite state for any  $k \geq 0$  and  $T$  is given by

$$x_{k,T}|_{\text{zero-input}} = (TA + I)^k x_{0,T} \quad (2.4)$$

where  $I$  is the identity matrix. A similar development can be carried out for the continuous-time control system of Figure 1.4(a).

Definitions 2.3.2 to 2.3.4 present the meaning of stability.

**Definition 2.3.2** A linear, time-invariant continuous-time closed-loop system is said to be *internally stable* if, given any finite initial condition to the composite state, the zero-input composite state approaches zero as  $t \rightarrow \infty$ .  $\square$

**Definition 2.3.3** A linear closed-loop system is said to be *internally stable at the sampling instants* if, given any finite initial condition to the composite state, the zero-input composite state approaches zero, at the discrete-time instants  $kT$ , as  $k \rightarrow \infty$ , for  $T \in (0, \infty)$ .  $\square$

**Definition 2.3.4** A linear system is *input-output stable* if every input in  $L_{PC}^{\infty}(0, \infty)$  results in an output in  $L_{PC}^{\infty}(0, \infty)$ .  $\square$

For a linear, time-invariant continuous-time closed-loop system, internal stability warrants internal stability at the sampling instants. For a sampled-data control system, the following theorem establishes internal stability in terms of the behavior at the sampling instants.

**Theorem 2.3.1** The sampled-data control system of Figure 1.4(b) is internally stable at the sampling instants if and only if all of the eigenvalues of the matrix  $A$  in (2.3) lie in the region of the  $\varepsilon$ -plane given by  $|T\varepsilon + 1| < 1$ .  $\square$

Proof: (i) If: Using equation (2.4), the norm on the zero-input composite state can be bounded as follows

$$\left\| x_{k,T} |_{\text{zero-input}} \right\| \leq \|(TA + I)^k\| \cdot \|x_{0,T}\| \quad (2.5)$$

for each  $k$ , where  $\|\cdot\|$  denotes vector or matrix norm depending on the case. As  $k \rightarrow \infty$ ,

$$\lim_{k \rightarrow \infty} \left\| x_{k,T} |_{\text{zero-input}} \right\| \leq \lim_{k \rightarrow \infty} \|(TA + I)^k\| \cdot \|x_{0,T}\| \quad (2.6)$$

which approaches zero when the eigenvalues of  $A$  lie in  $|T\varepsilon + 1| < 1$ .

(ii) Only if: The proof uses contradiction. Assume the opposite to what has to be shown; i.e., that at least one of the eigenvalues of  $A$  lies outside the stability region.

With the initial state selected to be the eigenvector  $p_j$  associated with an eigenvalue  $\lambda_j$  outside the stability region,

$$\begin{aligned} \lim_{k \rightarrow \infty} \left\| x_{k,T} \Big|_{\text{zero-input}} \right\| &= \lim_{k \rightarrow \infty} \left\| (TA + I)^k p_j \right\| \\ &= \lim_{k \rightarrow \infty} \left\| (T\lambda_j + 1)^k p_j \right\| \\ &= \lim_{k \rightarrow \infty} |(T\lambda_j + 1)^k| \cdot \|p_j\| \end{aligned} \quad (2.7)$$

does not approach zero. This contradicts the initial argument.  $\square$

Note that the rapprochement between the  $z$  and  $\varepsilon$  planes is simply given as  $\varepsilon = (z - 1)/T$  [29].

Necessary and sufficient conditions on the transfer functions of the individual discrete-time controllers can also be developed to guarantee internal stability at the sampling instants.

**Theorem 2.3.2** Consider the sampled-data control system of Figure 1.4(b) where

$$G_T(\varepsilon) = \frac{b(\varepsilon)}{a(\varepsilon)}, \quad \Omega_T(\varepsilon) = \frac{n_1(\varepsilon)}{d_1(\varepsilon)}, \quad \Pi_T(\varepsilon) = \frac{n_2(\varepsilon)}{d_2(\varepsilon)}, \quad \Gamma_T(\varepsilon) = \frac{n_3(\varepsilon)}{d_3(\varepsilon)}. \quad (2.8)$$

The closed-loop system is internally stable at the sampling instants if and only if the characteristic polynomial of the discrete-time closed-loop system,  $d_2(\varepsilon)(d_1(\varepsilon)d_3(\varepsilon)a(\varepsilon) + n_1(\varepsilon)n_3(\varepsilon)b(\varepsilon))$ , has no roots in  $|T\varepsilon + 1| \geq 1$ .  $\infty$

Proof: Obvious, by noticing that the roots of the characteristic polynomial are the same as the eigenvalues of the  $A$  matrix in (2.3).  $\square$

A consequence of internal stability at the sampling instants is given by the next theorem.

**Theorem 2.3.3** Consider a sampled-data control system which is internally stable at the sampling instants, as illustrated in Figure 2.1. When the reference input, disturbance and sensor noise are bounded at the sampling instants, then the following are bounded: the discrete-time control input  $u_{k,T}$ , the sampled controlled output  $y_{k,T}$ , the input to

$\Omega_T(\varepsilon)$ , and the outputs of the blocks  $\Gamma_T(\varepsilon)$  and  $\Pi_T(\varepsilon)$ .  $\bowtie$

Proof: Figure 2.1 shows the sampled-data control system with all the signals considered at the sampling instants. In the figure, the capital letters denote the Delta transforms of the corresponding discrete-time signals which are expressed in lower case letters. The disturbance input could be arising in the discrete-time domain or be the sampled version of  $d_T = HS\bar{d}$ , where  $\bar{d}$  is a bounded continuous-time signal and  $H$  is the same hold as that in the hold-equivalent model of the plant. The transfer functions relating the exogenous inputs  $R_T(\varepsilon)$ ,  $D_T(\varepsilon)$  and  $W_T(\varepsilon)$  to the outputs  $E_T(\varepsilon)$ ,  $U_T(\varepsilon)$ ,  $Z_T(\varepsilon)$ ,  $V_T(\varepsilon)$  and  $Y_T(\varepsilon)$  are given in matrix form as

$$\begin{bmatrix} E_T(\varepsilon) \\ U_T(\varepsilon) \\ Z_T(\varepsilon) \\ V_T(\varepsilon) \\ Y_T(\varepsilon) \end{bmatrix} = \frac{1}{p(\varepsilon)} \begin{bmatrix} \Pi_T(\varepsilon)d_1(\varepsilon)d_3(\varepsilon)a(\varepsilon) & -d_1(\varepsilon)n_3(\varepsilon)b(\varepsilon) & -d_1(\varepsilon)n_3(\varepsilon)a(\varepsilon) \\ \Pi_T(\varepsilon)n_1(\varepsilon)d_3(\varepsilon)a(\varepsilon) & d_1(\varepsilon)d_3(\varepsilon)a(\varepsilon) & -n_1(\varepsilon)n_3(\varepsilon)a(\varepsilon) \\ \Pi_T(\varepsilon)n_1(\varepsilon)d_3(\varepsilon)b(\varepsilon) & d_1(\varepsilon)d_3(\varepsilon)b(\varepsilon) & d_1(\varepsilon)d_3(\varepsilon)a(\varepsilon) \\ \Pi_T(\varepsilon)n_1(\varepsilon)n_3(\varepsilon)b(\varepsilon) & d_1(\varepsilon)n_3(\varepsilon)b(\varepsilon) & d_1(\varepsilon)n_3(\varepsilon)a(\varepsilon) \\ \Pi_T(\varepsilon)n_1(\varepsilon)d_3(\varepsilon)b(\varepsilon) & d_1(\varepsilon)d_3(\varepsilon)b(\varepsilon) & -n_1(\varepsilon)n_3(\varepsilon)b(\varepsilon) \end{bmatrix} \begin{bmatrix} R_T(\varepsilon) \\ D_T(\varepsilon) \\ W_T(\varepsilon) \end{bmatrix} \quad (2.9)$$

where

$$p(\varepsilon) = d_1(\varepsilon)d_3(\varepsilon)a(\varepsilon) + n_1(\varepsilon)n_3(\varepsilon)b(\varepsilon). \quad (2.10)$$

From the internal stability at the sampling instants of the closed-loop system, each transfer function of (2.9) has all of its poles in  $|T\varepsilon + 1| < 1$ . Thus, exogenous inputs bounded at the sampling instants result in bounded discrete-time loop signals [4].  $\square$

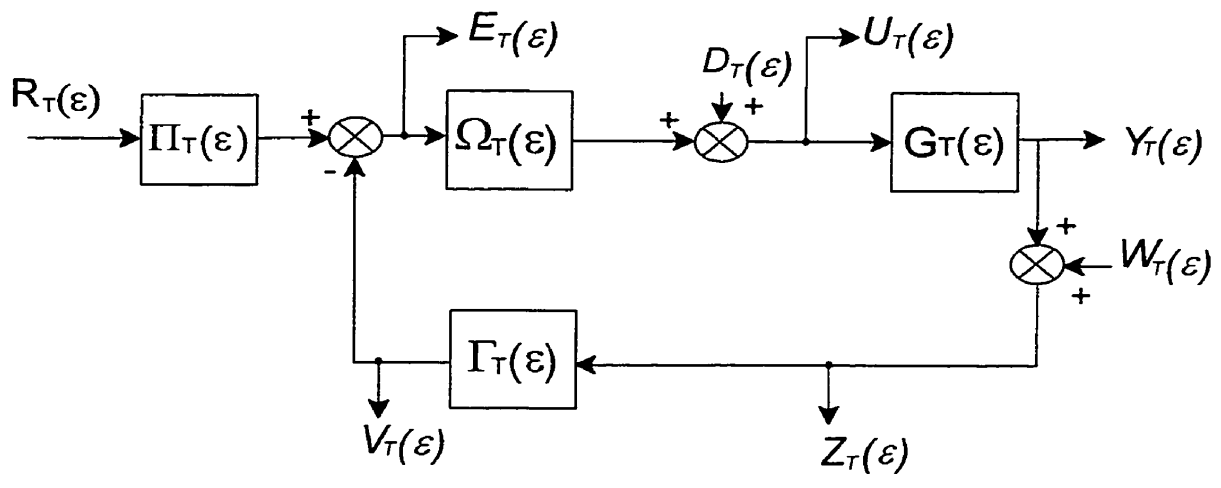


Figure 2.1: Discrete-time control system

The internal stability at the sampling instants as examined by Theorems 2.3.1 to 2.3.3 is connected to the input-output stability in Chapter 4.

## Chapter 3

# Global Digital Redesign Methods

The primary aim of this chapter is to propose global digital redesign methods which solve the issues of reducing the order and the number of controllers present in a PIM-based control system. The secondary goal is to show the existence of alternative digital redesign methods which are based on the matched pole-zero discretization of the closed-loop system relating the reference input to the controlled output, and the discretization of the PITF performed with a method other than the matched pole-zero technique. The chapter is organized as follows. Section 3.1 presents the regular PIM method and two means of solving the discrete-time polynomial Diophantine equation: the eliminant matrix method and the state-space factorization. Three modified PIM methods are provided in Section 3.2. These are the truncated, the reduced-order, and the reduced-order plus truncated PIM methods. The steps in obtaining the controllers with each method are detailed, and in Subsection 3.2.2, the behavior as  $T \rightarrow 0$  and the stability of the discrete-time control system obtained with the reduced-order PIM method are studied. Finally, two alternative digital redesign methods based on the classical discretization of a closed-loop system are given in Section 3.3.

## 3.1 Regular Plant Input Mapping Method

A description of the steps involved in performing the regular PIM method and two means of solving the Diophantine equation are provided in the next subsections.

### 3.1.1 Design Steps

The regular PIM-based discrete-time control system is obtained in four steps, as illustrated in Figure 1.1.

*Step 1:* Knowing the control blocks composing the internally stable continuous-time control system of Figure 1.4(a) and the plant given by

$$\bar{G}(s) = \frac{\bar{b}(s)}{\bar{a}(s)} = \frac{\bar{b}_m s^m + \bar{b}_{m-1} s^{m-1} + \cdots + \bar{b}_1 s + \bar{b}_0}{\bar{a}_n s^n + \bar{a}_{n-1} s^{n-1} + \cdots + \bar{a}_1 s + \bar{a}_0} \quad (3.1)$$

where  $m \leq n$ , the continuous-time PITF  $\bar{H}(s)$  can be calculated as

$$\bar{H}(s) = \frac{\bar{\Omega}(s)\bar{\Pi}(s)}{1 + \bar{\Omega}(s)\bar{\Gamma}(s)\bar{G}(s)}. \quad (3.2)$$

Furthermore, let

$$\bar{\Omega}(s) = \frac{\bar{n}_1(s)}{\bar{d}_1(s)}, \quad \bar{\Pi}(s) = \frac{\bar{n}_2(s)}{\bar{d}_2(s)}, \quad \bar{\Gamma}(s) = \frac{\bar{n}_3(s)}{\bar{d}_3(s)} \quad (3.3)$$

and rewrite the PITF as

$$\bar{H}(s) = \frac{\bar{n}_2(s)\bar{n}_1(s)\bar{d}_3(s)\bar{a}(s)}{\bar{d}_1(s)\bar{d}_2(s)\bar{d}_3(s)\bar{a}(s) + \bar{d}_2(s)\bar{n}_1(s)\bar{n}_3(s)\bar{b}(s)} \quad (3.4)$$

where the numerator degree is  $q$  and that of the denominator is  $p$ .

*Step 2:* Discretize  $\bar{H}(s)$  to  $H_T(\varepsilon)$  using the matched pole-zero method such that the

following conditions are met [27]:

$$\begin{aligned} \lim_{T \rightarrow 0} H_T(\varepsilon)|_{\varepsilon = \frac{e^{sT} - 1}{T}} &= \bar{H}(s), \text{ pointwise in } s, \\ H_T(\varepsilon)|_{\varepsilon = \varepsilon_0} &= \bar{H}(s)|_{s = s_0}, \end{aligned} \quad (3.5)$$

where  $s_0$  is a real constant such that  $0 \leq s_0 \ll 1$ ,  $\varepsilon_0 = (e^{s_0 T} - 1)/T$ ,  $T > 0$ , and  $H_T(\varepsilon) \triangleq H_T(z)|_{z = T\varepsilon + 1}$ . For a state-space formulation of the matched pole-zero discretization, the reader is referred to Appendix B.

*Step 3:* Discretize  $\bar{G}(s)$  to the hold-equivalent discrete-time model  $G_T \triangleq S\bar{G}H$  with transfer function

$$G_T(\varepsilon) = \frac{b(\varepsilon)}{a(\varepsilon)} = \frac{b_m \varepsilon^m + b_{m-1} \varepsilon^{m-1} + \dots + b_1 \varepsilon + b_0}{a_n \varepsilon^n + a_{n-1} \varepsilon^{n-1} + \dots + a_1 \varepsilon + a_0} \quad (3.6)$$

where  $m \leq m \leq n$ . This model depends on the hold selected at the control input of the sampled-data control system, as shown in Figure 1.4(b).

*Step 4:* Implement  $H_T(\varepsilon)$  as an internally stable, single-loop feedback control system with a structure as shown in Figure 1.4(b). In order to do so, first rewrite the discrete-time PITF as

$$H_T(\varepsilon) = \frac{m(\varepsilon)a(\varepsilon)}{d(\varepsilon)} \quad (3.7)$$

where  $m(\varepsilon)$  is of degree  $(q - n)$  and is that polynomial in the numerator of  $H_T(\varepsilon)$  whose roots are different from the poles of the hold-equivalent model of the plant, and

$$d(\varepsilon) = d_p \varepsilon^p + d_{p-1} \varepsilon^{p-1} + \dots + d_1 \varepsilon + d_0. \quad (3.8)$$

Then solve the Diophantine equation given by

$$u(\varepsilon)a(\varepsilon) + v(\varepsilon)b(\varepsilon) = d(\varepsilon) \quad (3.9)$$

for  $u(\varepsilon)$  and  $v(\varepsilon)$ , where

$$u(\varepsilon) = u_l \varepsilon^l + u_{l-1} \varepsilon^{l-1} + \dots + u_1 \varepsilon + u_0 \quad (3.10)$$

$$v(\varepsilon) = v_r \varepsilon^r + v_{r-1} \varepsilon^{r-1} + \dots + v_1 \varepsilon + v_0. \quad (3.11)$$

The conditions on the degrees of the polynomials in equation (3.9) which assure uniqueness of the solution are detailed in Section 3.1.2. Once  $u(\varepsilon)$  and  $v(\varepsilon)$  have been found, the transfer functions of the discrete-time controllers can always be obtained by letting  $w(\varepsilon)$  be an arbitrary stable polynomial of degree  $l$ , where  $r \leq l$  and  $(q - n) \leq l$ , and then calculating the controller transfer functions as

$$\Pi_T(\varepsilon) = \frac{m(\varepsilon)}{w(\varepsilon)}, \quad \Omega_T(\varepsilon) = \frac{w(\varepsilon)}{u(\varepsilon)}, \quad \Gamma_T(\varepsilon) = \frac{v(\varepsilon)}{w(\varepsilon)}. \quad (3.12)$$

A two-block implementation is possible whenever any of the following has its conditions satisfied:

1. If  $u(\varepsilon)$  is stable,  $r \leq l$  and  $(q - n) \leq l$ , set

$$\Pi_T(\varepsilon) = \frac{m(\varepsilon)}{u(\varepsilon)}, \quad \Omega_T(\varepsilon) = 1, \quad \Gamma_T(\varepsilon) = \frac{v(\varepsilon)}{u(\varepsilon)}. \quad (3.13)$$

2. If  $m(\varepsilon)$  is stable and  $r \leq (q - n) \leq l$ , set

$$\Pi_T(\varepsilon) = 1, \quad \Omega_T(\varepsilon) = \frac{m(\varepsilon)}{u(\varepsilon)}, \quad \Gamma_T(\varepsilon) = \frac{v(\varepsilon)}{m(\varepsilon)}. \quad (3.14)$$

3. If  $v(\varepsilon)$  is stable and  $(q - n) \leq r \leq l$ , set

$$\Pi_T(\varepsilon) = \frac{m(\varepsilon)}{v(\varepsilon)}, \quad \Omega_T(\varepsilon) = \frac{v(\varepsilon)}{u(\varepsilon)}, \quad \Gamma_T(\varepsilon) = 1. \quad (3.15)$$

**Remarks 3.1.1** (i) A polynomial in  $\varepsilon$  is stable when all its roots lie in  $|T\varepsilon + 1| < 1$ .  
(ii) The conditions on the stability of the polynomials  $w(\varepsilon)$  in (3.12),  $u(\varepsilon)$  in (3.13),

$m(\varepsilon)$  in (3.14) and  $v(\varepsilon)$  in (3.15) arise because of the requirement for internal stability of the closed-loop implementations, as formulated in Theorem 2.3.2. (iii) To apply the regular PIM method to a general MIMO system, the reader is referred to [27]. Still, for the particular case of a decoupled square system, where the off-diagonal elements of the transfer matrices are zero, the procedure detailed above and the modified PIM methods discussed in the following sections are applicable with each transfer function entry in the diagonal of the MIMO system considered independently.

### 3.1.2 Solutions to Diophantine Equation

Two means of solving the discrete-time Diophantine equation (3.9) are presented.

#### Eliminant Matrix Method

From the coefficients of like powers on both sides of (3.9), the following equation is obtained:

$$\underbrace{\begin{bmatrix}
 \overbrace{a_n \quad \dots \quad a_1}^{l+1} & \overbrace{b_m \quad b_{m-1} \quad \dots \quad b_0}^{r+1} \\
 a_{n-1} & \ddots & a_n & b_{m-1} & \ddots & b_m \\
 \vdots & \ddots & a_n & b_{m-1} & \ddots & b_m \\
 a_1 & & a_{n-1} & \vdots & \ddots & b_m \\
 a_0 & \ddots & \vdots & b_0 & & b_{m-1} \\
 & \ddots & a_1 & & \ddots & \vdots \\
 & & a_0 & & & b_0
 \end{bmatrix}}_{=A} \underbrace{\begin{bmatrix} u_l \\ \vdots \\ u_0 \\ v_r \\ \vdots \\ v_0 \end{bmatrix}}_{=X} = \underbrace{\begin{bmatrix} d_p \\ d_{p-1} \\ \vdots \\ d_1 \\ d_0 \end{bmatrix}}_{=Y} \quad (3.16)$$

For example, suppose the discrete-time PITF and plant model have been calculated as

$$H_T(\varepsilon) = \frac{2\varepsilon(\varepsilon + 0.9)(\varepsilon + 2)}{(\varepsilon + 3)(\varepsilon^2 + 5\varepsilon + 16)} \quad (3.17)$$

and

$$G_T(\varepsilon) = \frac{0.5\varepsilon + 9}{\varepsilon(\varepsilon + 0.9)} \quad (3.18)$$

for a given sampling period. With the degrees of  $u(\varepsilon)$  and  $v(\varepsilon)$  set to  $l = 1$  and  $r = 1$ , respectively, the discrete-time Diophantine equation is

$$\underbrace{(u_1\varepsilon + u_0)}_{=u(\varepsilon)} \underbrace{(\varepsilon^2 + 0.9\varepsilon)}_{=a(\varepsilon)} + \underbrace{(v_1\varepsilon + v_0)}_{=v(\varepsilon)} \underbrace{(0.5\varepsilon + 9)}_{=b(\varepsilon)} = \underbrace{\varepsilon^3 + 8\varepsilon^2 + 31\varepsilon + 48}_{=d(\varepsilon)} \quad (3.19)$$

and the linear system of equations is obtained as

$$\begin{bmatrix} 1 & 0 & 0 & 0 \\ 0.9 & 1 & 0.5 & 0 \\ 0 & 0.9 & 9 & 0.5 \\ 0 & 0 & 0 & 9 \end{bmatrix} \begin{bmatrix} u_1 \\ u_0 \\ v_1 \\ v_0 \end{bmatrix} = \begin{bmatrix} 1 \\ 8 \\ 31 \\ 48 \end{bmatrix}. \quad (3.20)$$

Lemma 3.1.1 and Theorem 3.1.1 give the conditions which guarantee the existence and uniqueness of the solution, provided  $p \geq 2n - 1$ . This is required to assure proper controllers as obtained with equations (3.12) to (3.15). If this degree requirement is not satisfied with the polynomials of the original system, add to  $\bar{H}(s)$  a stable, biproper, unity DC gain transfer function,  $\bar{\Sigma}(s)$ , of order greater than or equal to  $(2n - 1 - p)$  with identical sets of poles and zeros. The second step in obtaining the PIM-based control system then consists of discretizing  $\bar{H}(s)\bar{\Sigma}(s)$  to  $H_T(\varepsilon)$ .

**Lemma 3.1.1** Given an irreducible plant  $\bar{G}(s) = \bar{b}(s)/\bar{a}(s)$ , its hold-equivalent model  $G_T(\varepsilon) = b(\varepsilon)/a(\varepsilon)$  is composed of coprime polynomials  $b(\varepsilon)$  and  $a(\varepsilon)$ , provided  $T$  is non-pathological.  $\infty$

*Proof:* A transfer function with coprime polynomials can be minimally realized. With the main assumption on the hold at control input, where the hold is such that it does not introduce discrete-time zeros which cancel poles of the discrete-time plant model, controllability and observability of a continuous-time system are preserved in the trans-

formation to the hold-equivalent model of the plant with a non-pathological  $T$ . The case of a ZOH, which results in the step invariant model of the plant, is proven explicitly in [4].□

**Theorem 3.1.1** [29] Consider equation (3.16), where  $\mathbf{A} \in R^{(p+1) \times (l+r+2)}$  and the degrees of  $u(\varepsilon)$  and  $v(\varepsilon)$  are set to  $l = p - n$  and  $r = n - 1$ , respectively. There exists a unique solution  $X$  to (3.16) if and only if  $b(\varepsilon)$  and  $a(\varepsilon)$  are coprime.◻

**Remarks 3.1.2** (i) When  $p = 2n - 1$  and  $m = n$ ,  $\mathbf{A}$  is the Sylvester Matrix [73] associated with  $G_T(\varepsilon)$ . (ii) The solution to  $\mathbf{A}X = Y$  is obtained via Gaussian elimination in this thesis [74].

### State-Space Factorization

In order to use the state-space factorization method,  $\bar{H}(s)$  should be of order  $2n$ . If this condition is not satisfied, add to  $\bar{H}(s)$  a stable, biproper, unity DC gain transfer function,  $\bar{\Sigma}(s)$ , of order equal to  $(2n - p)$  with identical sets of poles and zeros. Then, the second step of the PIM method can be performed on  $\bar{\Sigma}(s)\bar{H}(s)$ , resulting in  $H_T(\varepsilon)$ , and equation (3.9) can be solved as follows. Write the denominator polynomial of  $H_T(\varepsilon)$  as  $d(\varepsilon) = \lambda(\varepsilon)\lambda'(\varepsilon)$ , where  $\lambda(\varepsilon)$  and  $\lambda'(\varepsilon)$  are stable polynomials each of degree  $n$ . Express  $G_T(\varepsilon)$  as a coprime factorization  $G_T(\varepsilon) = B(\varepsilon)A^{-1}(\varepsilon)$ , where  $A(\varepsilon) = a(\varepsilon)/\lambda(\varepsilon)$  and  $B(\varepsilon) = b(\varepsilon)/\lambda(\varepsilon)$  are irreducible transfer functions. From the coprimeness of  $a(\varepsilon)$  and  $b(\varepsilon)$ , there exist transfer functions  $U(\varepsilon)$  and  $V(\varepsilon)$ , where  $U(\varepsilon) = u(\varepsilon)/\lambda'(\varepsilon)$  and  $V(\varepsilon) = v(\varepsilon)/\lambda'(\varepsilon)$ , which satisfy  $A(\varepsilon)U(\varepsilon) + B(\varepsilon)V(\varepsilon) = 1$  [59]. To solve for  $U(\varepsilon)$  and  $V(\varepsilon)$ , obtain a realization of  $G_T(\varepsilon)$ ,  $C_{G_T}(\varepsilon I - A_{G_T})^{-1}B_{G_T} + D_{G_T}$ , and select  $f_T \in R^{1 \times n}$  such that the eigenvalues of  $A_{G_T} + B_{G_T}f_T$  equal the roots of  $\lambda(\varepsilon)$ . Select also  $h_T \in R^{n \times 1}$  such that  $A_{G_T} + h_TC_{G_T}$  has eigenvalues corresponding to the roots of  $\lambda'(\varepsilon)$ . Then set

$$U(\varepsilon) = [A_{G_T} + h_TC_{G_T}, -B_{G_T} - h_TD_{G_T}, f_T, 1] \quad (3.21)$$

$$V(\varepsilon) = [A_{G_T} + h_TC_{G_T}, h_T, f_T, 0] \quad (3.22)$$

from which the polynomials  $u(\varepsilon)$  and  $v(\varepsilon)$ , of degrees  $l = n$  and  $r = n - 1$ , respectively, can be found.

## 3.2 Modified Plant Input Mapping Methods

For simple, low-order control systems, such as those found in [26] and [31], uniquely solving the Diophantine equation is a simple task, free from numerical problems and polynomial degree constraints. However, in several applications, such as flight control, engine control and position control of a disk drive system, the design is generally performed on high-order plant models. For such cases, solving the discrete-time Diophantine equation with the means of Section 3.1.2 may result in discrete-time controllers whose orders are higher than those of the continuous-time control blocks. Furthermore, using any of (3.12) to (3.15) in the fourth step of the PIM method can yield a sampled-data control system with a greater number of control blocks than its continuous-time counterpart. In order to provide ways to overcome the problems of increased controller order and controller number, three new digital redesign methods are proposed in this section: truncated PIM, reduced-order PIM and reduced-order plus truncated PIM methods.

### 3.2.1 Truncated Plant Input Mapping Method

This method bears its name from the fact that, whenever the regular PIM method is used to discretize a continuous-time control system and the block  $\Pi_T(\varepsilon)$  appears in the implementation, whereas its continuous-time counterpart  $\bar{\Pi}(s)$  is not a dynamic block, the controller  $\Pi_T(\varepsilon)$  is truncated to a gain block to preserve a closed-loop DC or low frequency gain specification. The proposed truncated PIM method is carried out as follows: perform steps 1 to 4 of the regular PIM method, except that in the fourth step, with  $u(\varepsilon)$  and  $v(\varepsilon)$  known, the transfer functions of the discrete-time controllers are calculated with any applicable equations which follow:

1. Let  $w(\varepsilon)$  be an arbitrary stable polynomial of degree  $l$ , where  $r \leq l$  and  $(q - n) \leq l$ , and set

$$\Pi_T(\varepsilon) = \frac{m(\varepsilon)}{w(\varepsilon)} \Big|_{\varepsilon=\varepsilon_0}, \quad \Omega_T(\varepsilon) = \frac{w(\varepsilon)}{u(\varepsilon)}, \quad \Gamma_T(\varepsilon) = \frac{v(\varepsilon)}{w(\varepsilon)}. \quad (3.23)$$

2. If  $u(\varepsilon)$  is stable,  $r \leq l$  and  $(q - n) \leq l$ , set

$$\Pi_T(\varepsilon) = \frac{m(\varepsilon)}{u(\varepsilon)} \Big|_{\varepsilon=\varepsilon_0}, \quad \Omega_T(\varepsilon) = 1, \quad \Gamma_T(\varepsilon) = \frac{v(\varepsilon)}{u(\varepsilon)}. \quad (3.24)$$

3. If  $v(\varepsilon)$  is stable and  $(q - n) \leq r \leq l$ , set

$$\Pi_T(\varepsilon) = \frac{m(\varepsilon)}{v(\varepsilon)} \Big|_{\varepsilon=\varepsilon_0}, \quad \Omega_T(\varepsilon) = \frac{v(\varepsilon)}{u(\varepsilon)}, \quad \Gamma_T(\varepsilon) = 1. \quad (3.25)$$

In the above equations,  $0 \leq \varepsilon_0 \ll 1$ .

If one calculates the discrete-time PITF associated with the implementation resulting from any of (3.23) to (3.25), the discrete-time closed-loop poles are the same as those of  $H_T(\varepsilon)$ , which means that closed-loop internal stability at the sampling instants is guaranteed. However, the zeros of any of these implementations differ from those of  $H_T(\varepsilon)$ . For the controllers obtained with (3.23), if  $m(\varepsilon)$  has stable roots, the polynomial  $w(\varepsilon)$  can be selected such that its roots are stable and are as close as desired to those of  $m(\varepsilon)$ . Of course, if one can set  $w(\varepsilon) = m(\varepsilon)$ ,  $\Pi_T(\varepsilon)$  is unity.

### 3.2.2 Reduced-Order Plant Input Mapping Method

In the fourth step of the regular PIM technique, solving the discrete-time Diophantine equation with the eliminant matrix method and the state-space factorization results in discrete-time controllers with orders greater than or equal to  $(n - 1)$  and  $n$ , respectively, even if the original controllers have lower orders. To keep the orders of the discrete-time controllers as low as in the continuous-time case, the following procedure is proposed.



when  $(f + h + 1) < p$ . Then, by equating coefficients of like powers of  $\varepsilon$  on both sides of (3.9), there results the overdetermined system of equations (3.16). The dimensions of  $\mathbf{A}$ ,  $X$  and  $Y$ , in (3.16), are the same as those of  $\overline{\mathbf{A}}$ ,  $\overline{X}$  and  $\overline{Y}$ , in (3.30), respectively, since  $l = f$ ,  $r = h$ , the discrete-time plant model has the same order as that of the continuous-time plant, that is  $n$ , and the denominator of the discrete-time PITF has the same degree,  $p$ , as that of the continuous-time PITF. It is important to note that the difference between the discrete-time system of equations  $\mathbf{A}X=Y$  and the continuous-time system of equations  $\overline{\mathbf{A}}\overline{X}=\overline{Y}$  is that, in the former,  $Y$  and  $\mathbf{A}$  are known and the system of equations is solved for  $X$ , whereas, in the latter,  $\overline{\mathbf{A}}$  and  $\overline{X}$  are known and  $\overline{Y}$  comes from the calculation of the continuous-time PITF.

The system of equations (3.16) can be solved in a least-squares sense [75] as

$$\widehat{X} = (\mathbf{A}^T \mathbf{A})^{-1} \mathbf{A}^T Y \quad (3.31)$$

where  $\widehat{X}$  is the least-squares estimator of  $X$ , provided  $\mathbf{A}$  has full column rank. The following theorem shows that the irreducibility of the transfer function of the discrete-time plant model warrants the least-squares solution to (3.16).

**Theorem 3.2.1** Consider equation (3.16), where the degrees of  $u(\varepsilon)$  and  $v(\varepsilon)$  are  $l = p - n$  and  $r < n - 1$ , respectively, and  $r \leq l$ . There exists a unique solution to (3.16), obtained in a least-squares sense, when  $b(\varepsilon)$  and  $a(\varepsilon)$  are coprime.  $\blacktriangleright$

Proof: For the case  $p \geq n + m - 1$ , the coprimeness of  $b(\varepsilon)$  and  $a(\varepsilon)$  assures the full rank of a square matrix  $\mathbf{A} \in R^{(p+1) \times (p+1)}$  when  $l = p - n$  and  $r = n - 1$  from Theorem 3.1.1 since the theorem holds for the degree requirement  $p \geq n + m - 1$  [29]. Thus, with the degrees of  $u(\varepsilon)$  and  $v(\varepsilon)$  set to  $l = p - n$  and  $r < n - 1$ , respectively, the non-square matrix  $\mathbf{A} \in R^{(p+1) \times (l+r+2)}$  in (3.16) possesses  $l + r + 2$  linearly independent columns since it can be formed from the aforementioned square matrix by removing  $n - r - 1$  columns. With the null space of  $\mathbf{A} \in R^{(p+1) \times (l+r+2)}$ , where  $l = p - n$  and  $r < n - 1$ , composed of only the zero vector, the solution to (3.16) can be obtained in a least-squares sense with

equation (3.31).

For the case  $p < n + m - 1$ , consider the system of equations (3.32), which is obtained from the Diophantine equation (3.9) in the manner explained in Section 3.1, where  $m = n$ ,  $p = n + m - 1$ ,  $l = p - n$  and  $r = n - 1$ . The degree  $m$  could be smaller than  $n$ , however for simplicity only the case  $m = n$  is explicitly demonstrated.

$$\underbrace{\begin{bmatrix} \overbrace{a_n} & & \overbrace{b_n} \\ a_{n-1} & \ddots & b_{n-1} & \ddots \\ \vdots & \ddots & a_n & \vdots & \ddots & b_n \\ a_1 & & a_{n-1} & b_1 & & b_{n-1} \\ a_0 & \ddots & \vdots & b_0 & \ddots & \vdots \\ & \ddots & a_1 & & \ddots & b_1 \\ & & a_0 & & & b_0 \end{bmatrix}}_{=A} \underbrace{\begin{bmatrix} u_{n-1} \\ \vdots \\ u_0 \\ v_{n-1} \\ \vdots \\ v_0 \end{bmatrix}}_{=X} = \underbrace{\begin{bmatrix} d_{2n-1} \\ d_{2n-2} \\ \vdots \\ d_1 \\ d_0 \end{bmatrix}}_{=Y} \quad (3.32)$$

The degree  $r$  should be smaller than  $n - 1$ , according to the statement of the theorem, although this would only require eliminating a certain number of columns from the  $A$  matrix in (3.32), which does not alter the fact that the remaining columns are linearly independent if the  $A$  matrix in (3.32) has full column rank. The basic idea of the proof is to show that one can remove certain entries in the matrix and vectors of equation (3.32) in order to obtain a system of equations corresponding to the case  $p < n + m - 1$  whose matrix has full column rank. To transform the system of equations (3.32) to a system of equations corresponding to a Diophantine equation with degree  $p = n + m - 1 - j$ , where  $j \geq 1$  and  $m = n$ , requires filling with zeros the first  $j$  entries of the vector  $Y$  in (3.32)

resulting in  $Y'$  as shown in (3.33).

$$\underbrace{\begin{bmatrix}
 \overbrace{0 \ \cdots \ \cdots}^{n-j} & \overbrace{\cdots \ \cdots}^{n-j} & 0 \\
 \vdots & & \vdots \\
 0 & \cdots & \cdots & \cdots & 0 \\
 a_n & & & b_n & \\
 a_{n-1} & \ddots & & b_{n-1} & \ddots \\
 \vdots & \ddots & a_n & \vdots & \ddots & b_n \\
 a_0 & & a_{n-1} & b_0 & & b_{n-1} \\
 & \ddots & \vdots & \ddots & \vdots & \\
 & & a_0 & & & b_0
 \end{bmatrix}}_{=A'} \underbrace{\begin{bmatrix} u_{n-j-1} \\ \vdots \\ u_0 \\ v_{n-j-1} \\ \vdots \\ v_0 \end{bmatrix}}_{=X'} = \underbrace{\begin{bmatrix} 0 \\ \vdots \\ 0 \\ d_{2n-j-1} \\ \vdots \\ d_0 \end{bmatrix}}_{=Y'} \quad (3.33)$$

Consequently, in equation (3.33), the polynomial  $u(\varepsilon)$  has degree  $l = n - 1 - j$ , from the fact  $l = p - n$ , and since it is assumed that  $r \leq l$  the polynomial  $v(\varepsilon)$  has degree  $r = n - 1 - j$ . The matrix  $A'$  is the same as matrix  $A$  except for the columns of  $A$  multiplying the first  $j$  entries of  $u(\varepsilon)$  and of  $v(\varepsilon)$  which have been taken out. With the  $A$  matrix having full column rank, the columns composing  $A'$  are linearly independent; that is,  $A'$  has full column rank. It is clear that the first  $j$  rows of  $A' \in R^{(2n) \times (2n-2j)}$  in (3.33) are filled with zeros. These rows can be removed without affecting the column rank of  $A'$  which is equal to  $(2n - 2j)$ . Hence, a matrix  $A$  in (3.32) with column rank  $2n$  guarantees the full column rank  $(2n - 2j)$  of the matrix  $A'$  in (3.33), and the solution to (3.16) can be obtained in a least-squares sense when  $p < n + m - 1$ .  $\square$

**Remark 3.2.1** Numerically, (3.31) is solved with an algorithm using singular value decomposition of  $A$  [74].

The discrete-time controller transfer functions can be obtained with any applicable equations among (3.12)-(3.15) using the entries of  $\hat{X}$ . However, to guarantee that the orders of at least  $\Omega_T(\varepsilon)$  and  $\Gamma_T(\varepsilon)$  are as low as in the continuous-time case, additional

conditions must be imposed on the controller calculations for certain types of continuous-time control systems. First, for a continuous-time control system composed of the blocks  $\bar{\Omega}(s)$  and  $\bar{\Pi}(s)$  ( $\bar{\Gamma}(s) = 1$ ) or of the blocks  $\bar{\Gamma}(s)$  and  $\bar{\Pi}(s)$  ( $\bar{\Omega}(s) = 1$ ), steps 1 to 3 of the PIM process can be carried out by disregarding the block  $\bar{\Pi}(s)$ , although the block must be discretized with the matched pole-zero method to yield  $\Pi_T(\varepsilon)$  and be implemented as in Figure 1.4(b). Then, knowing the entries of  $\hat{X}$ , the discrete-time controller transfer functions can be obtained with any applicable equations among (3.12) to (3.15). Second, when either three control blocks are present in the continuous-time control system or only  $\bar{\Omega}(s)$  and  $\bar{\Gamma}(s)$  are part of the closed-loop system, after having obtained  $\hat{X}$ , write the solution polynomials  $u(\varepsilon)$  and  $v(\varepsilon)$  as

$$u(\varepsilon) = u_1(\varepsilon)u_3(\varepsilon) \quad (3.34)$$

and

$$v(\varepsilon) = v_1(\varepsilon)v_3(\varepsilon) \quad (3.35)$$

such that the degree of  $u_1(\varepsilon)$  equals that of  $\bar{d}_1(s)$ , the degree of  $u_3(\varepsilon)$  equals that of  $\bar{d}_3(s)$ , and similarly for the degrees of  $v_1(\varepsilon)$  and  $v_3(\varepsilon)$  with respect to those of  $\bar{n}_1(s)$  and  $\bar{n}_3(s)$ , respectively. It should be noted that this procedure must not be done if it results in a polynomial in  $\varepsilon$  with complex coefficients in order to avoid controller transfer functions with complex coefficients. If  $v_1(\varepsilon)$  and  $u_3(\varepsilon)$  are stable, the degree of  $v_1(\varepsilon)$  is less than or equal to that of  $u_1(\varepsilon)$ , the degree of  $v_3(\varepsilon)$  is less than or equal to that of  $u_3(\varepsilon)$ , and the degree of  $m(\varepsilon)$  is less than or equal to that of  $v_1(\varepsilon)u_3(\varepsilon)$ , then the controllers can be obtained as

$$\Pi_T(\varepsilon) = \frac{m(\varepsilon)}{v_1(\varepsilon)u_3(\varepsilon)}, \quad \Omega_T(\varepsilon) = \frac{v_1(\varepsilon)}{u_1(\varepsilon)}, \quad \Gamma_T(\varepsilon) = \frac{v_3(\varepsilon)}{u_3(\varepsilon)}. \quad (3.36)$$

As mentioned previously, for the 3-block continuous-time control system, the block  $\bar{\Pi}(s)$  can be taken out of the PIM process and discretized locally with the matched pole-zero method; therefore, the  $\Pi_T(\varepsilon)$  block given in (3.36) should be cascaded to the matched pole-zero model of  $\bar{\Pi}(s)$ , when steps 1 to 3 of the PIM method are performed with  $\bar{\Pi}(s)$

discarded.

The controllers form a system from  $R_T(\varepsilon)$  to  $U_T(\varepsilon)$  denoted as  $\widehat{H}_T(\varepsilon)$ . The resulting sampled-data control system has the structure shown in Figure 1.4(b). The discrete-time system  $\widehat{H}_T(\varepsilon)$  has the same set of zeros as that of  $H_T(\varepsilon)$ , but different pole locations. When  $\widehat{H}_T(\varepsilon)$  has all of its poles in the stability region  $|T\varepsilon + 1| < 1$ , a DC gain or low-frequency requirement can be met by cascading a gain  $K$  in front of  $\widehat{H}_T(\varepsilon)$  such that

$$\widehat{H}_T(\varepsilon) \Big|_{\varepsilon=\varepsilon_0} \cdot K = H_T(\varepsilon) \Big|_{\varepsilon=\varepsilon_0}. \quad (3.37)$$

The behavior, as  $T \rightarrow 0$ , and stability of the discrete-time control system are established with the following lemma and theorems.

**Lemma 3.2.1** Suppose that  $\mathbf{A}$ , for each  $T$  selected, and  $\overline{\mathbf{A}}$  have full column rank. Then the least-squares estimator  $\widehat{X}$ , obtained with (3.31), approaches  $\overline{X}$  as  $T \rightarrow 0$ .  $\blacktriangleright$

Proof: Since  $G_T(\varepsilon)$  is a discrete-time model [13] of  $\overline{G}(s)$  and  $H_T(\varepsilon)$  is a matched pole-zero model of  $\overline{H}(s)$ , one can write  $\mathbf{A} = \overline{\mathbf{A}} + \Delta\mathbf{A}$  and  $Y = \overline{Y} + \Delta Y$ , where  $\lim_{T \rightarrow 0} \Delta\mathbf{A} = 0_{(p+1) \times (l+r+2)}$  and  $\lim_{T \rightarrow 0} \Delta Y = 0_{(p+1) \times 1}$ . Knowing the solution  $\overline{X}$  exists, if the columns of  $\overline{\mathbf{A}}$  are linearly independent, the solution is unique and can still be expressed as  $(\overline{\mathbf{A}}^T \overline{\mathbf{A}})^{-1} \overline{\mathbf{A}}^T \overline{Y}$ . Then, a bound on the vector norm of  $\widehat{X} - \overline{X}$  is

$$\|\widehat{X} - \overline{X}\| \leq f_{1,T} + f_{2,T} + f_{3,T} \quad (3.38)$$

where

$$f_{1,T} = \left\| \left[ (\overline{\mathbf{A}} + \Delta\mathbf{A})^T (\overline{\mathbf{A}} + \Delta\mathbf{A}) \right]^{-1} (\overline{\mathbf{A}} + \Delta\mathbf{A})^T \right\| \cdot \|\Delta Y\| \quad (3.39)$$

$$f_{2,T} = \left\| \left[ (\overline{\mathbf{A}} + \Delta\mathbf{A})^T (\overline{\mathbf{A}} + \Delta\mathbf{A}) \right]^{-1} \right\| \cdot \|\overline{Y}\| \cdot \|\Delta\mathbf{A}^T\| \quad (3.40)$$

$$f_{3,T} = \left\| \left[ I + (\overline{\mathbf{A}}^T \overline{\mathbf{A}})^{-1} (\overline{\mathbf{A}}^T \Delta\mathbf{A} + \Delta\mathbf{A}^T \overline{\mathbf{A}} + \Delta\mathbf{A}^T \Delta\mathbf{A}) \right]^{-1} - I \right\|$$

$$\cdot \|\bar{Y}\| \cdot \|\bar{\mathbf{A}}^T\| \cdot \left\| \left( \bar{\mathbf{A}}^T \bar{\mathbf{A}} \right)^{-1} \right\|. \quad (3.41)$$

With the knowledge of equations (3.39) to (3.41), given any  $\xi > 0$ , there exists a  $T_1$  such that  $f_{1,T} < \xi/3$  for all  $T < T_1$ , a  $T_2$  such that  $f_{2,T} < \xi/3$  for all  $T < T_2$ , and a  $T_3$  such that  $f_{3,T} < \xi/3$  for all  $T < T_3$ . Choosing  $T < \kappa$ , where  $\kappa = \min \{T_1, T_2, T_3\}$ , implies  $\|\hat{X} - \bar{X}\| < \xi/3 + \xi/3 + \xi/3 = \xi$ .  $\square$

**Theorem 3.2.2** There exists a  $T_s > 0$  such that the system  $\hat{H}_T(\varepsilon)K$  has all of its poles inside the stability region  $|T\varepsilon + 1| < 1$  if  $0 < T < T_s$ .  $\bowtie$

Proof: First, let  $\hat{Y} = \mathbf{A}\hat{X}$ . Second, bound  $\|\hat{Y} - \bar{Y}\|$  as

$$\|\hat{Y} - \bar{Y}\| \leq \|\bar{\mathbf{A}}\| \cdot \|\hat{X} - \bar{X}\| + \|\Delta\mathbf{A}\| \cdot \|\hat{X}\|. \quad (3.42)$$

From Lemma 3.2.1, given any  $\varepsilon > 0$ , there exists a  $\kappa > 0$  such that whenever  $T < \kappa$ ,  $\|\hat{Y} - \bar{Y}\| < \varepsilon$ . This means that the coefficients of the denominator polynomial of  $\hat{H}_T(\varepsilon)$ ,  $\hat{d}(\varepsilon)$ , approach the corresponding coefficients of the denominator of  $\bar{H}(s)$ , as  $T \rightarrow 0$ .

Thus, one can write

$$\hat{d}(\varepsilon) = (\bar{d}_p + \Delta d_p)\varepsilon^p + \cdots + (\bar{d}_1 + \Delta d_1)\varepsilon + (\bar{d}_0 + \Delta d_0) \quad (3.43)$$

where  $\lim_{T \rightarrow 0} \Delta d_j = 0$  for  $0 \leq j \leq p$ . Third, apply the  $w$ -transformation [36]

$$\varepsilon = \frac{w}{1 - Tw/2} \quad (3.44)$$

to  $\hat{d}(\varepsilon)$  and write the polynomial as

$$\hat{d}(w) = (\bar{d}_p + \Delta d_p) \left( \frac{w}{1 - Tw/2} \right)^p + \cdots + (\bar{d}_1 + \Delta d_1) \left( \frac{w}{1 - Tw/2} \right) + (\bar{d}_0 + \Delta d_0). \quad (3.45)$$

Use the following facts: (i) the region of stability of the  $\varepsilon$ -plane corresponds to the left-half  $w$ -plane; (ii) when  $T$  is changed by an infinitesimal amount, the change in the coefficients

of (3.45) can be set arbitrarily small and so can that of the poles of this equation [40]; that is, there is no jumps in pole locations with relatively small changes in the sampling period; (iii) the roots of  $\hat{d}(w)$  approach the poles of  $\bar{H}(s)$ , as  $T \rightarrow 0$ . Then,  $\hat{H}_T(\varepsilon)K$  has all of its poles within the stability region  $|T\varepsilon + 1| < 1$  for a sufficiently small  $T$ .  $\square$

**Remark 3.2.2** Let  $\mathbf{A}X_{local} = Y_{local}$  be the system of equations associated with a 1-controller block control system obtained with a local digital redesign method. In this system of equations,  $X_{local}$  is obtained from  $\bar{X}$ ,  $\mathbf{A}$  comes from  $\bar{\mathbf{A}}$  and there is no guarantee that the resulting  $Y_{local}$  gives stable roots when expressed as a polynomial in  $\varepsilon$ . The coefficients of the powers of  $\varepsilon$  in the discrete-time controller transfer function, which correspond to the entries of  $X_{local}$ , can be recovered by performing the least-squares process on  $\mathbf{A}X_{local} = Y_{local}$ . On the other hand,  $\mathbf{A}X = Y$  is the system of equations associated with the reduced-order PIM-based control system, which is solved for  $X$ , given  $\mathbf{A}$  and  $Y$  are fixed for the sampling period selected. The sampling period used is the same for the reduced-order PIM and the local digital redesign. With the least-squares method carried out on  $\mathbf{A}X_{local} = Y_{local}$  and  $\mathbf{A}X = Y$ , the superiority of the reduced-order PIM method over the local digital redesign technique comes from the fact that  $Y$  forms a polynomial with stable roots, whereas there is no guarantee that  $Y_{local}$  gives stable roots when expressed as a polynomial in  $\varepsilon$ .

**Theorem 3.2.3**  $\hat{H}_T(\varepsilon) \Big|_{\varepsilon = \frac{e^{sT}-1}{T}} \cdot K$  converges to  $\bar{H}(s)$ , pointwise in  $s$ , as  $T \rightarrow 0$ .  $\square$

Proof: Since (i)  $\hat{Y} = \mathbf{A}\hat{X}$  approaches  $\bar{Y}$  as  $T \rightarrow 0$ , from Lemma 3.2.1, (ii) the zeros of  $\hat{H}_T(\varepsilon)$  equal those of  $H_T(\varepsilon)$ , and (iii)  $K$  is found from (3.37), it follows that, given any  $\epsilon > 0$ , there exists a  $\gamma > 0$  such that

$$\left| \hat{H}_T(\varepsilon) \Big|_{\varepsilon = \frac{e^{sT}-1}{T}} \cdot K - \bar{H}(s) \right| < \epsilon \quad (3.46)$$

for each fixed  $s$  in the region of convergence, whenever  $T < \gamma$ .  $\square$

**Remarks 3.2.3** (i) It is clear that the difference between the reduced-order and regular PIM methods lies in the closed-loop discrete-time pole locations. The simplest way to

compare systems obtained with these two methods is to investigate the closed-loop poles behavior. From Theorem 3.2.2, the poles of  $\widehat{H}_T(\varepsilon)$  approach those of  $\overline{H}(s)$  as the sampling period is reduced. (ii) If it is desired to improve the performance of the closed-loop system when the polynomial degrees of  $u(\varepsilon)$  and  $v(\varepsilon)$  of the discrete-time Diophantine equation are set to  $l = f$  and  $r = h$ , respectively, or if one is allowed to implement higher order controllers, although of orders smaller than those obtained with the regular PIM method, one can set  $l = f + k_1$  and  $r = h + k_2$ , where  $0 \leq k_2 \leq k_1$ ,  $0 \leq k_1 \leq (n - 2 - f)$  and  $k_2 \leq (p - 2 - f - h)$ . As was done in the case of the polynomial degree requirements in the Diophantine equation associated with the regular PIM method, one should add to  $\overline{H}(s)$  a stable, unity DC gain transfer function  $\overline{\Sigma}(s)$ , of order  $k_1$ , with identical sets of poles and zeros. Then  $\overline{H}(s)\overline{\Sigma}(s)$  is discretized to  $H_T(\varepsilon)$  in the second step of the digital redesign process.

### 3.2.3 Reduced-Order, Truncated Plant Input Mapping Method

This approach permits to restrict the number of controllers and their respective order. The price paid for such a simplification is the fact that the discrete-time closed-loop poles and zeros of the reduced-order, truncated PIM-based control system are different from those of the PIM-based control system. The proposed reduced-order, truncated PIM method is carried out as follows for a continuous-time control system where  $\overline{\Pi}(s)$  is a constant block:

*Step 1:* Perform the steps of the reduced-order PIM method up to the controller calculations.

*Step 2:* Obtain the controllers with any applicable equations among (3.23) to (3.25). These blocks form a system from  $R_T(\varepsilon)$  to  $U_T(\varepsilon)$  denoted as  $\widehat{H}'_T(\varepsilon)$ .

*Step 3:* Place a gain  $K'$  in front of  $\widehat{H}'_T(\varepsilon)$  such that

$$\widehat{H}'_T(\varepsilon)\Big|_{\varepsilon=\varepsilon_0} \cdot K' = H_T(\varepsilon)\Big|_{\varepsilon=\varepsilon_0}. \quad (3.47)$$

The poles of  $\widehat{H}'_T(\varepsilon)$  are the same as those of  $\widehat{H}_T(\varepsilon)$ . When the controllers are obtained with (3.23) and  $m(\varepsilon)$  has stable roots, the polynomial  $w(\varepsilon)$  can be selected such that its roots are stable and are as close as desired to those of  $m(\varepsilon)$ . This means that all the zeros of  $\widehat{H}'_T(\varepsilon)$  can be made arbitrarily close to those of  $H_T(\varepsilon)$ . When the implementation is performed with (3.24) or (3.25), the zeros of  $\widehat{H}'_T(\varepsilon)$  are the roots of  $a(\varepsilon)u(\varepsilon)$  and  $a(\varepsilon)v(\varepsilon)$ , respectively.

### 3.3 Alternative Digital Redesign Methods Based on the Classical Discretization of a Closed-Loop System

This section proposes two digital redesign methods which are based on the same rationale as that of PIM: the use of classical discretization on a closed-loop system. The methods are presented mainly to show the existence of alternatives to the PIM methods which result in sampled-data control systems with the structure of Figure 1.4(b). Their details can be found in Appendix C.

The first technique relies on the discretization of  $\overline{H}(s)$  with hold-equivalent and numerical integration methods. The steps in performing such digital redesign process are given in Appendix C.1. The resulting discrete-time closed-loop system satisfies (3.5) and, as is the case with the regular PIM method, internal stability at the sampling instants is guaranteed. Also, depending on the manner in which the design steps are carried out, truncated and reduced-order versions of the method can be obtained.

The second digital redesign method arises from the following interrogation. Knowing that the PIM techniques rely on the discretization of the system relating the, external,

reference input to the, internal, control input, from the viewpoint of exogenous input and output, is it possible to use the matched pole-zero method on the system relating the reference input to the controlled output, i.e. to perform a plant output mapping process? The answer is yes, as long as the hold at control input is an integral part of the digital redesign process. Appendix C.2 presents the steps involved in the plant output mapping method. The main features of the method are the following: (i) given that the continuous-time control system is internally stable, the sampled-data control system obtained with the plant output mapping method is internally stable at the sampling instants, for any non-pathological sampling period selected; and (ii) it can be interpreted as a procedure to discrete-time model following control, where the reference model is the matched pole-zero model of the system relating the reference input to the controlled output, except that the method is applicable to non-minimum phase plants and restrictions are placed on the hold at control input, as detailed in Appendix C.2, in order to obtain an intersample behavior for the control input and the controlled output signals which is exempt of large oscillations.

## Chapter 4

# Analysis of Digitally Redesigned Control Systems

The analysis of a sampled-data control system obtained with the digital redesign of a continuous-time control system consists in its characterization and performance evaluation. First of all, the characterization provided in this chapter is mainly concerned with (i) the time-domain behavior of the control input, controlled output, and other loop signals, (ii) the transfer functions of the discrete-time blocks, and (iii) the robustness characteristics of the sampled-data control systems, all as the sampling period approaches zero. The motivation of such study comes from the intuitive reasoning that a digitally redesigned control system should approach, in some sense, its continuous-time counterpart for sufficiently fast sampling rates. This idea is made clear in the present. Second of all, the performances obtained with the PIM-based systems, described in Chapter 3, are compared with those attained with systems based on the local digital redesign methods by using the modern approaches to performance quantification, as presented in Chapter 1. The performances are evaluated for any non-pathological sampling period, and not just for fast sampling frequencies.

The chapter is organized as follows. In Section 4.1, the sampled-data and continuous-time control systems are formulated under the lifting framework and the important hold

condition in the time domain is presented. This system representation forms the basis of the propositions and theorems given in the chapter which pertain to the time-domain behavior of sampled-data control systems. Section 4.2 addresses the issue of internal stability at the sampling instants and its relation with input-output stability, as introduced in Chapter 2. The development provided in Section 4.2 is different from the input-output stability analysis which can be found in [32] and [33] since it is based on the system formulation provided in Section 4.1, applies to the general 3-block structure with the possibility that the hold at control input is different from the ZOH, and emphasizes control systems obtained with the local digital redesign and the PIM methods. The main result of the time-domain characterization of sampled-data control systems is given in Section 4.3, where the conditions achieving uniform-in-time convergence of the control input and controlled output of a sampled-data control system to the respective signals of the continuous-time control system, as  $T \rightarrow 0$ , are established. In Section 4.4, the convergence in the transfer function of the discrete-time controller blocks to their continuous-time counterpart, as  $T \rightarrow 0$ , is defined. The theorems of Section 4.4 present the conditions achieving convergence in the transfer function. The consequence of such block convergence to the behavior of the loop signals other than the control input and controlled output is demonstrated. The robustness characteristics of PIM-based sampled-data control systems are investigated in the limit in Section 4.5. The  $L^2$  norm,  $L^\infty$  norm and ITAE index on the control-input and controlled-output errors, and the induced norms of the systems relating the reference and disturbance inputs to the control input are the means utilized to quantify the performances of digitally redesigned control systems. Their behavior with respect to the sampling period and the method of digital redesign is investigated in Section 4.6. The control input and controlled output responses of digitally redesigned control systems for relatively large sampling intervals are also investigated in Section 4.6.

## 4.1 Representation of Systems

Consider the systems in Figure 1.4. The lifted equivalent of the closed-loop continuous-time control system is  $\widehat{\overline{G}\overline{H}}$  and that of the sampled-data control system is  $\widehat{\overline{G}H\overline{H}_T S}$ . The state, control input and controlled output equations of the system  $\widehat{\overline{G}\overline{H}}$  are given by equations (4.1) to (4.3).

$$\delta\widehat{\overline{x}}_{k,T}(0) = \left( \frac{e^{\overline{A}T} - I}{T} \right) \widehat{\overline{x}}_{k,T}(0) + \frac{1}{T} \int_{v=0}^T e^{\overline{A}(T-v)} \overline{B} \widehat{\overline{r}}_{k,T}(v) dv \quad (4.1)$$

$$\widehat{\overline{u}}_{k,T}(\tau) = \overline{C} e^{\overline{A}\tau} \widehat{\overline{x}}_{k,T}(0) + \overline{C} \int_{v=0}^{\tau} e^{\overline{A}(\tau-v)} \overline{B} \widehat{\overline{r}}_{k,T}(v) dv + \overline{D} \widehat{\overline{r}}_{k,T}(\tau) \quad (4.2)$$

$$\begin{aligned} \widehat{\overline{y}}_{k,T}(\tau) = & \overline{C}_{\overline{G}} e^{\overline{A}_{\overline{G}}\tau} \widehat{\overline{x}}_{\overline{G},k,T}(0) + \left\{ \overline{D}_{\overline{G}} \overline{C} e^{\overline{A}\tau} \right. \\ & \left. + \overline{C}_{\overline{G}} \int_{v=0}^{\tau} e^{\overline{A}_{\overline{G}}(\tau-v)} \overline{B}_{\overline{G}} \overline{C} e^{\overline{A}v} dv \right\} \widehat{\overline{x}}_{k,T}(0) \\ & + \overline{D}_{\overline{G}} \left( \overline{C} \int_{v=0}^{\tau} e^{\overline{A}(\tau-v)} \overline{B} \widehat{\overline{r}}_{k,T}(v) dv \right. \\ & \left. + \overline{D} \widehat{\overline{r}}_{k,T}(\tau) \right) + \overline{C}_{\overline{G}} \int_{v=0}^{\tau} e^{\overline{A}_{\overline{G}}(\tau-v)} \overline{B}_{\overline{G}} \\ & \cdot \left\{ \overline{C} \int_{w=0}^v e^{\overline{A}(v-w)} \overline{B} \widehat{\overline{r}}_{k,T}(w) dw + \overline{D} \widehat{\overline{r}}_{k,T}(v) \right\} dv \end{aligned} \quad (4.3)$$

In the equations, the reference input  $\overline{r}(t)$ , state  $\overline{x}(t)$ , control input  $\overline{u}(t)$ , and controlled output  $\overline{y}(t)$  are lifted to  $\{\widehat{\overline{r}}_{k,T}(\tau)\}_0^\infty$ ,  $\{\widehat{\overline{x}}_{k,T}(\tau)\}_0^\infty$ ,  $\{\widehat{\overline{u}}_{k,T}(\tau)\}_0^\infty$ , and  $\{\widehat{\overline{y}}_{k,T}(\tau)\}_0^\infty$  ( $0 \leq \tau < T$ ), respectively. Also,  $\overline{A} \in R^{p \times p}$ ,  $\overline{B} \in R^{p \times 1}$ ,  $\overline{C} \in R^{1 \times p}$ , and  $\overline{D} \in R$  are the elements of a realization of the continuous-time system  $\overline{H}$  which corresponds to the composite state when the states of the block realizations present in the continuous-time control system are stacked according to Definition 2.3.1. Alternatively, one could calculate the continuous-time PITF, obtain any realization from the PITF, and then utilize the elements  $[\overline{A}, \overline{B}, \overline{C}, \overline{D}]$  in the equations (4.1)-(4.3). In both cases,  $\overline{x}(t)$  is the state of  $\overline{H}$  and  $\widehat{\overline{x}}_{k,T}(0) = \overline{x}(t)|_{t=kT}$ . The state-space elements of the continuous-time plant are  $\overline{A}_{\overline{G}} \in R^{n \times n}$ ,  $\overline{B}_{\overline{G}} \in R^{n \times 1}$ ,  $\overline{C}_{\overline{G}} \in R^{1 \times n}$ , and  $\overline{D}_{\overline{G}} \in R$ , the state of the plant realization is denoted as  $\overline{x}_{\overline{G}}(t)$ ,

and  $\widehat{\bar{x}}_{\bar{G},k,T}(0) = \bar{x}_{\bar{G}}(t)|_{t=kT}$ .

The state, control input and controlled output equations of  $\widehat{\bar{G}H}H_T S$  are given by equations (4.4) to (4.6).

$$\delta x_{k,T} = Ax_{k,T} + B\widehat{\bar{r}}_{k,T}(0) \quad (4.4)$$

$$\widehat{u}_{k,T}(\tau) = H(\tau)Cx_{k,T} + H(\tau)D\widehat{\bar{r}}_{k,T}(0) \quad (4.5)$$

$$\begin{aligned} \widehat{y}_{k,T}(\tau) = & \bar{C}_{\bar{G}}e^{\bar{A}_{\bar{G}}\tau}x_{G_T,k,T} + (\bar{D}_{\bar{G}}H(\tau)C \\ & + \bar{C}_{\bar{G}}\int_{v=0}^{\tau} e^{\bar{A}_{\bar{G}}(\tau-v)}\bar{B}_{\bar{G}}H(v)Cdv) x_{k,T} \\ & + (\bar{C}_{\bar{G}}\int_{v=0}^{\tau} e^{\bar{A}_{\bar{G}}(\tau-v)}\bar{B}_{\bar{G}}H(v)Ddv \\ & + \bar{D}_{\bar{G}}H(\tau)D)\widehat{\bar{r}}_{k,T}(0) \end{aligned} \quad (4.6)$$

As for the case of the continuous-time control system, the reference input  $\bar{r}(t)$ , control input  $u_T(t)$  and controlled output  $y_T(t)$  are lifted to  $\{\widehat{\bar{r}}_{k,T}(\tau)\}_0^\infty$ ,  $\{\widehat{u}_{k,T}(\tau)\}_0^\infty$ , and  $\{\widehat{y}_{k,T}(\tau)\}_0^\infty$  ( $0 \leq \tau < T$ ), respectively. However, the closed-loop state is a discrete-time signal and so is not lifted. In equations (4.4)-(4.6),  $A \in R^{p \times p}$ ,  $B \in R^{p \times 1}$ ,  $C \in R^{1 \times p}$ , and  $D \in R$  are the elements of a realization of the discrete-time system  $H_T$ . As in the continuous-time control system, the realization of  $H_T$  could be that describing the composite state or that obtained by first calculating the discrete-time PITF. In both cases,  $x_{k,T}$  ( $k \geq 0$ ) is the state of  $H_T$ . The former realization is useful to describe sampled-data control systems obtained with a local digital redesign method, whereas the latter realization is more suitable for the characterization of a PIM-based control system. In equations (4.4) to (4.6),  $\widehat{\bar{r}}_{k,T}(0) = \widehat{\bar{r}}_{k,T}(\tau)|_{\tau=0}$ , the sequence  $\{x_{G_T,k,T}\}_0^\infty$  corresponds to the state of the hold-equivalent model of the plant, and  $H(\tau)$  is the response function of the hold.

The *hold condition in the time domain* is defined as

$$\lim_{T \rightarrow 0} \sup_{0 \leq \tau < T} |H(\tau) - 1| = 0. \quad (4.7)$$

When a hold satisfies this condition, reducing the sampling interval results in a decrease in the supremum of the oscillations, if any, that are due to the hold at the control input. For instance, consider the hold function given by

$$H(\tau) = 1 + \tau, \quad \tau \in [0, T) \quad (4.8)$$

which satisfies the hold condition (4.7). For a given  $T$ , in each time interval  $[kT, (k+1)T)$ , the supremum deviation of the control input  $u_T(t)$  from the discrete-time control input amplitude at the  $k$ th step, i.e.  $u_{k,T}$ , is equal to  $u_{k,T} \cdot T$ . By reducing  $T$ , the deviation in each interval  $[kT, (k+1)T)$  can be made arbitrarily small. As another example, the most common hold device is the ZOH which satisfies the equation  $\sup_{0 \leq \tau < T} |H(\tau) - 1| = 0$  for each sampling period since its hold function is given by  $H(\tau) = 1$ . From now on in this chapter, unless stated otherwise, the hold at control input is assumed to satisfy the hold condition in the time domain.

It should be noted that the reference input to the continuous-time control system can be different from that entering the sampled-data system. However, for simplicity of notation, equations (4.1) to (4.6) use a unique description to the lifted reference inputs,  $\{\widehat{r}_{k,T}(\tau)\}_{k=0}^{\infty}$ .

## 4.2 Stability of Systems

The most important goal that must be achieved by a control system is closed-loop stability. In this section, internal stability at the sampling instants is connected to the input-output stability of sampled-data control systems with Theorem 4.2.1. In the theorem, it is assumed that the reference input is bounded and, as stated in the main

assumptions, that the sampling period is non-pathological with respect to the plant.

**Theorem 4.2.1** If the sampled-data control system of Figure 1.4(b) is internally stable at the sampling instants, it is also input-output stable.  $\square$

Proof: The norm equivalence between a continuous-time signal and its lifted form [56] is used. Consider the lifted formulation of the sampled-data system given by equations (4.4)-(4.6). Establishing input-output stability is equivalent to determining whether a system subjected to an input in  $l_{\overline{PC}[0,T]}^\infty$  generates an output in  $l_{\overline{PC}[0,T]}^\infty$ . To do so, write the composite state transition equation of the discrete-time closed-loop system, with zero initial conditions, as

$$x_{k,T} = \sum_{j=0}^{k-1} (TA + I)^{k-j-1} TB \widehat{r}_{j,T}(0) \quad (4.9)$$

where  $x_{k,T}$  is as defined in (2.2), to obtain the output equation given by

$$\widehat{y}_{k,T}(\tau) = C(\tau) \cdot \sum_{j=0}^{k-1} (TA + I)^{k-j-1} TB \widehat{r}_{j,T}(0) + D(\tau) \widehat{r}_{k,T}(0) \quad (4.10)$$

where

$$C(\tau) = \left[ 0_{1 \times (p-n)}, \overline{C}_{\overline{G}} e^{\overline{A}_{\overline{G}} \tau} \right] + \overline{D}_{\overline{G}} H(\tau) C + \overline{C}_{\overline{G}} \int_{v=0}^{\tau} e^{\overline{A}_{\overline{G}}(\tau-v)} \overline{B}_{\overline{G}} H(v) C dv \quad (4.11)$$

$$D(\tau) = \overline{C}_{\overline{G}} \int_{v=0}^{\tau} e^{\overline{A}_{\overline{G}}(\tau-v)} \overline{B}_{\overline{G}} H(v) D dv + \overline{D}_{\overline{G}} H(\tau) D. \quad (4.12)$$

Applying the vector norm, the matrix norm, and the absolute value where it is appropriate, the absolute value on the output sequence can be bounded as follows:

$$\begin{aligned} |\widehat{y}_{k,T}(\tau)| &\leq \|C(\tau)\| \cdot \sum_{j=0}^{k-1} \|(TA + I)^{k-j-1}\| T \cdot \|B\| \cdot \left| \widehat{r}_{j,T}(0) \right| \\ &\quad + |D(\tau)| \cdot \left| \widehat{r}_{k,T}(0) \right| \end{aligned} \quad (4.13)$$

for each  $k \geq 0$  and  $\tau \in [0, T)$ . Since the reference input is bounded, there exists a  $\tau_b < \infty$

such that

$$\sup_{k \geq 0} \left| \widehat{r}_{k,T}(0) \right| = r_b. \quad (4.14)$$

Then

$$\begin{aligned} \sup_{k \geq 0} \left\{ \sup_{0 \leq \tau < T} |\widehat{y}_{k,T}(\tau)| \right\} &\leq \sup_{0 \leq \tau < T} \|C(\tau)\| \cdot \sum_{j=0}^{\infty} \|(TA + I)^j\| T \\ &\quad \cdot \|B\| \cdot r_b + \sup_{0 \leq \tau < T} |D(\tau)| \cdot r_b. \end{aligned} \quad (4.15)$$

If the system is internally stable at the sampling instants, the  $A$  matrix has a set of eigenvalues lying in the stability region of the  $\varepsilon$ -plane,  $|T\varepsilon + 1| < 1$ , and [76]

$$\sum_{j=0}^{\infty} \|(TA + I)^j\| T < \infty. \quad (4.16)$$

It only remains to show that

$$\sup_{0 \leq \tau < T} \|C(\tau)\| < \infty \text{ and } \sup_{0 \leq \tau < T} |D(\tau)| < \infty. \quad (4.17)$$

Thus,

$$\begin{aligned} \sup_{0 \leq \tau < T} \|C(\tau)\| &\leq \sup_{0 \leq \tau < T} \left\| \left[ 0_{1 \times (p-n)}, \overline{C}_{\overline{G}} e^{\overline{A}_{\overline{G}} \tau} \right] \right\| + |\overline{D}_{\overline{G}}| \cdot \|C\| \sup_{0 \leq \tau < T} |H(\tau)| \\ &\quad + \|\overline{C}_{\overline{G}}\| \sup_{0 \leq \tau < T} \left\| \int_{v=0}^{\tau} e^{\overline{A}_{\overline{G}}(\tau-v)} \overline{B}_{\overline{G}} H(v) C dv \right\| \end{aligned} \quad (4.18)$$

which is finite, even if the plant is unstable, since  $\tau < T < \infty$  and each element of the plant and PITF realizations has a finite norm. Moreover,

$$\begin{aligned} \sup_{0 \leq \tau < T} |D(\tau)| &\leq \|\overline{C}_{\overline{G}}\| \sup_{0 \leq \tau < T} \left\| \int_{v=0}^{\tau} e^{\overline{A}_{\overline{G}}(\tau-v)} \overline{B}_{\overline{G}} H(v) D dv \right\| \\ &\quad + |\overline{D}_{\overline{G}}| \cdot |D| \sup_{0 \leq \tau < T} |H(\tau)| \end{aligned} \quad (4.19)$$

which is finite for each non-pathological  $T \in (0, \infty)$  for the reasons mentioned previously

and the fact the hold function  $H(\tau)$  is assumed to be bounded.  $\square$

**Remark 4.2.1** Theorem 4.2.1 can be modified such that it applies to MIMO systems. To do so, the absolute values should be substituted by vector or matrix norms, depending on the context. In particular, the absolute value of the response function of the hold in (4.7) should be changed to a matrix norm and the unity scalar should be replaced by the identity matrix. For MIMO systems, the hold is represented by a matrix response function with each of its entries satisfying the main assumptions on the hold function, as given in Chapter 2.

Theorem 4.2.1 shows that, to achieve input-output stability, the discrete-time closed-loop system should be internally stable and  $T$  should be non-pathological. However, depending on the digital redesign method and the sampling period employed, internal stability at the sampling instants can or cannot be achieved. For local digital redesign methods, care must be exercised in the selection of the sampling period as detailed below.

**Theorem 4.2.2** For a sampled-data control system obtained with the local digital redesign of an internally stable continuous-time control system, there exists a  $T^* > 0$  such that, whenever  $T < T^*$  and is non-pathological with respect to the plant, the sampled-data control system is internally stable at the sampling instants.  $\bowtie$

The following proposition is used in the proof of Theorem 4.2.2.

**Proposition 4.2.1** The discrete-time system  $G_T$ , which is composed of a hold that satisfies the hold condition in the time domain and the main assumptions provided in Chapter 2, the linear time-invariant continuous-time plant  $\bar{G} = [\bar{A}_{\bar{G}}, \bar{B}_{\bar{G}}, \bar{C}_{\bar{G}}, \bar{D}_{\bar{G}}]$ , and the ideal sampler, has one realization with elements  $[A_{G_T}, B_{G_T}, C_{G_T}, D_{G_T}]$  such that  $A_{G_T} \rightarrow \bar{A}_{\bar{G}}$ ,  $B_{G_T} \rightarrow \bar{B}_{\bar{G}}$ ,  $C_{G_T} \rightarrow \bar{C}_{\bar{G}}$ , and  $D_{G_T} \rightarrow \bar{D}_{\bar{G}}$ , as  $T \rightarrow 0$ .  $\bowtie$

Proof: Given in Appendix A.  $\square$

Proof of Theorem 4.2.2: Local digital redesign of a control block using any equi-order discretization method results in a discrete-time control block with at least one realization comprising matrices approaching those corresponding ones of a continuous-time realiza-

tion, according to [14]. The same can be said about the hold-equivalent discrete-time model of the plant, from Proposition 4.2.1. Consequently, with the sampled-data and continuous-time control systems having the same structure, and the states of the closed-loop discrete-time and continuous-time systems taken as composites of the local states, knowing there exists a realization of each discrete-time block which approaches that of its continuous-time counterpart as  $T \rightarrow 0$ , the  $A$  matrix of the closed-loop discrete-time system approaches its continuous-time counterpart, and so do the eigenvalues. In fact, for a small change in  $T$ , there results a small change in the matrix  $A$  and in its eigenvalues. The stability region of the  $\varepsilon$ -plane,  $|T\varepsilon + 1| < 1$ , is a circle centered at  $\varepsilon = -1/T$  with radius  $1/T$ . When the sampling period is sufficiently small and the eigenvalues of the  $\bar{A}$  matrix of the composite state realization of the continuous-time system are in the left-hand side of the  $s$ -plane, then the eigenvalues of the  $A$  matrix lie within the circle of stability in the  $\varepsilon$ -plane and stay in the stable region for any further reduction of  $T$ . The non-pathologicity of  $T$  is needed for closed-loop stability in the sense that if  $T$  is pathological with respect to the plant, it is possible that unstable poles of the plant be unaccounted for by the control system and instability would result.  $\square$

The stability of a PIM-based sampled-data control system for either short or large sampling periods can be established as follows.

**Theorem 4.2.3** A sampled-data control system obtained from an internally stable continuous-time control system with the regular PIM method, or its truncated version, is internally stable at the sampling instants for all non-pathological sampling periods.  $\blacktriangleright$

Proof: The discrete-time PITF has poles within the stability region of the  $\varepsilon$ -plane. The implementation process of equations (3.12) to (3.15) assures internal stability.  $\square$

As mentioned in Section 3.2, for the reduced-order PIM method, and its truncated alternative, stability can be guaranteed for a sufficiently small sampling period.

### 4.3 Behavior of Control Input and Controlled Output as $T \rightarrow 0$

Generally, it is expected that the responses of a digitally redesigned control system can be made as close as desired to those of a continuous-time control system that has satisfactory characteristics, when both systems are subjected to the same reference input, by selecting relatively fast sampling frequencies. In the present section, this intuitive idea is made clear; that is, conditions which guarantee the uniform-in-time convergence as  $T \rightarrow 0$  of the control input and controlled output responses of digitally redesigned control systems to those corresponding signals of the continuous-time control system, from which the digital redesign originates, are provided. Furthermore, for a brief investigation of the Laplace transform behavior of such signals, as  $T \rightarrow 0$ , the reader is referred to Appendix D.

The following definition presents the reference inputs which are admitted in the study.

**Definition 4.3.1** The admissible class of reference inputs to the control systems are those which satisfy either: (i) both control systems are subjected to an input which belongs to  $\mathcal{S}_1$  or is a staircase equivalent of a signal in  $\mathcal{S}_1$ ; or (ii) as  $T \rightarrow 0$ , the reference input to the sampled-data control system converges uniformly in time to that of the continuous-time control system, which lies in  $\mathcal{S}_1$ .  $\bowtie$

Knowing the reference inputs which can be applied to the control systems, the following theorem provides the conditions on a sampled-data control system to achieve uniform-in-time convergences of its control input and controlled output to the corresponding signals of a continuous-time control system.

**Theorem 4.3.1** Consider the continuous-time and sampled-data control systems described by equations (4.1)-(4.6). Suppose that a state-space form for the sampled-data control system has parameters  $A = \bar{A} + \Delta A$ ,  $B = \bar{B} + \Delta B$ ,  $C = \bar{C} + \Delta C$ , and  $D = \bar{D} + \Delta D$ ,

where the terms  $\Delta \cdot$  depend on  $\bar{A}$ ,  $\bar{B}$ ,  $\bar{C}$ ,  $\bar{D}$ , and  $T$ , and satisfy

$$\begin{aligned} \lim_{T \rightarrow 0} \Delta A &= 0_{p \times p}, & \lim_{T \rightarrow 0} \Delta B &= 0_{p \times 1} \\ \lim_{T \rightarrow 0} \Delta C &= 0_{1 \times p}, & \lim_{T \rightarrow 0} \Delta D &= 0. \end{aligned} \quad (4.20)$$

Then: (i)  $\widehat{HH}_T S$  is a sampled-data model of  $\widehat{H}$ , and (ii)  $\widehat{GHH}_T S$  is a sampled-data model of  $\widehat{GH}$ .  $\infty$

Proof: Given in Appendix A for the sake of brevity.

**Remark 4.3.1** Theorem 4.3.1 can be modified to consider the MIMO case. To do so, the condition on the reference input as given by Definition 4.3.1 should apply to each entry of the reference input vector, the absolute values found in (4.7) and in the proof should be replaced by vector norms, and the unity scalar in (4.7) should be substituted by the identity matrix.

The sampled-data control systems obtained with the local digital redesign methods, and the regular and reduced-order PIM methods satisfy Theorem 4.3.1. A system obtained with the reduced-order, truncated PIM method satisfies the theorem when the controllers are calculated with either (3.24) or (3.25). In the case the controllers are obtained with (3.23), if the coefficients of the powers of  $\varepsilon$  in  $w(\varepsilon)$  can be made arbitrarily close to those corresponding ones in  $m(\varepsilon)$ , as  $T \rightarrow 0$ , and if  $m(\varepsilon)$  is stable then the resulting sampled-data control system satisfies Theorem 4.3.1. For systems obtained with the truncated PIM method, the behavior, as  $T \rightarrow 0$ , of the Diophantine equation solution must first be assessed in order to determine if the systems satisfy the theorem. This is done in Section 4.4.

A corollary to Theorem 4.3.1 provides the conditions on the individual controller blocks to obtain a sampled-data model of a continuous-time control system.

**Corollary 4.3.1** Consider the systems of Fig. 1.4. If the elements of realization of each discrete-time block approach their respective continuous-time counterparts, as  $T \rightarrow 0$ , that is if  $A_{\Pi_T}$ ,  $B_{\Pi_T}$ ,  $C_{\Pi_T}$ , and  $D_{\Pi_T}$  of the realization of  $\Pi_T(\varepsilon)$  approach  $\bar{A}_{\Pi}$ ,  $\bar{B}_{\Pi}$ ,  $\bar{C}_{\Pi}$ , and

$\overline{D}_{\overline{\Pi}}$ , respectively, of the realization of  $\overline{\Pi}(s)$ , and similarly for the other blocks, then: (i)  $\widehat{HH}_T S$  is a sampled-data model of  $\widehat{H}$  and (ii)  $\widehat{GHH}_T S$  is a sampled-data model of  $\widehat{G}\widehat{H}$ .  $\bowtie$

Add the restriction that the  $L^2$  norm is finite on the admissible reference input which is applied to the continuous-time and sampled-data control systems. Then, Theorem 4.3.2 establishes the behavior, as  $T \rightarrow 0$ , of the  $L^2$  norms of the differences in control input and controlled output between sampled-data and continuous-time control systems.

**Theorem 4.3.2** Consider the systems of Fig. 1.4, where  $\widehat{HH}_T S$  is a sampled-data model of  $\widehat{H}$  and  $\widehat{GHH}_T S$  is a sampled-data model of  $\widehat{G}\widehat{H}$ . Also suppose that both control systems are subjected to an input which belongs to  $\mathcal{S}_1$ , or is a staircase equivalent of a signal in  $\mathcal{S}_1$ , and has a finite  $L^2$  norm. Then

$$\lim_{T \rightarrow 0} \left[ \sum_{k=0}^{\infty} \int_{\tau=0}^T |\widehat{u}_{k,T}(\tau) - \widehat{u}_{k,T}(\tau)|^2 d\tau \right]^{1/2} = 0 \quad (4.21)$$

and

$$\lim_{T \rightarrow 0} \left[ \sum_{k=0}^{\infty} \int_{\tau=0}^T |\widehat{y}_{k,T}(\tau) - \widehat{y}_{k,T}(\tau)|^2 d\tau \right]^{1/2} = 0. \bowtie \quad (4.22)$$

The following propositions are used in the proof of Theorem 4.3.2.

**Proposition 4.3.1** Let a signal  $\bar{r}(t)$  enter the ideal sampler of period  $T$  to obtain the sequence  $\{r_{k,T}\}_0^{\infty}$ . Then, for any  $T$ ,  $\{r_{k,T}\}_0^{\infty} \in l^2_R$ , the space of sequences of real numbers having finite  $l^2$  norm, if  $\bar{r}(t)$  is in, or is a staircase equivalent of a signal in,  $\mathcal{S}_1$  and has finite  $L^2$  norm.  $\bowtie$

Proof: Given in Appendix A.  $\square$

**Proposition 4.3.2** Consider the internally stable control system of Fig. 1.4(a). When the reference input is in  $L^2$ , then  $\bar{u}(t)$  and  $\bar{y}(t) \in L^2$ , where  $L^2$  is defined as the space of continuous-time functions with finite  $L^2$  norm given by equation (4.23) for the signal  $\bar{r}(t)$ .  $\bowtie$

$$\|\bar{r}(t)\|_{L^2} = \sqrt{\int_{t=0}^{\infty} |\bar{r}(t)|^2 dt} \quad (4.23)$$

Proof: Given in Appendix A.  $\square$

**Proposition 4.3.3** Consider the system of Fig. 1.4(b), which is internally stable at the sampling instants for the given sampling period. Suppose the reference input belongs to  $\mathcal{S}_1$  or is a staircase equivalent of a signal in  $\mathcal{S}_1$  having a finite  $L^2$  norm. Furthermore, assume that the hold satisfies the main assumptions given in Chapter 2 and the hold condition in the time domain. Then  $u_T(t)$  and  $y_T(t) \in L^2$ .  $\infty$

Proof: Given in Appendix A.  $\square$

Proof of Theorem 4.3.2: First, for the control input signal, with the linearity of the spaces,  $(u_T(t) - \bar{u}(t)) \in L^2$ . The lifted equivalent of the control-input error therefore belongs in the space of lifted signals which have a finite norm as given by

$$\left[ \sum_{k=0}^{\infty} \int_{\tau=0}^T |\hat{u}_{k,T}(\tau) - \bar{u}_{k,T}(\tau)|^2 d\tau \right]^{1/2}. \quad (4.24)$$

Since  $\widehat{HH}_T S$  is a sampled-data model of  $\widehat{H}$ , as  $T \rightarrow 0$  the integrand in (4.24) approaches zero for each  $\tau$ . Furthermore, for a given sampling period, as  $k \rightarrow \infty$ , the discrete-time control input  $u_{k,T}$  approaches zero [77] whereas  $\bar{u}_{k,T}(\tau) \rightarrow 0$  for each  $\tau$ . Thus, the 2-norm of the control-input error can be made arbitrarily small with a sufficiently short sampling period. Second, for the controlled output, the development is similar to that carried out for the control input.  $\square$

**Remark 4.3.2** A reference input which lies in  $\mathcal{S}_0$  and has a finite  $L^2$  norm can be admitted in Theorem 4.3.2 as long as it is passed through a strictly proper, stable, linear, time-invariant continuous-time system before entering the sampled-data control system. Then the output of this so called filter lies in  $\mathcal{S}_1$  and has a finite  $L^2$  norm [77].

## 4.4 Convergence of the Controller Blocks and Loop Signals as $T \rightarrow 0$

In order to assess if the input/output behavior of each discrete-time controller block of a digitally redesigned control system approaches that of the corresponding controller block in the continuous-time control system, a convergence study of the individual discrete-time controllers of PIM-based systems to their continuous-time counterparts, as  $T \rightarrow 0$ , is presented in this section. The convergence is that of the coefficients of a discrete-time transfer function in the complex variable  $\varepsilon$ , as defined in the following subsection. Concerning the local digital redesign methods studied in the present, each coefficient of a discrete-time controller transfer function is known to approach the corresponding coefficient of the continuous-time controller transfer function counterpart [14]. As an example, the coefficients of a discrete-time transfer function in  $\varepsilon$  obtained by discretizing a continuous-time block with the forward difference method [2] are the same as those of the continuous-time transfer function, for any  $T$ . In this case, the error between coefficients of corresponding powers of  $s$  and  $\varepsilon$  is zero, no matter which sampling period is selected in the design.

With the convergence of the discrete-time controller blocks known, the time-domain behavior of the loop signals can be established in the following sense: if one connects a discrete signal to the analog world with a digital-to-analog converter, the time trajectory of the output of the digital-to-analog converter approaches uniformly in time that of the corresponding signal of the continuous-time control system, as  $T$  is reduced. Figure 4.1 illustrates the situation, where the ZOH models the digital-to-analog converter.

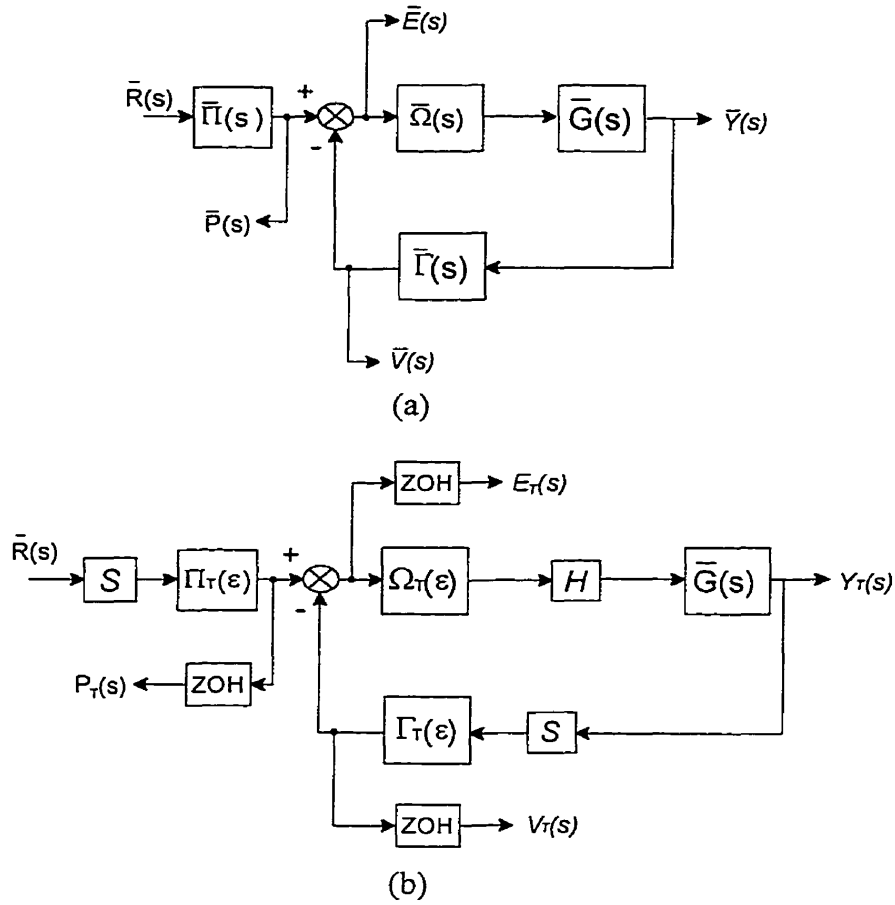


Figure 4.1: External connections for (a) the continuous-time and (b) the sampled-data control systems

#### 4.4.1 Preliminary Definition

The following definition clarifies the concept of convergence in the transfer function.

**Definition 4.4.1** Consider the general linear, time-invariant discrete-time system

$$\Lambda_T(\epsilon) = \frac{c_n \cdot \epsilon^n + \dots + c_1 \epsilon + c_0}{d_n \cdot \epsilon^n + \dots + d_1 \epsilon + d_0} \cdot \frac{a_n \epsilon^n + a_{n-1} \epsilon^{n-1} + \dots + a_1 \epsilon + a_0}{b_n \epsilon^n + b_{n-1} \epsilon^{n-1} + \dots + b_1 \epsilon + b_0} \quad (4.25)$$

where  $n^*$ ,  $n \in Z^+$ , and the linear, time-invariant continuous-time system represented as

$$\bar{\Lambda}(s) = \frac{\bar{a}_n s^n + \bar{a}_{n-1} s^{n-1} + \cdots + \bar{a}_1 s + \bar{a}_0}{\bar{b}_n s^n + \bar{b}_{n-1} s^{n-1} + \cdots + \bar{b}_1 s + \bar{b}_0}. \quad (4.26)$$

Given that the  $a_j$ s and  $b_j$ s can be written as

$$a_j = \bar{a}_j + \Delta a_j, \quad b_j = \bar{b}_j + \Delta b_j, \quad \text{for } j = 0, \dots, n \quad (4.27)$$

then the discrete-time system  $\Lambda_T(\varepsilon)$  is said to *converge in the transfer function* to  $\bar{\Lambda}(s)$  if

$$\begin{aligned} \text{(i)} \quad & \lim_{T \rightarrow 0} \Delta a_j = 0, \quad \lim_{T \rightarrow 0} \Delta b_j = 0, \quad \text{for } j = 0, \dots, n \\ \text{(ii)} \quad & \lim_{T \rightarrow 0} d_j = \bar{d}_j, \quad \text{for } j = 0, \dots, n^* \\ \text{(iii)} \quad & \lim_{T \rightarrow 0} (c_j - d_j) = 0, \quad \text{for } j = 0, \dots, n^* \end{aligned} \quad (4.28)$$

where  $\bar{d}_j \in R$  is fixed for  $j = 0, \dots, n^*$  and at least one  $\bar{d}_j$  is non-zero.  $\bowtie$

Note that the linear, time-invariant continuous-time system in Definition 4.4.1 can be a gain.

## 4.4.2 Block Convergence

The convergence in the transfer function of the discrete-time controller blocks obtained with the PIM methods is established in this subsection.

Consider the continuous-time control system of Figure 1.4(a), where there can be up to three controller blocks having irreducible transfer functions given by (3.3). The continuous-time PITF in (3.2) is rewritten as

$$\bar{H}(s) = \frac{\bar{m}(s)\bar{a}(s)}{\bar{d}(s)}. \quad (4.29)$$

In (4.29) and the continuous-time Diophantine equation (3.26) associated with the control

system, the known polynomials  $\bar{m}(s)$ ,  $\bar{u}(s)$  and  $\bar{v}(s)$  are given by

$$\begin{aligned}\bar{m}(s) &= \bar{n}_1(s)\bar{n}_2(s)\bar{d}_3(s) \\ \bar{u}(s) &= \bar{d}_1(s)\bar{d}_2(s)\bar{d}_3(s) \\ \bar{v}(s) &= \bar{n}_1(s)\bar{d}_2(s)\bar{n}_3(s).\end{aligned}\tag{4.30}$$

Assume that the degrees of  $\bar{m}(s)$ ,  $\bar{u}(s)$  and  $\bar{v}(s)$  in (4.30) are, respectively,  $(q - n)$ ,  $f = p - n$  and  $h \leq n - 1$ . It should be reminded that  $(q - n)$ ,  $f$  and  $h$  are fixed for a given continuous-time control system. Let the discrete-time counterpart of  $\bar{\Omega}(s)$  be  $\Omega_T(\varepsilon)$ , that of  $\bar{\Pi}(s)$  be  $\Pi_T(\varepsilon)$ , and that of  $\bar{\Gamma}(s)$  be  $\Gamma_T(\varepsilon)$ . Furthermore, let a non-unity block denote a block with a transfer function different from unity. Then, the main results of this section can be presented.

Theorem 4.4.1 provides the conditions yielding convergence in the transfer function of each discrete-time controller to its continuous-time counterpart when the 2-block discrete-time implementation is selected.

**Theorem 4.4.1** Consider the application of the regular PIM method to the continuous-time control system of Figure 1.4(a), where one or two control blocks are non-unity and the plant has irreducible transfer function. Each discrete-time controller converges in the transfer function to its continuous-time counterpart as  $T \rightarrow 0$  if, in the fourth step of the PIM method and for each non-pathological  $T$  selected, the eliminant matrix method is used to solve the Diophantine equation and the discrete-time controllers are calculated with any applicable equations among (3.13) to (3.15) such that each non-unity block in the continuous-time control system has a non-unity counterpart in the discrete-time control system.  $\blacktriangleright$

The following propositions are used in the proof of Theorem 4.4.1.

**Proposition 4.4.1** Consider the matrix equations  $\bar{\mathbf{A}}\bar{\mathbf{X}} = \bar{\mathbf{Y}}$  and  $\mathbf{A}\mathbf{X} = \mathbf{Y}$ , where  $\bar{\mathbf{A}}$  and  $\mathbf{A} \in R^{(p+1) \times (p+1)}$  have full rank, and  $\bar{\mathbf{X}}$ ,  $\mathbf{X}$ ,  $\bar{\mathbf{Y}}$ , and  $\mathbf{Y} \in R^{(p+1)}$ . The system of equations  $\bar{\mathbf{A}}\bar{\mathbf{X}} = \bar{\mathbf{Y}}$  has entries being the coefficients of the appropriate powers of  $s$

in the continuous-time Diophantine equation (3.26) of a given continuous-time control system, where  $f = p - n$  and  $h = n - 1$ , as shown in equation (3.30). Note that  $\bar{\mathbf{A}}$  and  $\bar{\mathbf{X}}$  are known and are used to calculate  $\bar{\mathbf{Y}}$ . By performing the regular PIM method on the continuous-time control system, as explained in Chapter 3, the discrete-time Diophantine equation (3.9) is obtained, where the degrees of  $u(\varepsilon)$  and  $v(\varepsilon)$  are set to  $l = p - n$  and  $r = n - 1$ , respectively. From (3.9), the system of equations  $\mathbf{A}X = Y$ , shown in (3.16), can be formulated. In this case,  $Y$  and  $\mathbf{A}$  are known and the system of equations is solved for  $X$ . Then,  $\lim_{T \rightarrow 0} X = \bar{\mathbf{X}}$ .  $\infty$

Proof: Given in Appendix A.

**Proposition 4.4.2** Suppose that a continuous-time control system has a Diophantine equation (3.26) with polynomials  $\bar{u}(s)$  and  $\bar{v}(s)$  of degrees  $f = p - n$  and  $h < n - 1$ , respectively. Also, assume that the plant has irreducible transfer function and that the denominator of the continuous-time PITF has degree  $p \geq 2n - 1$ . From the knowledge of  $\bar{d}(s)$ , i.e. the denominator of the continuous-time PITF, the following Diophantine equation can be formed:

$$\underbrace{(\bar{u}_{2,f_2} s^{f_2} + \dots + \bar{u}_{2,0})}_{=\bar{u}_2(s)} (\bar{a}_n s^n + \dots + \bar{a}_0) + \underbrace{(\bar{v}_{2,h_2} s^{h_2} + \dots + \bar{v}_{2,0})}_{=\bar{v}_2(s)} (\bar{b}_m s^m + \dots + \bar{b}_0) = \bar{d}_p s^p + \dots + \bar{d}_0 \quad (4.31)$$

where the unknown polynomials  $\bar{u}_2(s)$  and  $\bar{v}_2(s)$  are set to the degrees  $f_2 = p - n$  and  $h_2 = n - 1$ , respectively. Equation (4.31) can be solved uniquely for  $\bar{u}_2(s)$  and  $\bar{v}_2(s)$  with the eliminant matrix method by generating the system of equations (4.32), where  $\bar{\mathbf{A}}_2 \in R^{(p+1) \times (p+1)}$  is of rank  $(p + 1)$ , and  $\bar{\mathbf{X}}_2, \bar{\mathbf{Y}} \in R^{(p+1)}$ . Then  $\bar{u}_2(s) = \bar{u}(s)$  and

$$\bar{v}_2(s) = \bar{v}(s). \quad \bowtie$$

$$\underbrace{\begin{bmatrix} \bar{a}_n & & & & & \\ \bar{a}_{n-1} & \cdots & & \bar{b}_m & & \\ \vdots & \cdots & \bar{a}_n & \bar{b}_{m-1} & \cdots & \\ \bar{a}_1 & & \bar{a}_{n-1} & \vdots & \cdots & \bar{b}_m \\ \bar{a}_0 & \cdots & \vdots & \bar{b}_0 & & \bar{b}_{m-1} \\ & \cdots & \bar{a}_1 & & \cdots & \vdots \\ & & \bar{a}_0 & & & \bar{b}_0 \end{bmatrix}}_{=\bar{A}_2} \underbrace{\begin{bmatrix} \bar{u}_{2,f_2} \\ \vdots \\ \bar{u}_{2,0} \\ \bar{v}_{2,h_2} \\ \vdots \\ \bar{v}_{2,0} \end{bmatrix}}_{=\bar{X}_2} = \underbrace{\begin{bmatrix} \bar{d}_p \\ \bar{d}_{p-1} \\ \vdots \\ \bar{d}_1 \\ \bar{d}_0 \end{bmatrix}}_{=\bar{Y}} \quad (4.32)$$

Proof: Given in Appendix A.

**Proposition 4.4.3** Let a continuous-time control system have the Diophantine equation (3.26) which is composed of the polynomials  $\bar{u}(s)$  and  $\bar{v}(s)$  of degrees  $f = p - n$  and  $h < n - 1$ , respectively. Furthermore, suppose that the plant has irreducible transfer function and that  $p < 2n - 1$ . By multiplying the denominator of the continuous-time PITF, i.e.  $\bar{d}(s)$ , by a stable factor  $\bar{\phi}(s)$  of degree  $(2n - 1 - p) \leq c \leq (n - 1 - h)$ , one can form the following Diophantine equation, where  $\bar{u}_2(s)$  and  $\bar{v}_2(s)$ , of degrees set to  $f_2 = f + c$  and  $h_2 = h + c$ , respectively, are the unknowns:

$$\bar{u}_2(s)\bar{a}(s) + \bar{v}_2(s)\bar{b}(s) = \bar{\phi}(s) \cdot \bar{d}(s). \quad (4.33)$$

The unique solution to equation (4.33) is  $\bar{u}_2(s) = \bar{\phi}(s) \cdot \bar{u}(s)$  and  $\bar{v}_2(s) = \bar{\phi}(s) \cdot \bar{v}(s)$ .  $\bowtie$

Proof: Given in Appendix A.

Proof of Theorem 4.4.1: (i) Continuous-time control system. The main feature of a continuous-time control system is that the polynomials  $\bar{u}(s)$  and  $\bar{v}(s)$  given in (4.30)

uniquely solve a Diophantine equation of the form

$$\bar{u}(s)\bar{a}(s) + \bar{v}(s)\bar{b}(s) = \bar{d}(s) \quad (4.34)$$

provided the plant transfer function  $\bar{G}(s) = \bar{b}(s)/\bar{a}(s)$  is irreducible, as explained in the proof of Proposition 4.4.2. Then, the controller transfer functions can be recovered by using any equation among (4.35) to (4.37) whose unity block corresponds to that of, or to one of the unity blocks of, the given continuous-time control system:

1. If  $\bar{u}'(s)$  is stable,  $h' \leq f'$  and  $(q' - n) \leq f'$ , set

$$\bar{\Pi}(s) = \frac{\bar{m}'(s)}{\bar{u}'(s)}, \quad \bar{\Omega}(s) = 1, \quad \bar{\Gamma}(s) = \frac{\bar{v}'(s)}{\bar{u}'(s)}. \quad (4.35)$$

2. If  $\bar{m}'(s)$  is stable and  $h' \leq (q' - n) \leq f'$ , set

$$\bar{\Pi}(s) = 1, \quad \bar{\Omega}(s) = \frac{\bar{m}'(s)}{\bar{u}'(s)}, \quad \bar{\Gamma}(s) = \frac{\bar{v}'(s)}{\bar{m}'(s)}. \quad (4.36)$$

3. If  $\bar{v}'(s)$  is stable and  $(q' - n) \leq h' \leq f'$ , set

$$\bar{\Pi}(s) = \frac{\bar{m}'(s)}{\bar{v}'(s)}, \quad \bar{\Omega}(s) = \frac{\bar{v}'(s)}{\bar{u}'(s)}, \quad \bar{\Gamma}(s) = 1. \quad (4.37)$$

In equations (4.35) to (4.37),  $\bar{u}'(s)$  either corresponds to  $\bar{u}(s)$  or  $\bar{\phi}(s) \cdot \bar{u}(s)$  depending on the degree  $p$ , and similarly for  $\bar{v}'(s)$  in terms of  $\bar{v}(s)$  or  $\bar{\phi}(s) \cdot \bar{v}(s)$ . The multiplication by the stable polynomial  $\bar{\phi}(s)$ , of degree  $(2n - 1 - p) \leq c \leq (n - 1 - h)$ , should take place when  $p < 2n - 1$ . The relationship between the various solution polynomials is given by Propositions 4.4.2 and 4.4.3. Also note that for the case  $p < 2n - 1$ , the polynomial  $\bar{\phi}(s)$  should also multiply the numerator of the continuous-time PITF to yield  $\bar{m}'(s) = \bar{\phi}(s)\bar{m}(s)$ . Thus, in the equations,  $\bar{m}'(s)$  either corresponds to  $\bar{m}(s)$  or  $\bar{\phi}(s) \cdot \bar{m}(s)$  depending on  $p$ . The degrees involved in equations (4.35) to (4.37) are as

follows:  $h'$  is the degree of  $\bar{v}'(s)$ ,  $f'$  is the degree of  $\bar{u}'(s)$ , and  $(q' - n)$  is the degree of  $\bar{m}'(s)$ .

(ii) Discrete-time control system obtained with the regular PIM method. The degree of  $d(\varepsilon)$  in the discrete-time Diophantine equation (3.9) is assumed to be correctly set for the use of the eliminant matrix method; that is, the continuous-time system has been modified to meet the requirement  $p \geq 2n - 1$ , if necessary, in the second step of the regular PIM method. This means that the polynomials  $u(\varepsilon)$  and  $v(\varepsilon)$  have the same degrees as the polynomials  $\bar{u}'(s)$  and  $\bar{v}'(s)$ , respectively, which are introduced in part (i) of the proof. Then, from Proposition 4.4.1, each coefficient of  $u(\varepsilon)$  approaches the coefficient of  $\bar{u}'(s)$  of corresponding power of  $s$ , and similarly for  $v(\varepsilon)$  with respect to  $\bar{v}'(s)$ , as  $T \rightarrow 0$ . Furthermore, since the regular PIM method provides convergence of  $H_T(\varepsilon)$  to  $\bar{H}(s)$ , in the transfer function sense, if one writes  $H_T(\varepsilon) = m(\varepsilon)a(\varepsilon)/d(\varepsilon)$ , each coefficient of  $m(\varepsilon)$  approaches that of the corresponding power of  $s$  in  $\bar{m}(s)$ , or  $\bar{m}'(s)$ , depending on the case, as  $T \rightarrow 0$ .

When one or two non-unity controller blocks are present in the continuous-time control system, any of (3.13) to (3.15) can be used to obtain the discrete-time controllers as long as the conditions of application of the equations are met and each non-unity continuous-time controller has a non-unity discrete-time counterpart. Since the polynomials present in these equations have each of their coefficients approaching that of the corresponding power of  $s$  in the corresponding polynomial of the continuous-time system, as  $T \rightarrow 0$ , the controller convergence in the transfer function is obtained.  $\square$

Theorem 4.4.2 provides the conditions to achieve convergence in the transfer function of each discrete-time block to its continuous-time counterpart when the 3-block discrete-time implementation is chosen.

**Theorem 4.4.2** When the regular PIM method is applied to the continuous-time control system of Figure 1.4(a), which has one, two or three non-unity control blocks and a plant with irreducible transfer function, each discrete-time controller converges in the transfer function to its continuous-time counterpart, as  $T \rightarrow 0$ , if, in the fourth step of the

PIM method and for each non-pathological  $T$  selected, the eliminant matrix method is used to solve the Diophantine equation and the discrete-time controllers can be calculated with (3.12), where each coefficient of the polynomial  $w(\varepsilon)$  approaches the corresponding coefficient of a polynomial defined as  $\bar{w}(s) = \bar{n}_1(s)\bar{d}_2(s)\bar{d}_3(s)$ , provided  $\bar{\Omega}(s)$  is minimum-phase and  $\bar{\Gamma}(s)$  is stable.  $\blacktriangleright$

Proof: (i) Continuous-time control system. Following the rationale of the proof of Theorem 4.4.1, by letting  $\bar{w}(s) = \bar{n}_1(s)\bar{d}_2(s)\bar{d}_3(s)$ , the controller transfer functions can be recovered by using

$$\bar{\Pi}(s) = \frac{\bar{m}'(s)}{\bar{w}'(s)}, \quad \bar{\Omega}(s) = \frac{\bar{w}'(s)}{\bar{u}'(s)}, \quad \bar{\Gamma}(s) = \frac{\bar{v}'(s)}{\bar{w}'(s)}. \quad (4.38)$$

In the equations,  $\bar{u}'(s)$ ,  $\bar{v}'(s)$  and  $\bar{m}'(s)$  are defined as in part (i) of the proof of Theorem 4.4.1, whereas  $\bar{w}'(s)$  either corresponds to  $\bar{w}(s)$  or  $\bar{\phi}(s) \cdot \bar{w}(s)$  depending on the degree  $p$ . When  $p < 2n - 1$ ,  $\bar{d}(s)$ ,  $\bar{w}(s)$  and  $\bar{m}(s)$  should be multiplied by a stable factor  $\bar{\phi}(s)$ , of degree  $(2n - 1 - p) \leq c \leq (n - 1 - h)$ . From Propositions 4.4.2 and 4.4.3,  $\bar{u}'(s) = \bar{\phi}(s)\bar{u}(s)$  and  $\bar{v}'(s) = \bar{\phi}(s)\bar{v}(s)$ .

(ii) Discrete-time control system obtained with the regular PIM method. The 3-block discrete-time implementation should be chosen if three controllers are present in the continuous-time control system or if none of (3.13) to (3.15) has its conditions satisfied. For this, define  $w(\varepsilon) = n_1(\varepsilon)d_2(\varepsilon)d_3(\varepsilon)$  or  $w'(\varepsilon) = \phi(\varepsilon)w(\varepsilon)$ , depending on the original continuous-time PITF, as stable polynomials of degrees equal to those of  $\bar{w}(s) = \bar{n}_1(s)\bar{d}_2(s)\bar{d}_3(s)$  or  $\bar{w}'(s) = \bar{\phi}(s)\bar{w}(s)$ . Let each coefficient of  $\phi(\varepsilon)$ ,  $n_1(\varepsilon)$ ,  $d_2(\varepsilon)$  and  $d_3(\varepsilon)$  approach that of the corresponding power of  $s$  in  $\bar{\phi}(s)$ ,  $\bar{n}_1(s)$ ,  $\bar{d}_2(s)$  and  $\bar{d}_3(s)$ , respectively, as  $T \rightarrow 0$ . Equation (3.12) then serves to calculate the discrete-time controller blocks with the appropriate polynomial  $w(\varepsilon)$  or  $w'(\varepsilon)$  utilized. Since  $m(\varepsilon) \rightarrow \bar{m}(s)$ , or  $m(\varepsilon) \rightarrow \bar{m}'(s)$  depending on  $p$ ,  $w(\varepsilon) \rightarrow \bar{w}(s)$ ,  $w'(\varepsilon) \rightarrow \bar{w}'(s)$ ,  $u(\varepsilon) \rightarrow \bar{u}'(s)$  and  $v(\varepsilon) \rightarrow \bar{v}'(s)$ , as  $T \rightarrow 0$ , in terms of their polynomial coefficients, for instance each coefficient of  $m(\varepsilon)$  approaches the corresponding coefficient of  $\bar{m}(s)$ , the convergence in the

transfer function of each discrete-time controller block to its continuous-time counterpart is assured.

It must be emphasized that the conditions pertaining to  $\bar{\Omega}(s)$  being minimum-phase and  $\bar{\Gamma}(s)$  being stable concern the internal stability of the discrete-time closed-loop system at relatively short sampling intervals since some roots of  $w(\varepsilon)$  approach the zeros of  $\bar{\Omega}(s)$  whereas some other roots approach the poles of  $\bar{\Gamma}(s)$ , as  $T \rightarrow 0$ . If the aforementioned conditions on  $\bar{\Omega}(s)$  and  $\bar{\Gamma}(s)$  are not satisfied, the closed-loop sampled-data system is not internally stable at the sampling instants.  $\square$

For the truncated PIM method, when the conditions of Theorems 4.4.1 and 4.4.2 are satisfied, each discrete-time block converges in the transfer function to its continuous-time counterpart. For the reduced-order PIM method, with the convergence of the polynomials  $u(\varepsilon)$  and  $v(\varepsilon)$  to  $\bar{u}(s)$  and  $\bar{v}(s)$ , respectively, in terms of the coefficients, and the conditions of Theorems 4.4.1 and 4.4.2 satisfied, except for the Diophantine equation which is solved with the least-squares method instead of the eliminant matrix method, each discrete-time controller converges in the transfer function to its continuous-time counterpart. Knowing the convergence of the blocks for the reduced-order and truncated PIM methods, the convergence of the controllers obtained with the reduced-order plus truncated PIM method is obvious.

### 4.4.3 Loop Signal Convergence

Knowing the convergence in the transfer function of each discrete-time controller block, the time-domain behavior of the loop signals as  $T \rightarrow 0$  can be determined. The following theorem establishes the conditions which guarantee the uniform-in-time convergence of the loop signals of a digitally redesigned control system to the corresponding signals in the continuous-time control system.

**Theorem 4.4.3** Sufficient conditions to assure uniform-in-time convergence of the loop signals  $p_T(t)$ ,  $v_T(t)$  and  $e_T(t)$  of the digitally redesigned control system of Figure 4.1(b) to respectively  $\bar{p}(t)$ ,  $\bar{v}(t)$  and  $\bar{e}(t)$  of the linear, time-invariant continuous-time system

of Figure 4.1(a) are that: (i) the reference input is in  $\mathcal{S}_1$  or is a staircase equivalent of a signal in  $\mathcal{S}_1$ , (ii) the continuous-time and sampled-data control systems are internally stable at the sampling instants, and (iii) the discrete-time controllers converge in the transfer function to their continuous-time counterpart.  $\infty$

The following proposition is used in the proof of Theorem 4.4.3.

**Proposition 4.4.4** Consider a general discrete-time system

$$W_T(\varepsilon) = \frac{(\bar{a}_n + \Delta a_n) \varepsilon^n + (\bar{a}_{n-1} + \Delta a_{n-1}) \varepsilon^{n-1} + \cdots + (\bar{a}_0 + \Delta a_0)}{\varepsilon^n + (\bar{b}_{n-1} + \Delta b_{n-1}) \varepsilon^{n-1} + \cdots + (\bar{b}_0 + \Delta b_0)} \quad (4.39)$$

where the  $\bar{a}_j$ s and  $\bar{b}_j$ s are the coefficients of the transfer function of a continuous-time system given as

$$\bar{W}(s) = \frac{\bar{a}_n s^n + \bar{a}_{n-1} s^{n-1} + \cdots + \bar{a}_0}{s^n + \bar{b}_{n-1} s^{n-1} + \cdots + \bar{b}_0}. \quad (4.40)$$

Then

$$\lim_{T \rightarrow 0} \Delta a_j = 0 \text{ and } \lim_{T \rightarrow 0} \Delta b_j = 0 \text{ for } j = 0, 1, \dots, n \quad (4.41)$$

if and only if there exists at least one realization of  $W_T(\varepsilon)$  with elements  $(\bar{A} + \Delta A)$ ,  $(\bar{B} + \Delta B)$ ,  $(\bar{C} + \Delta C)$  and  $(\bar{D} + \Delta D)$ , where  $[\bar{A}, \bar{B}, \bar{C}, \bar{D}]$  are the elements of a realization of the system  $\bar{W}(s)$ , such that

$$\begin{aligned} \lim_{T \rightarrow 0} \Delta A &= 0_{n \times n}, & \lim_{T \rightarrow 0} \Delta B &= 0_{n \times 1} \\ \lim_{T \rightarrow 0} \Delta C &= 0_{1 \times n}, & \lim_{T \rightarrow 0} \Delta D &= 0_{1 \times 1}. \infty \end{aligned} \quad (4.42)$$

Proof: Given in Appendix A.  $\square$

Proof of Theorem 4.4.3: (i)  $v_T(t)$ : Write the transfer function relating  $R_T(\varepsilon)$  to  $V_T(\varepsilon)$  as

$$\frac{V_T(\varepsilon)}{R_T(\varepsilon)} = \frac{\Gamma_T(\varepsilon)G_T(\varepsilon)\Omega_T(\varepsilon)\Pi_T(\varepsilon)}{1 + \Gamma_T(\varepsilon)G_T(\varepsilon)\Omega_T(\varepsilon)} \quad (4.43)$$

and proceed similarly for the continuous-time transfer function relating  $\bar{V}(s)$  to  $\bar{R}(s)$ .

When each discrete-time block has the same order as that of its continuous-time counterpart, as is the case when discretizing each continuous-time block to obtain equi-order discrete-time models, the conditions of the theorem assure uniform-in-time convergence of  $v_T(t)$  to  $\bar{v}(t)$  by using Proposition 4.4.4, and a variant of Theorem 4.3.1. When some, or all, discrete-time blocks have order larger than their continuous-time counterpart, by  $n^*$ , while they converge in transfer function to these according to Definition 4.4.1, one can multiply the continuous-time blocks concerned with such convergence by a stable biproper transfer function with identical sets of poles and zeros, such as

$$\frac{\bar{d}_n \cdot s^{n^*} + \cdots + \bar{d}_1 s + \bar{d}_0}{\bar{d}_n \cdot s^{n^*} + \cdots + \bar{d}_1 s + \bar{d}_0}$$

in reference to Definition 4.4.1. Performing such modifications to the continuous-time control system does not affect the input-output behavior of each continuous-time block and is done strictly for demonstrative purposes. Then, Proposition 4.4.4 and a variant of Theorem 4.3.1 can be applied and the uniform-in-time convergence demonstrated.

(ii)  $e_T(t)$  : Perform the same process as in (i) except that the transfer function relating  $R_T(\varepsilon)$  to  $E_T(\varepsilon)$ ,

$$\frac{E_T(\varepsilon)}{R_T(\varepsilon)} = \frac{\Pi_T(\varepsilon)}{1 + \Gamma_T(\varepsilon)G_T(\varepsilon)\Omega_T(\varepsilon)}, \quad (4.44)$$

is now considered.

(iii)  $p_T(t)$  : The signal can be expressed as  $p_T = H\Pi_T S\bar{r}$ , where the hold  $H$  is the ZOH,  $\bar{r} \in \mathcal{S}_1$  or is a staircase equivalent of a signal in  $\mathcal{S}_1$ , and  $\Pi_T(\varepsilon)$  has all its poles within the stability region of the  $\varepsilon$ -plane for each  $T$  selected. Two cases are possible, either  $\bar{\Pi}(s)$  is a dynamic block and  $\Pi_T(\varepsilon)$  converges in transfer function to this system, or  $\bar{\Pi}(s) = \bar{K}$  and  $\Pi_T(\varepsilon)$  converges to this non-zero gain. For the former case, one can perform a process similar to that carried out in part (i), except that the system  $\Pi_T(\varepsilon)$  replaces the system relating  $R_T(\varepsilon)$  to  $V_T(\varepsilon)$ . For the latter case, the continuous-time signal can be written as  $\bar{p}(t) = \bar{K} \cdot \bar{r}(t)$ . The discrete-time block can be realized as  $\Pi_T(\varepsilon) = [A_\Pi, B_\Pi, C_\Pi, D_\Pi]$ , where  $\lim_{T \rightarrow 0} \|C_\Pi\| = 0$  and  $\lim_{T \rightarrow 0} D_\Pi = \bar{K}$  from the convergence of  $\Pi_T(\varepsilon)$  to  $\bar{K}$ . The

lifted form of  $p_T(t)$  is given by

$$\widehat{p}_{k,T}(\tau) = \sum_{j=0}^{k-1} C_{\Pi}(TA_{\Pi} + I)^{k-j-1} \cdot TB_{\Pi}\widehat{r}_{j,T}(0) + D_{\Pi} \cdot \widehat{r}_{k,T}(0). \quad (4.45)$$

Therefore, using the lifted form of the signal  $\bar{p}(t)$ , one can write

$$\left| \widehat{p}_{k,T}(\tau) - \widehat{\bar{p}}_{k,T}(\tau) \right| = \left| \sum_{j=0}^{k-1} C_{\Pi}(TA_{\Pi} + I)^{k-j-1} \cdot TB_{\Pi}\widehat{r}_{j,T}(0) + D_{\Pi} \cdot \widehat{r}_{k,T}(0) - \bar{K} \cdot \widehat{r}_{k,T}(\tau) \right|. \quad (4.46)$$

Taking the limit on a bound on the supremum yields

$$\begin{aligned} & \limsup_{T \rightarrow 0} \left\{ \sup_{k \geq 0} \left\{ \sup_{0 \leq \tau < T} \left| \widehat{p}_{k,T}(\tau) - \widehat{\bar{p}}_{k,T}(\tau) \right| \right\} \right\} \\ & \leq \lim_{T \rightarrow 0} \|C_{\Pi}\| \cdot \|B_{\Pi}\| \sum_{j=0}^{\infty} \|(TA_{\Pi} + I)^j\| \cdot T \cdot r_b \\ & \quad + \limsup_{T \rightarrow 0} \left\{ \sup_{k \geq 0} \left\{ \sup_{0 \leq \tau < T} \left| D_{\Pi} \cdot \widehat{r}_{k,T}(0) - \bar{K} \cdot r_{k,T} - \bar{K} \omega_{k,T}(\tau) \right| \right\} \right\} \end{aligned} \quad (4.47)$$

where  $r_b$  is the supremum of the reference input and  $\widehat{r}_{k,T}(\tau) = r_{k,T} + \omega_{k,T}(\tau)$ , for  $0 \leq \tau < T$ , with the meaning of the variable component of  $\widehat{r}_{k,T}(\tau)$ , i.e.  $\omega_{k,T}(\tau)$ , being more easily understood by looking at Figure A.1 in Appendix A. Simplifying:

$$\begin{aligned} & \limsup_{T \rightarrow 0} \left\{ \sup_{k \geq 0} \left\{ \sup_{0 \leq \tau < T} \left| \widehat{p}_{k,T}(\tau) - \widehat{\bar{p}}_{k,T}(\tau) \right| \right\} \right\} \\ & \leq \lim_{T \rightarrow 0} \|C_{\Pi}\| \cdot \|B_{\Pi}\| \cdot \sum_{j=0}^{\infty} \|(TA_{\Pi} + I)^j\| \cdot T \cdot r_b \\ & \quad + \lim_{T \rightarrow 0} |D_{\Pi} - \bar{K}| \cdot r_b + |\bar{K}| \cdot \limsup_{T \rightarrow 0} \left\{ \sup_{k \geq 0} \left\{ \sup_{0 \leq \tau < T} |\omega_{k,T}(\tau)| \right\} \right\}. \end{aligned} \quad (4.48)$$

The limiting behavior of  $\omega_{k,T}(\tau)$  is given as

$$\lim_{T \rightarrow 0} \sup_{0 \leq k < \infty} \left\{ \sup_{0 \leq \tau < T} |\omega_{k,T}(\tau)| \right\} = 0 \quad (4.49)$$

when the reference input is in  $\mathcal{S}_1$ , or as

$$\sup_{0 \leq k < \infty} \left\{ \sup_{0 \leq \tau < T} |\omega_{k,T}(\tau)| \right\} = 0, \quad \forall T \quad (4.50)$$

when the reference input is a staircase equivalent of a signal in  $\mathcal{S}_1$ — see Proposition A.1 in Appendix A. Then, with a sufficiently small sampling period, each term on the right-hand side of (4.48) can be made as small as desired.  $\square$

## 4.5 Robustness Characteristics of PIM-Based Sampled-Data Control Systems as $T \rightarrow 0$

The PIM methods revolve around the transfer function from the reference input to the control input without considering other characteristics of closed-loop systems such as disturbance rejection and sensitivity to changes in parameters of the controllers and plant. On the other hand, sampled-data control systems obtained with the local digital redesign methods possess robustness properties, perceived in discrete-time, which can be shown to approach those of the continuous-time control system as  $T$  is reduced. In order to guarantee known behaviors for the disturbance responses and sensitivities of PIM-based sampled-data systems, at least as  $T \rightarrow 0$ , the following developments show that it is required that the solution to the discrete-time Diophantine equation approaches that of the continuous-time equation, in some sense, as the sampling period is reduced.

The discrete-time sensitivity functions are first investigated. Then, the behavior in the time-domain of the disturbance responses of a digitally redesigned control system is assessed for the case when the sampling interval is made arbitrarily small.

### 4.5.1 Sensitivity to Controller and Plant Uncertainties

Consider the closed-loop transfer functions  $\bar{M}(s)$ , which relates  $\bar{R}(s)$  to  $\bar{Y}(s)$  as shown in Figure 1.4(a), and  $M_T(\varepsilon)$ , which relates  $R_T(\varepsilon)$  to  $Y_T(\varepsilon)$  in Figure 1.4(b), i.e.  $M_T \triangleq$

$S\overline{G}HH_T S$ , where  $Y_T(\varepsilon)$  denotes the Delta transform of the sampled controlled output; that is,

$$Y_T(\varepsilon) = \mathcal{D} \{ \widehat{y}_{k,T}(0) \} = \sum_{k=0}^{\infty} \widehat{y}_{k,T}(0) (T\varepsilon + 1)^{-k} T. \quad (4.51)$$

The sensitivities to variations in the plant transfer functions  $\overline{G}(s)$  and  $G_T(\varepsilon)$  are given by  $\overline{S}_{\overline{G}}^{\overline{M}}(s) = 1/(1 + \overline{\Omega}(s)\overline{\Gamma}(s)\overline{G}(s))$  for the continuous-time system and as  $S_{G_T}^{M_T}(\varepsilon) = 1/(1 + \Omega_T(\varepsilon)\Gamma_T(\varepsilon)G_T(\varepsilon))$  for the discrete-time system. Similarly, the sensitivities of the closed-loop systems to small changes in the controller block transfer functions are given as:

$$\overline{S}_{\overline{H}}^{\overline{M}}(s) = 1, \quad \overline{S}_{\overline{\Omega}}^{\overline{M}}(s) = \overline{S}_{\overline{G}}^{\overline{M}}(s), \quad \overline{S}_{\overline{\Gamma}}^{\overline{M}}(s) = \frac{-\overline{\Omega}(s)\overline{G}(s)\overline{\Gamma}(s)}{1 + \overline{\Omega}(s)\overline{\Gamma}(s)\overline{G}(s)} \quad (4.52)$$

$$S_{\Pi_T}^{M_T}(\varepsilon) = 1, \quad S_{\Omega_T}^{M_T}(\varepsilon) = S_{G_T}^{M_T}(\varepsilon), \quad S_{\Gamma_T}^{M_T}(\varepsilon) = \frac{-\Omega_T(\varepsilon)G_T(\varepsilon)\Gamma_T(\varepsilon)}{1 + \Omega_T(\varepsilon)\Gamma_T(\varepsilon)G_T(\varepsilon)}. \quad (4.53)$$

The next theorem gives the relationships between the discrete-time and continuous-time sensitivities, as  $T \rightarrow 0$ .

**Theorem 4.5.1** Consider a general 3-block sampled-data control system shown in Figure 1.4(b) which has been obtained by performing the regular, the truncated, the reduced-order or the reduced-order plus truncated PIM method on the system of Figure 1.4(a). When the coefficients of the solution polynomials  $u(\varepsilon)$  and  $v(\varepsilon)$  of the discrete-time Diophantine equation (3.9) converge to those of  $\overline{u}(s)$  and  $\overline{v}(s)$ , respectively, of (3.26), or to those of the modified version of the equation when  $p < 2n - 1$ , each discrete-time sensitivity function, as given by (4.53), converges in the transfer function to the corresponding sensitivity function of the continuous-time control system, given by (4.52), as  $T \rightarrow 0$ .  $\square$

Proof: The proof is shown for  $S_{\Omega_T}^{M_T}(\varepsilon)$  and  $S_{\Gamma_T}^{M_T}(\varepsilon)$ . First, for  $S_{\Omega_T}^{M_T}(\varepsilon)$ ,

$$\begin{aligned} S_{\Omega_T}^{M_T}(\varepsilon) &= \frac{1}{1 + \Omega_T(\varepsilon)\Gamma_T(\varepsilon)G_T(\varepsilon)} \\ &= \frac{u(\varepsilon)a(\varepsilon)}{u(\varepsilon)a(\varepsilon) + v(\varepsilon)b(\varepsilon)} \end{aligned} \quad (4.54)$$

whatever is the implementation chosen among equations (3.12) to (3.15) and (3.23) to (3.25). On the other hand,

$$\begin{aligned}\bar{S}_{\bar{\Omega}}^{\bar{M}}(s) &= \frac{1}{1 + \bar{\Omega}(s)\bar{\Gamma}(s)\bar{G}(s)} \\ &= \frac{\bar{u}(s)\bar{a}(s)}{\bar{u}(s)\bar{a}(s) + \bar{v}(s)\bar{b}(s)}\end{aligned}\quad (4.55)$$

where  $\bar{u}(s)$  and  $\bar{v}(s)$  come from (3.26), or a modified version of the equation, and have the same degrees as those of  $u(\varepsilon)$  and  $v(\varepsilon)$ , respectively. With each coefficient of  $u(\varepsilon)$  approaching its counterpart in  $\bar{u}(s)$ , and similarly for  $v(\varepsilon)$ , and knowing that each coefficient of the numerator and denominator polynomials of the transfer function of the hold-equivalent model of the plant approaches that of the plant transfer function, as  $T \rightarrow 0$ , the convergence in the transfer function is immediate. Second, for  $S_{\Gamma T}^{M_T}(\varepsilon)$ ,

$$S_{\Gamma T}^{M_T}(\varepsilon) = \frac{-v(\varepsilon)b(\varepsilon)}{u(\varepsilon)a(\varepsilon) + v(\varepsilon)b(\varepsilon)}\quad (4.56)$$

and

$$\bar{S}_{\bar{\Gamma}}^{\bar{M}}(s) = \frac{-\bar{v}(s)\bar{b}(s)}{\bar{u}(s)\bar{a}(s) + \bar{v}(s)\bar{b}(s)}.\quad (4.57)$$

The convergence in the transfer function is shown by using the same arguments as for the case of  $S_{\Omega T}^{M_T}(\varepsilon)$ .  $\square$

## 4.5.2 Responses to Disturbance Input

Assume that the reference input is zero, i.e.  $\bar{r}(t) = 0$  for all  $t \in [0, \infty)$ , and the only non-zero exogenous input to the closed-loop continuous-time and sampled-data control systems is a disturbance  $\bar{d}(t)$  which lies in  $S_1$  or is a staircase equivalent of a signal in  $S_1$ . The disturbance enters the sampled-data control system as shown in Figure 4.2(a), where  $H$  is the ZOH. The reformulation of the system is shown in Figure 4.2(b), where the reference input is discarded. A similar reformulation can be carried out for the continuous-time control system.

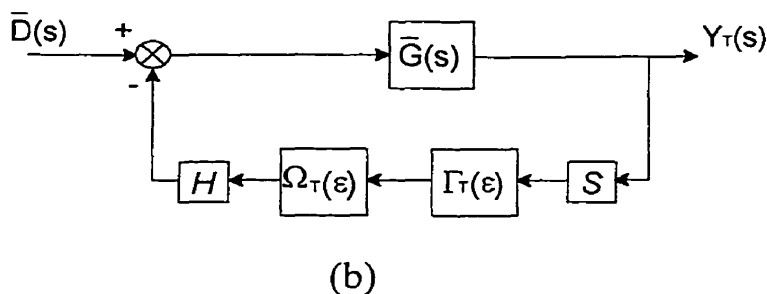
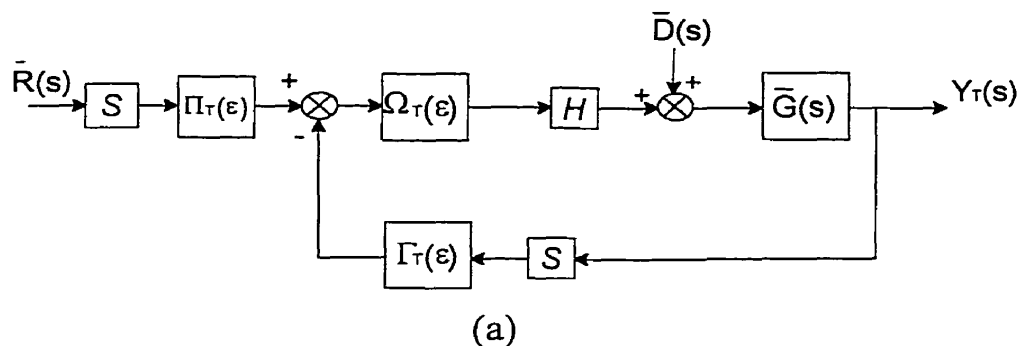


Figure 4.2: Disturbance input to sampled-data control system

The next theorem establishes sufficient conditions to achieve uniform-in-time convergence of the plant input and output of the sampled-data control system to those signals of the continuous-time control system, as the sampling rate is increased, when the reference input is zero and a disturbance is applied to both control systems.

**Theorem 4.5.2** Consider a sampled-data control system which is internally stable at the sampling instants, and has been obtained with the regular, the truncated, the reduced-order or the reduced-order plus truncated PIM method. Suppose that the reference input to this system is set to zero over all time instants and that the hold at control input is the ZOH. If the coefficients of the solution polynomials  $u(\epsilon)$  and  $v(\epsilon)$  of the discrete-time Diophantine equation converge to those of  $\bar{u}(s)$  and  $\bar{v}(s)$ , respectively, of (3.26), or to those of the modified version of the equation when  $p < 2n - 1$ , and if the fixed disturbance input  $\bar{d}(t)$  lies in  $S_1$  or is a staircase equivalent of a signal in  $S_1$ ,

the control input and controlled output converge uniformly in time, as  $T \rightarrow 0$ , to those corresponding signals of the internally stable continuous-time control system which is subjected to the same disturbance.  $\square$

Proof: The lifted form of the disturbance input is denoted as  $d_{k,T} + \omega_{d,k,T}(\tau)$  for  $k \geq 0$  and  $\tau \in [0, T)$ , where  $d_{k,T}$  is the staircase equivalent of the disturbance signal and  $\omega_{d,k,T}(\tau)|_{\tau=0} = 0$ . Equation (4.49) applies to  $\omega_{d,k,T}(\tau)$  when  $\bar{d}(t)$  lies in  $S_1$ , whereas equation (4.50) holds true for  $\omega_{d,k,T}(\tau)$  when the reference input is a staircase equivalent of a signal in  $S_1$  (see Proposition A.1 for the proof). From the linearity of the systems, the disturbance response can be expressed as the sum of the outputs due to the staircase equivalent of the disturbance and the intersample signal  $\omega_{d,k,T}(\tau)$ . With the assumption on the stability of the systems and the behavior of  $\omega_{d,k,T}(\tau)$ , the supremum norms at control input and controlled output, which are due to  $\omega_{d,k,T}(\tau)$ , can be made arbitrarily close to zero with a sufficiently small sampling period. Concerning the responses due to the staircase equivalent of the disturbance, the sampled-data control system can be reformulated as in Figure 4.3.

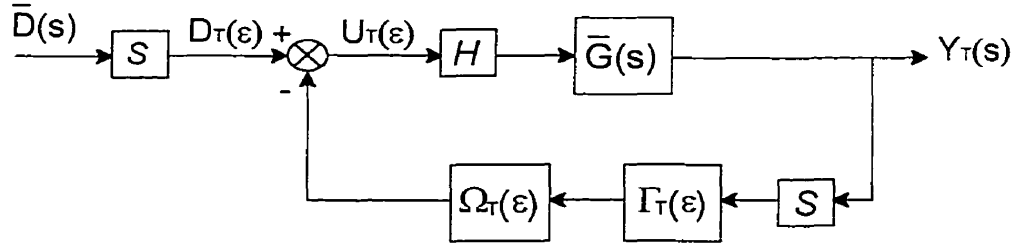


Figure 4.3: Disturbance as a staircase equivalent

The transfer function from the sampled disturbance input to the discrete-time control input is

$$\begin{aligned} \frac{U_T(\epsilon)}{D_T(\epsilon)} &= S_{G_T}^{M_T}(\epsilon) \\ &= \frac{u(\epsilon)a(\epsilon)}{u(\epsilon)a(\epsilon) + v(\epsilon)b(\epsilon)} \end{aligned} \quad (4.58)$$

for all the controller equations (3.12) to (3.15) and (3.23) to (3.25). It is clear that the discrete-time transfer function converges to its continuous-time counterpart as  $T$  is reduced with the conditions set forth in the theorem. If this is so, there exists a realization for the discrete-time system whose elements approach the corresponding elements of the continuous-time system, according to Proposition 4.4.4. Using a variant of Theorem 4.3.1, where the disturbance to control input transfer function replaces the reference to control input transfer function and  $\bar{d}(t)$  is applied to the continuous-time and sampled-data systems, the control input and controlled output of the sampled-data control system converge uniformly in time to their continuous-time counterpart.  $\square$

With the above theorem satisfied, the systems relating the disturbance input to the control input and the controlled output can be considered as sampled-data models of their continuous-time counterparts.

## 4.6 Performance Evaluation of Sampled-Data Control Systems

In this section, three means of evaluating the performance of digitally redesigned control systems, for any non-pathological sampling interval, are presented from a time-domain perspective. These are: (i) norms of control-input and controlled-output errors between the continuous-time and sampled-data control systems; (ii) induced norms, or system gains, of sampled-data control systems; and (iii) ITAE index on the control-input and controlled-output error signals.

These performance measures are motivated by the practical usefulness of bounding the energy and maximum magnitude of a signal and by the simplicity in generating plots of performance, i.e. a scalar, versus sampling period. On the one hand, norms and ITAE index on the control-input and controlled-output errors are especially useful when one wants to bound the error signals, and is interested in knowing for what range of sampling periods the response of a sampled-data system remains within a specified

tolerance of that of the continuous-time system. On the other hand, induced norms provide least upper bounds on the energy and maximum magnitude of a signal, given an input with known norm, and thus their use is relevant in that sense. Generally, since the continuous-time control system is assumed to perform in a satisfactory fashion, the preferred sampled-data control system is the one whose performances are the closest to those of the continuous-time control system according to the quantification means put forward in this section.

A practical example of the use of norms in sampled-data control is when one wants to be able to guarantee that the threshold of control input magnitudes, which can be restrained for instance because of actuators and saturation consideration, is not violated. In such a case, the problem becomes one of determining the range of sampling periods such that a sampled-data control system has a control input response within the tolerance. Additional examples of the use of norms and ITAE index are: (i) to determine the range of sampling periods for a sampled-data control system to reject input disturbances with values of norm and ITAE index on the controlled output response being smaller than a prescribed magnitude; (ii) to distinguish among the digital redesign methods tested which ones possess a tracking error within a desired tolerance for a given sampling period; and (iii) to obtain the range of sampling periods for which each digital redesign method offers control-input and controlled-output error norms and index smaller than or equal to fixed values.

At the end of the section, a time-domain characterization of the control-input and controlled-output errors between sampled-data and continuous-time control systems is established in order to complement the performance measures aforementioned. In particular, the effect of the movement of the closed-loop discrete-time poles with increasing  $T$  on the responses of sampled-data control systems is clarified.

### 4.6.1 Norms of Control-Input and Controlled-Output Error Signals

A designer often wants to know the range of  $T$  values which can be used in a digital redesign process such that upper bounds on the error signal's  $L^2$  and  $L^\infty$  norms, as defined in Section 1.2, are satisfied with the digitally redesigned control systems. Such preoccupation may arise for practical reasons, such as actuator saturation, and/or performance requirements, such as a relative closeness among the responses. The norms are an indication of the deterioration of performance obtained with a digitally redesigned control system from that of a continuous-time control system. Being able to determine the range of sampling frequencies for which this deterioration is tolerable is one goal that can be accomplished by using the  $L^2$  and  $L^\infty$  norms. The following theorem provides a general rule that distinguishes among the regular PIM-based and locally redesigned control systems. It should be noted that the restrictions on the admissible reference input, defined in Section 4.3, apply to Theorem 4.6.1.

**Theorem 4.6.1** For a sampled-data model of a continuous-time control system obtained with the regular PIM method, or its truncated version, associated with each finite, non-pathological sampling period is a finite, prescribed value  $\beta > 0$  on the  $L^2$  and  $L^\infty$  norms of the control-input and controlled-output error signals. On the other hand, for sampled-data models obtained with a local digital redesign, there is an upper limit on the value of  $T$ ,  $T < T_\beta$ , such that a finite bound  $\beta$  can be met.  $\times$

Proof: For sampled-data models obtained with the local digital redesign, from Theorem 4.2.2,  $T_\beta = T^*$ , where  $T^*$  is the critical sampling period below which the sampled-data system is internally stable at the sampling instants. If  $0 < T < T^*$ , any non-zero, finite bound can be met, from the definition of a sampled-data model. For sampled-data models obtained with the regular PIM method, or its truncated version, since the closed-loop discrete-time poles lie in the stable region of the discrete-time plane for all finite, non-pathological  $T$  selected, finite bounds on the norms at control input and controlled

output can be established for each fixed  $T$ .  $\square$

**Remark 4.6.1** Theorem 4.6.1 does not say that any finite bound on the norm of an error signal can be met by a PIM-based system for sampling periods at which sampled-data control systems obtained with the local digital redesign methods are unstable. For a particular control system and for sampling intervals which are relatively long, it is possible that the error signal norms calculated for the PIM-based systems, although finite, be larger than what is acceptable.

For sampled-data systems obtained with the reduced-order, and reduced-order plus truncated PIM methods, unless the sampling period is sufficiently small, no guarantee exists that a finite bound  $\beta$  can be met.

## 4.6.2 Induced Norm

In general, the gains of a digitally redesigned control system should be relatively close to those of the continuous-time control system, for a given  $T$ , since then characteristics of the sampled-data system such as disturbance rejection, maximum magnitude at control input and at controlled output, and energy of control input and controlled output signals can be as close as desired to those of the continuous-time control system. Knowing that the continuous-time control system performs in a satisfactory fashion for the aforementioned aspects, then so is the sampled-data control system.

The induced norm computations for systems relating reference and disturbance inputs to control input and controlled output for a given sampling period are well established. For instance, the  $L^\infty$ -induced norm of an internally stable sampled-data control system, such as  $\overline{G}HH_T S$ , can be obtained according to an algorithm described in [62], whereas a method to obtain the  $L^2$ -induced norm of a system such as  $\overline{G}HH_T S$  can be found in [20]. The novelty of this subsection is the establishment of conditions which guarantee that the  $L^2$ - and  $L^\infty$ -induced norms of a digitally redesigned sampled-data control system approach, as  $T \rightarrow 0$ , those respective induced norms of the continuous-time control system from which the digital redesign originates, and the explanation of the difference

in the induced norms between the regular PIM method, and its truncated version, and the local digital redesign methods for relatively large sampling periods.

The  $L^\infty$ -induced norm is first considered, followed by the  $L^2$ -induced norm.

### $L^\infty$ -Induced Norm

Theorem 4.6.2 establishes the behavior, as  $T \rightarrow 0$ , of the  $L^\infty$ -induced norm of the sampled-data system  $HH_T S$ , as shown on Figure 1.4(b). In the theorem, the admissible inputs are those which lie in  $\mathcal{S}_0$  or are staircase equivalents of signals in  $\mathcal{S}_0$ . It should be noted that the theorem applies as well to the sampled-data system which relates the disturbance input to the control input when the disturbance input is confined to be a staircase equivalent of a signal in  $\mathcal{S}_0$ , as shown on Figure 4.2(a). In that case, the sampled-data control system can be reformulated as in Figure 4.3.

**Theorem 4.6.2** Consider a linear, time-invariant discrete-time system  $H_T = [A, B, C, D]$  with sampling period  $T$  and a linear, time-invariant continuous-time system  $\bar{H} = [\bar{A}, \bar{B}, \bar{C}, \bar{D}]$ , where  $A, \bar{A} \in R^{p \times p}$ ,  $B, \bar{B} \in R^{p \times 1}$ ,  $C, \bar{C} \in R^{1 \times p}$ , and  $D, \bar{D} \in R$ . With both systems being internally stable, given  $A = \bar{A} + \Delta A$ ,  $B = \bar{B} + \Delta B$ ,  $C = \bar{C} + \Delta C$ , and  $D = \bar{D} + \Delta D$ , and if

$$\lim_{T \rightarrow 0} \Delta A = 0_{p \times p}, \quad \lim_{T \rightarrow 0} \Delta B = 0_{p \times 1}, \quad \lim_{T \rightarrow 0} \Delta C = 0_{1 \times p}, \quad \lim_{T \rightarrow 0} \Delta D = 0 \quad (4.59)$$

then

$$\lim_{T \rightarrow 0} \|HH_T S\|_{L^\infty} = \|\bar{H}\|_{L^\infty} \quad (4.60)$$

where  $H$  is the ZOH and  $S$  is the ideal sampler, as defined in Section 1.2, both having period  $T$ .  $\infty$

Proof: Given in Appendix A for the sake of brevity.  $\square$

**Remark 4.6.2** It can be deduced from the proof of Theorem 4.6.2 that the  $l^\infty$ -induced norm of a linear, time-invariant discrete-time system approaches the  $L^\infty$ -induced norm

of a linear, time-invariant continuous-time system, as  $T \rightarrow 0$ , when each element of at least one realization of the discrete-time system approaches that of a realization of the continuous-time system.

It follows that one analysis of sampled-data control systems based on the  $L^\infty$ -induced norm is to determine the range of sampling periods for which the following inequality is satisfied

$$|\|HH_T S\|_{L^\infty} - \|\bar{H}\|_{L^\infty}| \leq \chi_T \quad (4.61)$$

where  $\chi_T \in R^+$  has been specified by the control designer. At least, from Theorem 4.6.2, by sampling sufficiently fast, the bound in (4.61) can be satisfied for any  $\chi_T$ . As an example of the practical use of such design specification, consider the system relating the disturbance input to the control input. If a disturbance input of unit  $L^\infty$  norm is applied to the continuous-time and sampled-data control systems, then  $\chi_T$  could be the worst possible difference in supremum norms of the control inputs of the sampled-data and continuous-time control systems which is physically tolerable.

For a  $T$  relatively long, the guarantee of internal stability of PIM-based systems results in finite induced norms for such systems whereas this may not be the case for systems obtained with the local digital redesign. Furthermore, due in part to the movement of at least one closed-loop discrete-time pole toward the stability boundary on the  $\varepsilon$ -plane, with an increase in  $T$ , as explained in subsection 4.6.4, the sampled-data system obtained with the local digital redesign shows an impulse response  $g_{k,T}$ ,  $k \geq 0$ , which becomes more oscillatory. The consequence is that the value of the  $L^\infty$ -induced norm increases. This adverse phenomenon does not take place with a sampled-data system obtained with the regular PIM method, as detailed in subsection 4.6.4.

### **$L^2$ -Induced Norm**

Theorem 4.6.3 provides the conditions which guarantee that the induced norm of  $HH_T S$ , which maps signals lying in, or being staircase equivalents of signals in,  $\mathcal{S}_1$  and having a finite  $L^2$  norm to signals with a finite  $L^2$  norm, approaches the induced norm of  $\bar{H}$ , acting

on the same spaces, as  $T \rightarrow 0$ . Without loss of generality, such induced norm is named  $L^2$ -induced norm in this subsection with the understanding that the input to  $HH_T S$  and  $\bar{H}$  is so restricted in order to warrant that the output of the sampler is a sequence with finite  $l^2$  norm, as clarified in Proposition 4.3.1. Furthermore, it should be mentioned that a variant of the theorem can be applied to the system which relates the disturbance input to the control input when the disturbance signal is a staircase equivalent of a signal in  $S_1$  with finite  $L^2$  norm.

**Theorem 4.6.3** Consider a linear, time-invariant discrete-time system  $H_T = [A, B, C, D]$  with sampling period  $T$ , and a linear, time-invariant continuous-time system  $\bar{H} = [\bar{A}, \bar{B}, \bar{C}, \bar{D}]$ , where  $A, \bar{A} \in R^{p \times p}$ ,  $B, \bar{B} \in R^{p \times 1}$ ,  $C, \bar{C} \in R^{1 \times p}$ , and  $D, \bar{D} \in R$ . Both systems are internally stable in their respective domain. Given  $A = \bar{A} + \Delta A$ ,  $B = \bar{B} + \Delta B$ ,  $C = \bar{C} + \Delta C$ , and  $D = \bar{D} + \Delta D$ , if

$$\lim_{T \rightarrow 0} \Delta A = 0_{p \times p}, \quad \lim_{T \rightarrow 0} \Delta B = 0_{p \times 1}, \quad \lim_{T \rightarrow 0} \Delta C = 0_{1 \times p}, \quad \lim_{T \rightarrow 0} \Delta D = 0 \quad (4.62)$$

and the input to the sampled-data system  $HH_T S$  and the continuous-time system  $\bar{H}$  is confined to lie in, or to be a staircase equivalent of a signal in,  $S_1$  and to have finite  $L^2$  norm, then

$$\lim_{T \rightarrow 0} \|HH_T S\|_{L^2} = \|\bar{H}\|_{L^2} \cdot \infty \quad (4.63)$$

Proof: Given in Appendix A for the sake of brevity.  $\square$

**Remarks 4.6.3** (i) The  $l^2$ -induced norm of  $H_T$  is the  $H^\infty$  norm of its transfer function [20]. The computational algorithm used to obtain the  $H^\infty$  norm of the discrete-time system is a binary search process [78] which is applied to the transfer function  $H_T(w)$ . The transfer function  $H_T(w)$  is obtained by transforming  $H_T(\varepsilon)$  to the  $w$  domain [36] via the inverse bilinear transformation

$$\varepsilon = \frac{2w}{2 - Tw}. \quad (4.64)$$

(ii) From the proof of Theorem 4.6.3, the  $l^2$ -induced norm of a linear, time-invariant discrete-time system such as  $M_T$ , which relates the sampled reference input to the sampled controlled output, approaches the  $L^2$ -induced norm of the linear, time-invariant continuous-time system  $\bar{M}$ , which is the system relating the reference input to the controlled output, as  $T \rightarrow 0$ , when each element of at least one realization of  $M_T$  approaches that of a realization of  $\bar{M}$ .

One advantage of the regular and truncated PIM methods over the local digital redesign in the context of the  $l^2$ -induced norm of the discrete-time PITF  $H_T(\varepsilon)$  is that the poles and zeros of the discrete-time PITF obtained with PIM are known for each  $T$ . With the local digital redesign methods, the movement of the poles and zeros with an increasing  $T$  can result in an amplification of the supremum of the magnitude of the frequency response. Subsection 4.6.4 treats the pole movement in more details.

### 4.6.3 ITAE index

The ITAE index  $I_{T_i}$  on the signal  $e(t) \in L_{PC}^\infty[0, \infty)$  is given by

$$I_{T_i} = \int_{t=0}^{T_i} t |e(t)| dt \quad (4.65)$$

where  $0 < T_i < \infty$  is fixed. The index reduces contributions of the time response errors occurring initially while it emphasizes errors which take place at later times, and penalizes errors sustained over relatively long time periods. In this research, the ITAE index is calculated for the error signals at control input and controlled output between the continuous-time and sampled-data control systems, and for the difference between the constant reference input and the controlled output response. Obviously, a small value of the ITAE index is desired, for a given sampling period. For a signal represented with

the continuous-time lifting, the expression for the ITAE index is alternatively given by

$$I_{T_i} = \sum_{k=0}^{Q-1} \int_{\tau=0}^T (\tau + kT) |\widehat{e}_{k,T}(\tau)| d\tau + \int_{\tau=0}^{T_i-QT} (\tau + QT) |\widehat{e}_{Q,T}(\tau)| d\tau \quad (4.66)$$

for  $0 < T_i < \infty$  and  $T_i \geq QT$ , assuming the integration and summation are finite,  $T$  and  $T_i$  are fixed, and  $0 \leq (T_i - QT) < T$ , where  $Q \in Z^+$ . A discrete-time approximation to (4.66) can be obtained as

$$\widetilde{I}_{T_i} = \sum_{k=0}^{Q-1} \sum_{j=0}^{N-1} \left( kT + j \frac{T}{N} \right) |\widetilde{e}_{k,T}(j)| \frac{T}{N} + \sum_{j=0}^M \left( QT + j \frac{T}{N} \right) |\widetilde{e}_{Q,T}(j)| \frac{T}{N} \quad (4.67)$$

where  $\widetilde{e}_{k,T}$  is a vector of length  $N$  comprising the values of  $\widehat{e}_{k,T}(\tau)$  at time instants  $\tau = jT/N$  for  $j = 0, 1, \dots, N-1$ , as given by

$$\widetilde{e}_{k,T} = \left[ \widehat{e}_{k,T}(0), \widehat{e}_{k,T}(T/N), \dots, \widehat{e}_{k,T}((N-1)T/N) \right]^T \quad (4.68)$$

and  $M$  corresponds to the number of time intervals of length  $T/N$  in the span  $T_i - QT$ ; that is  $M = \text{int}\{N(T_i - QT)/T\}$ , where  $\text{int}\{\cdot\}$  represents the integer portion of its argument.

**Theorem 4.6.4** For fixed  $T$  and  $T_i$ ,  $\lim_{N \rightarrow \infty} \widetilde{I}_{T_i} = I_{T_i}$ .  $\square$

Proof: Since  $T$  and  $T_i$  are fixed, the summations from 0 to  $M$  and from 0 to  $N-1$  in (4.67) are performed over fixed time intervals on the continuous-time axis. Suppose that  $\widehat{e}_{k,T}(\tau)$  is continuous over  $\tau \in [0, T)$  for each step  $k$ . As  $N \rightarrow \infty$ , it follows that  $M \rightarrow \infty$  and the vector  $\widetilde{e}_{k,T}(j)$  increases in dimension for each  $k \geq 0$ ; that is, the vector takes values of  $\widehat{e}_{k,T}(\tau)$  at more time instants within each lifting interval. With  $\widetilde{e}_{k,T}(j) = \widehat{e}_{k,T}(\tau)|_{\tau=jT/N}$ , for  $j = 0, 1, \dots, N-1$ , in the  $k$ th lifting period, let each point  $\widetilde{e}_{k,T}(j)$  be held constant over the time frame  $T/N$ . Within a lifting interval, sum the norm of each element of the

vector scaled by the partition size  $T/N$ . Then, for each  $k \geq 0$ , let  $N \rightarrow \infty$  to obtain [79]

$$\lim_{N \rightarrow \infty} \sum_{j=0}^{N-1} |\tilde{e}_{k,T}(j)| \frac{T}{N} = \int_{\tau=0}^T |\hat{e}_{k,T}(\tau)| d\tau \quad (4.69)$$

$$\lim_{N \rightarrow \infty} \sum_{j=0}^{N-1} \frac{jT}{N} |\tilde{e}_{k,T}(j)| \frac{T}{N} = \int_{\tau=0}^T \tau |\hat{e}_{k,T}(\tau)| d\tau \quad (4.70)$$

$$\lim_{N \rightarrow \infty} \sum_{j=0}^M |\tilde{e}_{k,T}(j)| \frac{T}{N} = \int_{\tau=0}^{T_i-QT} |\hat{e}_{k,T}(\tau)| d\tau \quad (4.71)$$

$$\lim_{N \rightarrow \infty} \sum_{j=0}^M \frac{jT}{N} |\tilde{e}_{k,T}(j)| \frac{T}{N} = \int_{\tau=0}^{T_i-QT} \tau |\hat{e}_{k,T}(\tau)| d\tau. \quad (4.72)$$

Since the above limiting behaviors are valid for each  $k \geq 0$ , it follows that  $\widetilde{I}_{T_i}$  approaches  $I_{T_i}$  as  $T \rightarrow 0$ .  $\square$

In terms of the variations of the index with the sampling period, as  $T \rightarrow 0$ , the ITAE index on the difference between the constant reference input and the controlled output response of the sampled-data system approaches that of the continuous-time control system if it is a sampled-data model of the continuous-time system. Furthermore, when the responses of the error systems  $(HH_T S - \bar{H})$  and  $(\bar{G}HH_T S - \bar{G}\bar{H})$  approach zero, uniformly in time, as  $T \rightarrow 0$ , so do their ITAE indices. For relatively large, and finite, values of  $T$ , equation (4.67) is computed for a given sampled-data system and fixed value of  $N$ , and the graph of  $\widetilde{I}_{T_i}$  versus  $T$  determines the performance of the sampled-data system. The advantage of the regular and truncated PIM-based control systems over those obtained with the local digital redesign is that stability can be achieved for the relatively large sampling intervals and thus the ITAE index on an error signal can meet a finite bound.

The following subsection gives helpful insight to the understanding of the responses of digitally redesigned control systems for any non-pathological sampling period.

#### 4.6.4 Error System Responses to Inputs in $\mathcal{S}_2$

The signal norms do not give information as to the shape of a response; for example, signals with different transient behaviors can possess the same  $L^\infty$  and  $L^2$  norms. In addition, it would be useful to have more insight as to the performances obtained with the various digital redesign methods; for instance, the knowledge of the closed-loop pole locations could complement the use of error signal norms and index in the performance evaluation. In order to achieve the aforementioned objectives, this subsection studies the responses of the error systems  $(\widehat{HH}_T S - \widehat{H})$  and  $(\widehat{GHH}_T S - \widehat{G}\widehat{H})$ , which are subjected to a known set of reference inputs, as expressed in terms of the PITF, the plant and the hold at control input. The restriction of the analysis to inputs in  $\mathcal{S}_2$ , defined in Chapter 2, simplifies the notation and allows one to clearly understand the phenomena involved in the control-input and controlled-output errors associated with the digital redesign performed at relatively large sampling periods.

Any signal in  $\mathcal{S}_2$  can be expressed in the lifted form as follows: for a given  $T$  and step  $k$ ,

$$\widehat{r}_{k,T}(\tau) = C_{k,T}, \quad 0 \leq \tau < T, \quad k \geq 0, \quad C_{k,T} \in R. \quad (4.73)$$

With the knowledge of the reference input and the representation of the continuous-time and sampled-data control systems presented in Section 4.1, the influence of the closed-loop discrete-time poles on the responses and the differences between the responses of PIM-based and locally redesigned control systems are explained.

The control-input error is first presented followed by the controlled-output error.

##### Control-Input Error

In the equations that follow, the system representation of Section 4.1, more specifically that found in equations (4.1) to (4.6), is used. Let

$$R_T(\varepsilon) = \mathcal{D} \left\{ \widehat{r}_{k,T}(\tau) \Big|_{\tau=0} \right\}. \quad (4.74)$$

An expression for the control input response of the continuous-time control system is

$$\begin{aligned} \widehat{u}_{k,T}(\tau) &= \overline{C}e^{\overline{A}\tau} \cdot \mathcal{D}^{-1} \left\{ \frac{\text{Adj}(\varepsilon I - (e^{\overline{A}T} - I)/T) \frac{1}{T} \int_{v=0}^T e^{\overline{A}(T-v)} \overline{B} dv}{|\varepsilon I - (e^{\overline{A}T} - I)/T|} R_T(\varepsilon) \right\} \\ &\quad + \left( \overline{C} \int_{v=0}^T e^{\overline{A}(\tau-v)} \overline{B} dv + \overline{D} \right) \cdot \mathcal{D}^{-1} \{R_T(\varepsilon)\} \end{aligned} \quad (4.75)$$

for  $k = 0, 1, 2, \dots$ , and  $\tau \in [0, T)$ . In (4.75),  $\text{Adj}(\cdot)$  represents the adjoint of its matrix argument [76]. On the other hand, the control input response of the sampled-data system is

$$\widehat{u}_{k,T}(\tau) = H(\tau) \cdot \mathcal{D}^{-1} \left\{ \frac{C \text{Adj}(\varepsilon I - A) B}{|\varepsilon I - A|} R_T(\varepsilon) \right\} + H(\tau) \cdot D \cdot \mathcal{D}^{-1} \{R_T(\varepsilon)\}. \quad (4.76)$$

Hence, the response of the error system ( $\widehat{H\overline{H}_T S} - \widehat{H}$ ) is

$$\begin{aligned} &\widehat{u}_{k,T}(\tau) - \widehat{u}_{k,T}(\tau) \\ &= \underbrace{H(\tau)C \cdot \mathcal{D}^{-1} \left\{ \frac{\text{Adj}(\varepsilon I - A) B}{|\varepsilon I - A|} R_T(\varepsilon) \right\}}_{=f_1(\tau,k)} \\ &\quad - \underbrace{\overline{C}e^{\overline{A}\tau} \cdot \mathcal{D}^{-1} \left\{ \frac{\text{Adj}(\varepsilon I - (e^{\overline{A}T} - I)/T) \frac{1}{T} \int_{v=0}^T e^{\overline{A}(T-v)} \overline{B} dv}{|\varepsilon I - (e^{\overline{A}T} - I)/T|} R_T(\varepsilon) \right\}}_{=f_2(\tau,k)} \\ &\quad + \underbrace{\left( H(\tau) \cdot D - \overline{C} \int_{v=0}^T e^{\overline{A}(\tau-v)} \overline{B} dv - \overline{D} \right) \cdot \mathcal{D}^{-1} \{R_T(\varepsilon)\}}_{=f_3(\tau,k)}. \end{aligned} \quad (4.77)$$

For a regular PIM-based sampled-data control system, using the hold-equivalent structure of the matched pole-zero discrete-time model as described in Appendix B, the expression for the control-input error can be written as:

$$\begin{aligned} &\widehat{u}_{k,T}(\tau) - \widehat{u}_{k,T}(\tau) \\ &= H(\tau)\overline{C} \cdot \mathcal{D}^{-1} \left\{ \frac{\text{Adj}(\varepsilon I - (e^{\overline{A}T} - I)/T) \frac{1}{T} \int_{v=0}^T e^{\overline{A}(T-v)} H_{MPZ}(v) \overline{B} dv \cdot K}{|\varepsilon I - (e^{\overline{A}T} - I)/T|} R_T(\varepsilon) \right\} \end{aligned}$$

$$\begin{aligned}
& -\bar{C}e^{\bar{A}\tau} \cdot \mathcal{D}^{-1} \left\{ \frac{\text{Adj}(\varepsilon I - (e^{\bar{A}T} - I)/T) \frac{1}{T} \int_{v=0}^T e^{\bar{A}(T-v)} \bar{B} dv}{|\varepsilon I - (e^{\bar{A}T} - I)/T|} R_T(\varepsilon) \right\} \\
& + \left( H(\tau) \cdot K\bar{D} - \bar{C} \int_{v=0}^{\tau} e^{\bar{A}(\tau-v)} \bar{B} dv - \bar{D} \right) \cdot \mathcal{D}^{-1} \{R_T(\varepsilon)\}
\end{aligned} \tag{4.78}$$

for  $k = 0, 1, 2, \dots$  and  $\tau \in [0, T)$ , where  $H_{MPZ}$  represents the hold in the matched pole-zero discrete-time model of the continuous-time PITF, as described in Appendix B.

The following observations can be made about the responses of the error systems to inputs in  $\mathcal{S}_2$  for any non-pathological sampling period, according to equations (4.77) and (4.78).

*Observation 1* With hold and plant dynamics fixed, one can only modify  $H_T$ , and consequently its elements of realization  $A$ ,  $B$ ,  $C$  and  $D$ , to obtain a satisfactory error system's output. In (4.77), to have the control-input error relatively small,  $f_1(\tau, k)$  should be close to  $f_2(\tau, k)$ , and  $f_3(\tau, k)$  should be small for  $k = 0, 1, 2, \dots$ , and  $\tau \in [0, T)$ . For all the digital redesign methods, reducing  $T$  guarantees that  $f_1(\tau, k)$  is as close as required to  $f_2(\tau, k)$ , and that  $f_3(\tau, k)$  is as small as needed over all times. On the other hand, when  $T$  is set to a relatively large value,  $f_3(\tau, k)$  generally has a significant magnitude,  $H(\tau)C$  is a function very much disparate from  $\bar{C}e^{\bar{A}\tau}$ , and the zeros of the transfer functions

$$\frac{\text{Adj}(\varepsilon I - A)B}{|\varepsilon I - A|} R_T(\varepsilon)$$

and

$$\frac{\text{Adj}(\varepsilon I - (e^{\bar{A}T} - I)/T) \frac{1}{T} \int_{v=0}^T e^{\bar{A}(T-v)} \bar{B} dv}{|\varepsilon I - (e^{\bar{A}T} - I)/T|} R_T(\varepsilon)$$

can differ significantly.

*Observation 2* For the regular PIM method and its truncated version,

$$|\varepsilon I - A| = \left| \varepsilon I - (e^{\bar{A}T} - I)/T \right|. \tag{4.79}$$

This is the most salient difference between regular PIM-based sampled-data control systems and systems obtained by using local digital redesign methods; that is, with the local methods, the closed-loop poles can go everywhere when  $T$  is increased, whereas it is not the case with the regular PIM method.

*Observation 3* The poles of the discrete-time PITF of an internally stable, regular or truncated PIM-based control system approach the location  $-1/T$  in the  $\varepsilon$ -plane, as  $T \rightarrow \infty$ . The influence of the closed-loop discrete-time poles on the control input response is explained as follows. For a sampled-data system obtained with the regular or the truncated PIM method, each discrete-time closed-loop pole  $\lambda_\varepsilon$  is given by

$$\lambda_\varepsilon = \frac{(e^{\bar{\lambda}_s T} - 1)}{T} \quad (4.80)$$

where  $\bar{\lambda}_s$  is a pole of the continuous-time PITF. As  $T \rightarrow \infty$ , the distance between each pole  $\lambda_\varepsilon$  and the stability boundary approaches zero. Furthermore, each pole  $\lambda_\varepsilon$  approaches the point  $-1/T$  in the  $\varepsilon$ -plane, as  $T \rightarrow \infty$ . A discrete-time system with poles at the location  $-1/T$  in the  $\varepsilon$ -plane, or equivalently the location 0 in the  $z$ -plane, is known to settle to its steady-state value in a finite number of steps [2]. For a regular or a truncated PIM-based control system, the control input response to a constant reference input approaches to this so called deadbeat behavior, at the sampling instants, as  $T \rightarrow \infty$ .

From a continuous-time point of view, the complex discrete-time pole  $\lambda_\varepsilon$  maps to a pole in the  $s$ -plane,  $\bar{\lambda}'_s$ , according to

$$\bar{\lambda}'_s = \frac{1}{T} \ln(T\lambda_\varepsilon + 1). \quad (4.81)$$

If the sampling period is such that the upper limit of the primary strip in the  $s$ -plane, given by  $j\pi/T$ , is larger than the complex part of the pole  $\bar{\lambda}_s$  of the continuous-time PITF, then  $\bar{\lambda}'_s$  equals  $\bar{\lambda}_s$  [80]. However, for a sufficiently large  $T$ ,  $\bar{\lambda}_s$  is absent from the primary strip. In such a case,  $\bar{\lambda}'_s$  is different from  $\bar{\lambda}_s$ ; in fact,  $\bar{\lambda}'_s$  has a smaller complex

part, in absolute terms, than that of  $\bar{\lambda}_s$ , although  $\bar{\lambda}'_s$  and  $\bar{\lambda}_s$  have the same real part. This means that, by increasing the sampling interval, the control input response of the PIM-based control system approaches, at the sampling instants, the control input response of a continuous-time system with stable real poles.

*Observation 4* For a sampled-data control system obtained with a local digital redesign method, the control input response to a constant reference input can be oscillatory when the sampling interval is relatively large. This is explained as follows. First, it is known that, for a given sampling period, when a discrete-time pole is relatively close to the stability boundary, an oscillatory response is obtained [2]. For sampled-data systems based on the local digital redesign method, as the sampling period is increased to  $T^*$ , the sampling period below which a system is internally stable according to Theorem 4.2.2, at least one pole of the discrete-time closed-loop system moves toward the stability boundary. Second, with the local digital redesign there is no control over the movement of the closed-loop discrete-time poles with  $T$ . The consequence may be that some discrete-time poles continualize to poles having small damping ratio since the real part of each continualized pole is not fixed unlike the poles of PIM-based systems. Thus, systems obtained with the local digital redesign and subjected to a constant reference input can exhibit the oscillatory responses associated with complex poles with low damping ratios, when  $T$  is relatively large, or equivalently to discrete-time poles close to the stability boundary in the  $\epsilon$ -plane, as shown graphically in [2] and [5].

*Observation 5* The time-domain expression (4.77) reveals that, in order to have an error system's output with zero amplitude at the sampling instants, one should discretize the continuous-time PITF with the step invariant method [2] and select a hold  $H(\tau)$  at control input which satisfies  $H(\tau)|_{\tau=0} = 1$ . However, the structure of the sampled-data control system, as shown in Figure 1.4(b), renders impossible such a process since the set of discrete-time zeros of the discrete-time PITF includes the poles of the discrete-time plant model, which cannot be achieved with a step invariant discretization of the

continuous-time PITF.

*Observation 6* In the case of a sampled-data system obtained with the regular or truncated PIM method which is internally stable at the sampling instants and subjected to a constant input, the maximum magnitude of its control input generally occurs in the time interval  $[0, T)$  and has a known behavior as  $T \rightarrow \infty$ , as explained next. The control-input error over  $[0, T)$  is given by

$$\widehat{u}_{0,T}(\tau) - \widehat{u}_{0,T}(\tau) = \left( H(\tau) \cdot K\overline{D} - \overline{C} \int_{v=0}^{\tau} e^{\overline{A}(\tau-v)} \overline{B} dv - \overline{D} \right) \cdot \mathcal{D}^{-1} \{R_T(\varepsilon)\} \quad (4.82)$$

for the regular PIM-based system. When  $\overline{D} = 0$ , for any value of  $T$ , the control input of the sampled-data control system in the interval  $[0, T)$  has zero magnitude. When  $\overline{D} \neq 0$ , the gain  $K$ , obtained with equation (B.10), and the hold determine the control input response of the PIM-based sampled-data control system. It can be shown, with the development of Appendix B, that the discrete-time PITF, which is obtained by discretizing the continuous-time PITF  $\overline{H}(s)$  with the matched pole-zero method and is expressed as

$$H_T(\varepsilon) = K \cdot \frac{\varepsilon^q + n_q \varepsilon^{q-1} + \dots + n_1 \varepsilon + n_0}{\varepsilon^p + d_p \varepsilon^{p-1} + \dots + d_1 \varepsilon + d_0}, \quad (4.83)$$

has the following limiting behavior:

$$\lim_{T \rightarrow \infty} H_T(\varepsilon) = \left( \lim_{T \rightarrow \infty} K \right) \cdot \frac{(\varepsilon + 1/T)^{w_1} \varepsilon^{w_2}}{(\varepsilon + 1/T)^p} \quad (4.84)$$

where  $w_1 + w_2$  equals to the degree of the numerator polynomial,  $q$ , minus the number of zeros in the region of the  $\varepsilon$ -plane given by  $|T\varepsilon + 1| > 1$ ,  $w_1$  represents the number of zeros inside the stability boundary,  $w_2$  denotes the number of zeros at origin, and

$$\lim_{T \rightarrow \infty} K = \overline{H}(s) \Big|_{s=s_o} \cdot \frac{(\varepsilon_o + 1/T)^p}{(\varepsilon_o + 1/T)^{w_1} \varepsilon_o^{w_2}}. \quad (4.85)$$

In equation (4.85),  $s_o$  is a real number which satisfies  $0 \leq s_o \ll 1$ , and  $\varepsilon_o = (e^{s_o T} - 1)/T$ .

If the discrete-time PITF is biproper and all of its zeros are within the stability boundary, then

$$\lim_{T \rightarrow \infty} K = \bar{H}(s)|_{s=s_0}. \quad (4.86)$$

In the case  $\bar{H}(s)$  contains  $w_2$  ( $\geq 1$ ) zeros at origin, its DC gain is zero and  $\bar{H}(s)|_{s=s_0}$  is close to zero with a small value of  $s_0$ . Hence, for this case the gain  $K$  approaches zero as the sampling interval increases; i.e.

$$\lim_{T \rightarrow \infty} K = \frac{\bar{H}(s)|_{s=s_0}}{\varepsilon_0^{w_2}} \cdot \frac{(\varepsilon_0 + 1/T)^p}{(\varepsilon_0 + 1/T)^{w_1}} = 0, \quad w_1 < p. \quad (4.87)$$

As an example, consider the continuous-time PITF

$$\bar{H}(s) = \frac{2.993s(s+1)(s+2.404)}{(s+3.471)(s^2+4.724s+20.728)} \quad (4.88)$$

where one zero is at the origin, the remaining ones are in the stability region of the  $s$ -plane, and the three poles are stable. The continuous-time PITF is discretized with the matched pole-zero method to yield  $H_T(\varepsilon)$  [14]. Let the systems  $\bar{H}$  and  $H_T$  be subjected to a unit step input and the ZOH be placed at the output of  $H_T$ . Equations (4.89) and (4.90) give the discrete-time transfer functions for  $T = 0.1$  and  $T = 5$ , respectively, and Figure 4.4 shows the responses of  $\bar{H}$  and  $H_T$  for various sampling periods. In the figure, the solid line corresponds to the response of the continuous-time system. The figure clearly shows that the control input of the sampled-data system approaches zero with an increase in sampling period.

$$H_T(\varepsilon) = 2.342 \cdot \frac{\varepsilon(\varepsilon^2 + 3.088\varepsilon + 2.033)}{\varepsilon^3 + 8.321\varepsilon^2 + 32.041\varepsilon + 47.617} \quad (4.89)$$

$$H_T(\varepsilon) = 0.02 \cdot \frac{\varepsilon(\varepsilon^2 + 0.399\varepsilon + 0.04)}{\varepsilon^3 + 0.6\varepsilon^2 + 0.12\varepsilon + 0.008} \quad (4.90)$$

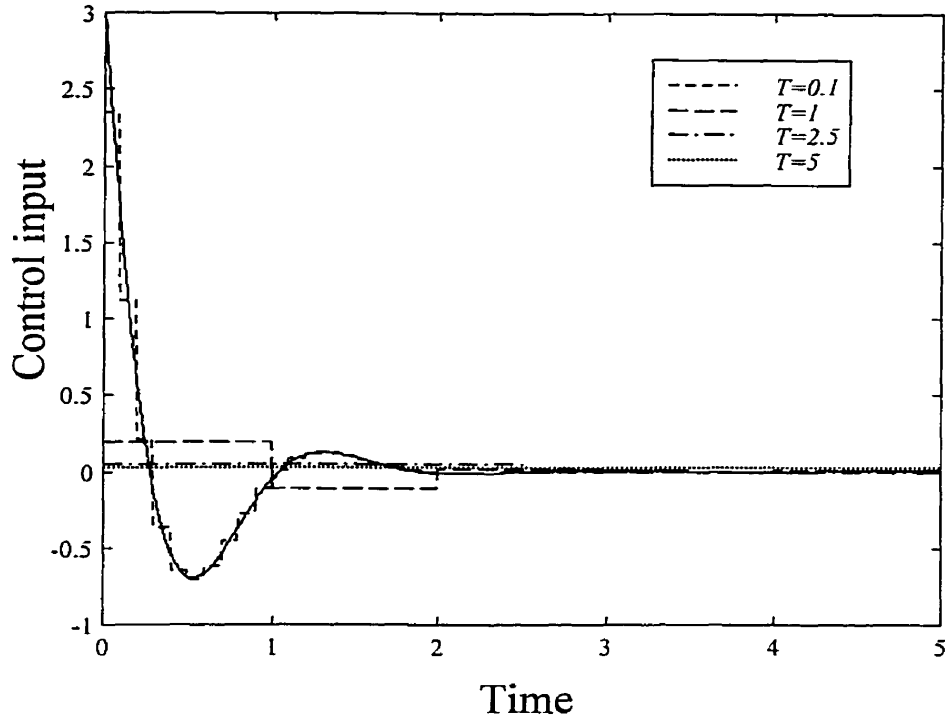


Figure 4.4: Control input responses for the example

For a continuous-time PITF with at least one zero at origin and discretized with the matched pole-zero method to a discrete-time PITF, the  $L^\infty$  norm of the control-input error approaches the supremum magnitude of the control input of the continuous-time control system as  $T \rightarrow \infty$ , whereas the  $L^2$  norm of the control-input error approaches the  $L^2$  norm of the control input of the continuous-time control system as  $T \rightarrow \infty$ . This is clearly an advantage of the PIM method over a local digital redesign method employed on the same continuous-time control system.

### Controlled-Output Error

For a sampled-data control system, the plant output can be expressed as

$$\hat{y}_{k,T}(\tau) = \underbrace{\overline{C}_G e^{\overline{A}_G \tau}}_{=g_1(\tau)} x_{G_T,k,T} + \underbrace{\left( \overline{C}_G \int_{v=0}^{\tau} e^{\overline{A}_G(\tau-v)} \overline{B}_G H(v) dv + \overline{D}_G H(\tau) \right)}_{=g_2(\tau)} u_{k,T} \quad (4.91)$$

whereas the plant output of the continuous-time control system is

$$\widehat{y}_{k,T}(\tau) = \overline{C}_{\overline{G}} e^{\overline{A}_{\overline{G}}\tau} \widehat{x}_{\overline{G},k,T}(0) + \overline{C}_{\overline{G}} \int_{v=0}^{\tau} e^{\overline{A}_{\overline{G}}(\tau-v)} \overline{B}_{\overline{G}} \widehat{u}_{k,T}(v) dv + \overline{D}_{\overline{G}} \widehat{u}_{k,T}(\tau). \quad (4.92)$$

Denoting

$$\widehat{u}_{k,T}(\tau) = \widehat{u}_{k,T}(0) + w_{u,k,T}(\tau), \quad w_{u,k,T}(0) = 0, \quad (4.93)$$

the output of the error system  $(\widehat{G} \widehat{H} \widehat{H}_T S - \widehat{G} \widehat{H})$  is

$$\begin{aligned} & \widehat{y}_{k,T}(\tau) - \widehat{y}_{k,T}(\tau) \\ &= g_1(\tau) \cdot (x_{G_T,k,T} - \widehat{x}_{\overline{G},k,T}(0)) + g_2(\tau) \cdot u_{k,T} \\ & \quad - \underbrace{\left( \overline{C}_{\overline{G}} \int_{v=0}^{\tau} e^{\overline{A}_{\overline{G}}(\tau-v)} \overline{B}_{\overline{G}} dv + \overline{D}_{\overline{G}} \right)}_{=g_3(\tau)} \widehat{u}_{k,T}(0) \\ & \quad - \underbrace{\left( \overline{C}_{\overline{G}} \int_{v=0}^{\tau} e^{\overline{A}_{\overline{G}}(\tau-v)} \overline{B}_{\overline{G}} w_{u,k,T}(v) dv + \overline{D}_{\overline{G}} w_{u,k,T}(\tau) \right)}_{=g_4(\tau)} \end{aligned} \quad (4.94)$$

where

$$\widehat{u}_{k,T}(\tau) \Big|_{\tau=0} = \mathcal{D}^{-1} \left\{ \frac{\overline{C} \text{Adj}(\varepsilon I - \frac{(e^{\overline{A}T} - I)}{T}) \frac{1}{T} \int_{v=0}^T e^{\overline{A}(T-v)} \overline{B} dv}{\left| \varepsilon I - \frac{(e^{\overline{A}T} - I)}{T} \right|} R_T(\varepsilon) \right\} + \overline{D} \cdot \mathcal{D}^{-1} \{R_T(\varepsilon)\} \quad (4.95)$$

$$u_{k,T} = \mathcal{D}^{-1} \left\{ \frac{C \text{Adj}(\varepsilon I - A) B}{|\varepsilon I - A|} R_T(\varepsilon) \right\} + D \cdot \mathcal{D}^{-1} \{R_T(\varepsilon)\}. \quad (4.96)$$

The following observations can be made about the controlled output responses.

*Observation 1* The difference between the state of the discrete-time plant model and that of the continuous-time plant at the sampling instants, i.e.  $(x_{G_T,k,T} - \widehat{x}_{\overline{G},k,T}(0))$ , and the discrete-time control input  $u_{k,T}$  are what distinguishes a digital redesign method from another one, as perceived from the controlled-output error. The intersample behavior of the controlled output of a sampled-data control system is dominated by the functions

$g_1(\tau)$  and  $g_2(\tau)$ , given in equation (4.91), which are fixed for a given hold, plant, and value of  $T$ .

*Observation 2* When the sampling period is relatively large, the control input within the time interval  $[0, T)$  significantly influences the rise time of the controlled output response. In particular, depending on the value of  $D$ , the rise time can be long or short; that is,  $D$  acts as a weighting factor whose magnitude directly affects the rise time. Moreover, when  $D = 0$ , an increase in the sampling interval results in an increased time lag.

*Observation 3* For a regular PIM-based system, as  $T \rightarrow \infty$ , its controlled output response at the sampling instants approaches that of a system with poles at  $-1/T$  in the  $\varepsilon$ -plane. This fact can be seen by rewriting equation (4.91), for the sampling instants, as

$$\hat{y}_{k,T}(\tau)|_{\tau=0} = g_1(\tau)|_{\tau=0} \cdot \mathcal{D}^{-1}\{X_{G_T}(\varepsilon)\} + g_2(\tau)|_{\tau=0} \cdot \mathcal{D}^{-1}\{U_T(\varepsilon)\}. \quad (4.97)$$

The Delta transform of the state of the discrete-time plant model, i.e.  $X_{G_T}(\varepsilon)$ , is obtained in the second part of the proof of Theorem 4.3.1. There it is shown that the system relating the discrete-time reference input to the discrete-time plant state has the same set of poles as that of the discrete-time PITF, which are known to approach  $-1/T$  in the  $\varepsilon$ -plane, as  $T \rightarrow \infty$ , for a regular or truncated PIM-based system.

## Chapter 5

# Applications of Digitally Redesigned Control Systems

In the preceding chapters, several characteristics of sampled-data systems obtained with the digital redesign of a continuous-time control system were studied. In this chapter, the performances of the digital redesign methods are evaluated and some of their characteristics are investigated through five examples.

The first case involves an optimal digital redesign of a continuous-time control system, which provides an alternative closed-loop discretization to the use of PIM. Two types of controller implementations are tested: (i) an ideal setup, with floating-point arithmetic and relatively large number of bits; and (ii) a worst-case scenario, with fixed-point arithmetic and restricted number of bits. The comparison uses the step response plots of the various sampled-data control systems to determine which digital redesign methods offer the fastest rise time, the smallest overshoot, the shortest settling time, and the required DC gain, and relies on the  $L^\infty$  and  $L^2$  norms, and the ITAE index of the error signals. The second case concerns the digital pitch attitude control system of the T-2 aircraft. The time-domain performances of flight control systems based on the conventional local discretization techniques are compared with those systems obtained with the PIM methods via numerical simulations. The disturbance-rejection behavior of the sampled-data

control systems is also investigated. Thirdly, experiments are conducted on the control of a voice-coil-driven flexible positioner system in order to study the effectiveness of the proposed modified PIM methods and to compare them with the conventional approaches under a real-time setting. The fourth practical case is the digital redesign of a gas-turbine engine speed control system. The main objective in carrying out such a design is to employ the newly developed methods to a typical industrial application and assess their performances against conventionally designed digital control laws. The fifth example validates the convergence theorems derived in Chapter 4 for MIMO control systems.

The last section provides a summary of the results obtained with the digitally redesigned control systems considered in this chapter.

It should be noted that the simulations for the first, second and fifth examples are performed on Matlab/Simulink<sup>1</sup> whereas the gas-turbine engine simulations are carried out with the software MatrixX/SystemBuild<sup>2</sup>.

## 5.1 Example Taken from the Optimal Digital Redesign Literature

The method of optimal digital redesign can be found in [24]. It consists in the following: Given a continuous-time plant and a well-designed continuous-time controller, design a discrete-time control system such that its continuous-time, closed-loop step responses, at control input and controlled output, optimally match those of the continuous-time system in the sense that a weighted sum of the energy of the associated error signals is minimized. In [24], the conclusion is that the performance achieved with such an optimal approach on a given control system is superior to that found with the local digital redesign methods. The comparison is now further extended to include the PIM methods.

Consider the linear, time-invariant continuous-time control system used in [24] as a

---

<sup>1</sup>Matlab and Simulink are registered trademarks of The MathWorks, Inc.

<sup>2</sup>MatrixX is a registered trademark and SystemBuild is a trademark of Integrated Systems, Inc.

benchmark with the structure of Figure 1.4(a) and blocks given by:

$$\bar{\Pi}(s) = 1, \bar{\Gamma}(s) = 1, \bar{\Omega}(s) = \frac{s^2 + 10.42s + 20}{s^2 + 32.44s + 20}, \bar{G}(s) = \frac{20}{s(1 + s/10)(1 + s/30)}. \quad (5.1)$$

Digital redesign is performed using the optimal technique of [24], the regular PIM method, the regular plus truncated PIM method, and the Tustin's and matched pole-zero discretizations of  $\bar{\Omega}(s)$ , for sampling periods of  $T = 0.1$  (which corresponds to half the rise time  $t_r$ ) and 0.4, as used in [24]. In this case, the orders of  $\bar{\Omega}(s)$  and  $\bar{G}(s)$  are such that the reduced-order PIM method is the same as the regular PIM method. The resulting sampled-data control systems have the structure shown in Figure 1.4(b), where some blocks can be unity depending on the digital redesign method used, with the ZOH at control input.

The set of discrete-time controllers calculated with the various methods is given in the following tables, where MPZ denotes the matched pole-zero discretization of the local control block.

Optimal Digital Redesign (with order reduction)	$\Omega_T(\varepsilon) = \frac{0.511\varepsilon^6 + 21.762\varepsilon^5 + 377.15\varepsilon^4 + 3370.8\varepsilon^3 + 16194\varepsilon^2 + 39000\varepsilon + 35800}{\varepsilon^6 + 49.271\varepsilon^5 + 971.98\varepsilon^4 + 9678.4\varepsilon^3 + 49803\varepsilon^2 + 117290\varepsilon + 78800}$
Regular PIM	$\Omega_T(\varepsilon) = \frac{0.098\varepsilon^2 + 1.379\varepsilon + 5.643}{\varepsilon^2 + 14.730\varepsilon + 56.335}, \Pi_T(\varepsilon) = \frac{0.462\varepsilon^2 + 3.553\varepsilon + 5.643}{0.098\varepsilon^2 + 1.379\varepsilon + 5.643}$
Regular, Truncated PIM	$\Omega_T(\varepsilon) = \frac{0.098\varepsilon^2 + 1.379\varepsilon + 5.643}{\varepsilon^2 + 14.730\varepsilon + 56.335}, \Pi_T(\varepsilon) = 1$
Tustin's Method	$\Omega_T(\varepsilon) = \frac{0.588\varepsilon^2 + 4.648\varepsilon + 7.485}{\varepsilon^2 + 12.889\varepsilon + 7.485}$
MPZ	$\Omega_T(\varepsilon) = \frac{0.478\varepsilon^2 + 3.677\varepsilon + 5.840}{\varepsilon^2 + 10.194\varepsilon + 5.840}$

Table 5.1: Controller parameters for  $T = 0.1$

Optimal Digital Redesign (with order reduction)	$\Omega_T(\varepsilon) = \frac{0.162\varepsilon^4+1.46\varepsilon^3+4.9\varepsilon^2+7.278\varepsilon+4.041}{\varepsilon^4+9.77\varepsilon^3+35.038\varepsilon^2+54.731\varepsilon+31.414}$
Regular PIM	$\Omega_T(\varepsilon) = \frac{0.094\varepsilon^2+0.47\varepsilon+0.586}{\varepsilon^2+5.426\varepsilon+7.32}, \Pi_T(\varepsilon) = \frac{0.154\varepsilon^2+0.612\varepsilon+0.586}{0.094\varepsilon^2+0.47\varepsilon+0.586}$
Regular, Truncated PIM	$\Omega_T(\varepsilon) = \frac{0.094\varepsilon^2+0.47\varepsilon+0.586}{\varepsilon^2+5.426\varepsilon+7.32}, \Pi_T(\varepsilon) = 1$
Tustin's Method	$\Omega_T(\varepsilon) = \frac{0.469\varepsilon^2+2.222\varepsilon+2.413}{\varepsilon^2+4.879\varepsilon+2.413}$
MPZ	$\Omega_T(\varepsilon) = \frac{0.364\varepsilon^2+1.453\varepsilon+1.390}{\varepsilon^2+3.056\varepsilon+1.390}$

Table 5.2: Controller parameters for  $T = 0.4$

The next figures present the step responses at control input and controlled output, where CT denotes the continuous-time system.

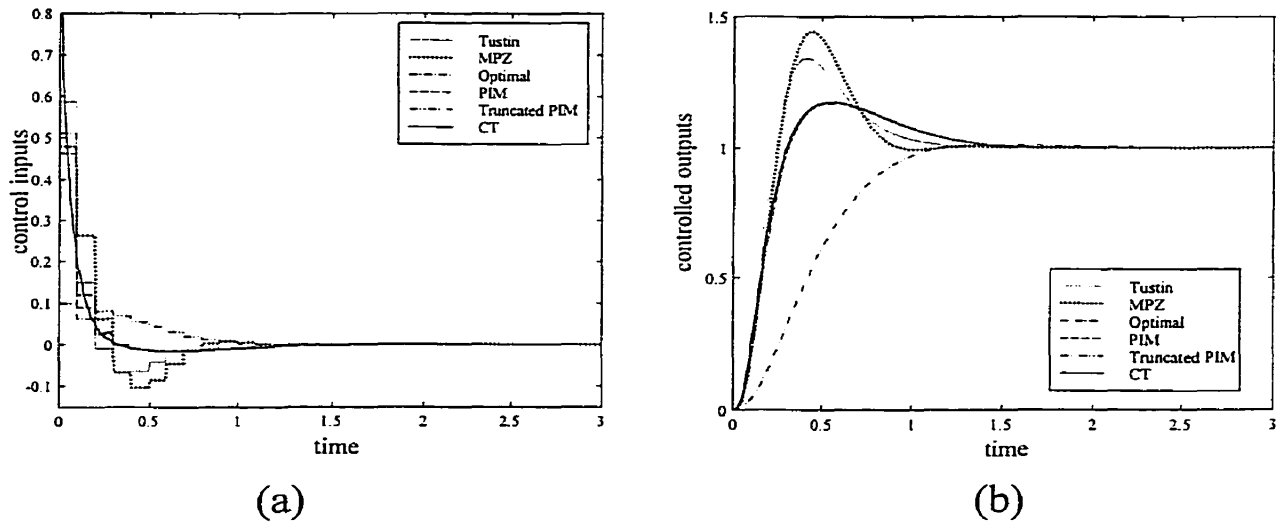


Figure 5.1: (a) Control inputs and (b) controlled outputs for  $T = 0.1$

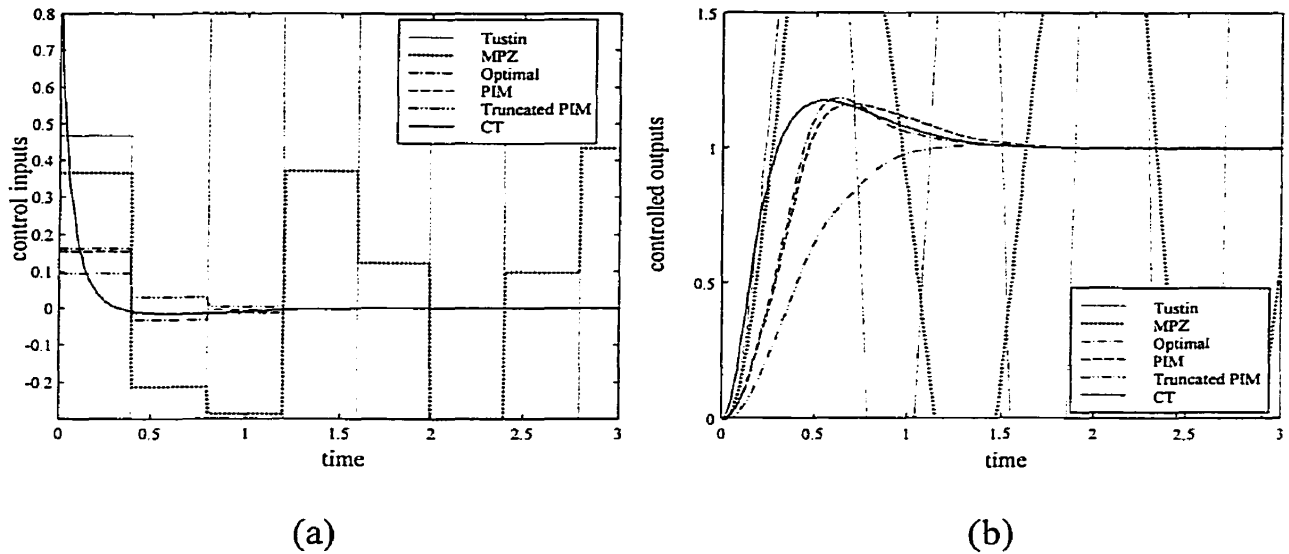


Figure 5.2: (a) Control inputs and (b) controlled outputs for  $T = 0.4$

The responses are almost identical for the regular PIM and optimal digital redesign methods for both values of  $T$ . On the other hand, the local digital redesign methods result in unstable closed-loop systems at the largest sampling period, and the regular, truncated PIM method offers no overshoot in the controlled output although it presents a slow rise time for the two sampling periods. Hence, by comparing the behavior of the regular and the regular, truncated PIM methods, one sees that the discrete-time zeros can affect the rise time, a well-known result for continuous-time systems [5]. The sampled-data control system resulting from the regular PIM method has one advantage over the optimal digital redesign method: it consists of low order controllers. Yet, the regular PIM-based sampled-data system possesses one drawback: two discrete-time controllers are implemented instead of only one. This problem can be solved by using the regular, truncated PIM method if a slower rise time is tolerable.

Tables 5.3 and 5.4 provide the performance measures as applied to the control-input and controlled-output error signals. In the tables, for  $T = 0.4$ , the norms and index are not calculated for the Tustin's and MPZ methods since they result in unstable closed-loop

systems. For  $T = 0.1$ , the truncated PIM method offers the worst performance of all the digital redesign techniques, whereas for both  $T = 0.1$  and  $T = 0.4$  the optimal digital redesign has a slight edge over the PIM method. This is especially true at the controlled output and for  $T = 0.4$  where the slower settling time of the PIM-based system as compared to that of the system based on the optimal redesign, as seen on Figure 5.2(b), renders the  $L^2$  norm and ITAE index of the error signal larger than those calculated for the optimal redesign.

	$L^\infty$	$L^2$	ITAE
Tustin	$4.12 \times 10^{-1}$ —	$8.68 \times 10^{-2}$ —	$1.27 \times 10^{-2}$ —
MPZ	$5.22 \times 10^{-1}$ —	$1.01 \times 10^{-1}$ —	$2.22 \times 10^{-2}$ —
PIM	$5.38 \times 10^{-1}$ $8.46 \times 10^{-1}$	$7.84 \times 10^{-2}$ $1.51 \times 10^{-1}$	$2.18 \times 10^{-3}$ $1.34 \times 10^{-2}$
Truncated PIM	$9.02 \times 10^{-1}$ $9.06 \times 10^{-1}$	$1.58 \times 10^{-1}$ $1.60 \times 10^{-1}$	$2.48 \times 10^{-2}$ $2.34 \times 10^{-2}$
Optimal	$4.90 \times 10^{-1}$ $8.38 \times 10^{-1}$	$7.89 \times 10^{-2}$ $1.52 \times 10^{-1}$	$2.49 \times 10^{-3}$ $1.73 \times 10^{-2}$

Table 5.3: Quantitative measures on the control-input errors for  $T = 0.1$  (top of each entry) and  $T = 0.4$  (bottom)

	$L^\infty$	$L^2$	ITAE
Tustin	$2.27 \times 10^{-1}$ —	$1.17 \times 10^{-1}$ —	$5.42 \times 10^{-2}$ —
MPZ	$2.94 \times 10^{-1}$ —	$1.52 \times 10^{-1}$ —	$7.74 \times 10^{-2}$ —
PIM	$6.88 \times 10^{-2}$ $4.87 \times 10^{-1}$	$2.85 \times 10^{-2}$ $2.38 \times 10^{-1}$	$5.81 \times 10^{-3}$ $6.89 \times 10^{-2}$
Truncated PIM	$6.85 \times 10^{-1}$ $6.73 \times 10^{-1}$	$4.43 \times 10^{-1}$ $4.21 \times 10^{-1}$	$2.04 \times 10^{-1}$ $1.87 \times 10^{-1}$
Optimal	$4.53 \times 10^{-2}$ $4.64 \times 10^{-1}$	$1.50 \times 10^{-2}$ $2.20 \times 10^{-1}$	$2.94 \times 10^{-3}$ $4.71 \times 10^{-2}$

Table 5.4: Quantitative measures on the controlled-output errors for  $T = 0.1$  (top of each entry) and  $T = 0.4$  (bottom)

### 5.1.1 Simulations with Fixed-Point Arithmetic and Finite Number of Bits

A control system is truly practical when it performs relatively well under fixed- and/or floating-point arithmetic and finite number of bits. With the worst-case scenario being the fixed-point arithmetic computations, it is expected that the orders of the discrete-time controllers should influence the performance of the sampled-data control system, as opposed to the case when simulations are performed with floating-point arithmetic and a relatively large number of bits, e.g.  $\geq 32$ . The discrete-time controllers of the sampled-data control systems obtained with the optimal digital redesign and PIM methods are subjected to fixed-point arithmetic, and 8- and 16-bit representations and computations with scaling used when the coefficients of a transfer function lie outside the acceptable

range of values. The step responses for  $T = 0.1$  and  $T = 0.4$  are shown in Figures 5.3 and 5.4.

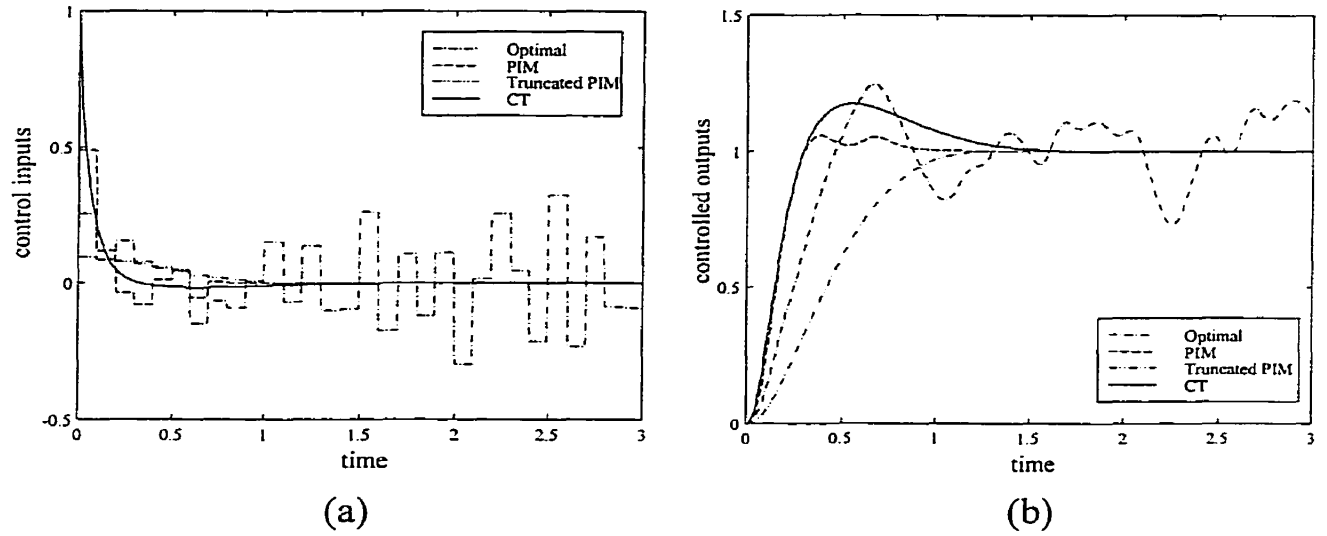


Figure 5.3: Step responses for  $T = 0.1$

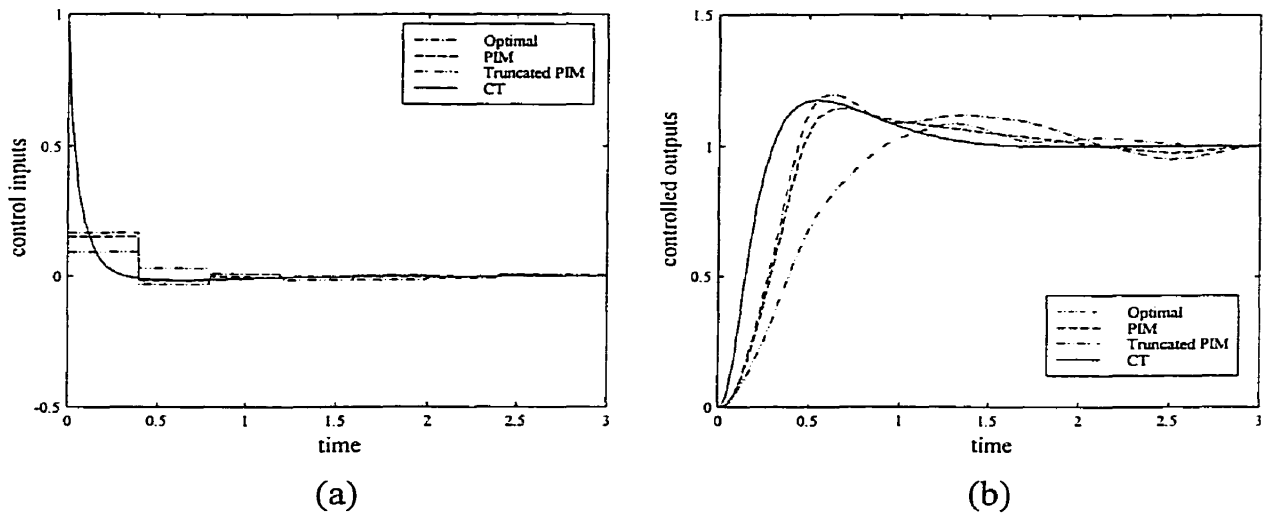


Figure 5.4: Step responses for  $T = 0.4$

The graphs show that the regular PIM-based sampled-data control system with controllers implemented with 8-bit controllers offers a superior performance to that obtained with the regular, truncated PIM method and the optimal digital redesign method. It is worth noticing that the control blocks obtained with the optimal digital redesign are implemented with 8 bits for  $T = 0.1$  and 16 bits for  $T = 0.4$ , and that doubling the number of bits for  $T = 0.4$  is still not sufficient for the optimal digital redesign to match the performance attained with the regular PIM method.

## 5.2 Digital Flight Control of T-2 Aircraft

Consider the pitch-angle control system of the T-2 aircraft in the short period mode [81] shown in Figure 5.5, where

$$\bar{G}_1(s) = \frac{1}{0.1s + 1}, \quad \bar{G}_2(s) = -\frac{22.062s + 19.079}{s^2 + 2.099s + 3.112}, \quad \bar{\Omega}(s) = \frac{s + 2}{s + 20}. \quad (5.2)$$

In the figure,  $\bar{G}_2(s)$  represents the transfer function of the aircraft from the elevator deflection, in radians, to the pitch rate (in rad./sec.), with poles at  $s = -1.0495 \pm j1.4179$ .  $\bar{G}_1(s)$  is the transfer function of the actuator from the controller's output to the elevator deflection, and  $\bar{\Omega}(s)$  that of the lead controller, which sets the closed-loop poles at  $s = -20.923, -8.0457, -1.377 \pm j2.0321, -0.3761$ .

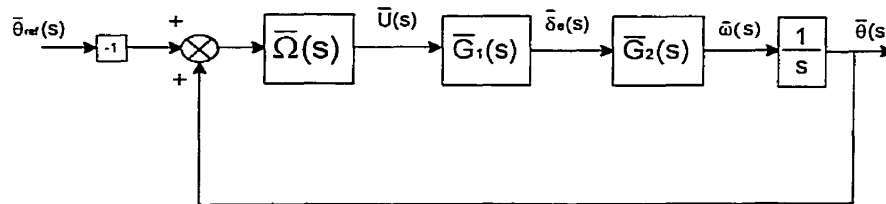


Figure 5.5: Continuous-time pitch control system

Digital redesign is performed by discretizing the continuous-time PITF, which relates  $\bar{\theta}_{ref}(s)$  to  $\bar{U}(s)$ , with the PIM methods and by discretizing  $\bar{\Omega}(s)$  with the matched pole-zero and Tustin's methods. The next figure shows the general block diagram of the

digitally redesigned pitch control systems, where one or more controller blocks can be unity.

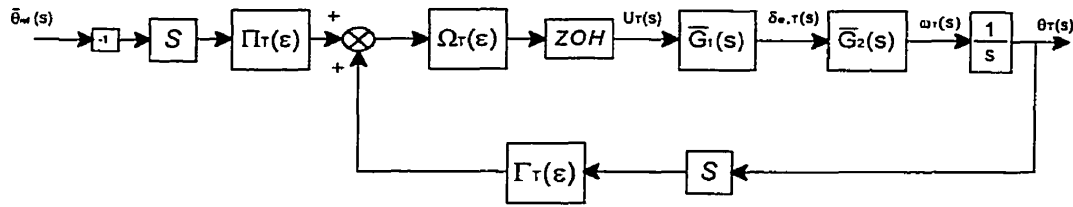


Figure 5.6: Digitally redesigned pitch control system

The controllers obtained with the local digital redesign methods are

$$\Omega_T(\epsilon) = \frac{(1 - e^{-20T})}{10(1 - e^{-2T})} \cdot \frac{\epsilon + (1 - e^{-2T})/T}{\epsilon + (1 - e^{-20T})/T} \text{ (MPZ)}, \quad (5.3)$$

$$\Omega_T(\epsilon) = \frac{\epsilon(\frac{T+1}{1+10T}) + (\frac{2}{1+10T})}{\epsilon + (\frac{20}{1+10T})} \text{ (Tustin)} \quad (5.4)$$

whereas the blocks obtained with the PIM methods are given in the following tables for the two extreme values of sampling period; that is,  $T = 0.05$  second and  $T = 4.4$  seconds.

Reduced-order PIM	$\Omega_T(\epsilon) = \frac{0.69\epsilon + 1.26}{1.11\epsilon + 12.73}$ $\Pi_T(\epsilon) = \frac{0.66\epsilon + 1.26}{0.69\epsilon + 1.26}$
Regular PIM (Elim. matrix)	$\Omega_T(\epsilon) = \frac{0.55\epsilon^3 + 2.91\epsilon^2 + 4.46\epsilon + 2.35}{\epsilon^3 + 15.65\epsilon^2 + 41.86\epsilon + 26.43}$ $\Pi_T(\epsilon) = \frac{0.66\epsilon^3 + 3.18\epsilon^2 + 4.87\epsilon + 2.35}{0.55\epsilon^3 + 2.91\epsilon^2 + 4.46\epsilon + 2.35}$
Regular PIM (State-space)	$\Omega_T(\epsilon) = \frac{0.66\epsilon^4 + 5.03\epsilon^3 + 13.72\epsilon^2 + 15.92\epsilon + 6.54}{\epsilon^4 + 18.48\epsilon^3 + 90.35\epsilon^2 + 239.9\epsilon + 152.13}$ $\Gamma_T(\epsilon) = \frac{-1.07\epsilon^3 + 1.66\epsilon^2 + 1.96\epsilon + 6.54}{0.66\epsilon^4 + 5.03\epsilon^3 + 13.72\epsilon^2 + 15.92\epsilon + 6.54}$

Table 5.5: Controllers obtained with PIM for  $T = 0.05$  second

Reduced-order PIM	$\Omega_T(\varepsilon) = \frac{0.0309\varepsilon+0.007}{\varepsilon+0.2107}$ $\Pi_T(\varepsilon) = \frac{0.0307\varepsilon+0.007}{0.0309\varepsilon+0.007}$
Regular PIM (Elim. matrix)	$\Omega_T(\varepsilon) = \frac{0.0309\varepsilon^3+0.0209\varepsilon^2+0.0047\varepsilon+0.0004}{\varepsilon^3+0.6628\varepsilon^2+0.1463\varepsilon+0.0108}$ $\Pi_T(\varepsilon) = \frac{0.0307\varepsilon^3+0.0209\varepsilon^2+0.0047\varepsilon+0.0004}{0.0309\varepsilon^3+0.0209\varepsilon^2+0.0047\varepsilon+0.0004}$
Regular PIM (State-space)	$\Omega_T(\varepsilon) = \frac{0.0307\varepsilon^4+0.0278\varepsilon^3+0.0095\varepsilon^2+0.0014\varepsilon+0.0001}{\varepsilon^4+1.0955\varepsilon^3+0.4325\varepsilon^2+0.0738\varepsilon+0.0046}$ $\Gamma_T(\varepsilon) = \frac{0.007\varepsilon^3+0.0048\varepsilon^2+0.0011\varepsilon+0.0001}{0.0307\varepsilon^4+0.0278\varepsilon^3+0.0095\varepsilon^2+0.0014\varepsilon+0.0001}$

Table 5.6: Controller blocks obtained with the PIM methods for  $T = 4.4$  seconds

Each non-unity discrete-time controller is realized in the so called direct form II structure [40]. The operator  $\varepsilon^{-1}$  is used as the basic operation on discrete-time signals because of its superior numerical characteristics than  $z^{-1}$  in the presence of a finite number of bits [29, 48]. The control systems based on the local discretization become unstable at around  $T = t_r/2$  sec. using the matched pole-zero method, and  $T = t_r/4$  sec. using Tustin's method, where  $t_r$  ( $= 4.4$  seconds) is the rise time of the continuous-time control system's step response. On the other hand, the reduced-order PIM-based control system is stable for *all* the sampling periods tested.

The poles of the continuous-time PITF are calculated and mapped to the  $\varepsilon$ -plane. The poles of the discrete-time PITF of each sampled-data control system are also obtained. Then, the relative error between each pole of each digitally redesigned sampled-data control system and the closest pole of the continuous-time PITF, seen in the  $\varepsilon$ -plane, is calculated and the maximum pole relative error is determined for each sampled-data system. Figure 5.7 shows the graph of the maximum closed-loop pole relative errors versus  $T$ . The relative errors between the  $\varepsilon$ -plane poles of the regular PIM-based system and the continuous-time control system are zero. From the figure, one expects a deterioration of the performances of the sampled-data control systems obtained with the local digital redesign methods, with respect to that obtained with the continuous-time and PIM-based

control systems, for  $T \geq 0.55$  second.

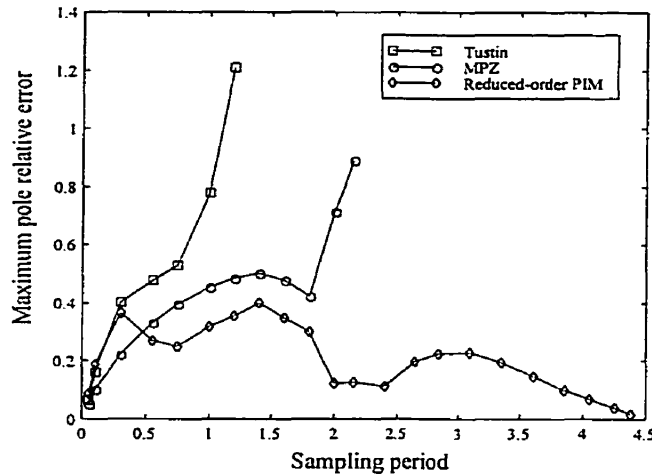


Figure 5.7: Maximum closed-loop pole relative errors with  $T$

Figure 5.8 shows the maximum relative differences between continuous-time and discrete-time coefficients corresponding to the same powers of  $s$  in  $\bar{\Omega}(s)$  and  $\varepsilon$  in  $\Omega_T(\varepsilon)$ , respectively, for different sampling periods and for the matched pole-zero, Tustin's and PIM methods. Note that for the regular PIM method,  $\Omega_T(\varepsilon)$  approaches the following as  $T \rightarrow 0$ :

$$\bar{\Omega}(s) = \frac{(s+1)(s+2)}{(s+1)(s+2)} \cdot \frac{(s+2)}{(s+20)} \quad (5.5)$$

and so the comparison takes this fact into account. It is seen in the figure that as the sampling period is reduced the differences in coefficients diminish, as expected from the convergence in the transfer function of the blocks. Referring to the stability property of the various sampled-data control systems, it can be appreciated from the figure that a closed-loop system with coefficients of  $\Omega_T(\varepsilon)$  relatively close to those of  $\bar{\Omega}(s)$  does not

imply superior closed-loop performance for a given sampling period.

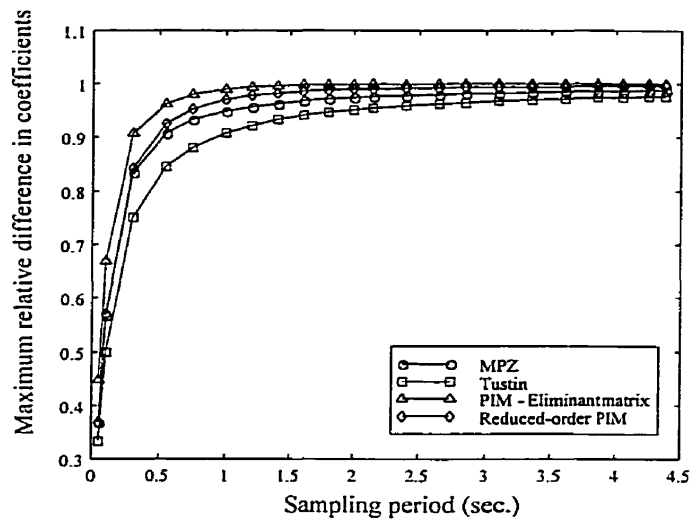


Figure 5.8: Maximum relative differences between corresponding coefficients of  $\Omega_T(\varepsilon)$  and  $\bar{\Omega}(s)$

For the  $\Pi_T(\varepsilon)$  block obtained with the PIM methods, it was found that each coefficient in the numerator approaches that in the denominator.

### 5.2.1 Responses to Reference Input

Figure 5.9 provides graphs of pitch angle  $\bar{\theta}(t)$ , pitch rate  $\bar{\omega}(t)$  and elevator deflection  $\bar{\delta}_e(t)$  of the continuous-time flight control system subjected to a signal  $\bar{r}(t) \in \mathcal{S}_1$  described as

$$\bar{r}(t) = \begin{cases} t/\alpha, & t \in [0, \alpha) \\ 1, & t \in [\alpha, \infty) \end{cases} \quad (5.6)$$

where  $\alpha = t_r/900$ . The control systems are not subjected to the unit step defined by  $\bar{r}(t) = 1$  for  $t > 0$  since it violates the restrictions imposed on the admissible reference inputs as explained in Definition 4.3.1 and the analytical methods developed in Chapter 4 cannot be used. The control input and controlled output responses of the digital flight

control systems are shown on Figure 5.10, for  $T = 0.3$  second, and on Figure 5.11, for  $T = 1$  second. It should be noted that for the smallest sampling period tested,  $T = 0.05$  second, all the digitally redesigned control systems have responses relatively close to those of the continuous-time flight control system. Figures 5.10 and 5.11 clearly show a deterioration in the responses with an increase in  $T$ . The deterioration occurring with the systems based on the local methods is mainly characterized by increased oscillations whereas that associated with the PIM-based systems is one of increased rise time and settling time. Moreover, in Figure 5.11, it is seen that the control input behaves according to the observations made in subsection 4.6.4; that is, with an increase in  $T$ , the magnitude of the control input approaches its steady-state value over all time instants.

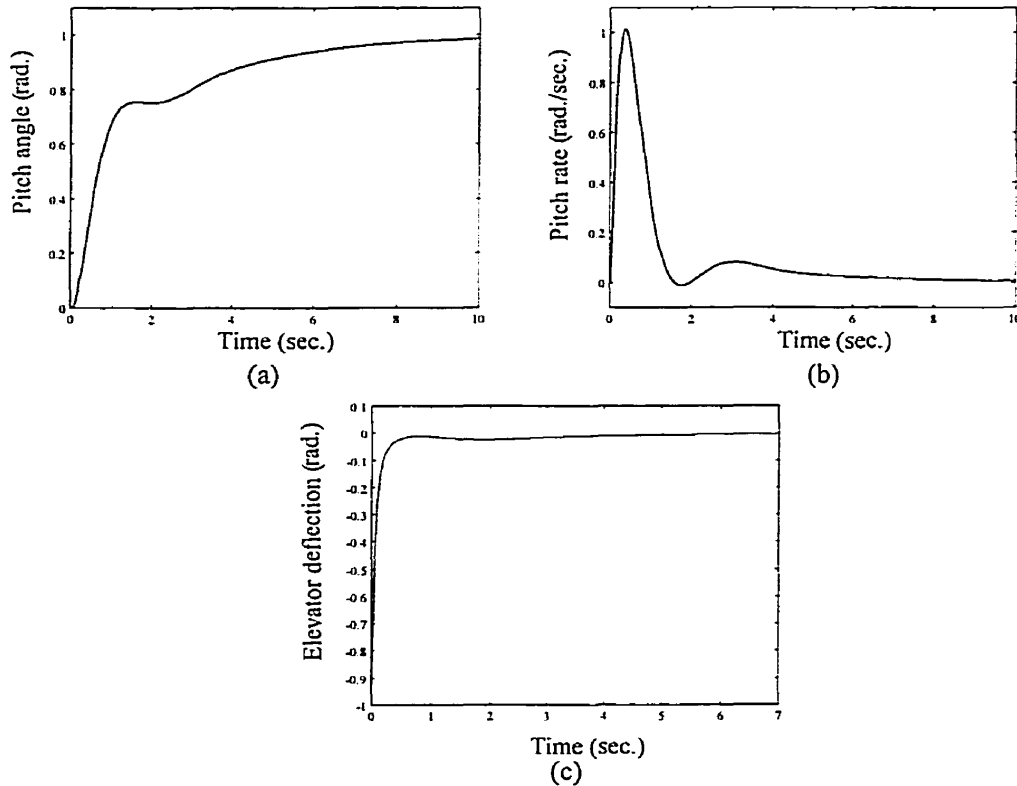
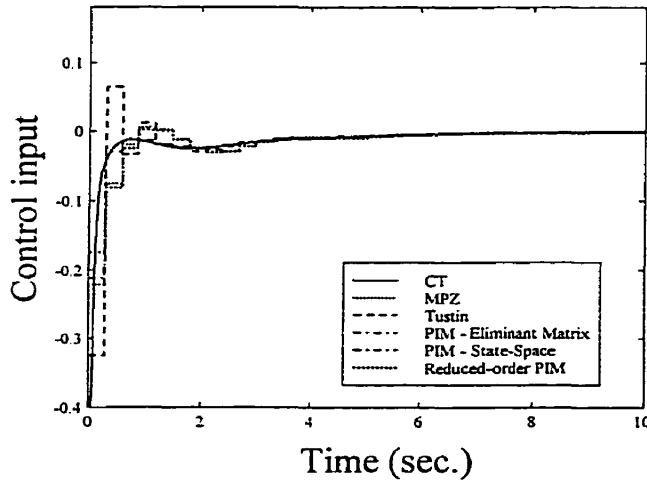
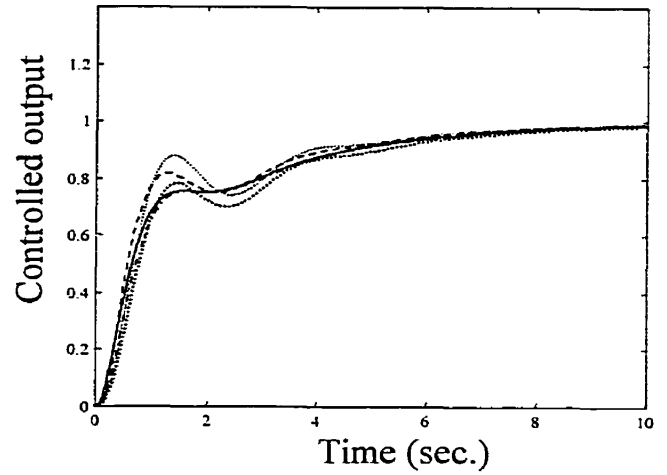


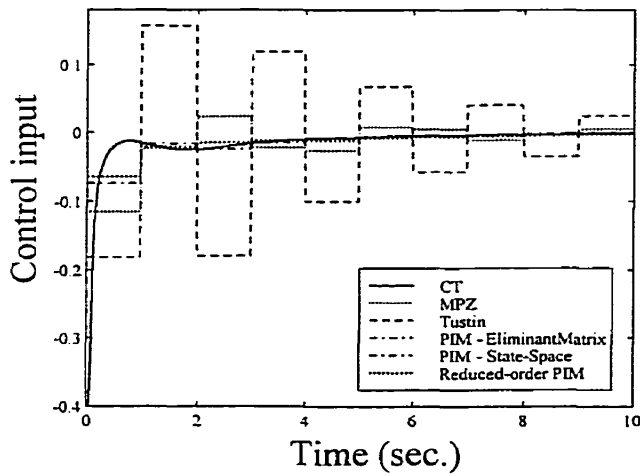
Figure 5.9: (a) Pitch angle  $\bar{\theta}(t)$ , (b) pitch rate  $\bar{\omega}(t)$ , and (c) elevator deflection  $\bar{\delta}_e(t)$



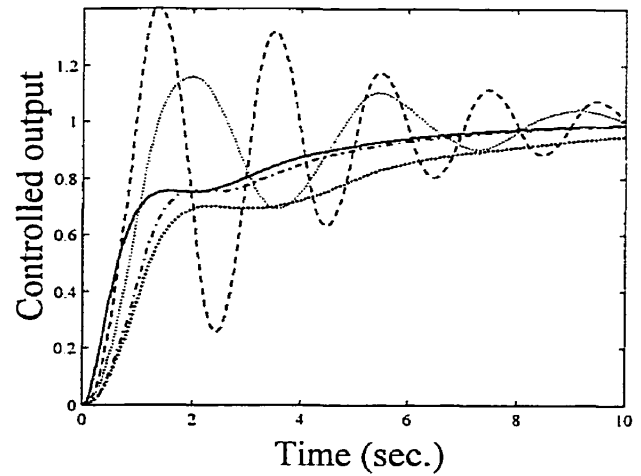
(a)



(b)

Figure 5.10: Control input and controlled output responses for  $T = 0.3$  second

(a)

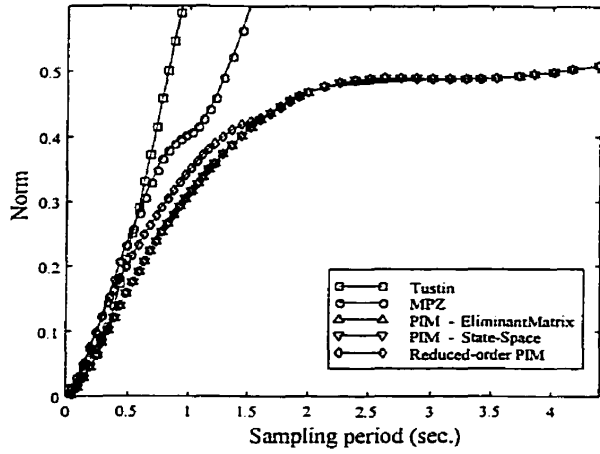


(b)

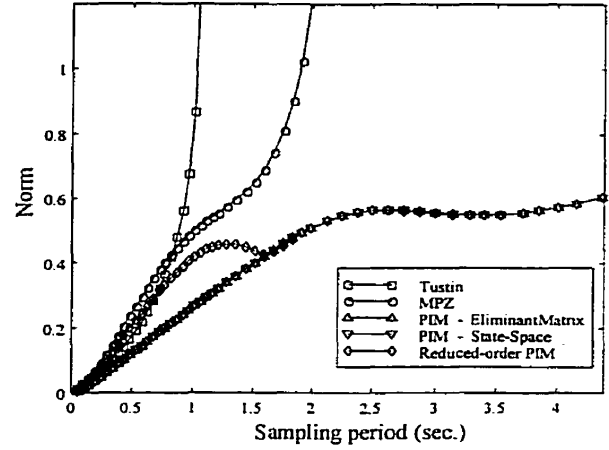
Figure 5.11: Control input and controlled output responses for  $T = 1$  second

With the digital flight control systems subjected to the input of (5.6), the angular position error (controlled-output error) is defined as  $\Delta\theta_T(t) = \theta_T(t) - \bar{\theta}(t)$ , the angular ve-

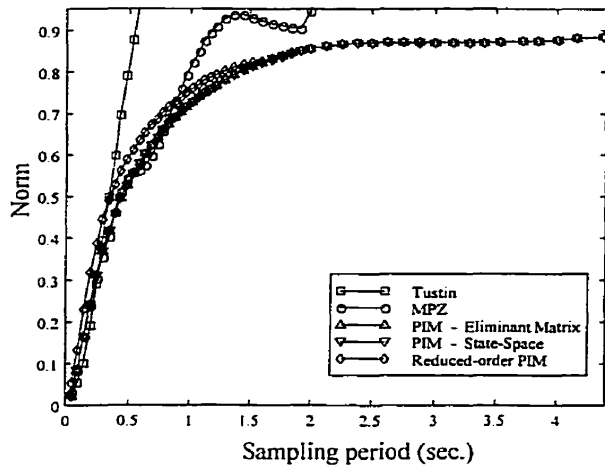
locity error as  $\Delta\omega_T(t) = \omega_T(t) - \bar{\omega}(t)$  and the control-input error as  $\Delta u_T(t) = u_T(t) - \bar{u}(t)$ . Furthermore, over the range of sampling frequencies for which internal stability of the discrete-time control systems takes place, the  $L^2$  and  $L^\infty$  norms of  $\Delta\theta_T(t)$ ,  $\Delta\omega_T(t)$  and  $\Delta u_T(t)$  are finite. However, because quantization effects can alter the steady-state gains for simulations performed with a limited number of bits, the  $L^2$  norm is evaluated over a finite and fixed time interval. Figures 5.12, 5.13 and 5.14 show the  $L^\infty$  and  $L^2$  norms of  $\Delta\theta_T(t)$ ,  $\Delta\omega_T(t)$  and  $\Delta u_T(t)$  for  $T \in [t_r/88, t_r]$ , when the computations and implementations are carried out using 32 bits with floating-point arithmetic. The norms of  $\Delta\theta_T(t)$ ,  $\Delta\omega_T(t)$  and  $\Delta u_T(t)$  approach zero for all the discrete-time flight control systems, as  $T \rightarrow 0$ . For most sampling periods, the PIM-based systems have smaller controlled-output error norms than the systems based on the local digital redesign methods. The  $L^\infty$  norm on the control-input errors can be smaller for the systems based on the local digital redesign methods than for the PIM-based systems. The response plots generated for each sampling period tested, although shown only for  $T = 0.3$  second and  $T = 1$  second in this thesis for brevity, reveal that this is caused by a low-magnitude control input for the PIM-based systems, at the  $k = 0$  sampling instant, whereas the continuous-time and sampled-data systems based on the local digital redesign methods have relatively large magnitude. It can be seen also that the regular PIM-based systems, whose Diophantine equations are solved with the eliminant matrix and state-space methods, have indistinguishable values of norm. Furthermore, the reduced-order PIM-based control system has an inferior performance at relatively fast sampling rates than the regular PIM-based systems, while, for slower sampling frequencies, the performances are alike. In other words, as the sampling rates are reduced ( $T \rightarrow \infty$ ), the responses obtained with all three PIM methods become relatively close to one another. Although not shown here, simulations of 16-bit, fixed-point arithmetic flight control systems have patterns of error norms essentially the same as those in the 32-bit, floating-point arithmetic case.



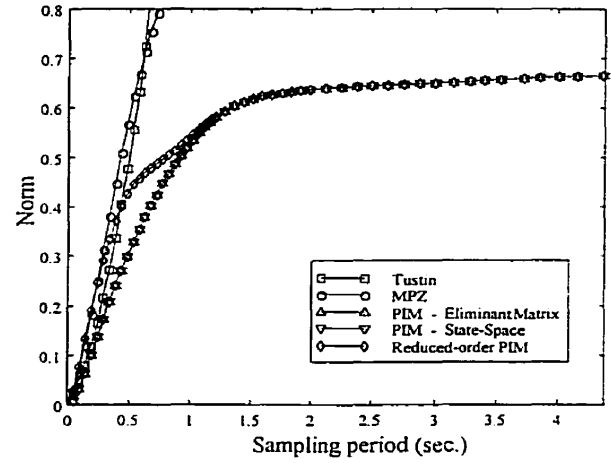
(a)



(b)

Figure 5.12: (a)  $\|\Delta\theta_T(t)\|_{L^\infty}$  and (b)  $\|\Delta\theta_T(t)\|_{L^2}$  with  $T$ 

(a)



(b)

Figure 5.13: (a)  $\|\Delta\omega_T(t)\|_{L^\infty}$  and (b)  $\|\Delta\omega_T(t)\|_{L^2}$  against  $T$

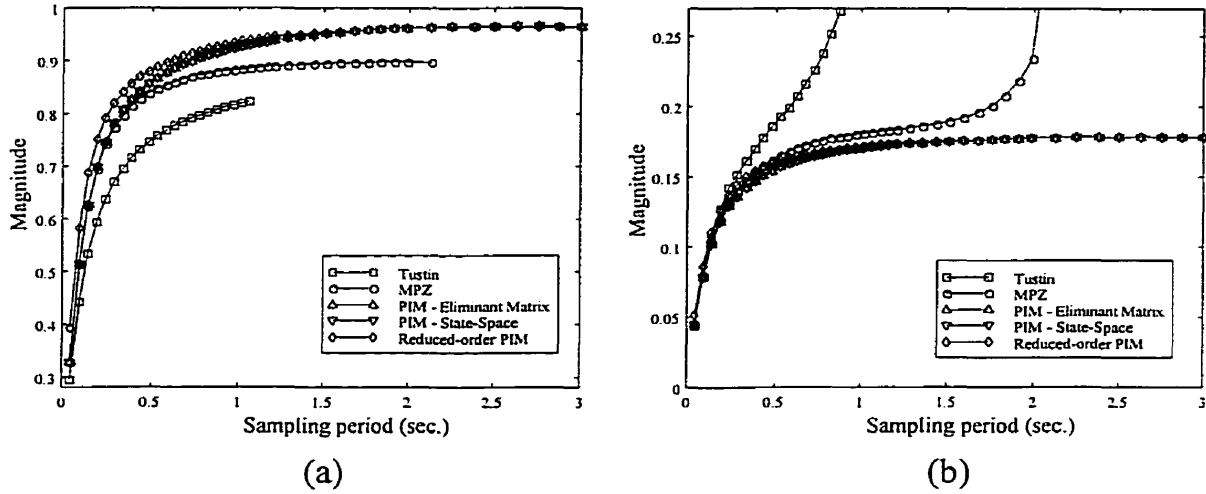


Figure 5.14: (a)  $\|\Delta u_T(t)\|_{L^\infty}$  and (b)  $\|\Delta u_T(t)\|_{L^2}$  with respect to  $T$

The ITAE index on the control-input and controlled-output errors as a function of the sampling period is plotted on Figure 5.15. In the figure, it is seen that the values of the index diminish with a reduction of the sampling period for all the digital redesign methods tested. Moreover, the regular PIM method has a smaller value of the index than that calculated with the local digital redesign methods for each sampling period, whereas the reduced-order PIM method offers a superior performance to the local methods for  $T \geq 1.4$  seconds. It can be seen also that the largest ITAE index, over  $T$ , attained by the regular PIM method is the smallest among the maximum ITAE indices obtained with all

the methods studied.

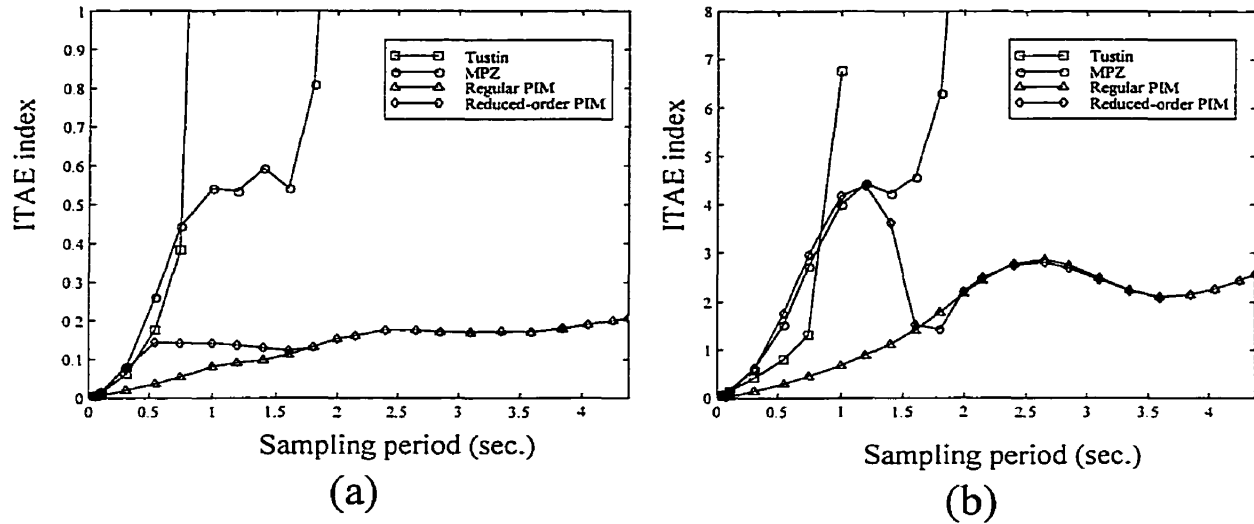
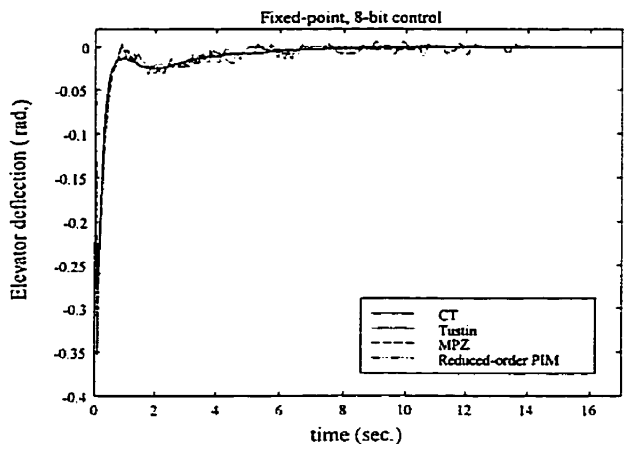
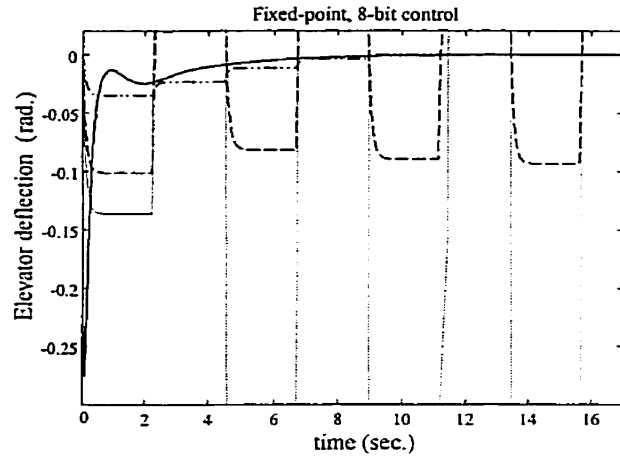


Figure 5.15: ITAE index on (a) the control-input and (b) the controlled-output errors

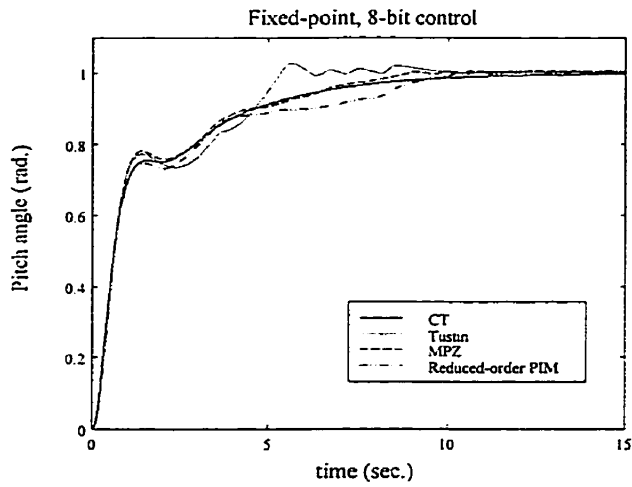
The elevator deflections and pitch angles of the low-order digital control systems subjected to the reference input described in (5.6) and implemented with 8-bit, fixed-point arithmetic are shown in Figures 5.16 and 5.17. At  $T = t_r/40$ , the performance of the reduced-order PIM-based control system is comparable to that of the Tustin- and matched pole-zero-based digital control systems. At the relatively long sampling period of  $T = t_r/2$ , only the reduced-order PIM-based control system offers a satisfactory performance. On the other hand, the response obtained with the regular PIM-based control system settles with an 11% error at steady-state for  $T = t_r/40$ , and is oscillatory for  $T = t_r/2$ , as shown in Figure 5.18. This shows that the orders of the controllers should be kept as low as possible in a practical implementation, even when using the Euler operator, especially at relatively slow sampling rates.



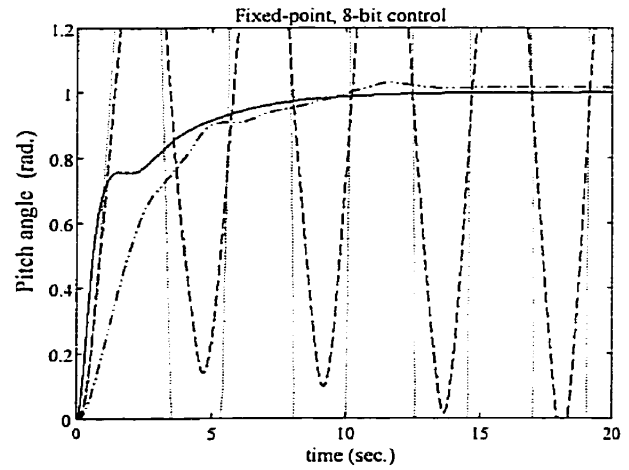
(a)



(b)

Figure 5.16: Elevator deflections for (a)  $T = t_r/40$  and (b)  $T = t_r/2$ 

(a)



(b)

Figure 5.17: Pitch angles for (a)  $T = t_r/40$  and (b)  $T = t_r/2$

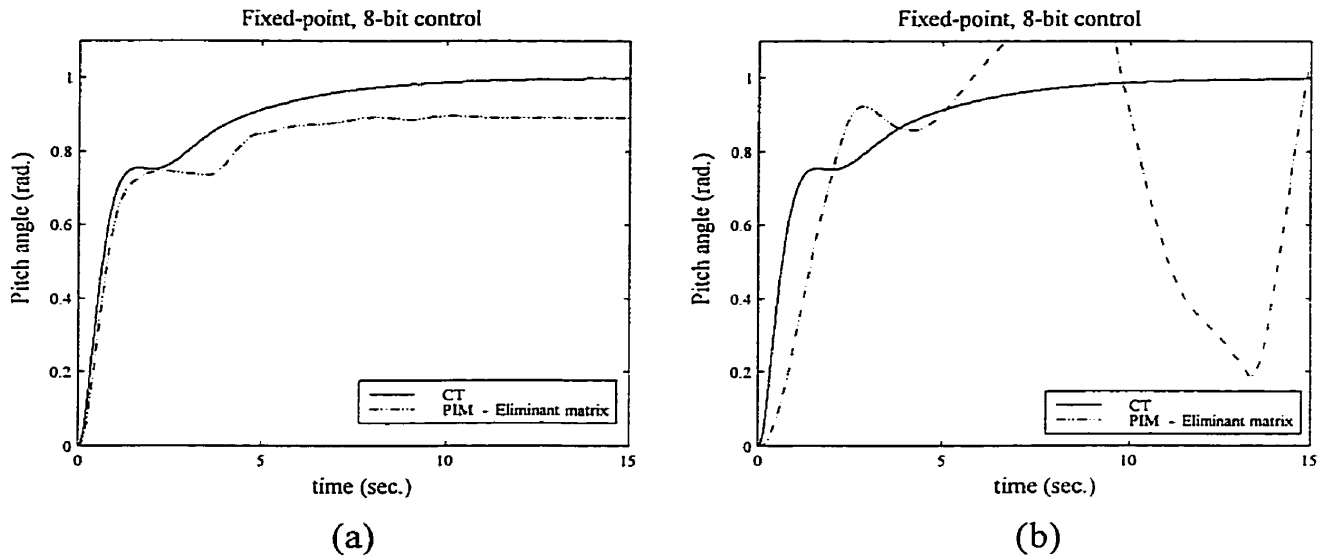


Figure 5.18: Pitch angles for (a)  $T = t_r/40$  and (b)  $T = t_r/2$

### 5.2.2 Response to Disturbance Input

Suppose that a wind gust enters the pitch control system as a disturbance  $\bar{d}(t)$  to the plant input. Although stochastic disturbance signals are better suited than deterministic ones for a general evaluation of the disturbance response, this thesis is concerned with deterministic signals only. Therefore, consider the simple test signal  $\bar{d}(t) \in \mathcal{S}_1$  shown in Figure 5.19, where  $\alpha = t_r/900$ .

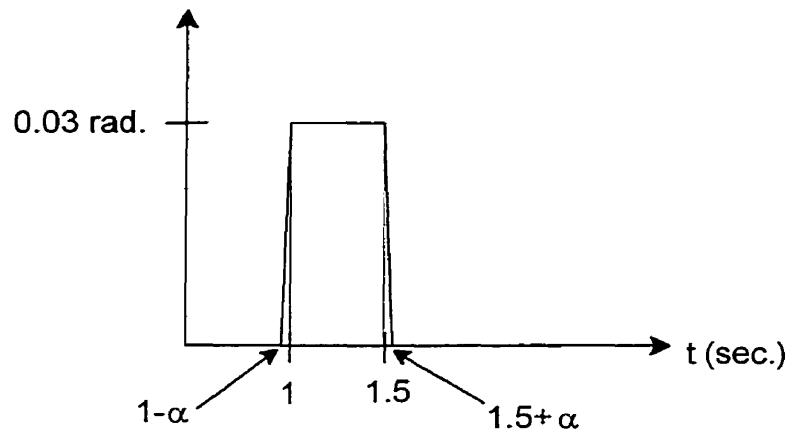


Figure 5.19: Disturbance to the plant input

It is desired to study the controlled output responses of the sampled-data control systems over a range of sampling periods when the only exogenous input to the pitch control system is  $\bar{d}(t)$ . The norms are calculated for each fixed  $T$  and the plots are shown in Figure 5.20.

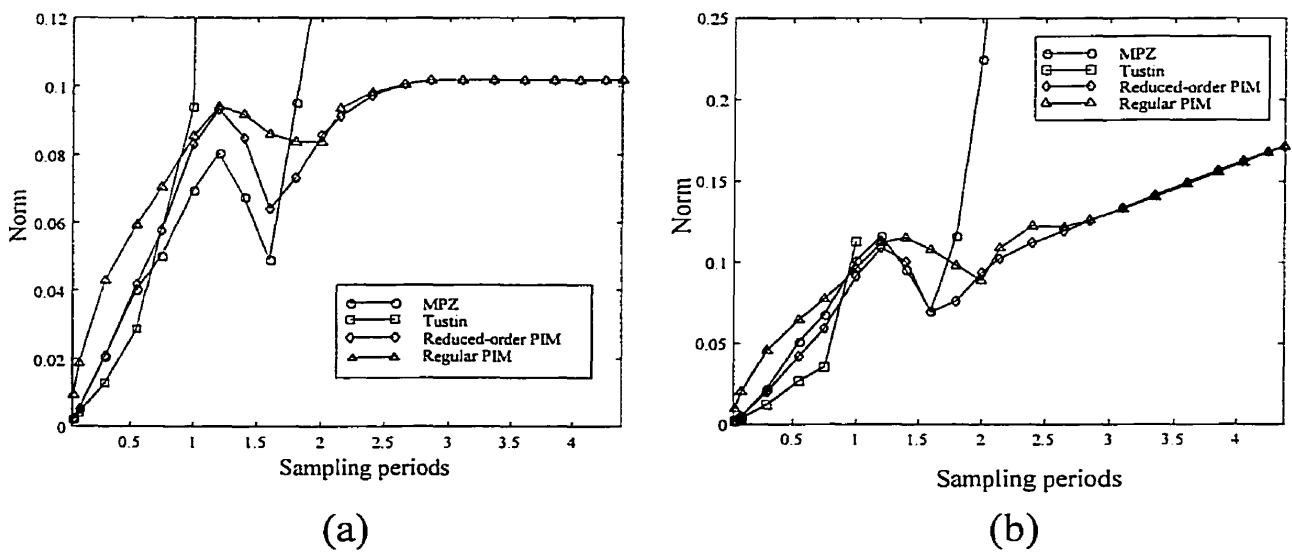


Figure 5.20: (a)  $L^\infty$  and (b)  $L^2$  norms on the controlled-output errors

The  $L^\infty$  and  $L^2$  norms shown in Figure 5.20 behave according to Theorem 4.5.2 for a diminishing sampling interval. Also, it can be seen that the PIM methods result in smaller error norms than those calculated for the local digital redesign methods when  $T \geq 1.8$  seconds and that the error norms associated with the PIM methods become indistinguishable from the graph for increasing sampling period. For the sampling periods below 1.8 seconds, the PIM methods do not always possess the smallest error norms. For instance, consider the systems obtained with a sampling period of 0.55 second. The controlled output responses are plotted in Figure 5.21. Despite the fact the regular PIM method exhibits a less oscillatory response than the responses obtained with the reduced-order PIM, MPZ and Tustin's methods, the disturbance response of the PIM-based system has an undershoot which is the largest in amplitude ( $L^\infty$  norm) and the discrepancy with the response of the continuous-time system is the greatest among the four digital redesign techniques ( $L^2$  norm).

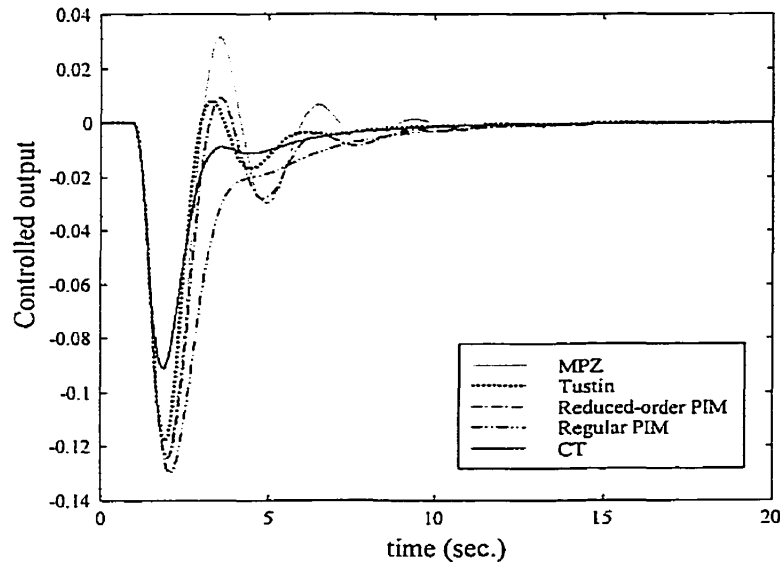


Figure 5.21: Controlled output responses to disturbance input ( $T = 0.55$  second)

The  $l^\infty$ - and  $l^2$ -induced norms of the system relating the sampled disturbance input to the discrete-time control input versus  $T$  are plotted on Figure 5.22. The  $L^\infty$ -induced

norm of the continuous-time control system relating the disturbance input to the control input is approximately 2 and its  $L^2$ -induced norm, 1.18.

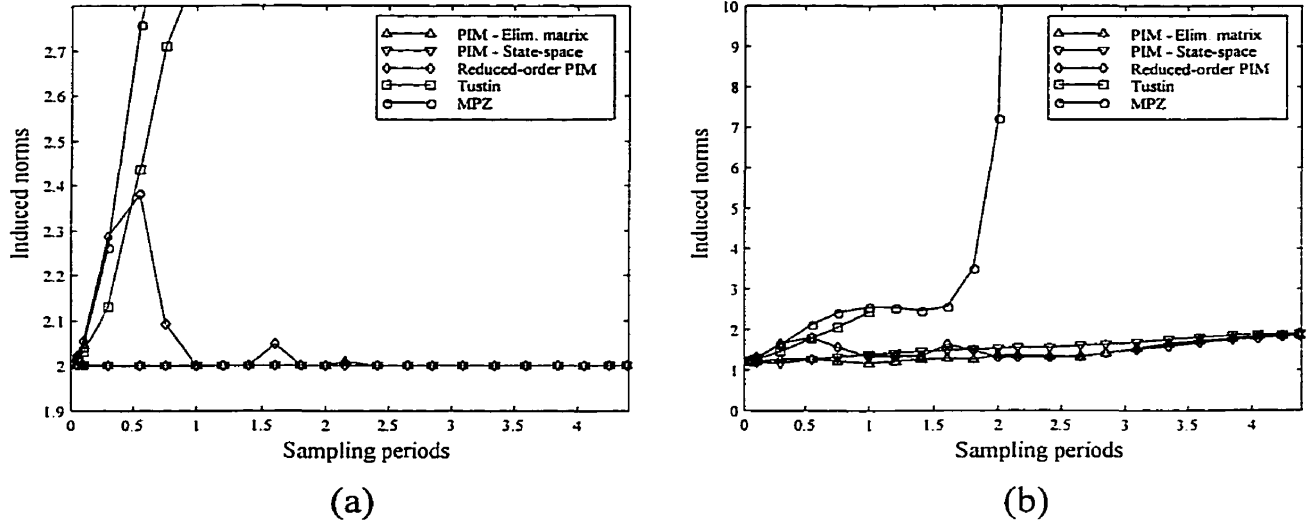


Figure 5.22: (a)  $l^\infty$ - and (b)  $l^2$ -induced norms with  $T$

In Figure 5.22, it is seen that the induced norms of the discrete-time systems approach the induced norms of the continuous-time system, as  $T \rightarrow 0$ . The induced norms associated with the reduced-order PIM fluctuate over the lower range of sampling periods compared with those of the other methods, although the reduced-order PIM still yields a superior performance than that obtained with the local methods for  $T \geq 0.55$  second. At relatively large sampling periods, the PIM-based control systems have finite induced norms which are almost identical for all three of them; in fact, as  $T \rightarrow \infty$ , the  $l^\infty$ - and  $l^2$ -induced norms approach a value of 2.

### 5.3 Control of Voice-Coil-Driven Flexible Positioner

Simulations and experiments are performed on the feedback control of a voice-coil-driven flexible positioner (VCFP) plant, which is a typical fast positioning mechanism, having

the following mathematical model in state-space form [82]:

$$\begin{aligned}
 \frac{d\bar{x}(t)}{dt} &= \begin{bmatrix} \frac{-d_1-d_{12}}{J_1} & \frac{-c_{12}}{J_1} & \frac{d_{12}}{J_1} & \frac{c_{12}}{J_1} & 0 & 0 & \frac{k_M}{J_1} \\ 1 & 0 & 0 & 0 & 0 & 0 & 0 \\ \frac{d_{12}}{J_2} & \frac{c_{12}}{J_2} & \frac{-d_{12}-d_{23}-d_2}{J_2} & \frac{-c_{12}-c_{23}}{J_2} & \frac{d_{23}}{J_2} & \frac{c_{23}}{J_2} & 0 \\ 0 & 0 & 1 & 0 & 0 & 0 & 0 \\ 0 & 0 & \frac{d_{23}}{J_3} & \frac{c_{23}}{J_3} & \frac{-d_{23}-d_3}{J_3} & \frac{-c_{23}}{J_3} & 0 \\ 0 & 0 & 0 & 0 & 1 & 0 & 0 \\ \frac{-k_E}{L} & 0 & 0 & 0 & 0 & 0 & \frac{-R}{L} \end{bmatrix} \bar{x}(t) \\
 &+ \begin{bmatrix} 0 & 0 & 0 & 0 & 0 & 0 & 1/L \end{bmatrix}^T \bar{u}(t) \\
 \bar{y}(t) &= \begin{bmatrix} 0 & 0 & 0 & 0 & 0 & k_r \cdot k_x & 0 \end{bmatrix} \bar{x}(t)
 \end{aligned} \tag{5.7}$$

where the constants are given in the following table.

$R = 1 \Omega$	$L = 1 \times 10^4 \text{ H}$
$k_E = 1 \text{ V}/(\text{rad/s})$	$k_M = 0.1 \text{ Nm/A}$
$k_x = 1 \times 10^5 \text{ V/m}$	$J_1 = 1.1 \times 10^{-4} \text{ kg} \cdot \text{m}^2$
$J_2 = 2.6 \times 10^{-4} \text{ kg} \cdot \text{m}^2$	$J_3 = 1.1 \times 10^{-4} \text{ kg} \cdot \text{m}^2$
$d_1 = 0.08 \text{ Nm}/(\text{rad/s})$	$d_2 = 0.08 \text{ Nm}/(\text{rad/s})$
$d_3 = 0.03 \text{ Nm}/(\text{rad/s})$	$c_{12} = 1 \times 10^4 \text{ Nm/rad}$
$c_{23} = 1 \times 10^4 \text{ Nm/rad}$	$d_{12} = 0.08 \text{ Nm}/(\text{rad/s})$
$d_{23} = 0.08 \text{ Nm}/(\text{rad/s})$	$k_r = 0.1 \text{ m/rad}$

Table 5.7: Plant parameters

The control system consists of the VCFP in closed-loop with a lead controller given by

$$\bar{\Omega}(s) = 5000 \cdot \frac{0.00112s + 0.7}{s + 5000} \tag{5.8}$$

and with structure as in Figure 1.4(a), where  $\bar{\Pi}(s) = \bar{\Gamma}(s) = 1$ . The controlled output

voltage represents the position of the end of a mechanical arm and the reference input voltage stands for the commanded position. The analog control system's performance, in terms of a unit step reference input, is provided in Table 5.8.

Rise time	$t_r = 3 \times 10^{-4}$ second
Settling time	$t_s = 3 \times 10^{-3}$ second
Maximum overshoot	$M_p = 0.18$
DC gain	$K_{DC} = 1$

Table 5.8: Performance parameters of continuous-time control system

Digital redesign is performed on this system with the most common local methods, Tustin's mapping and matched pole-zero, and the regular PIM, reduced-order PIM, and reduced-order, truncated PIM methods. For the regular PIM method, the Diophantine equation is solved with the state-space factorization. The discrete-time controllers are calculated for  $T \in [t_r/2, 1.7t_r]$ , and shown for  $T = 1.5t_r$  in Table 5.9. For ease of reading the table, the coefficients are shown with limited precision. The resulting sampled-data control systems have the structure of Fig. 1.4(b), where some blocks can be unity

depending on the digital redesign method used, and the ZOH is placed at control input.

Tustin	$\Omega_T(\varepsilon) = \frac{3.006\varepsilon+1647.059}{\varepsilon+2352.941}$
MPZ	$\Omega_T(\varepsilon) = \frac{2.554\varepsilon+1391.601}{\varepsilon+1988.002}$
Regular PIM	$\Omega_T(\varepsilon) = \frac{\left( \begin{array}{l} 2.021\varepsilon^7 + 2.059 \cdot 10^4\varepsilon^6 + 8.786 \cdot 10^7\varepsilon^5 \\ +2.026 \cdot 10^{11}\varepsilon^4 + 2.714 \cdot 10^{14}\varepsilon^3 + 2.099 \cdot 10^{17}\varepsilon^2 \\ +8.631 \cdot 10^{19}\varepsilon + 1.444 \cdot 10^{22} \end{array} \right)}{\left( \begin{array}{l} \varepsilon^7 + 1.423 \cdot 10^4\varepsilon^6 + 8.588 \cdot 10^7\varepsilon^5 \\ +2.855 \cdot 10^{11}\varepsilon^4 + 5.417 \cdot 10^{14}\varepsilon^3 + 5.082 \cdot 10^{17}\varepsilon^2 \\ +3.197 \cdot 10^{19}\varepsilon - 2.488 \cdot 10^{23} \end{array} \right)}$ $\Gamma_T(\varepsilon) = \frac{\left( \begin{array}{l} 483.903\varepsilon^6 + 1.852 \cdot 10^7\varepsilon^5 + 1.182 \cdot 10^{11}\varepsilon^4 \\ +3.316 \cdot 10^{14}\varepsilon^3 + 4.191 \cdot 10^{17}\varepsilon^2 + 1.735 \cdot 10^{20}\varepsilon \\ +1.444 \cdot 10^{22} \end{array} \right)}{\left( \begin{array}{l} 2.021\varepsilon^7 + 2.059 \cdot 10^4\varepsilon^6 + 8.786 \cdot 10^7\varepsilon^5 \\ +2.026 \cdot 10^{11}\varepsilon^4 + 2.714 \cdot 10^{14}\varepsilon^3 + 2.099 \cdot 10^{17}\varepsilon^2 \\ +8.631 \cdot 10^{19}\varepsilon + 1.444 \cdot 10^{22} \end{array} \right)}$
Reduced-order PIM	$\Omega_T(\varepsilon) = \frac{1.976\varepsilon+1100.794}{1.109\varepsilon+4107.366}$ $\Pi_T(\varepsilon) = \frac{2.021\varepsilon+1100.794}{1.976\varepsilon+1100.794}$
Reduced-order truncated PIM	$\Omega_T(\varepsilon) = \frac{1.976\varepsilon+1100.794}{1.109\varepsilon+4107.366}$

Table 5.9: Controller transfer functions for  $T = 1.5t_r$ .

### 5.3.1 Experimental Results

Both the fixed- and floating-point sampled-data control systems have the configuration illustrated in Figure 5.23, where the arrows indicate the direction of the flow of information, and A/D and D/A respectively denote analog-to-digital and digital-to-analog converters. The discrete-time part of the control system uses the Texas Instruments'

TMS320C31 digital signal processor (DSP), which performs floating-point computations on 32-bit data words. The digital-to-analog converter has a 12-bit resolution and the two analog-to-digital converters are 16-bit successive approximation converters [83]. The connections between the VCFP plant and the converters are made through standard BNC cables, whereas the converters are connected to the DSP via 32-bit buses [84].

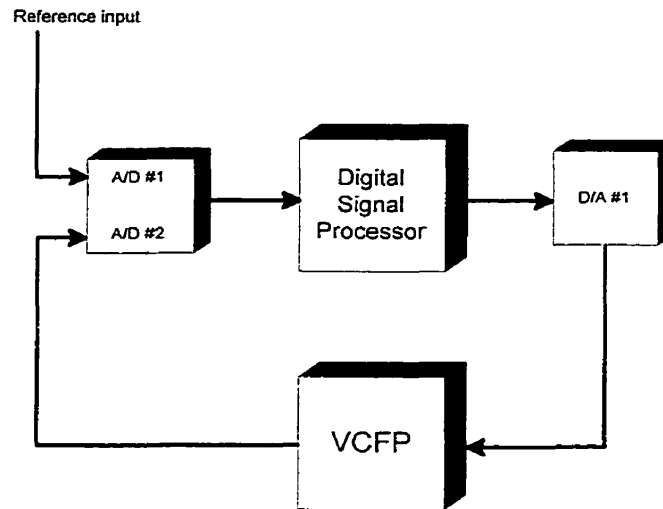
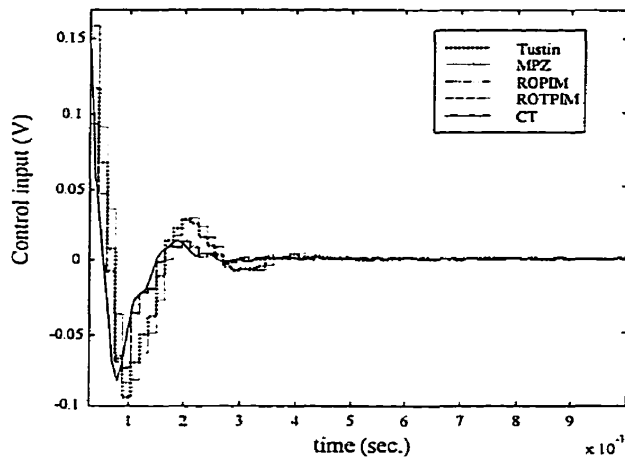


Figure 5.23: Sampled-data control system configuration

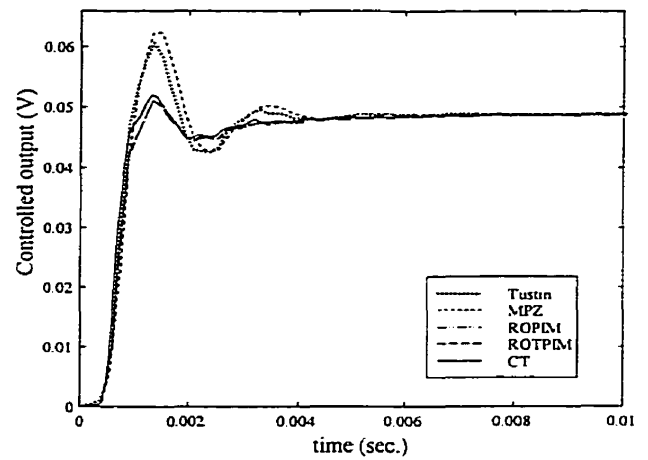
The reference input applied to the control systems is a constant signal with amplitude of 50 mV for  $t \geq 0$  which is part of the space  $\mathcal{S}_1$ .

### Floating-Point Controllers

The control input and controlled output responses of the sampled-data control systems, for the two extreme values of sampling, are shown in Figures 5.24 and 5.25, where ROPIM and ROTPIM are the acronyms for reduced-order PIM and reduced-order, truncated PIM, respectively. A qualitative comparison with the responses of the continuous-time control system reveals the superiority of the PIM techniques to the Tustin's and matched pole-zero methods, especially when the sampling period is relatively long.

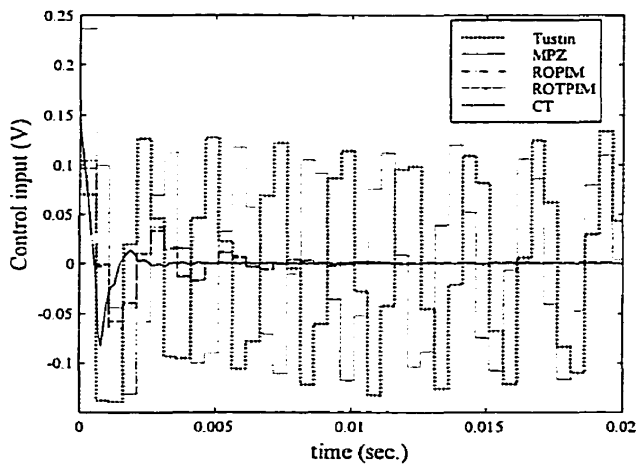


(a)

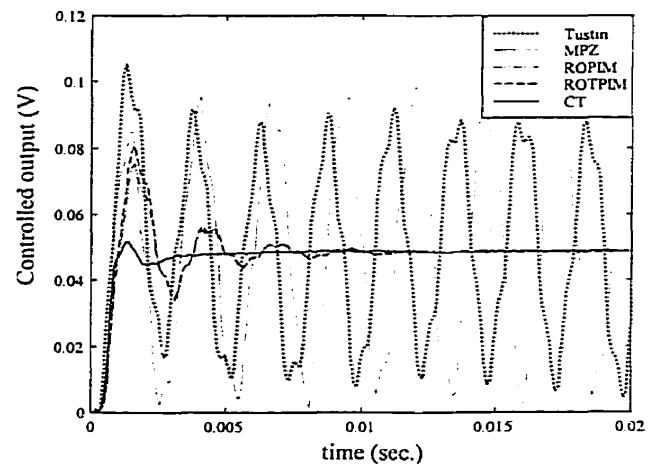


(b)

Figure 5.24: Control input and controlled output responses ( $T = t_r/2$ )



(a)



(b)

Figure 5.25: Control input and controlled output responses ( $T = 1.7t_r$ )

The norms of control-input and controlled-output error responses are calculated over a finite time interval and their values against  $T$  are shown in Figures 5.26 and 5.27. The

ITAE indices are also evaluated for the error signals  $(u_T(t) - \bar{u}(t))$  and  $(y_T(t) - \bar{y}(t))$  over a fixed, finite time interval and the graphs are given in Figure 5.28. The controlled-output error is smaller in the norms and in the ITAE performance index for the PIM methods than for the local redesign methods for all the sampling frequencies considered in the experiments. On the other hand, the supremum norm of the control-input error can be smaller for the local methods over a limited range of sampling periods.

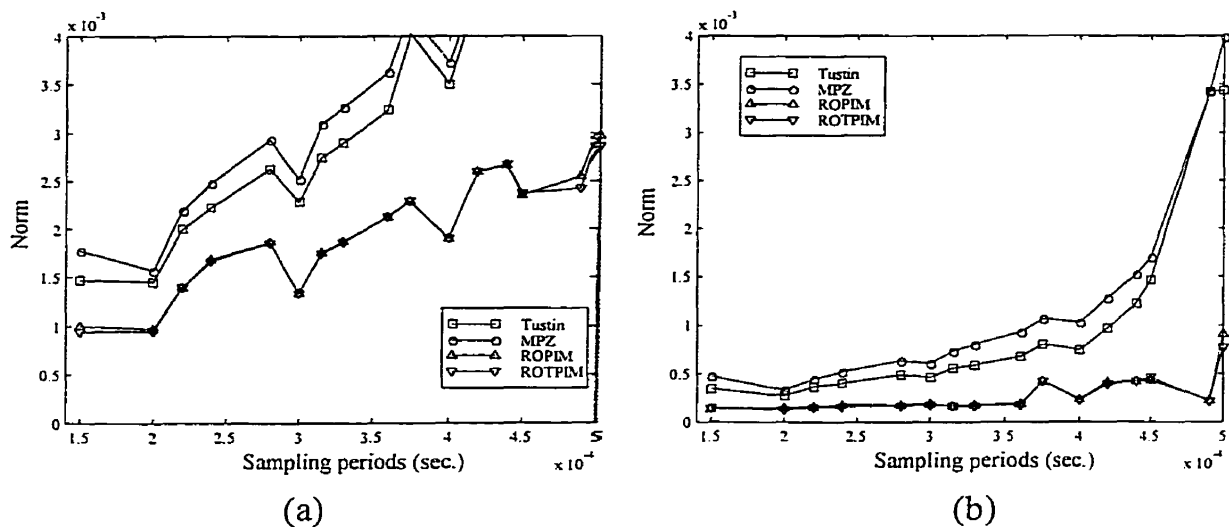
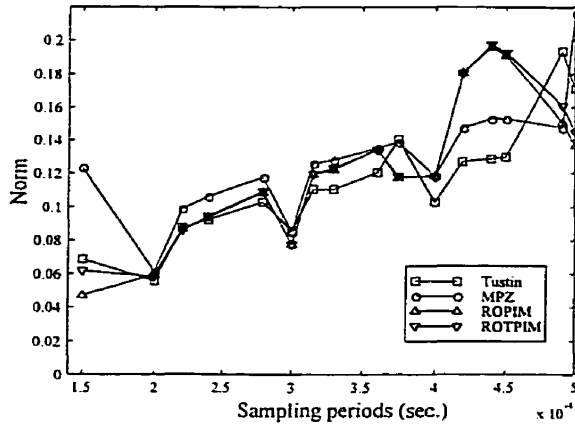
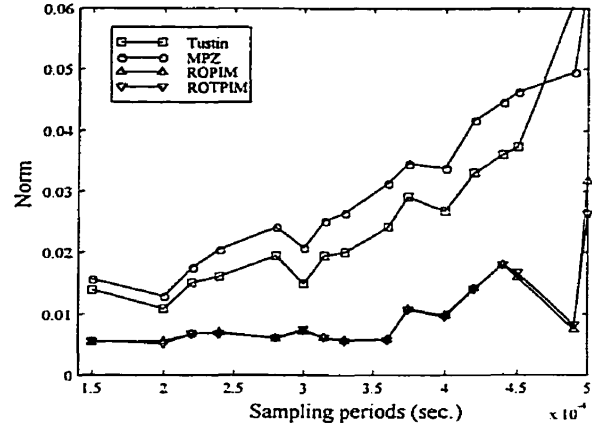


Figure 5.26:  $L^2$  error norms at (a) control input and (b) controlled output vs.  $T$

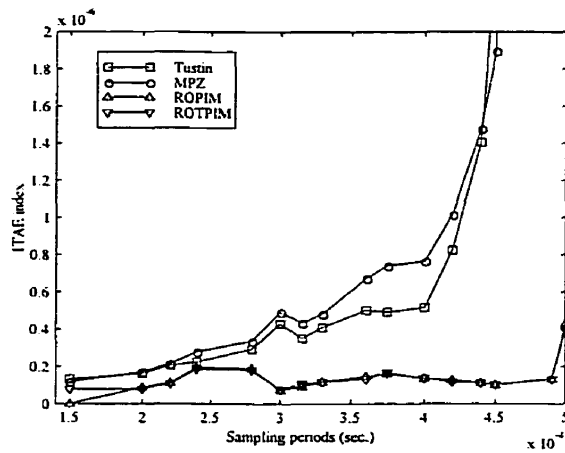


(a)

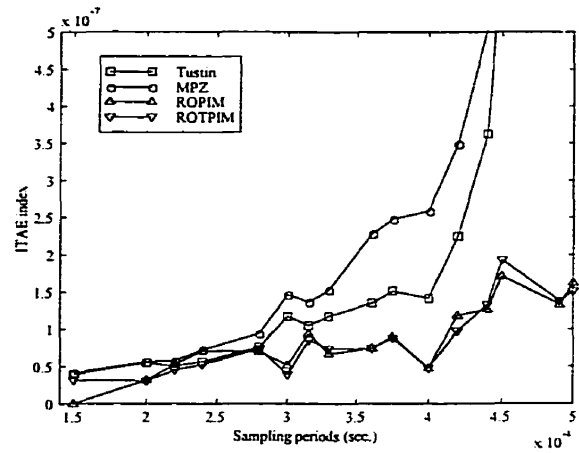


(b)

Figure 5.27:  $L^\infty$  error norms at (a) control input and (b) controlled output with respect to  $T$



(a)



(b)

Figure 5.28: ITAE indices for (a) the control-input and (b) the controlled-output errors against  $T$

The plots for the regular PIM method are not shown since the implementation and processing of the seventh order controllers  $\Pi(\varepsilon)$  and  $\Omega(\varepsilon)$ , which require considerably more instructions than the low-order controllers obtained with the other digital redesign methods, cannot be carried out with the DSP for the sampling rates selected; that is,

the computational time necessary to process the controllers with the DSP is longer than the sampling intervals selected.

When the amplitude of the reference input is too large, the operational amplifiers of the VCFP can saturate. One consequence may be that the controlled output response looks satisfactory, yet its shape is mainly due to the rate limiters present in the plant. A linear system analysis is then contaminated by the nonlinearities and the theoretical concepts conveyed in Chapters 3 and 4 become irrelevant. For example, by carrying out an experiment with a constant reference input of 1 V amplitude and for a sampling period of  $5 \times 10^{-4}$  second, it is found that the control inputs and controlled outputs behave in a satisfactory manner, as shown in Figure 5.29, even for the case of the matched pole-zero and Tustin's methods, which result in an oscillatory response in the linear range of operation of the control system, as shown in Figure 5.25. However, the actual control input to the plant is different from the plant input calculated with the controllers. It should be noted that, although stable in this particular case, once saturation takes place, the control system becomes nonlinear and instability can result in general.

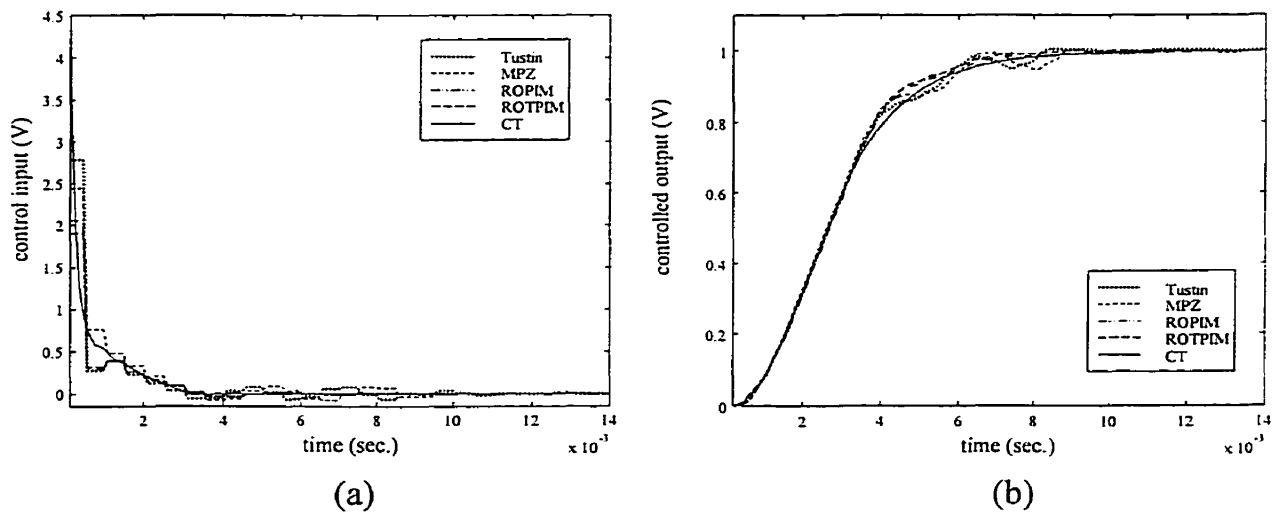


Figure 5.29: Responses of sampled-data control systems

## Fixed-Point Controllers

Experiments with 32-bit fixed-point representations and computations are carried out with the same physical setup as that used in the floating-point experiments. The responses are shown for two sampling periods in Figures 5.30 and 5.31. For the shortest sampling period, the responses of the sampled-data systems obtained with the ROPIM and ROTPIM methods are almost identical. Their control input behavior is less oscillatory than that obtained with the Tustin's mapping and matched pole-zero methods and their controlled output offers less overshoot. For the longer sampling interval, the control inputs of the PIM-based control systems are closer to that of the continuous-time system than those obtained with the local methods of digital redesign, and the controlled output responses of the PIM-based systems settle down, whereas the responses of the systems obtained with the local methods remain oscillatory.

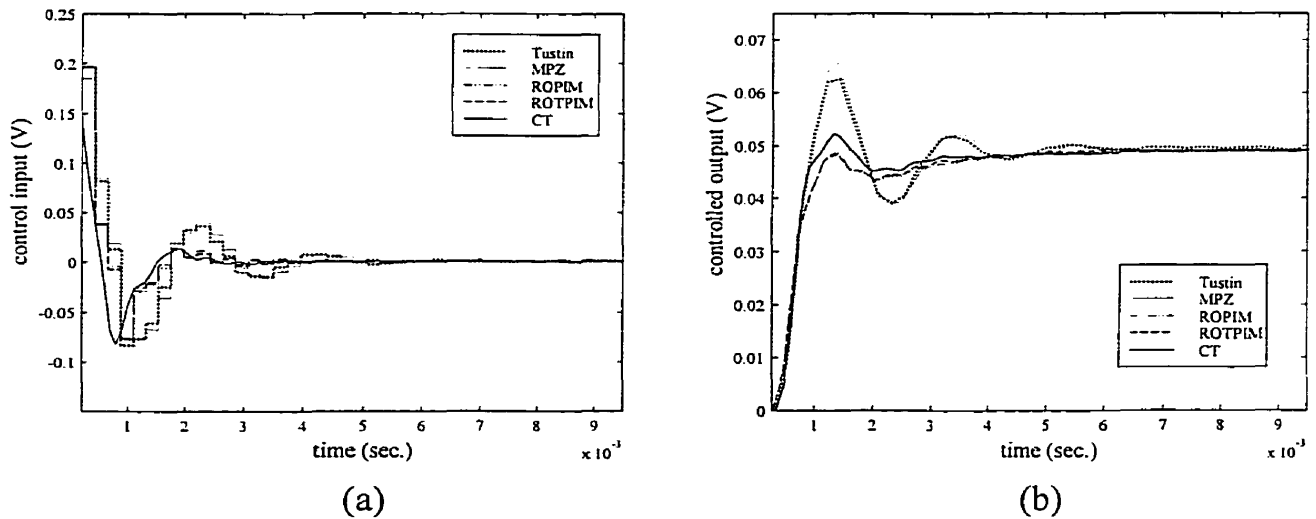


Figure 5.30: Control inputs and controlled outputs ( $T = 2t_r/3$ )

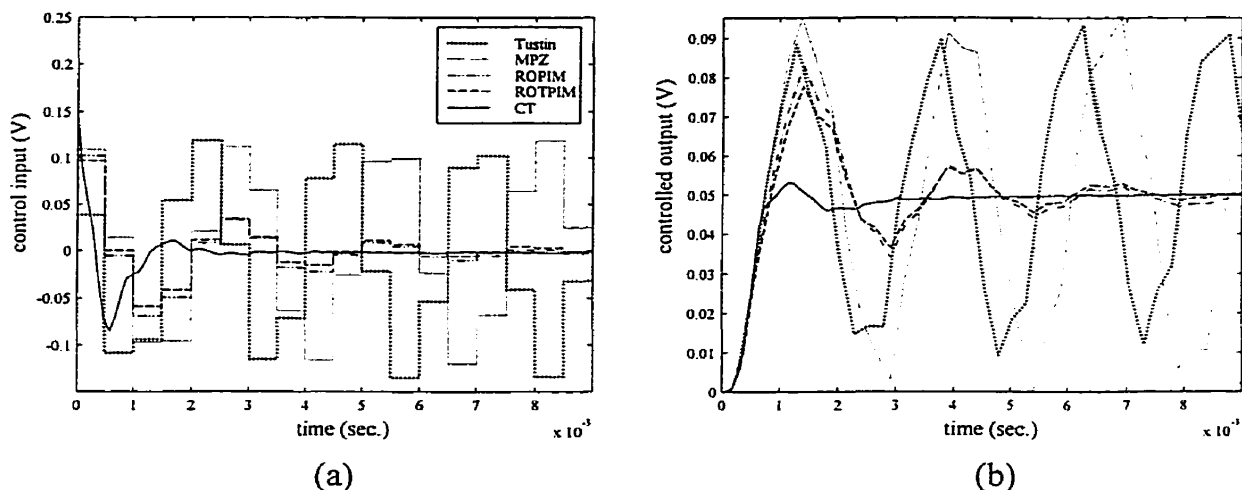


Figure 5.31: Control inputs and controlled outputs ( $T = 1.7t_r$ )

It should be pointed out that control laws implemented with as low as 16 bits provide unacceptable responses for all the methods tested and for the entire range of sampling periods considered.

## 5.4 Gas-Turbine Engine Speed Control<sup>3</sup>

Consider a turboshaft engine [85, 86] which can drive a helicopter's main and tail rotors. The operation of the engine can be briefly described as follows with reference to the schematics of Figure 5.32(a): air enters the engine inlet where it is compressed and mixed with fuel and the mixture is then ignited in the combustion chamber. The hot gas coming out of the combustion chamber is expanded through gas generator and power turbines. The power turbine drives the engine output shaft, whereas the gas generator, or compressor, turbine provides the energy to drive the compressor.

<sup>3</sup>The material is based on a collaborative research work with Pratt & Whitney Canada, Inc., which has authorized the release of information contained in this section.

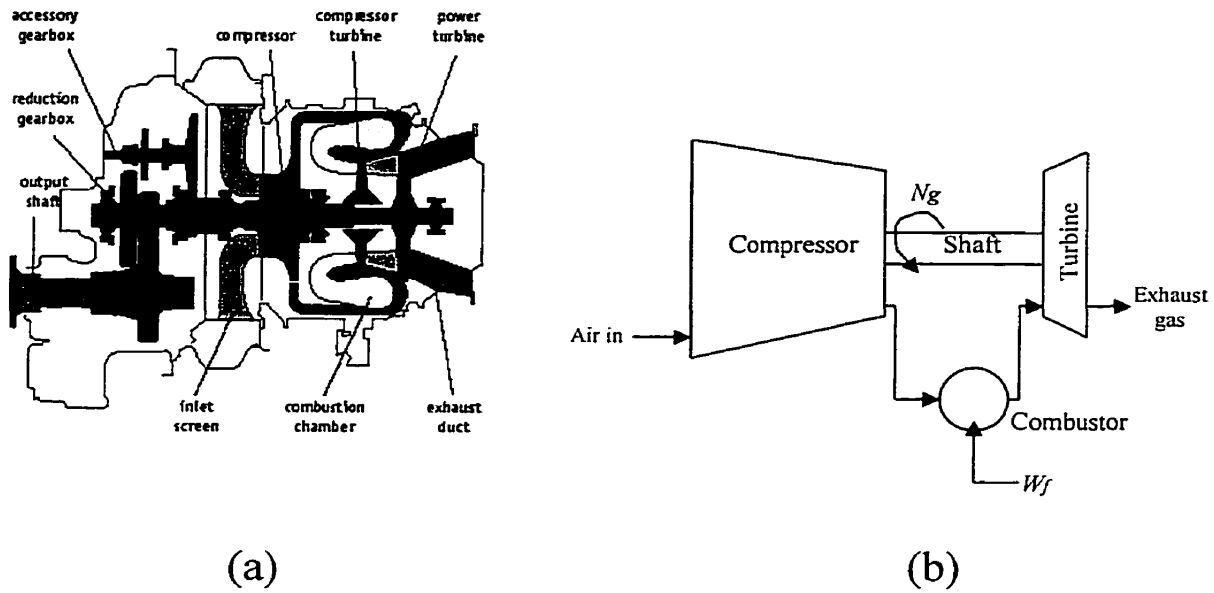


Figure 5.32: Schematics of (a) turboshaft engine and (b) gas generator

In this section, the compressor-combustor-turbine part of the engine, also known as the gas generator and shown schematically in Figure 5.32(b), is considered. In the figure, the shaft speed of the gas generator turbine, referred to as gas generator speed  $N_g$  with units of rpm, can be increased or decreased by appropriately varying the flow of fuel,  $W_f$ , in the combustor, or combustion chamber. The fuel flow is modulated by varying the current, denoted as  $I_{tm}$  with units of Amperes (A), to a torque motor interface from an electronic controller [87]. From a control perspective, the task consists of sending a torque motor current to the system having input  $I_{tm}$  and output  $N_g$  which follows the commanded gas generator speed within an acceptable level of error. The block diagram of the simplified feedback control system taken as an independent system in this thesis is shown in Figure 5.33. Several variables such as pressure and temperature of the fluids at different stages of the engine are omitted in the figure to simplify the notation. In Figure 5.33, the plant is composed of the fuel metering unit in cascade with the engine. The fuel metering unit is the electro-hydraulic system relating the control signal  $I_{tm}$  to the fuel flow entering the combustor,  $W_f$ . The engine relates  $W_f$  to  $N_g$ , assuming

constant ambient pressure and temperature. The plant is nonlinear due to the presence of rate limiters in the fuel metering unit to the values of  $I_{tm}$  ( $0 \text{ A} \leq I_{tm} \leq 150 \text{ A}$ ) and  $W_f$  ( $17 \text{ kg/h} \leq W_f \leq f(P_c) \text{ kg/h}$ , where  $f(P_c)$  is some function of  $P_c$ , the compressor discharge pressure, and kg/h represents kilograms per hour), and the nonlinear dynamics of the compressor, combustor and gas generator turbine [87].

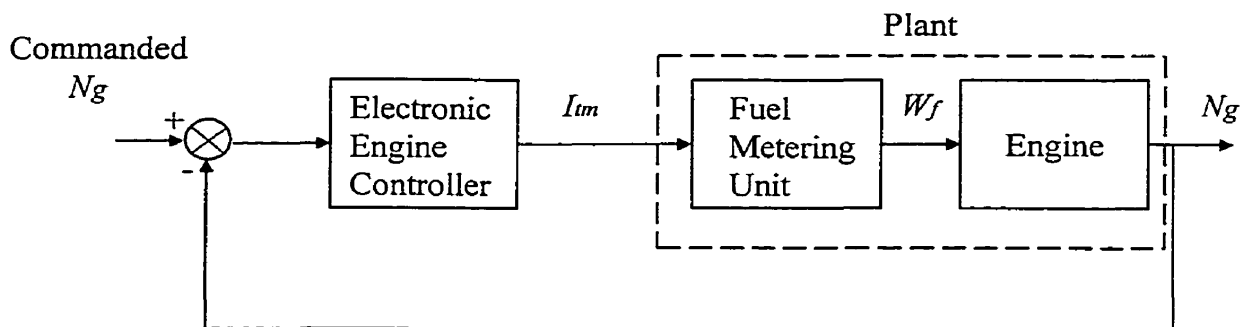


Figure 5.33: Block diagram of feedback control system

The continuous-time control system design starts with the linearization of the plant at the operating points. Although the linearized models are only approximating the nonlinear plant, they are convenient for performing analysis and give much insight as to the behavior of the nonlinear sampled-data control system near the equilibrium points, as remarked in [88]. At each of these points, a proportional plus integral block cascaded with a lead controller is designed for the linear, incremental plant model. The controller transfer function has the form

$$\bar{\Omega}(s) = \left( K_p + \frac{K_I}{s} \right) \frac{s/\omega_1 + 1}{s/\omega_2 + 1} \quad (5.9)$$

where the parameters  $K_p$ ,  $K_I$ ,  $\omega_1$  and  $\omega_2$  depend on the time-domain requirements associated with the unit step response and the linear plant model for each operating point. Once the linear designs have been completed, the feedback control system comprising the nonlinear plant is simulated with a gain scheduling routine which reads the controller parameters  $K_p$ ,  $K_I$ ,  $\omega_1$  and  $\omega_2$  from an interpolation table. Since the controllers are real-

ized on a digital device, a digital redesign method is used to convert the continuous-time control system to a sampled-data system. After the simulation runs, if the performance of the nonlinear control system is satisfactory, the control law is implemented on processors for extensive real-time tests. However, in this thesis, the real-time tests are not carried out.

### 5.4.1 Control of Linearized System

The operating point studied is the one for which the linear, time-invariant continuous-time control system has the shortest rise time when subjected to a unit step input; that is, at 84% of the full engine power, denoted as  $\%Ng = 84$ . It should be mentioned, however, that results similar to those detailed in the present subsection were obtained with the other 18 operating points.

The linear, time-invariant plant model relates deviations of the control input to deviations of the controlled output from the operating point and has irreducible transfer function given as

$$\bar{G}(s) = \frac{\left( \begin{array}{l} 1.510145501047373 \cdot 10^2 \cdot s^5 + 1.870741957332588 \cdot 10^5 \cdot s^4 \\ + 7.057640312298997 \cdot 10^7 \cdot s^3 + 7.836469084174614 \cdot 10^9 \cdot s^2 \\ + 2.378787016907578 \cdot 10^{11} \cdot s + 2.871475439369421 \cdot 10^9 \end{array} \right)}{\left( \begin{array}{l} s^8 + 1.187017375630150 \cdot 10^3 \cdot s^7 + 4.351278988897174 \cdot 10^5 \cdot s^6 \\ + 5.189920309018213 \cdot 10^7 \cdot s^5 + 2.729795397644238 \cdot 10^9 \cdot s^4 \\ + 6.453392192641624 \cdot 10^{10} \cdot s^3 + 5.582734248200342 \cdot 10^{11} \cdot s^2 \\ + 2.568942104303842 \cdot 10^{11} \cdot s + 2.917766247100640 \cdot 10^9 \end{array} \right)}. \quad (5.10)$$

The controller block is given by

$$\bar{\Omega}(s) = \left( 17.75 + \frac{8.62}{s} \right) \frac{0.0956s + 1}{0.025s + 1}. \quad (5.11)$$

The continuous-time control system is digitally redesigned with the local approaches by discretizing  $\bar{\Omega}(s)$  with the Tustin's, matched pole-zero, backward difference (BDM), step invariance (SIM), and forward difference (FDM) methods [2], as well as with the global approaches of the PIM methods. The controllers are calculated for  $T \in [t_r/7, 2t_r]$ , where  $t_r = 0.15$  second, and their transfer functions are shown in Tables 5.10 and 5.11 for  $T = t_r/7$ , where the coefficients are truncated to facilitate the reading of the table. The sampled-data control systems have the structure of Fig. 1.4(b), where some blocks can be unity depending on the digital redesign method used and the ZOH is placed at the control input. Only the PIM methods result in internally stable closed-loop systems for the entire set of operating points and sampling periods tested.

BDM	$\Omega_T(\varepsilon) = \frac{45.567\varepsilon^2+413.3769\varepsilon+188.2096}{\varepsilon^2+21.8341\varepsilon}$
FDM	$\Omega_T(\varepsilon) = \frac{67.876\varepsilon^2+742.9629\varepsilon+344.8}{\varepsilon^2+40\varepsilon}$
SIM	$\Omega_T(\varepsilon) = \frac{67.876\varepsilon^2+507.1452\varepsilon+234.0752}{\varepsilon^2+27.1549\varepsilon}$
Tustin	$\Omega_T(\varepsilon) = \frac{53.4182\varepsilon^2+529.7562\varepsilon+243.5028}{\varepsilon^2+28.2486\varepsilon}$
MPZ	$\Omega_T(\varepsilon) = \frac{51.533\varepsilon^2+509.3382\varepsilon+234.0752}{\varepsilon^2+27.1549\varepsilon}$

Table 5.10: Controller transfer functions obtained with the local digital redesign methods for  $T = t_r/7$

Regular PIM	$\Omega_T(\varepsilon) = \frac{\begin{pmatrix} 7.91 \cdot 10^{-8}\varepsilon^7 + 9.16 \cdot 10^{-6}\varepsilon^6 + 4.26 \cdot 10^{-4}\varepsilon^5 \\ +1.02 \cdot 10^{-2}\varepsilon^4 + 1.31 \cdot 10^{-1}\varepsilon^3 + 8.72 \cdot 10^{-1}\varepsilon^2 \\ +2.46\varepsilon + 1 \end{pmatrix}}{\begin{pmatrix} 1.23 \cdot 10^{-8}\varepsilon^7 + 1.74 \cdot 10^{-6}\varepsilon^6 + 1.26 \cdot 10^{-4}\varepsilon^5 \\ +7.32 \cdot 10^{-3}\varepsilon^4 + 3.23 \cdot 10^{-1}\varepsilon^3 + 8.18\varepsilon^2 \\ +8.38 \cdot 10^1\varepsilon + 1 \end{pmatrix}}$ $\Gamma_T(\varepsilon) = \frac{\begin{pmatrix} -1.06 \cdot 10^{-6}\varepsilon^7 - 1.73 \cdot 10^{-4}\varepsilon^6 - 1.09 \cdot 10^{-2}\varepsilon^5 \\ -3.29 \cdot 10^{-1}\varepsilon^4 - 4.82\varepsilon^3 - 2.78 \cdot 10^1\varepsilon^2 \\ -10\varepsilon + 1 \end{pmatrix}}{\begin{pmatrix} 7.91 \cdot 10^{-8}\varepsilon^7 + 9.16 \cdot 10^{-6}\varepsilon^6 + 4.26 \cdot 10^{-4}\varepsilon^5 \\ +1.02 \cdot 10^{-2}\varepsilon^4 + 1.31 \cdot 10^{-1}\varepsilon^3 + 8.72 \cdot 10^{-1}\varepsilon^2 \\ +2.46\varepsilon + 1 \end{pmatrix}}$
Reduced-order PIM	$\Omega_T(\varepsilon) = \frac{1025\varepsilon^2 + 10586.67\varepsilon + 4875.21}{19.58\varepsilon^2 + 639.17\varepsilon + 1}$ $\Pi_T(\varepsilon) = \frac{0.22\varepsilon^2 + 2.18\varepsilon + 1}{0.21\varepsilon^2 + 2.17\varepsilon + 1}$
Reduced-order, truncated PIM	$\Omega_T(\varepsilon) = \frac{1025\varepsilon^2 + 10586.67\varepsilon + 4875.21}{19.58\varepsilon^2 + 639.17\varepsilon + 1}$ $\Pi_T(\varepsilon) = 1.000229$

Table 5.11: Controller transfer functions obtained with the PIM methods for  $T = t_r/7$

The linearized control systems are subjected to an incremental reference input of 1% of the full engine power for  $t \geq 0$ . The  $L^2$  and  $L^\infty$  norms of the control-input and controlled-output errors are shown in Figures 5.34 and 5.35. Note that the FDM, SIM and Tustin's methods yield stable systems for the shorter sampling periods tested and, thus, the norms are evaluated for these sampling periods only. It is clear from the figures that, for the sampling periods used, the three PIM methods provide superior performances to the local methods at the controlled output. However, at the control input, the  $L^\infty$  norm of the error can be smaller for the local methods. This is due to the fact that, at

the initial sampling interval, the control input magnitude may be closer to zero for the PIM-based systems than for the systems based on the local digital redesign methods, depending on the matched pole-zero model of the PITF, whereas the continuous-time control system's response is large initially. This can be considered as an advantage of PIM since it avoids large initial jumps, although it has for effect to prolong the rise time at controlled output.

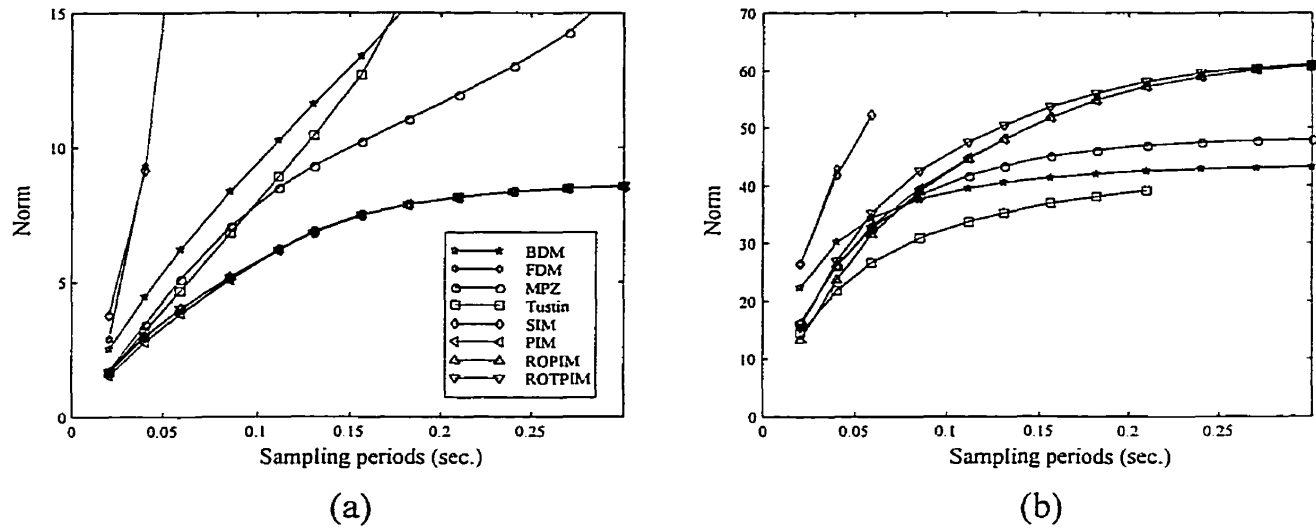
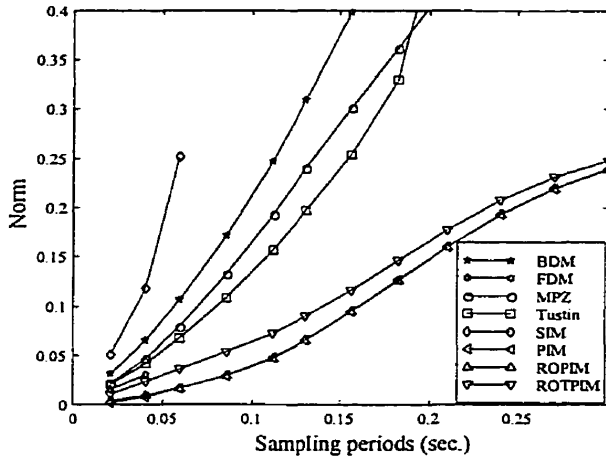
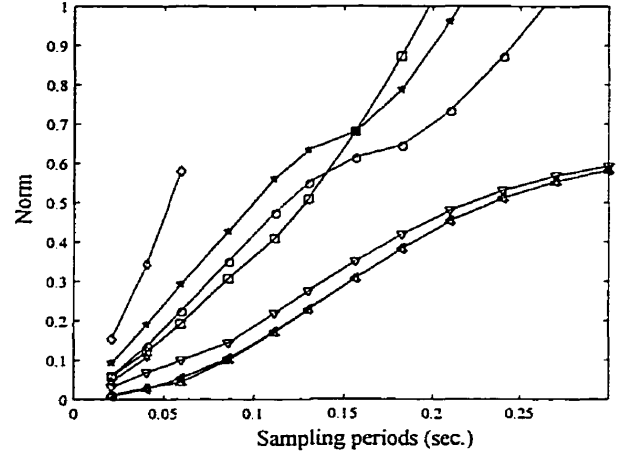


Figure 5.34: (a)  $L^2$  and (b)  $L^\infty$  norms of the control-input errors



(a)



(b)

Figure 5.35: (a)  $L^2$  and (b)  $L^\infty$  norms of the controlled-output errors

The ITAE index on the control-input and controlled-output errors is plotted against the sampling period in Figure 5.36. The PIM methods result in finite values of the index for all the sampling periods used in the simulations. Moreover, these ITAE index values are the smallest among those obtained with all the digital redesign methods employed for each sampling period.

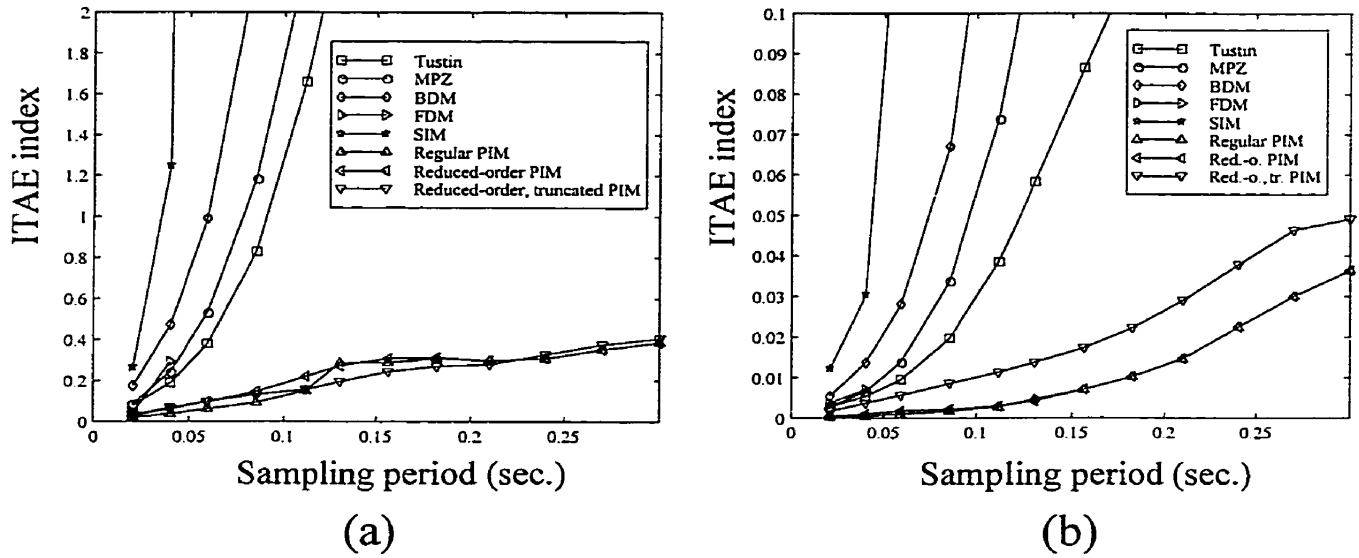


Figure 5.36: ITAE index on (a) the control-input and (b) the controlled-output errors

At the largest sampling period tested ( $T = 0.3$  second), the local BDM and MPZ, and the global PIM methods result in responses shown in Figure 5.37. In the figure, the regular and reduced-order PIM methods are assigned the same line type since their responses cannot be distinguished on the graph. The classical digital redesign techniques result in responses with large oscillations, which are due to the closeness of a complex pair of poles to the stability boundary in the complex discrete-time plane, as discussed in Section 4.6. On the other hand, the controlled output response of the PIM-based closed-loop system has a long rise time and is non-oscillatory. The slow rise time of the systems obtained with the PIM methods is expected since the control inputs within the time interval  $[0, T)$  are of low magnitude as compared with the other control systems.

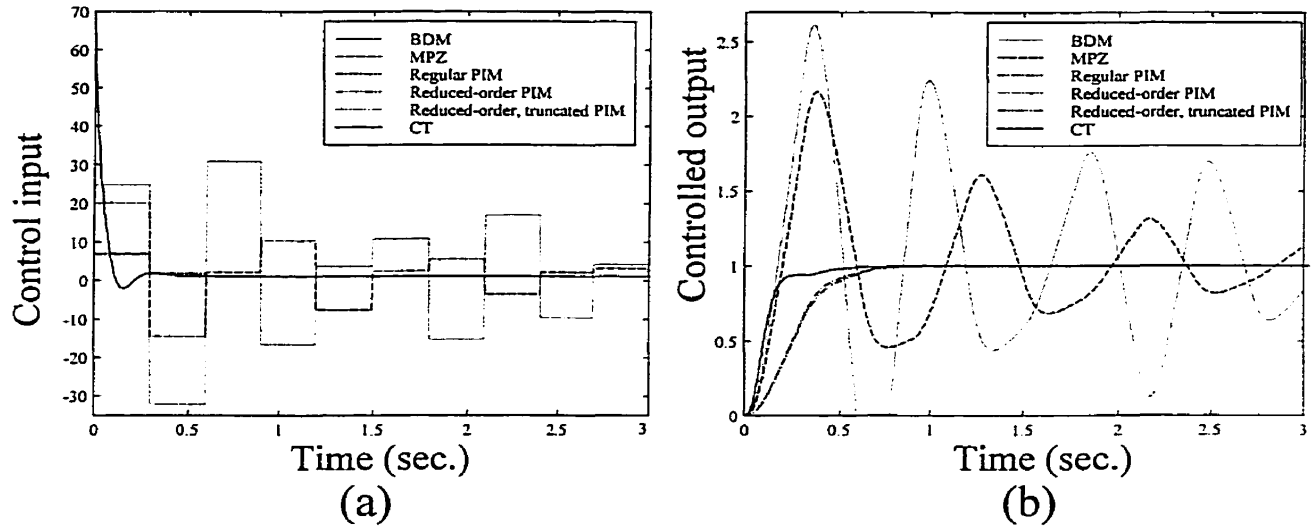


Figure 5.37: (a) Control input and (b) controlled output responses for  $T = 0.3$  second

The simulation results obtained with 16-bit, fixed-point arithmetic, low-order controller implementations are shown in Figure 5.38 for  $T = 0.0208$  second and  $T = 0.5$  second. The figure shows that all the methods perform relatively well for the shortest sampling interval. However, the backward difference and step invariance methods offer responses which are more oscillatory than the others. For  $T = 0.5$  second, the local digital redesign methods result in unstable closed-loop systems, and hence their responses are not provided. On the other hand, for the half-second sampling interval, the PIM-based systems are stable and present almost identical non-oscillatory responses, relatively small steady-state errors, and rise times approximately three times slower than that of

the continuous-time control system.

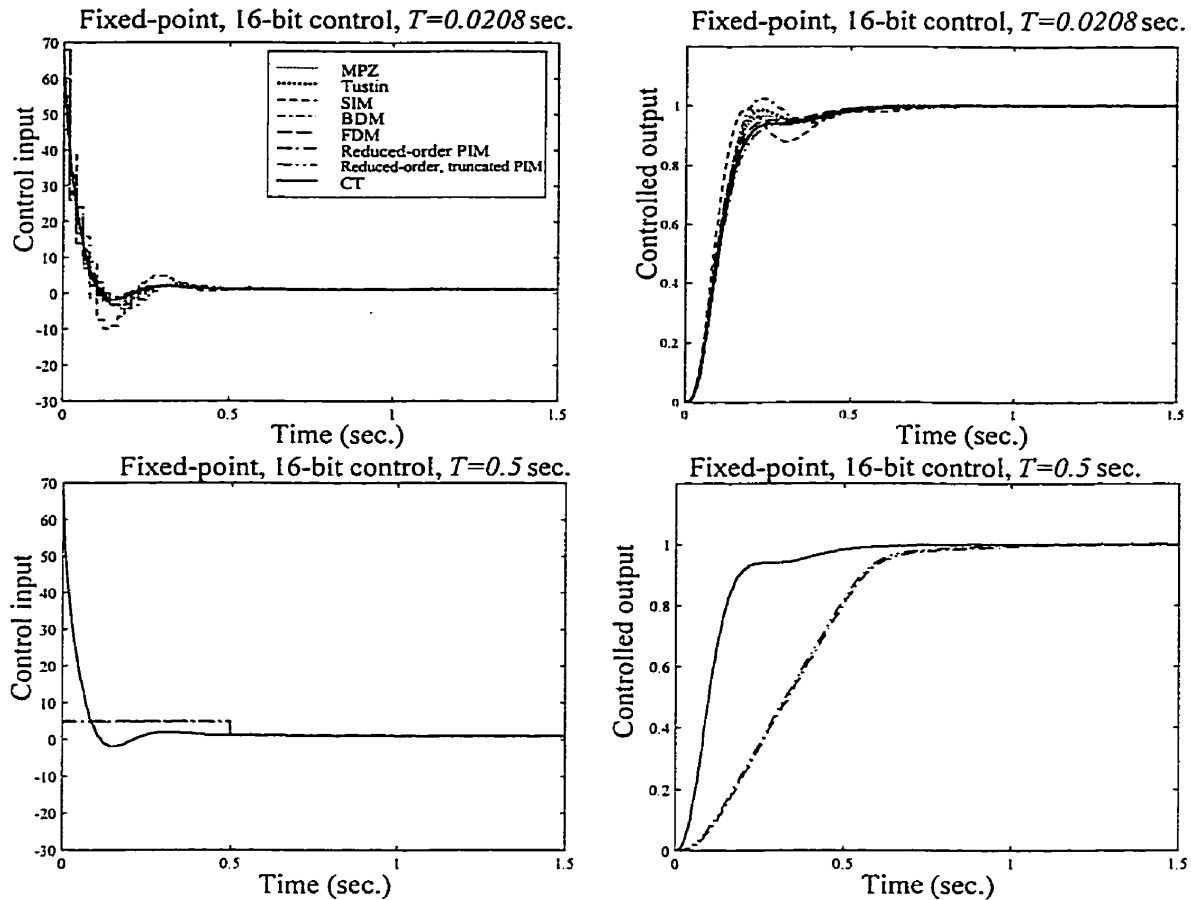


Figure 5.38: Fixed-point simulation responses

The responses to a constant 1% disturbance input to the plant, for  $t \geq 0$ , are shown in Figure 5.39 for  $T = 0.0208$  second and  $T = 0.3$  second. In the figure, the reduced-order and reduced-order plus truncated PIM methods are assigned the same line type since their responses are not distinguishable from the graphs. For the smallest sampling period, the responses of all the sampled-data control systems are relatively close to that of the continuous-time control system although the PIM-based systems offer the largest overshoot in their controlled output responses among the sampled-data systems and are the only ones having a non-zero steady-state error of magnitude  $2.0935 \times 10^{-4}$ . For the largest sampling period, only the responses of the stable systems are presented.

The BDM- and MPZ-based systems have oscillatory control input and controlled output responses, and zero steady-state error since  $\Omega_T(\varepsilon)$  has a pole at  $\varepsilon = 0$ . On the other hand, the PIM-based systems have a non-oscillatory controlled output response with steady-state error of  $3.4782 \times 10^{-3}$ . It should be noted that, with the block convergence of the PIM-based systems, one pole of  $\Omega_T(\varepsilon)$  approaches 0 as  $T \rightarrow 0$  and consequently the steady-state error of the disturbance response of the PIM-based systems can be made arbitrarily small with a sufficiently short sampling interval.

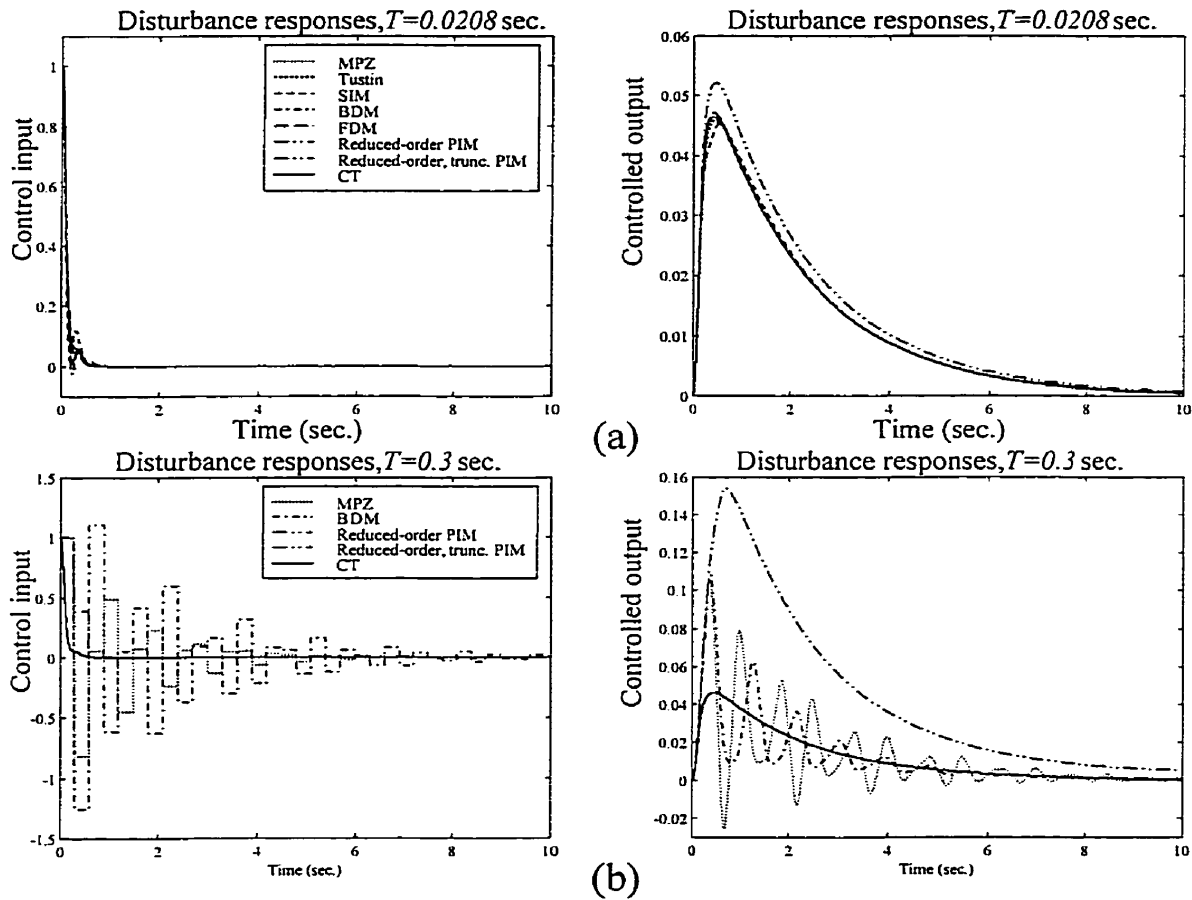


Figure 5.39: Disturbance responses for (a)  $T = 0.0208$  sec. and (b)  $T = 0.3$  sec.

### 5.4.2 Gain-Scheduled Control of the Engine

Simulations are performed on the nonlinear plant model in closed-loop with the controller blocks, whose parameters are obtained from a gain scheduling routine. The scheduling

is based on the controlled output, which is the so called scheduling variable [89]. A 1-block scheduled sampled-data control system is shown in Figure 5.40. The *ad hoc* scheduling methodology is explained as follows. The controller coefficients for each of the 19 operating points, which range from  $\%Ng = 60$  to  $\%Ng = 102$ , are entered in a table. For instance, in the case of the continuous-time controller given by equation (5.9), the table entries are obtained from the knowledge of  $K_I$ ,  $K_p$ ,  $\omega_1$  and  $\omega_2$ , as provided in Appendix E. The discrete-time and continuous-time controllers are either assigned linearly interpolated values of coefficients, when  $\%Ng$  has a value lying between two operating points, or the coefficients of the table when  $\%Ng$  equals to one of the operating points. Figure 5.41 presents the test input applied to the gain-scheduled control systems, and the resulting control input and controlled output responses of the continuous-time control system. Some of the responses obtained with the sampled-data control systems can be found in Appendix E. In Figure 5.41(b), it can be seen that the gain-scheduled continuous-time control system suffers from a large amplitude of control input over a short time interval at around  $t = 76$  seconds. During that time interval, the controlled output spans the operating points  $\%Ng = 86$ ,  $\%Ng = 88$  and  $\%Ng = 92$ . Table E.1 in Appendix E reveals that at the operating point  $\%Ng = 86$ ,  $K_I = 11.9$ , at  $\%Ng = 88$ ,  $K_I = 35.71$ , and at  $\%Ng = 92$ ,  $K_I = 12.31$ . The changes in  $K_I$  from 11.9 to 35.71 and from 35.71 to 12.31 were found to result in relatively large changes in the coefficient in front of  $s^0$  in the numerator polynomial of  $\bar{\Omega}(s)$ . Such abrupt modifications to one of the controller coefficients could be the cause of the undesired behavior. To verify this statement, one should redo the continuous-time controller design at the operating point  $\%Ng = 88$  with a lower value of  $K_I$  and perform extensive simulations. Still, for the purpose of comparing the digital redesign techniques, the current continuous-time control

system is assumed to behave in a satisfactory manner.

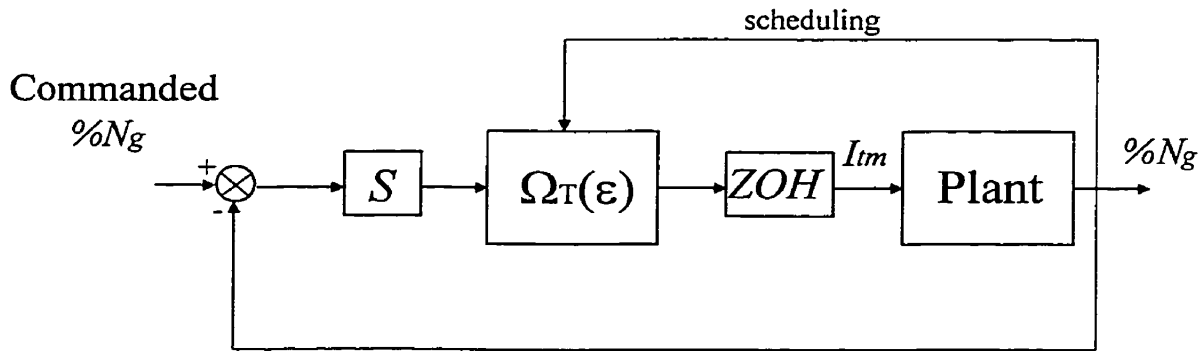


Figure 5.40: Block diagram of a gain-scheduled sampled-data control system

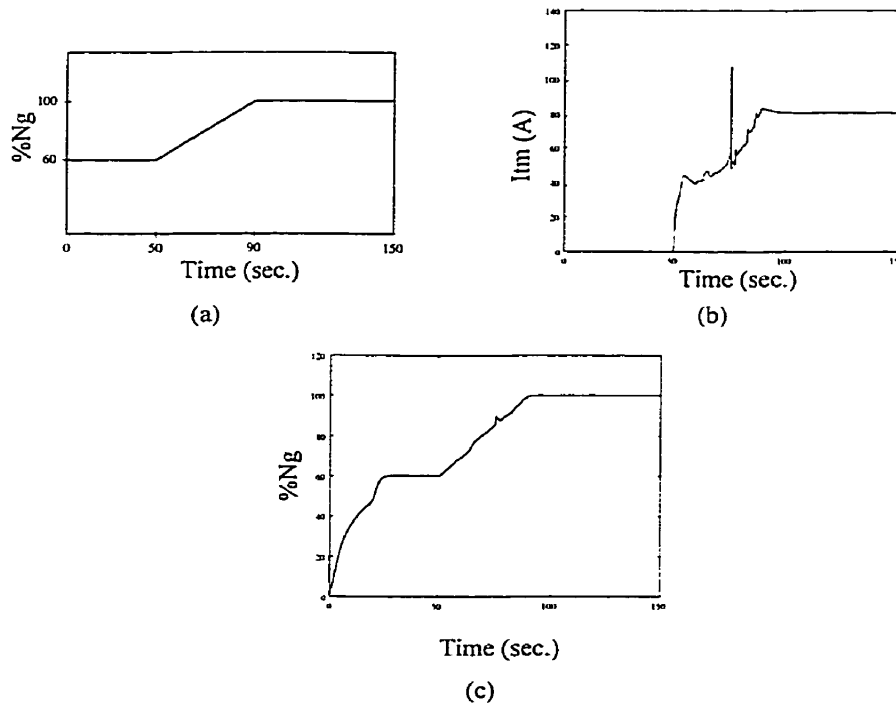


Figure 5.41: (a) Reference input, (b) control input and (c) controlled output

The discrete-time controllers are obtained with the local BDM, FDM, MPZ and Tustin's methods, and with the reduced-order and reduced-order plus truncated PIM methods for each operating point. Since the regular PIM method results in seventh order controllers whose coefficients have values ranging from  $10^1$  to  $10^{-8}$ , this approach

is discarded from the tests. The norms of the control-input errors between the sampled-data and continuous-time control systems are calculated for  $T \in \{0.0208, 0.1, 0.208, 0.35, 0.5\}$  (units in seconds) and the graphs are shown in Figure 5.42. It can be seen from the figure that the reduced-order, truncated PIM method offers an improvement in control input response over the conventional methods for  $T = 0.35$  second and  $T = 0.5$  second, based on the  $L^2$  norm quantification. At the smallest sampling interval, the responses of all the methods tested behave in a similar fashion except for the reduced-order PIM method. In fact, for most sampling periods, the reduced-order PIM method offers the worst performance among the methods studied according to the  $L^2$  and  $L^\infty$  norms. This behavior is different from that obtained with the linear simulations. What differentiates systems obtained with the reduced-order PIM method from systems obtained with the reduced-order, truncated PIM method is that the former possesses two dynamic control blocks instead of one. The performance of systems obtained with the reduced-order PIM method suggests that an increase in the number of controller blocks is detrimental to the gain-scheduled, PIM-based sampled-data control system.

One point to mention is that the behavior of the control input is not reflected at the controlled output. This is in the sense that the  $L^2$  norm of the controlled-output errors, not shown for the sake of brevity, are relatively close for all the methods tested even if it is not the case at control input. One possible explanation to this behavior is the presence of rate limiters in the plant model. As was shown for the VCFP experiments, it is possible that the local digital redesign approaches result in satisfactory responses when saturation takes place. Still, the nonlinear nature of the problem goes beyond the intent of this thesis and the qualitative hypothesis put forward about the behavior of the controlled-output error needs to be validated in a future expansion of this research work.

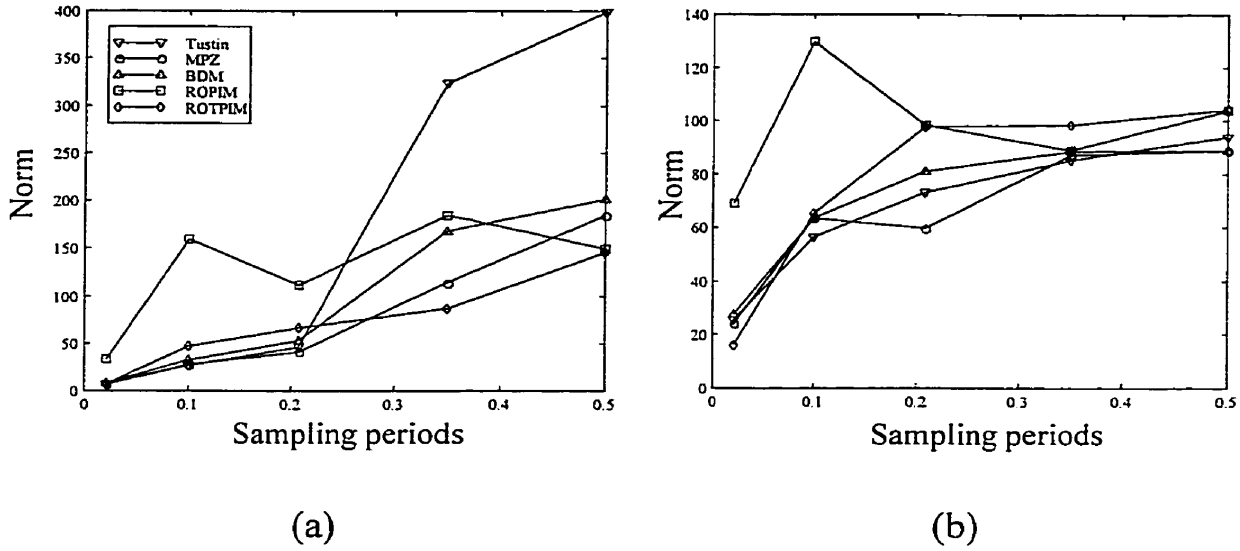


Figure 5.42: (a)  $L^2$  and (b)  $L^\infty$  norms of control-input errors with  $T$

## 5.5 Example of a MIMO Control System

The following example, first studied in [27] in a qualitative manner, is shown here to demonstrate that the theoretical analysis on the convergence of control inputs and controlled outputs of SISO sampled-data control systems in the time domain, as  $T \rightarrow 0$ , can readily be extended to the MIMO case.

Consider a continuous-time control system having the structure of Figure 1.4(a) and composed of  $\bar{\Pi}(s) = \bar{\Gamma}(s) = I_{2 \times 2}$  and

$$\bar{G}(s) = \frac{\begin{bmatrix} s+1 & s \\ s & s+1 \end{bmatrix}}{s(s+1)}, \quad \bar{\Omega}(s) = \frac{\begin{bmatrix} (s+2)(s+1)^3 & -(s+1)^2 \\ -(s+1)^2 & (s+2)(s+1)^3 \end{bmatrix}}{s^4 + 6s^3 + 13s^2 + 12s + 3}. \quad (5.12)$$

The controller block  $\bar{\Omega}(s)$  is discretized with the matched pole-zero, Tustin's, and step invariance methods, whereas the closed-loop system is discretized with the regular MIMO PIM method as described in [27]. All four sampled-data control systems have

the structure of Figure 1.4(b), where the blocks  $\Pi_T(\varepsilon)$  and  $\Gamma_T(\varepsilon)$  are non-unity only for the PIM-based system, and  $H$  is the ZOH. The range of sampling periods tested is  $[0.1, 0.85]$ . A reference input  $\bar{r}(t) = 1, t \geq 0$ , is applied to the first channels of the continuous-time and sampled-data control systems. The control input responses of the continuous-time control system and sampled-data systems, for the relatively large sampling interval  $T = 0.7$ , are shown for the two channels in Figures 5.43 and 5.44 so that one has a better idea of the time trajectories involved. It is seen that the time trajectories of the control inputs of the sampled-data control systems are the closest to those of the continuous-time control system with the PIM method.

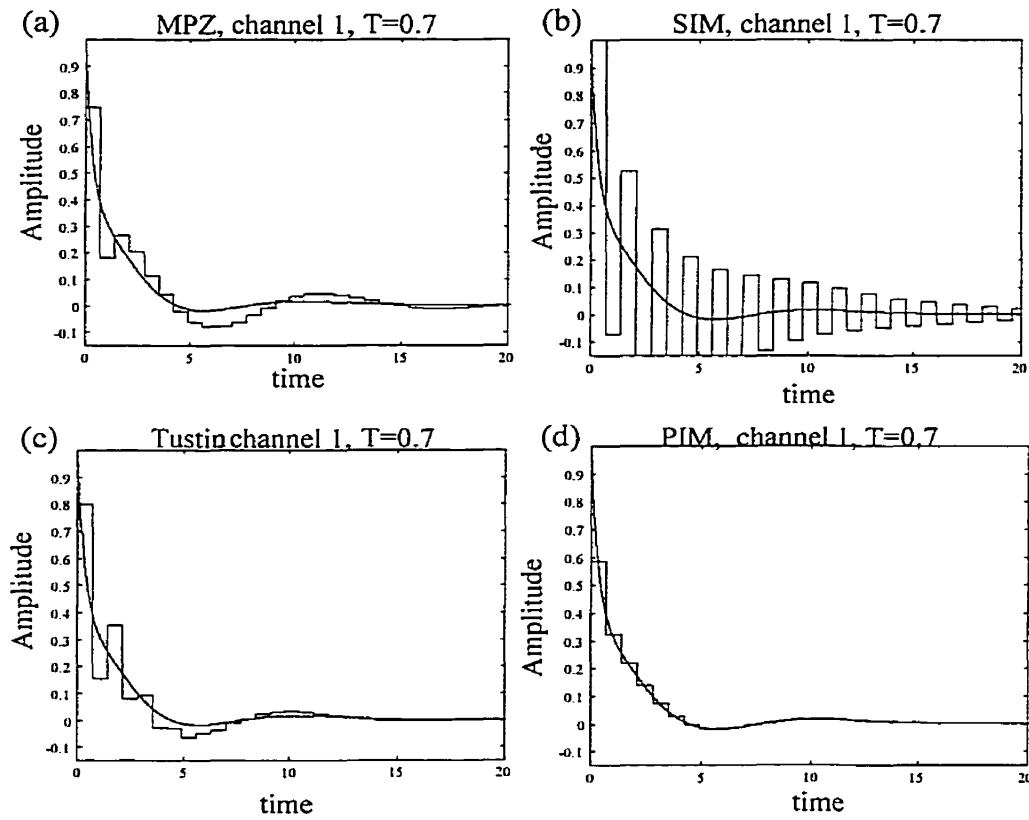


Figure 5.43: Control inputs (channel 1) for (a) MPZ method, (b) SIM, (c) Tustin, and (d) PIM

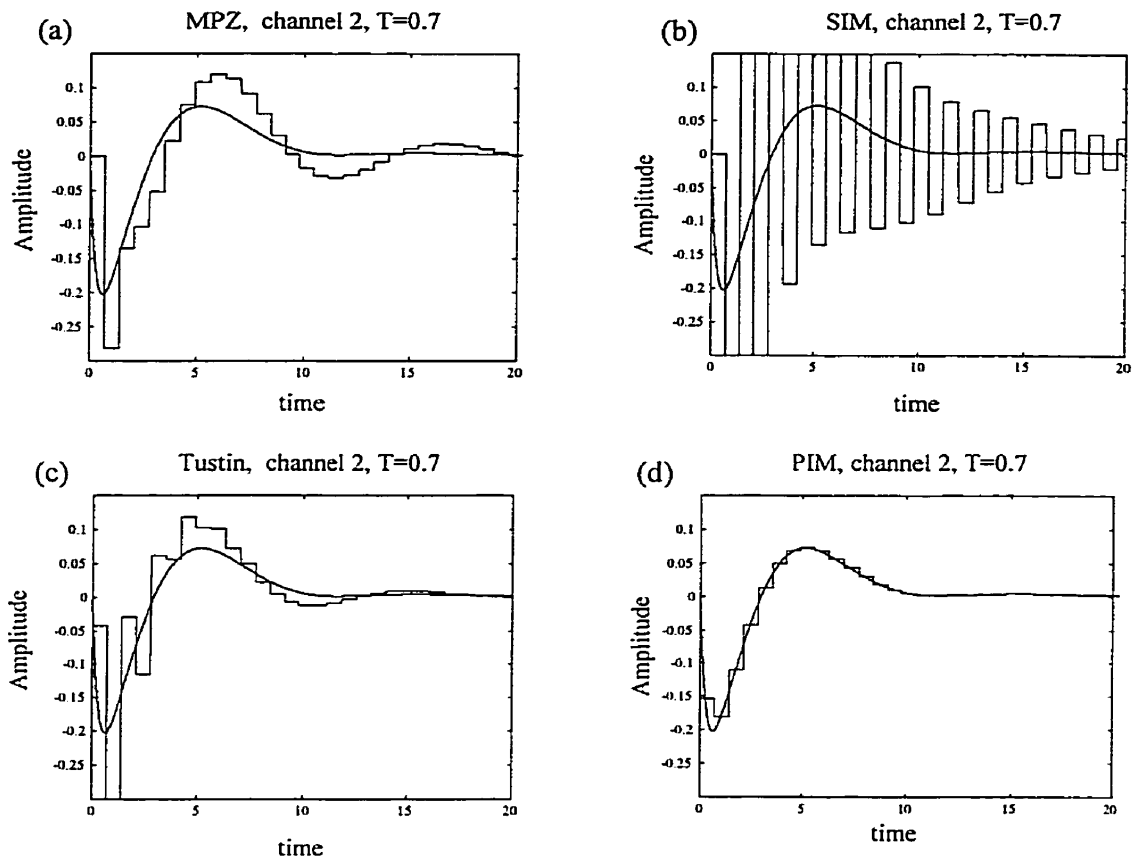


Figure 5.44: Control inputs (channel 2) for (a) MPZ method, (b) SIM, (c) Tustin, and (d) PIM

Figure 5.45 provides graphs of the  $L^\infty$  norms on the control-input errors against  $T$  and Figure 5.46, graphs of the  $L^\infty$  norms of the errors at controlled output. Since the four discretization methods result in sampled-data models of the continuous-time control system, the norms of the errors at control input and controlled output approach zero as  $T \rightarrow 0$ .

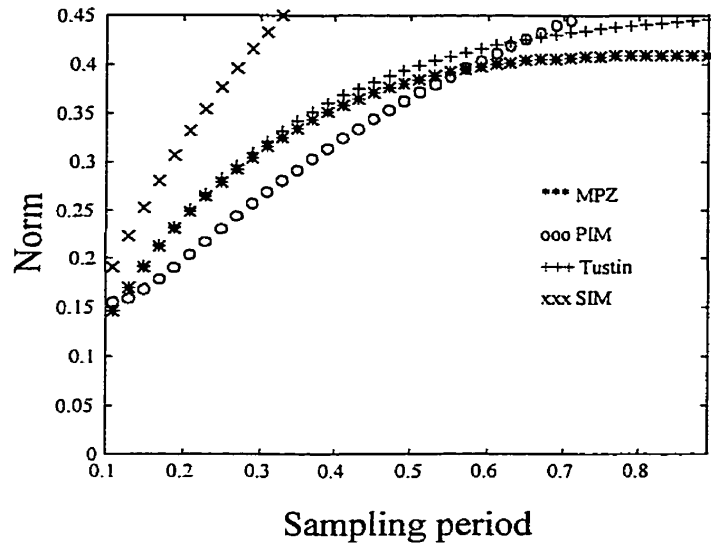


Figure 5.45:  $L^\infty$  norms of control-input errors

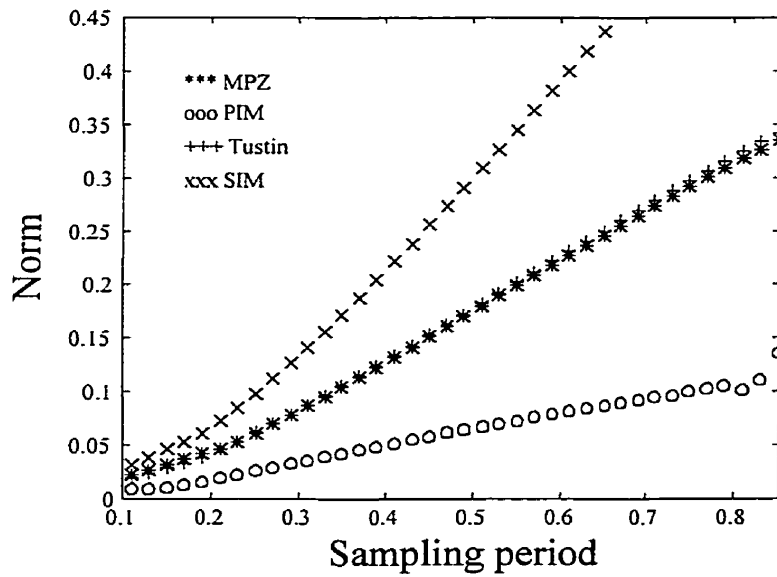


Figure 5.46:  $L^\infty$  norms of controlled-output errors

## 5.6 Summary of the Performances Achieved with the Examples

Table 5.12 provides a summary of the performances achieved with the linear control systems. In the table, TPIM denotes the truncated PIM method, LOCAL, the local digital redesign methods, and Y (N) signifies that a performance criterion is (not) achieved.

	PIM	TPIM	ROPIM	ROTPIM	LOCAL
Controller block convergence with $T$	Y	Y	Y	Y	Y
Induced norm convergence with $T$	Y	Y	Y	Y	Y
Stability for all $T$ values selected	Y	Y	Y	Y	N
Finite norms/ITAE index of control-input and controlled-output errors for large $T$	Y	Y	Y	Y	N
Diminishing error norms and values of ITAE index as $T$ is reduced	Y	Y	Y	Y	Y
Finite induced norms for large $T$	Y	Y	Y	Y	N
Smallest $L^2$ error norms, when subjected to a constant reference input, for all $T$ values selected	Y	N	N	N	N
Closest responses to continuous-time control system's when realized with fixed-point arithmetic and restricted number of bits for large $T$ values	N <sup>4</sup>	N	Y	N	N

Table 5.12: Observed performances of the digitally redesigned control systems

<sup>4</sup>In the example of Section 5.1, the PIM method is the same as the reduced-order PIM method.

# Chapter 6

## Conclusions

### 6.1 Contributions of the Research Work

This thesis has proposed solutions to some of the unresolved issues associated with the regular PIM method, presented a characterization of digitally redesigned control systems, applied quantitative measures to assess the performance of sampled-data control systems, and validated the theoretical concepts via numerical simulations and experiments.

#### 6.1.1 Solutions to Unresolved Issues of the Regular PIM Method

The truncated, reduced-order and reduced-order plus truncated PIM methods were proposed in Chapter 3. These new methods constitute the first global digital redesign techniques which generally result in low-order controllers while providing satisfactory closed-loop performances for sampling frequencies at which the local digital redesign techniques fail to do so. In Section 3.3 and Appendix C, global digital redesign methods were proposed which rely on discretization techniques other than the matched pole-zero method to discretize the continuous-time PTF and on the discretization of the closed-loop system relating the reference input to the controlled output. Finally, the first set of guidelines in solving the Diophantine equations associated with the PIM methods was presented in Chapter 3, rendering the PIM approaches more systematic and suitable to

numerical methods.

### 6.1.2 Characterization and Performance Evaluation of Digitally Redesigned Control Systems

The sampled-data control systems were investigated for a decreasing sampling interval. The conditions on the discrete-time controller blocks, the hold at control input, and the exogenous inputs were established in Sections 4.3 and 4.5 such that the systems relating the exogenous input to the control input and the controlled output are sampled-data models of the corresponding continuous-time systems. Since the output of a sampled-data model of a continuous-time system, as defined in Chapter 2, approaches that of the continuous-time system uniformly in time, when the sampling period is reduced, the sampled-data model concept bridges the gap between sampled-data and continuous-time control systems in the context of time-domain responses. This was made possible by using the lifting reformulation of systems as presented in Section 4.1. The PIM and the local digital redesign techniques result in sampled-data models of continuous-time systems, provided the hold at control input, as seen on Figure 1.4(b), satisfies the hold condition in the time domain given in Section 4.1. Furthermore, conditions ensuring that the discrete-time controller transfer functions of PIM-based sampled-data control systems approach, in the sense defined in Section 4.4, their continuous-time counterpart for sufficiently fast sampling frequencies were given. This results in the input and output signals of each block to approach their counterparts in the continuous-time control system.

The PIM-based sampled-data control systems were studied for relatively large sampling periods in Section 4.6. On the one hand, it was found that systems based on the regular and truncated PIM methods and subjected to a constant reference input present control input and controlled output responses exempt from oscillations, at the sampling instants, when relatively large sampling periods are used. This characteristic has a practical implication since physical devices, such as the actuator, could experience early wear, produce noises, and waste power due to repeated oscillations. On the other

hand, the main disadvantage of increasing the sampling period with PIM-based systems is the increase in rise time.

Concerning the performance evaluation of digitally redesigned control systems, it was shown that there is an upper limit on the sampling period such that a sampled-data control system obtained with a local digital redesign method satisfies a prescribed bound on the  $L^\infty$  and  $L^2$  norms at the control-input and controlled-output errors, whereas with the regular and truncated PIM methods, a finite bound on the error norms can be met for all non-pathological sampling periods. More generally, the advantages of the PIM-based systems over the other methods for relatively large sampling periods, in terms of the performance measures and the shapes of the responses, were clarified in Section 4.6. For a diminishing sampling period, it was found that the value of the ITAE index on the error signals approaches zero in the presence of sampled-data models of continuous-time systems. Furthermore, the  $L^\infty$ - and  $L^2$ -induced norms of sampled-data systems relating the reference and disturbance inputs to the control input were shown to become close to their continuous-time counterparts, provided certain conditions are satisfied according to Theorems 4.6.2 and 4.6.3.

### 6.1.3 Summary of Numerical Simulation and Experimental Results

In Chapter 5, the four PIM methods were compared with the most common local digital redesign approaches and the modern optimal digital redesign method of [24]. Table 5.12 gives a summary of the performances achieved with the various digital redesign methods. In addition to the observations of Table 5.12, the following results were obtained with the simulations and experiments. First, the  $L^\infty$  norms of the error signals can be smaller for the local methods than for the PIM methods for certain sampling periods. This is due to the fact that, at the initial sampling interval ( $k = 0$ ), the control inputs of the PIM-based systems can have a magnitude closer to zero than that of a system obtained with the local digital redesign, whereas the control input of the continuous-time control system

is large initially. This result confirms the investigation of the control input provided in Section 4.6. Second, two limitations associated with the implementation of discrete-time controllers obtained with the regular PIM method were exposed during the experiment: (i) for a plant model transfer function with relatively large coefficients, the transfer functions of the discrete-time control blocks can also contain high-magnitude coefficients, thus making them impractical for fixed-point implementations using a relatively small number of bits; and (ii) knowing that the implementation hardware can perform a finite number of computations per sampling period and that high-order controllers require considerably more instructions than low-order ones, a lower bound on the usable sampling periods is then imposed for the controllers obtained with the regular PIM method whereas controllers of lower orders, such as those obtained with the reduced-order PIM method, could be performing in a satisfactory manner for sampling intervals much shorter than this lower bound. Third, all four PIM-based control systems have similar output responses, as  $T$  becomes large, when subjected to the same exogenous input. Finally, although the poor performance of the gain-scheduled gas-turbine engine control system obtained with the reduced-order PIM method could not be explained, this thesis laid the groundwork for a linear analysis of the nonlinear control system at the operating points.

## 6.2 Future Research Work

The following are suggested areas for future research:

1. For the non-decoupled MIMO control systems, especially of interest in the aircraft industry [90], order-reduced and modified PIM methods could be developed.
2. A more thorough study of the stability of the reduced-order PIM-based control systems, for relatively large sampling periods, could be initiated. This would answer the question regarding the possibility of having a wider range of sampling periods for which the stability of the reduced-order PIM-based system is preserved over that associated with a sampled-data control system obtained with any of the local digital

redesign methods. In parallel with the stability analysis, the generalized least-squares method [75] should be investigated as a means to improve the performance of a reduced-order PIM-based system.

3. An expansion to the gas-turbine engine control system analysis, which includes the nonlinearities, should be undertaken in order to understand the behavior of a digitally redesigned control system using gain scheduling.
4. For the plant output mapping method to be of any practical interest when the plant model is of order greater than or equal to two, hold functions which can provide a satisfactory intersample performance at control input, as discussed in Appendix C, should be determined.
5. The case of multiple-interval holds [53], such as the first-order hold, could be included in the characterization of digitally redesigned control systems. There would result a higher-order sampled-data model study.
6. In order to predetermine the performance of digitally redesigned control systems with respect to that obtained with the continuous-time control system by using the PITF parameters, upper bounds on  $L^\infty$  and  $L^2$  norms can be calculated. For instance, equation (A.11) in the proof of Theorem 4.3.1 can serve as an upper bound to the  $L^\infty$  norm of the control-input error. However, such a bound is conservative. The possibility of establishing simple, yet useful and tight, bounds on the  $L^2$  and  $L^\infty$  norms of the control-input and controlled-output errors should be investigated.

# Bibliography

- [1] G.F. Franklin, J.D. Powell and M.L. Workman, *Digital Control of Dynamic Systems*, 2nd edition, Addison-Wesley, Reading, MA, 1990.
- [2] K.J. Astrom & B. Wittenmark, *Computer-Controlled Systems: Theory and Design*, Prentice Hall, NJ, 1990.
- [3] S. Hara, Y. Yamamoto and H. Fujioka, "Modern and Classical Analysis/Synthesis Methods in Sampled-Data Control — A Brief Overview with Numerical Examples", *Proc. 35th Conf. Decision and Control*, pp. 1251-1256, Kobe, Japan, 1996.
- [4] T. Chen and B. Francis, *Optimal Sampled-Data Control Systems*, Springer-Verlag, London, England, 1995.
- [5] J.D. Powell and A. Emami-Naeini, *Feedback Control of Dynamic Systems*, 3rd edition, Addison Wesley, Reading, MA, 1994.
- [6] P. Kabamba and S. Hara, "Worst-Case Analysis and Design of Sampled-Data Control Systems", *IEEE Trans. Aut. Control*, Vol. AC-38, No. 9, pp. 1337-1357, 1993.
- [7] S. Hara and H.-K. Sung, "Ripple-Free Conditions in Sampled-Data Control Systems", *Proc. 30th Conf. Decision and Control*, pp. 2670-2671, Brighton, England, 1991.
- [8] S. Urikura and A. Nagata, "Ripple-Free Deadbeat Control for Sampled-Data Systems", *IEEE Trans. Aut. Control*, Vol. AC-32, No. 6, pp. 474-482, 1987.

- [9] N. Hori, R. Cormier and K. Kanai, "On Matched Pole-Zero Discrete-Time Models", *IEE Proceedings-D*, Vol. 139, No. 3, pp. 273-278, May 1992.
- [10] P. Katz, *Digital Control Using Microprocessors*, Prentice Hall, Englewood Cliffs, NJ, 1981.
- [11] C.A. Rabbath and N. Hori, "A Hold-Equivalent Structure for Matched Pole-Zero Discrete-time Models", *Proc. Society of Instrumentation and Control Engineers (SICE) Conference*, pp. 659-660, Shiba, Japan, 1998.
- [12] N. Hori, T. Mori, and P.N. Nikiforuk, "A New Perspective for Discrete-Time Models of a Continuous-Time System", *IEEE Trans. Aut. Control*, Vol AC-37, No 7, pp. 1013-1017, 1992.
- [13] T. Mori, P.N. Nikiforuk, M.M. Gupta and N. Hori, "A Class of Discrete-Time Models for a Continuous-Time System", *IEE Proceedings-D*, Vol. 136, No. 2, pp. 79-83, March 1989.
- [14] N. Hori, T. Mori and P.N. Nikiforuk, "Discrete-time Models of Continuous-time Systems", *Control and Dynamic Systems*, No. 66, pp. 1-45, Academic Press, 1994.
- [15] N. Hori, A.R. Comeau and K. Kanai, "On the first-order and slewer-hold equivalent discrete-time models", *Proc. Int. Conf. Control '94*, pp. 911-915, Coventry, UK, 1994.
- [16] N. Hori and A.R. Comeau, "A State-Space Form for Higher Order Discrete-Time Mapping Models", *Proc. Society of Instrumentation and Control Engineers (SICE) Conference*, pp. 829-832, Tokyo, Japan, 1994.
- [17] J.D. Powell and P. Katz, "Sample Rate Selection for Aircraft Digital Control", *AIAA Journal*, Vol. 13, No. 8, pp. 975-978, 1975.
- [18] T. Chen and B.A. Francis, " $H_2$ -Optimal Sampled-Data Control", *IEEE Trans. Aut. Control*, Vol. AC-36, No. 4, pp. 387-397, 1991.

- [19] B.D.O. Anderson, "Controller Design: Moving from Theory to Practice", *IEEE Control Systems Magazine*, pp. 16-25, August 1993.
- [20] J.P. Keller and B.D.O. Anderson, "A New Approach to the Discretization of Continuous-Time Controllers", *IEEE Trans. Aut. Control*, vol. AC-37, pp. 214-223, 1992.
- [21] K.S. Rattan and H.H. Yeh, "Discretizing Continuous-Data Control systems", *Computer Aided Design*, vol. 10, pp. 299-306, 1984.
- [22] K.S. Rattan, "Digitalization of Existing Continuous Control Systems", *IEEE Trans. Aut. Control*, Vol. AC-29, No. 3, pp. 282-285, 1984.
- [23] R. Kennedy and R. Evans, "Digital Redesign of a Continuous Controller Based on Closed Loop Performance", *Proc. 29th Conf. Decision and Control*, pp. 1898-1901, Honolulu, Hawaii, 1990.
- [24] N. Rafee, T. Chen and O.P. Malik, "A Technique for Optimal Digital Redesign of Analog Controllers", *IEEE Trans. on Control Systems Technology*, Vol. 5, No. 1, pp. 89-99, Jan. 1997.
- [25] B.D.O. Anderson and Y. Liu, "Controller Reduction: Concepts and Approaches", *IEEE Trans. Aut. Control*, Vol. AC-34, No. 8, pp. 802-812, 1989.
- [26] A.H.D. Markazi and N. Hori, "A New Method with Guaranteed Stability for Discretization of Continuous-Time Control Systems", *Proc. American Control Conf.*, vol.2, pp. 1397-1402, Chicago, USA, 1992.
- [27] A.H.D. Markazi, *A New Approach to the Digital Implementation of Analog Controllers and Continuous-Time Reference Models*, Ph.D. Thesis, McGill University, Montreal, 1994.

- [28] N. Hori and A.H.D. Markazi, "A New Approach to Digital Control System Design", *Proc. Motion and Vibration International Conference (MOVIC)*, pp. 918-923, Yokohama, Japan, 1992.
- [29] G.C. Goodwin and R.H. Middleton, *Digital Control and Estimation— A Unified Approach*, Prentice Hall, Englewood Cliffs, NJ, 1990.
- [30] N. Hori, A.H.D. Markazi, P.N. Nikiforuk, K. Kanai and T. Ieko, "Digital Model-Reference Flight Control of Aircraft with Unstable Sampling Zeros", *Proc. 12th World Congress of International Federation of Automatic Control (IFAC)*, pp. 297-302, Sydney, Australia, 1993.
- [31] N. Hori and A.H.D. Markazi, "A New Approach to the Design of Digital Model Reference Control Systems", *JSME International Journal*, Vol. 38, No. 4, pp. 712-718, 1995.
- [32] B.A. Francis and T.T. Georgiou, "Stability Theory for Linear Time-Invariant Plants with Periodic Digital Controllers", *IEEE Trans. Aut. Control*, Vol. AC-33, No. 9, pp. 820-832, September 1988.
- [33] T. Chen and B.A. Francis, "Input-Output Stability of Sampled-Data Systems", *IEEE Trans. Aut. Control*, Vol. AC-36, No. 1, pp. 50-58, 1991.
- [34] N. Hori, "On System Representations and Discrete-time Models of a Multivariable System", *Proc. American Control Conf.*, pp. 2407-2412, Boston, USA, 1991.
- [35] A.H.D. Markazi, N. Hori, K. Kanai and T. Ieko, "A New Discretization of Continuous-Time Control Systems and its Application to the Design of a Flight Control System", *Proc. Society of Instrumentation and Control Engineers (SICE) Conference*, pp. 1199-1203, Kanazawa, Japan, 1993.
- [36] B.C. Kuo, *Digital Control Systems*, 2nd edition, Saunders College Publishing, Philadelphia, 1992.

- [37] B.C. Kuo, *Automatic Control Systems*, 6th edition, Prentice Hall, Englewood Cliffs, NJ, 1991.
- [38] V. Kucera, "Diophantine Equations in Control — A Survey", *Automatica*, 29, No. 6, pp. 1361-1375, 1993.
- [39] C.A. Desoer, R.-W. Liu, J. Murray and R. Saeks, "Feedback System Design: The Fractional Representation Approach to Analysis and Synthesis", *IEEE Trans. Aut. Control*, Vol. AC-25, No. 3, pp. 399-412, 1980.
- [40] J.G. Proakis and D.G. Manolakis, *Digital Signal Processing — Principles, Algorithms, and Applications*, Second Edition, Macmillan Publishing Co., New York, NY, 1992.
- [41] P. Lapsley, J. Bier, A. Shoham and E.A. Lee, *DSP Processor Fundamentals — Architectures and Features*, IEEE Press, New York, NY, 1997.
- [42] J.E. Ciolfi, The Mathworks Inc., *Fixed-Point Blockset — User's Guide*, Natick, MA, 1995.
- [43] C.A. Rabbath, N. Hori, P.N. Nikiforuk and K. Kanai, "Order Reduction of PIM-Based Digital Flight Control Systems", *Proceedings of the IFAC World Congress*, Beijing, China, 1999.
- [44] A.H.D. Markazi and N. Hori, "Discretisation of Continuous-Time Control Systems with Guaranteed Stability", *IEE Proc.- Control Theory Appl.*, Vol. 142, No. 4, pp. 323-328, July 1995.
- [45] B. Bamieh, "Intersample and Finite wordlength Effects in Sampled-Data Problems", *Proc. 35th Conf. Decision and Control*, pp. 1272-1277, Kobe, Japan, 1996.
- [46] H. Oz, L. Meirovitch and C.R. Johnson, "Some Problems Associated with Digital Control of Dynamical Systems", *J. Guidance and Control*, Vol. 3, No. 6, pp. 523-528, 1980.

- [47] R.H. Middleton and G.C. Goodwin, "Improved Finite Word Length Characteristics in Digital Control Using Delta Operators", *IEEE Trans. Aut. Control*, Vol. AC-31, No. 11, pp. 1015-1021, 1986.
- [48] C.A. Rabbath and N. Hori, "On the Implementation of Filters Subjected to Quantization of Coefficients", *Proc. 13th International Conference on Digital Signal Processing*, pp. 665-669, Santorini, Greece, 1997.
- [49] C.A. Rabbath and N. Hori, "Sensitivity of the Continualization of Poles and its Effect in System Identification", *Proc. 6th IEEE Conference on Control Applications*, pp. 511-516, Hartford, USA, 1997.
- [50] G.C. Goodwin, R.H. Middleton and H.V. Poor, "High Speed Digital Signal Processing and Control", *Proc. IEEE*, 80, pp. 240-259, 1992.
- [51] A.H.D. Markazi and N. Hori, Reply to the comment on "Discretisation of continuous-time control systems with guaranteed stability", *IEE Proc.- Control Theory Appl.*, Vol. 144, No. 3, pp. 277-279, May 1997.
- [52] T. Ieko, Y. Ochi, K. Kanai, N. Hori and K.-I. Okamoto, "Digital Redesign Methods Based on Plant Input Mapping and a New Discrete-Time Model", *Proc. 35th Conf. Decision and Control*, pp. 1569-1574, Kobe, Japan, 1996.
- [53] M. Araki, "Recent developments in digital control theory", *Proc. of IFAC Congress*, Volume 9, pp. 251-260, Sydney, Australia, 1993.
- [54] Y. Yamamoto, "New Approach to Sampled-Data Control Systems — A Function Space Method", *Proc. 29th Conf. Decision and Control*, pp. 1882-1887, Honolulu, Hawaii, 1990.
- [55] B. Bamieh, J.B. Pearson, B.A. Francis and A. Tannenbaum, "A lifting technique for linear periodic systems with applications to sampled-data control", *Systems & Control Letters*, 17, pp 79-88, 1991.

- [56] B.A. Bamieh and J.B. Pearson, "A General Framework for Linear Periodic Systems with Applications to  $H^\infty$  Sampled-Data Control", *IEEE Trans. Aut. Control*, Vol. AC-37, No. 4, pp. 418-435, 1992.
- [57] Y. Yamamoto, "A Function Space Approach to Sampled Data Control Systems and Tracking Problems", *IEEE Trans. Aut. Control*, Vol. AC-39, No. 4, pp 703-713, April 1994.
- [58] A.N. Michel and C.J. Herget, *Mathematical Foundations in Engineering and Science — Algebra and Analysis*, Prentice-Hall, Inc., Englewood Cliffs, NJ, 1981.
- [59] J.C. Doyle, B.A. Francis and A.R. Tannenbaum, *Feedback Control Theory*, Macmillan Publishing, New York, NY, 1992.
- [60] M.A. Dahleh and J.B. Pearson, " $l^1$ -Optimal Feedback Controllers for MIMO Discrete-Time Systems", *IEEE Trans. Aut. Control*, Vol. AC-32, No. 4, pp. 314-322, 1987.
- [61] E.G. Collins and T. Song, "A Delta Operator Approach to Discrete-Time  $H_\infty$  Control", *Proc. American Control Conf.*, pp. 1980-1984, Philadelphia, PA, 1998.
- [62] N. Sivashankar and P.P. Khargonekar, " $\mathcal{L}_\infty$ -Induced Norm of Sampled-Data Systems", *Proc. American Control Conf.*, pp. 167-172, Boston, MA, 1991.
- [63] Y. Yamamoto, "On the state-space and frequency domain characterization of  $H^\infty$ -norm of sampled-data systems", *Systems & Control Letters*, 21, pp 163-172, 1993.
- [64] G.M.H. Leung, T.P. Perry and B.A. Francis, "Performance Analysis of Sampled-data Control Systems", *Automatica*, 27, No. 4, pp. 699-704, 1991.
- [65] B. Bamieh, M.A. Dahleh and J.B. Pearson, "Minimization of the  $L^\infty$ -Induced Norm for Sampled-Data Systems", *IEEE Trans. Aut. Control*, Vol. AC-38, No. 5, pp. 717-732, 1993.

- [66] G.E. Dullerud and B.A. Francis, " $\mathcal{L}_1$  Analysis and Design of Sampled-Data Systems", *IEEE Trans. Aut. Control*, Vol. AC-37, No. 4, pp. 436-446, 1992.
- [67] H.T. Toivonen, "Sampled-data Control of Continuous-time Systems with an  $H_\infty$  Optimality Criterion", *Automatica*, 20, No. 4, pp. 45-54, 1993.
- [68] T. Chen and B.A. Francis, "On the  $\mathcal{L}_2$ -induced norm of a sampled-data system", *Systems & Control Letters*, 15, pp 211-219, 1990.
- [69] D. Graham and R.C. Lathrop, "The Synthesis of Optimum Transient Response: Criteria and Standard Forms", *Trans. AIEE*, vol. 72, part II, pp. 273-288, 1953.
- [70] R.C. Dorf, *Modern Control Systems*, 6th edition, Addison-Wesley, Reading, MA, 1992.
- [71] C.A. Rabbath and N. Hori, "Continuous-time Lifting Analysis of Digitally-Redesigned Control Systems", *Proc. Society of Instrumentation and Control Engineers (SICE) Conference*, pp. 779-784, Shiba, Japan, 1998.
- [72] R. Middleton and J. Xie, "Non-Pathological Sampling for High Order Generalised Sampled-Data Hold Functions", *Proc. American Control Conf.*, pp. 1498-1502, Seattle, USA, 1993.
- [73] S. Barnett, *Polynomials and Linear Control Systems*, Marcel Dekker, Inc., New York, NY, 1983.
- [74] G.H. Golub and C.F. Van Loan, *Matrix Computations*, The Johns Hopkins University Press, Baltimore, Maryland, 1996.
- [75] T.C. Hsia, *System Identification—Least Squares Methods*, Lexington Books, Lexington, MA, 1977.
- [76] W.J. Rugh, *Linear System Theory*, 2nd edition, Prentice Hall, Englewood Cliffs, NJ, 1996.

- [77] C.A. Desoer and M. Vidyasagar, *Feedback Systems: Input-Output Properties*, Academic Press, New York, NY, 1975.
- [78] M.G. Safonov, D.J.N. Limebeer and R.Y. Chiang, "Simplifying the  $H^\infty$  theory via loop-shifting, matrix-pencil and descriptor concepts", *Int. J. Control*, Vol. 50, No. 6, pp. 2467-2488, 1989.
- [79] A.E. Taylor, *Advanced Calculus*, Blaisdell Publishing Company, New York, NY, 1965.
- [80] C.A. Rabbath, *Sensitivity of the Discrete- to Continuous-Time Pole Transformation at Fast Sampling Rates*, Master's Thesis, McGill University, Montreal, 1995.
- [81] K. Kanai, *Flight Control*, Maki-Publishing, Tokyo, 1985.
- [82] dSPACE GmbH, *VCFP Demo*, Germany, 1994.
- [83] C.L. Phillips and H.T. Nagle, *Digital Control System Analysis and Design*, Prentice-Hall, Englewood Cliffs, NJ, 1990.
- [84] dSPACE GmbH, *Floating-Point Controller Board — DS1102 User's Guide*, Germany, 1996.
- [85] I.E. Treager, *Aircraft — Gas Turbine Engine Technology*, Third Edition, Glencoe, McGraw-Hill, New York, NY, 1995.
- [86] J.D. Mattingly, *Elements of Gas Turbine Propulsion*, McGraw-Hill, Inc., New York, NY, 1996.
- [87] Pratt & Whitney Canada, *Engineering Report #4237*, Longueuil, Quebec, Canada, 1997 [Proprietary Data].
- [88] D. S. Bernstein, "A Student's Guide to Classical Control", *IEEE Control Systems Magazine*, pp. 96-100, August 1997.

- [89] J.S. Shamma and M. Athans, "Gain Scheduling: Potential Hazards and Possible Remedies", *IEEE Control Systems Magazine*, Vol. 12, pp. 101-107, 1992.
- [90] D. McRuer, I. Ashkenas and D. Graham, *Aircraft Dynamics and Automatic Control*, Princeton University Press, Princeton, NJ, 1973.
- [91] A. Raymond Comeau, *Higher Order Discrete-Time Models with Applications to Multi-Rate Control*, Ph.D. Thesis, McGill University, Montreal, 1997.
- [92] R. M. McLeod, *The Generalized Riemann Integral*, The Mathematical Association of America, 1980.
- [93] G. Strang, *Linear Algebra and Its Applications*, 3rd edition, Saunders College Publishing, Orlando, Florida, 1988.
- [94] M. Artin, *Algebra*, Prentice-Hall, Englewood Cliffs, NJ, 1991.
- [95] P.T. Kabamba, "Control of Linear Systems Using Generalized Sampled-Data Hold Functions", *IEEE Trans. Aut. Control*, Vol. AC-32, No. 9, pp. 772-783, 1987.
- [96] T. Kailath, *Linear Systems*, Prentice-Hall, Englewood Cliffs, NJ, 1980.
- [97] A. Feuer and G.C. Goodwin, *Sampling in Digital Signal Processing and Control*, Birkhauser, Boston, MA, 1996.
- [98] G.C. Goodwin and A. Feuer, "Generalised Sample Hold Functions: Facts and Fallacies", *Proc. 31st Conf. Decision and Control*, pp. 1955-1960, Tucson, AZ, USA, 1992.
- [99] A. Feuer and G.C. Goodwin, "Generalized Sample Hold Functions — Frequency Domain Analysis of Robustness, Sensitivity, and Intersample Difficulties", *IEEE Trans. Aut. Control*, Vol. AC-39, No. 5, pp. 1042-1047, 1994.
- [100] Y.-C. Juan and P.T. Kabamba, "Optimal Hold Functions for Sampled Data Regulation", *Automatica*, 27, No. 1, pp. 177-181, 1991.

# Appendix A

## Mathematical Details

This appendix provides proofs of some propositions and theorems presented in Chapter 4.

### A.1 Proof of Proposition 4.2.1

The discrete-time system can be represented as follows

$$\begin{aligned} \delta x_{k,T} &= \underbrace{\left( \frac{e^{\bar{A}_G T} - I}{T} \right)}_{=A_{G_T}} x_{G_T, k, T} + \underbrace{\frac{1}{T} \left( \int_{v=0}^T e^{\bar{A}_G(T-v)} \bar{B}_G H(v) dv \right)}_{=B_{G_T}} u_{k, T}, \quad x_{G_T, 0, T} = 0_{n \times 1}, \\ y_{k, T} &= \underbrace{\bar{C}_G}_{=C_{G_T}} x_{G_T, k, T} + \underbrace{\bar{D}_G \cdot H(\tau)|_{\tau=0}}_{=D_{G_T}} u_{k, T}. \end{aligned} \quad (\text{A.1})$$

From the hold condition in the time domain,

$$\begin{aligned} \lim_{T \rightarrow 0} D_{G_T} &= \bar{D}_G \cdot \lim_{T \rightarrow 0} H(\tau)|_{\tau=0} \\ &= \bar{D}_G. \end{aligned} \quad (\text{A.2})$$

Also,

$$\begin{aligned} & \left\| B_{G_T} - \frac{1}{T} \int_{v=0}^T e^{\bar{A}_{\bar{G}}(T-v)} \bar{B}_{\bar{G}} H(v) dv \right\| \\ & \leq \left\| B_{G_T} - \frac{1}{T} \int_{v=0}^T e^{\bar{A}_{\bar{G}}(T-v)} \bar{B}_{\bar{G}} dv \right\| + \left\| \frac{1}{T} \int_{v=0}^T e^{\bar{A}_{\bar{G}}(T-v)} \bar{B}_{\bar{G}} (H(v) - 1) dv \right\|. \quad (\text{A.3}) \end{aligned}$$

Given any  $\epsilon > 0$ , there exists a  $\gamma > 0$  such that whenever  $T < \gamma$  the two terms on the right-hand side of (A.3) add up to a value less than  $\epsilon$ . Furthermore,  $\lim_{T \rightarrow 0} A_{G_T} = \bar{A}_{\bar{G}}$  and  $C_{G_T} = \bar{C}_{\bar{G}}$ .

## A.2 Proof of Theorem 4.3.1

In order to prove Theorem 4.3.1, the following proposition is used.

**Proposition A.1** For a signal in  $\mathcal{S}_1$  or a staircase equivalent of a signal in  $\mathcal{S}_1$ , denoted as  $\bar{r}(t)$  and with lifted representation  $\{\widehat{r}_{k,T}(\tau)\}_0^\infty = \{r_{k,T} + \omega_{k,T}(\tau)\}_0^\infty$ ,  $0 \leq \tau < T$ , where  $\omega_{k,T}(\tau)|_{\tau=0} = 0$ , as shown on Figure A.1,

$$\lim_{T \rightarrow 0} \sup_{k \geq 0} \left\{ \sup_{0 \leq \tau < T} |\omega_{k,T}(\tau)| \right\} = 0. \quad (\text{A.4})$$

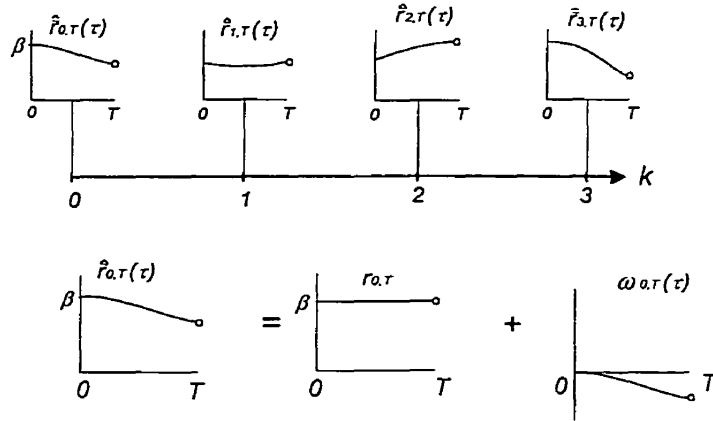


Figure A.1: Lifted representation of a signal in  $\mathcal{S}_1$

Proof: (i)  $\bar{r}(t) \in \mathcal{S}_1$ . The proof is given by contradiction. The signal  $\bar{r}(t)$  is bounded, uniformly continuous and independent of  $T$ . Assume the contrary to what has to be shown; that is,  $\sup_{k \geq 0} \sup_{0 \leq \tau < T} |\omega_{k,T}(\tau)|$  cannot be made as small as desired by choosing a  $T$  sufficiently small. This means that there exists at least one time instant for which the supremum norm cannot be arbitrarily reduced. If this is so, since the lifted signal  $\{\omega_{k,T}(\tau)\}_{k=0}^{\infty}$  represents the difference between lifted forms of a signal in  $\mathcal{S}_1$  and its staircase equivalent, as can be appreciated from Figure A.1, the initial assumption of uniform continuity of  $\bar{r}(t)$  is violated.

(ii)  $\bar{r}(t)$  is a staircase equivalent of a signal in  $\mathcal{S}_1$ . For this  $T$ -dependent signal,  $\omega_{k,T}(\tau) = 0$ ,  $0 \leq \tau < T$ , for all  $k$  and each  $T$  selected. The limiting behavior is immediate.  $\square$

The proof of Theorem 4.3.1 is divided into two parts: one treats the control input, the other investigates the controlled output. For both cases, to satisfy the definition of a sampled-data model, Definition 2.2.7, knowing the condition on the reference inputs as established by Definition 4.3.1, equations (A.5) and (A.6) must be satisfied.

$$\lim_{T \rightarrow 0} \left[ \sup_{k \in [0, \infty)} \left\{ \sup_{\tau \in [0, T)} \left| \hat{u}_{k,T}(\tau) - \widehat{u}_{k,T}(\tau) \right| \right\} \right] = 0 \quad (\text{A.5})$$

$$\lim_{T \rightarrow 0} \left[ \sup_{k \in [0, \infty)} \left\{ \sup_{\tau \in [0, T)} \left| \hat{y}_{k,T}(\tau) - \widehat{y}_{k,T}(\tau) \right| \right\} \right] = 0 \quad (\text{A.6})$$

(i) Control input. Let  $\widehat{e}_{k,T}(\tau) = \hat{u}_{k,T}(\tau) - \widehat{u}_{k,T}(\tau)$ , for any  $k \geq 0$ . Write the lifted equivalent of the reference input to the continuous-time control system as  $\widehat{r}_{CT,k,T}(\tau)$  and that to the sampled-data control system, as  $\widehat{r}_{SD,k,T}(\tau)$ . Then

$$\begin{aligned} & |\widehat{e}_{k,T}(\tau)| \\ &= \left| \sum_{j=0}^{k-1} \{H(\tau)(\bar{C} + \Delta C)(T(\bar{A} + \Delta A) + I)^{k-j-1} \right. \\ & \quad \left. \cdot T(\bar{B} + \Delta B) \cdot \widehat{r}_{SD,j,T}(0) - \bar{C}e^{\bar{A}\tau} (e^{\bar{A}T})^{k-j-1} \right| \end{aligned}$$

$$\begin{aligned}
& \cdot \int_{v=0}^T e^{\bar{A}(T-v)} \bar{B} \cdot \widehat{r}_{CT,j,T}(v) dv \Big\} \\
& - \bar{C} \int_{v=0}^{\tau} e^{\bar{A}(\tau-v)} \bar{B} \cdot \widehat{r}_{CT,k,T}(v) dv \\
& + H(\tau)(\bar{D} + \Delta D) \cdot \widehat{r}_{SD,k,T}(0) - \bar{D} \cdot \widehat{r}_{CT,k,T}(\tau) \Big| \tag{A.7}
\end{aligned}$$

where the sum  $\sum_{j=0}^{k-1}$  is zero for  $k = 0$ . Let

$$\sup_{k \geq 0} \left\{ \sup_{0 \leq \tau < T} \left| \widehat{r}_{CT,k,T}(\tau) \right| \right\} = r_{b,CT} \tag{A.8}$$

and

$$\sup_{k \geq 0} \left\{ \sup_{0 \leq \tau < T} \left| \widehat{r}_{SD,k,T}(\tau) \right| \right\} = r_{b,SD}. \tag{A.9}$$

Use the triangle inequality, for fixed  $\bar{A}$ ,  $\bar{B}$ ,  $\bar{C}$ ,  $\bar{D}$ , and  $T$ , to bound  $|\widehat{e}_{k,T}(\tau)|$  as

$$\begin{aligned}
& \sup_{0 \leq k < \infty} \left\{ \sup_{0 \leq \tau < T} |\widehat{e}_{k,T}(\tau)| \right\} \\
\leq & \sup_{0 \leq k < \infty} \left\{ \sup_{0 \leq \tau < T} \left| \sum_{j=0}^{k-1} \{ (\bar{C} + \Delta C) \right. \right. \\
& \cdot (T(\bar{A} + \Delta A) + I)^{k-j-1} T(\bar{B} + \Delta B) \widehat{r}_{SD,j,T}(0) \\
& \left. \left. - \bar{C} e^{\bar{A}\tau} \left( e^{\bar{A}T} \right)^{k-j-1} \int_{v=0}^T e^{\bar{A}(T-v)} \bar{B} \widehat{r}_{CT,j,T}(v) dv \right\} \right\} \\
& + \sup_{0 \leq k < \infty} \left\{ \sup_{0 \leq \tau < T} \left| -\bar{C} \int_{v=0}^{\tau} e^{\bar{A}(\tau-v)} \bar{B} \widehat{r}_{CT,k,T}(v) dv \right. \right. \\
& \left. \left. + (\bar{D} + \Delta D) \widehat{r}_{SD,k,T}(0) - \bar{D} \widehat{r}_{CT,k,T}(\tau) \right| \right\} \\
& + \sup_{0 \leq \tau < T} |H(\tau) - 1| \cdot \sup_{0 \leq k < \infty} \left| \sum_{j=0}^{k-1} \{ (\bar{C} + \Delta C) \right. \\
& \cdot (T(\bar{A} + \Delta A) + I)^{k-j-1} T(\bar{B} + \Delta B) \widehat{r}_{SD,j,T}(0) \} \\
& \left. \left. + (\bar{D} + \Delta D) \widehat{r}_{SD,k,T}(0) \right| \right\}. \tag{A.10}
\end{aligned}$$

From the assumption on the reference inputs, one can write  $\widehat{r}_{SD,k,T}(0) = \widehat{r}_{CT,k,T}(0) + \Delta r_{k,T}$ , where  $\Delta r_{k,T} \rightarrow 0$  for each  $k$ , as  $T \rightarrow 0$ . Therefore, equation (A.10) can be

rewritten as follows:

$$\begin{aligned}
& \sup_{0 \leq k < \infty} \left\{ \sup_{0 \leq \tau < T} |\widehat{e}_{k,T}(\tau)| \right\} \\
\leq & \underbrace{\sup_{0 \leq k < \infty} \left\{ \sup_{0 \leq \tau < T} \left| \sum_{j=0}^{k-1} \{(\overline{C} + \Delta C) \cdot (T(\overline{A} + \Delta A) + I)^{k-j-1} T(\overline{B} + \Delta B) \cdot (\widehat{r}_{CT,j,T}(0) + \Delta r_{j,T}) - \overline{C} e^{\overline{A}\tau} (e^{\overline{A}T})^{k-j-1} \int_{v=0}^T e^{\overline{A}(T-v)} \overline{B} \widehat{r}_{CT,j,T}(v) dv\} \right| \right\}}_{=F_1(T)} \\
& + \underbrace{\sup_{0 \leq k < \infty} \left\{ \sup_{0 \leq \tau < T} \left| -\overline{C} \int_{v=0}^{\tau} e^{\overline{A}(\tau-v)} \overline{B} \widehat{r}_{CT,k,T}(v) dv + (\overline{D} + \Delta D) \cdot (\widehat{r}_{CT,k,T}(0) + \Delta r_{k,T}) - \overline{D} \widehat{r}_{CT,k,T}(\tau) \right| \right\}}_{=F_2(T)} \\
& + \underbrace{\sup_{0 \leq \tau < T} |H(\tau) - 1| \cdot \sup_{0 \leq k < \infty} \left| \sum_{j=0}^{k-1} \{(\overline{C} + \Delta C) \cdot (T(\overline{A} + \Delta A) + I)^{k-j-1} T(\overline{B} + \Delta B) (\widehat{r}_{CT,j,T}(0) + \Delta r_{j,T})\} + (\overline{D} + \Delta D) (\widehat{r}_{CT,k,T}(0) + \Delta r_{k,T}) \right|}_{=F_3(T)}. \tag{A.11}
\end{aligned}$$

A bound on the first term on the right-hand side of (A.11),  $F_1(T)$ , is thus

$$\begin{aligned}
& F_1(T) \\
\leq & \|\overline{C}\| \cdot \|(\overline{B} + \Delta B)\| f_1(T) r_{b,CT} \\
& + \|\overline{C}\| f_2(T) f_3(T) r_{b,CT} + \|\overline{C}\| f_5(T) \omega_{b,T} f_3(T) \\
& + \|\overline{C}\| \sup_{0 \leq \tau < T} \|e^{\overline{A}\tau} - I\| f_3(T) f_5(T) r_{b,CT} \\
& + \|\Delta C\| f_4(T) \|(\overline{B} + \Delta B)\| r_{b,CT} \\
& + f_4(T) \|\overline{C} + \Delta C\| \cdot \|(\overline{B} + \Delta B)\| \cdot \Delta r_{b,T} \tag{A.12}
\end{aligned}$$

where

$$f_1(T) = \sum_{j=0}^{\infty} T \left\| (T(\bar{A} + \Delta A) + I)^j - e^{\bar{A}Tj} \right\| \quad (\text{A.13})$$

$$f_2(T) = \left\| (\bar{B} + \Delta B) - \frac{1}{T} \int_{v=0}^T e^{\bar{A}(T-v)} \bar{B} dv \right\| \quad (\text{A.14})$$

$$f_3(T) = \sum_{j=0}^{\infty} T \left\| e^{\bar{A}Tj} \right\| \quad (\text{A.15})$$

$$f_4(T) = \sum_{j=0}^{\infty} T \left\| (T(\bar{A} + \Delta A) + I)^j \right\| \quad (\text{A.16})$$

$$f_5(T) = \frac{1}{T} \int_{v=0}^T \left\| e^{\bar{A}(T-v)} \bar{B} \right\| dv \quad (\text{A.17})$$

$$\omega_{b,T} = \sup_{0 \leq k < \infty} \left( \sup_{0 \leq \tau < T} |\omega_{k,T}(\tau)| \right) \quad (\text{A.18})$$

$$\Delta r_{b,T} = \sup_{0 \leq k < \infty} |\Delta r_{k,T}|. \quad (\text{A.19})$$

The first term on the right-hand side of (A.12) comprises  $f_1(T)$  which can be bounded as

$$f_1(T) \leq \sum_{j=0}^{\infty} T \left\| (T(\bar{A} + \Delta A) + I)^j \right\| + \sum_{j=0}^{\infty} T \left\| e^{\bar{A}Tj} \right\|. \quad (\text{A.20})$$

The right-hand side of the last inequality is finite since the two series converge for each fixed  $T$  which yields internal stability of the discrete-time system. In fact, there exist finite positive  $T$ -dependent parameters  $\gamma_{1,T}$ ,  $\gamma_{2,T}$ ,  $0 \leq \eta_{1,T} < 1$ , and  $0 \leq \eta_{2,T} < 1$  such that [76]

$$\left\| (T(\bar{A} + \Delta A) + I)^k \right\| \leq \gamma_{1,T} \cdot \eta_{1,T}^k \quad (\text{A.21})$$

and

$$\left\| e^{\bar{A}Tk} \right\| \leq \gamma_{2,T} \cdot \eta_{2,T}^k \quad (\text{A.22})$$

for all  $k \geq 0$ .  $f_1(T)$  approaches zero when the sampling interval is reduced since the terms of the series in (A.13) (i) approach zero in an exponentially decaying fashion when  $k \rightarrow \infty$ , and (ii) approach zero for each step  $k$ .

Alternatively,  $f_1(T)$  can be related to the difference in zero-input state responses, at the sampling instants, between the continuous- and discrete-time systems subjected to the same finite initial state  $x_0$  :

$$x_{k,T} - \widehat{x}_{k,T}(0) = \left\{ (T(\overline{A} + \Delta A) + I)^k - e^{\overline{A}Tk} \right\} x_0. \quad (\text{A.23})$$

As  $k \rightarrow \infty$ ,  $(x_{k,T} - \widehat{x}_{k,T}(0)) \rightarrow 0_{p \times 1}$  since the systems are internally stable. It can be shown that [91]

$$\lim_{T \rightarrow 0} (T(\overline{A} + \Delta A) + I)^j = \lim_{T \rightarrow 0} e^{\overline{A}Tj} \quad (\text{A.24})$$

for each  $j \geq 0$ . Also, as  $j \rightarrow \infty$ ,  $(T(\overline{A} + \Delta A) + I)^j \rightarrow 0_{p \times p}$ , and  $e^{\overline{A}Tj} \rightarrow 0_{p \times p}$ . The weighting factor  $T$  in the series makes  $f_1(T)$  become close to an integral over  $[0, \infty)$  [92] with integrand approaching zero over all time instants, as  $T \rightarrow 0$ , and decaying exponentially as time becomes large. Therefore, the series approaches zero by reducing  $T$ .

The consequence of the behavior of  $f_1(T)$ , as  $T \rightarrow 0$ , is that the first term in (A.12) becomes infinitesimally small. The second term in (A.12) approaches zero as  $T \rightarrow 0$  since  $\lim_{T \rightarrow 0} f_2(T) = 0$  and the series  $f_3(T)$  is finite ( $\overline{A}$  is Hurwitz). The third term of (A.12) vanishes as  $T \rightarrow 0$  since  $\omega_{b,T} \rightarrow 0$  (from Proposition A.1). For the fourth term, integral and summation are finite and  $\sup_{0 \leq \tau < T} \|e^{\overline{A}\tau} - I\| \rightarrow 0$  as  $T \rightarrow 0$ . The fifth term can be made arbitrarily small since  $\|\Delta C\| \rightarrow 0$  ( $T \rightarrow 0$ ). Finally, the sixth term approaches zero as the sampling period is reduced from the conditions on the reference inputs.

The second term on the right-hand side of (A.11),  $F_2(T)$ , can be bounded as follows:

$$\begin{aligned} F_2(T) \leq & \|\overline{C}\| \cdot T f_5(T) r_{b,CT} \\ & + |\Delta D| r_{b,CT} + |\overline{D}| \cdot \omega_{b,T} + |\overline{D} + \Delta D| \cdot \Delta r_{b,T} \end{aligned} \quad (\text{A.25})$$

where  $\lim_{T \rightarrow 0} T f_5(T) = 0$ . The third term on the right-hand side of (A.11),  $F_3(T)$ , can be made arbitrarily small from the hold condition in the time domain. Thus, given

any  $\xi > 0$ , one can select a  $T < \kappa_1(\xi)$  such that  $F_1(T) < \xi/3$ , a  $T < \kappa_2(\xi)$  such that  $F_2(T) < \xi/3$  and a  $T < \kappa_3(\xi)$  such that  $F_3(T) < \xi/3$ . Let  $\kappa = \min \{\kappa_1, \kappa_2, \kappa_3\}$ , and take  $T < \kappa(\xi)$ . Then  $\sup_{k \geq 0} \sup_{0 \leq \tau < T} |\widehat{e}_{k,T}(\tau)| \leq \xi$ .

(ii) Controlled output. The norm on the error at controlled output can be written as follows:

$$\begin{aligned}
& \sup_{0 \leq k < \infty} \left\{ \sup_{0 \leq \tau < T} \left| \widehat{y}_{k,T}(\tau) - \widehat{\bar{y}}_{k,T}(\tau) \right| \right\} \\
= & \sup_{0 \leq k < \infty} \left\{ \sup_{0 \leq \tau < T} \left| \overline{C}_{\overline{G}} e^{\overline{A}_{\overline{G}} \tau} \sum_{j=0}^{k-1} \left[ \left( e^{\overline{A}_{\overline{G}} T} \right)^{k-j-1} \int_{v=0}^T e^{\overline{A}_{\overline{G}}(T-v)} \overline{B}_{\overline{G}} \left( \widehat{u}_{k,T}(v) - \widehat{\bar{u}}_{k,T}(v) \right) dv \right] \right. \right. \\
& + \overline{C}_{\overline{G}} \int_{v=0}^{\tau} e^{\overline{A}_{\overline{G}}(\tau-v)} \overline{B}_{\overline{G}} \left( \widehat{u}_{k,T}(v) - \widehat{\bar{u}}_{k,T}(v) \right) dv \\
& \left. \left. + \overline{D}_{\overline{G}} \left( \widehat{u}_{k,T}(\tau) - \widehat{\bar{u}}_{k,T}(\tau) \right) \right| \right\} \tag{A.26}
\end{aligned}$$

for all  $k \geq 0$ , where  $\widehat{\bar{x}}_{\overline{G},0,T}(0) = 0_{n \times 1}$ ,  $\overline{G}$  has realization elements given by  $[\overline{A}_{\overline{G}}, \overline{B}_{\overline{G}}, \overline{C}_{\overline{G}}, \overline{D}_{\overline{G}}]$ , and  $T$  is selected such that the sampled-data control system is internally stable at the sampling instants. The following fact is the basis for the rest of the proof: the nature of feedback is such that control inputs  $\{\widehat{u}_{k,T}(\tau)\}_{k=0}^{\infty}$  and  $\{\widehat{\bar{u}}_{k,T}(\tau)\}_{k=0}^{\infty}$  stabilize the plant for each fixed  $T$  in the allowable range of values; for instance, all non-pathological sampling periods for a digital redesign carried out with PIM. Stabilizing the plant for the sampled-data system means that, for each  $T$  and at the sampling instants, the discrete-time control input provides stability for the closed-loop discrete-time system, i.e. the unstable factors of the discrete-time plant model are exactly cancelled out by the control input and the overall output response is composed of decaying factors, those of the discrete-time PITF, and factors of the discrete reference input. In between the sampling instants, the hold is such that the plant output is bounded. For the continuous-time control system, its stabilization over all time instants implies that at the sampling instants. The state of the plant at the sampling instants then takes on finite values. Define

$\widehat{e}_{k,T}(\tau) = \widehat{u}_{k,T}(\tau) - \widehat{\bar{u}}_{k,T}(\tau)$  and

$$e_{b,T} = \sup_{0 \leq k < \infty} \left\{ \sup_{0 \leq \tau < T} |\widehat{e}_{k,T}(\tau)| \right\}. \quad (\text{A.27})$$

Then, using the aforementioned facts and the lifting formalism, the norm of the output response error is finite and can be written as follows:

$$\begin{aligned} & \sup_{0 \leq k < \infty} \sup_{0 \leq \tau < T} \left| \widehat{y}_{k,T}(\tau) - \widehat{\bar{y}}_{k,T}(\tau) \right| \\ = & \sup_{0 \leq k < \infty} \sup_{0 \leq \tau < T} \left| \overline{C}_{\overline{G}} e^{\overline{A}_{\overline{G}} \tau} \sum_{j=0}^{k-1} \left[ \left( e^{\overline{A}_{\overline{G}} T} \right)^{k-j-1} \int_{v=0}^T e^{\overline{A}_{\overline{G}}(T-v)} \overline{B}_{\overline{G}} \widehat{e}_{j,T}(v) dv \right] \right. \\ & \left. + \overline{C}_{\overline{G}} \int_{v=0}^{\tau} e^{\overline{A}_{\overline{G}}(\tau-v)} \overline{B}_{\overline{G}} \widehat{e}_{k,T}(v) dv + \overline{D}_{\overline{G}} \widehat{e}_{k,T}(\tau) \right|. \end{aligned} \quad (\text{A.28})$$

Moreover, if one separates the state of the plant, in terms of its discrete-time part, and the intersample information at the  $k$ th lifting interval, it follows that each element of (A.28) is bounded. Then

$$\sup_{0 \leq k < \infty} \sup_{0 \leq \tau < T} \left| \widehat{y}_{k,T}(\tau) - \widehat{\bar{y}}_{k,T}(\tau) \right| \leq f_{1,T} + f_{2,T} + f_{3,T} \quad (\text{A.29})$$

where

$$f_{1,T} = \sup_{0 \leq \tau < T} \left\| \overline{C}_{\overline{G}} e^{\overline{A}_{\overline{G}} \tau} \right\| \cdot \sup_{0 \leq k < \infty} \left\| \sum_{j=0}^{k-1} \left[ \left( e^{\overline{A}_{\overline{G}} T} \right)^{k-j-1} \int_{v=0}^T e^{\overline{A}_{\overline{G}}(T-v)} \overline{B}_{\overline{G}} \widehat{e}_{j,T}(v) dv \right] \right\| \quad (\text{A.30})$$

$$f_{2,T} = \sup_{0 \leq k < \infty} \sup_{0 \leq \tau < T} \left| \overline{C}_{\overline{G}} \int_{v=0}^{\tau} e^{\overline{A}_{\overline{G}}(\tau-v)} \overline{B}_{\overline{G}} \widehat{e}_{k,T}(v) dv \right| \quad (\text{A.31})$$

$$f_{3,T} = \sup_{0 \leq k < \infty} \sup_{0 \leq \tau < T} \left| \overline{D}_{\overline{G}} \widehat{e}_{k,T}(\tau) \right| \quad (\text{A.32})$$

Note: From part (i),  $\widehat{e}_{k,T}(\tau)$  approaches zero for each  $\tau \in [0, T)$  and for each step  $k$ , as  $T \rightarrow 0$ , while it preserves stability.

In (A.30), the first term is finite. The right-most term of (A.30) represents the

supremum over all time steps of the norm of the difference in the zero-state responses of the plant, at the sampling instants, as governed by the sampled-data and continuous-time control inputs. In both cases, the plant is stabilized and so, at each sampling instant, the two states take on finite values. Invoke Proposition 4.2.1. The key to the demonstration is to investigate the zero-state responses of the plant under sampled-data and continuous-time control, at the sampling instants. For the continuous-time control system, the zero-state in the transform domain is given by

$$\bar{X}_{\bar{G}}(s) = \frac{Adj(sI - \bar{A}_{\bar{G}})\bar{B}_{\bar{G}}\bar{m}(s)}{\bar{d}(s)}\bar{R}_{CT}(s) \quad (\text{A.33})$$

where  $\bar{R}_{CT}(s)$  is the transform of the reference input applied to the continuous-time control system, and  $\bar{m}(s)$  and  $\bar{d}(s)$  come from  $\bar{H}(s) = \bar{m}(s)\bar{a}(s)/\bar{d}(s)$ . Note that  $\bar{a}(s) = |sI - \bar{A}_{\bar{G}}|$  if the plant transfer function is irreducible,  $\bar{X}_{\bar{G}}(s) = (sI - \bar{A}_{\bar{G}})^{-1}\bar{B}_{\bar{G}}\bar{U}(s)$ , and the rational transfer function vector relating  $\bar{X}_{\bar{G}}(s)$  to  $\bar{R}_{CT}(s)$  in (A.33) has strictly proper entries. One can associate a realization to (A.33) with elements  $[\bar{A}_2, \bar{B}_2, \bar{C}_2]$ , where  $\bar{A}_2$  is Hurwitz, and the lifting on this realization yields the following plant state evolution at the sampling instants:

$$\hat{\bar{x}}_{\bar{G},k,T}(0) = \bar{C}_2 \sum_{j=0}^{k-1} \left[ \left( e^{\bar{A}_2 T} \right)^{k-j-1} \int_{v=0}^T e^{\bar{A}_2(T-v)} \bar{B}_2 \hat{\bar{r}}_{CT,j,T}(v) dv \right]. \quad (\text{A.34})$$

For the sampled-data control system, the zero-state of the hold-equivalent model of the plant in the transform domain is given by

$$X_{GT}(\varepsilon) = \frac{Adj\left(\varepsilon I - (e^{\bar{A}_{\bar{G}}T} - I)/T\right) \left(\frac{1}{T} \int_{v=0}^T e^{\bar{A}_{\bar{G}}v} \bar{B}_{\bar{G}} H(v) dv\right) m(\varepsilon)}{d(\varepsilon)} R_{SD,T}(\varepsilon) \quad (\text{A.35})$$

where  $R_{SD,T}(\varepsilon)$  is the transform of the sampled reference input applied to the sampled-data control system, and  $m(\varepsilon)$  and  $d(\varepsilon)$  come from  $H_T(\varepsilon) = m(\varepsilon)a(\varepsilon)/d(\varepsilon)$ . Note that  $a(\varepsilon) = \left| \varepsilon I - (e^{\bar{A}_{\bar{G}}T} - I)/T \right|$  if the hold-equivalent model of the plant transfer function is

irreducible, and

$$X_{G_T}(\varepsilon) = \left( \varepsilon I - (e^{\bar{A}_G T} - I)/T \right)^{-1} \left( \frac{1}{T} \int_{v=0}^T e^{\bar{A}_G v} \bar{B}_G H(v) dv \right) U_T(\varepsilon). \quad (\text{A.36})$$

The transfer function vector (A.35) has the same dimension as that of the continuous-time system and  $d(\varepsilon)$  has the same degree as  $\bar{d}(s)$ . One can associate a realization to (A.35) with elements  $[A_2, B_2, C_2]$ , where  $A_2$  has all its eigenvalues in the region  $|T\varepsilon + 1| < 1$ , which yields the following state evolution for the hold-equivalent model of the plant:

$$x_{G_T, k, T} = C_2 \sum_{j=0}^{k-1} \left[ (TA_2 + I)^{k-j-1} TB_2 \widehat{r}_{SD, j, T}(0) \right]. \quad (\text{A.37})$$

With the assumption on the reference inputs, the difference in zero-state responses of the plant, at the sampling instants, can then be written as:

$$\begin{aligned} x_{G_T, k, T} - \widehat{x}_{\bar{G}, k, T}(0) &= \sum_{j=0}^{k-1} \left[ C_2 (TA_2 + I)^{k-j-1} TB_2 (\widehat{r}_{CT, j, T}(0) + \Delta r_{j, T}) \right. \\ &\quad \left. - \bar{C}_2 \left( e^{\bar{A}_2 T} \right)^{k-j-1} \int_{v=0}^T e^{\bar{A}_2 (T-v)} \bar{B}_2 \widehat{r}_{CT, j, T}(v) dv \right]. \quad (\text{A.38}) \end{aligned}$$

From the structure of the problem, the fact the hold satisfies the hold condition in the time domain, and Proposition 4.4.4, proved in this Appendix, there exists one discrete-time realization such that its elements satisfy:  $\lim_{T \rightarrow 0} A_2 = \bar{A}_2$ ,  $\lim_{T \rightarrow 0} B_2 = \bar{B}_2$ , and  $\lim_{T \rightarrow 0} C_2 = \bar{C}_2$ . The supremum over all time steps of the norm of the difference in the zero-state responses of the plant, at the sampling instants, can then be bounded as follows for any finite  $T$ :

$$\begin{aligned} &\sup_{0 \leq k < \infty} \left\| x_{G_T, k, T} - \widehat{x}_{\bar{G}, k, T}(0) \right\| \\ &\leq \|\bar{C}_2\| \cdot \sup_{0 \leq k < \infty} \sum_{j=0}^{k-1} \left\| \left[ (TA_2 + I)^{k-j-1} - \left( e^{\bar{A}_2 T} \right)^{k-j-1} \right] TB_2 \right\| \cdot r_{b, CT} \end{aligned}$$

$$\begin{aligned}
& + \|\bar{C}_2\| \cdot \sup_{0 \leq k < \infty} \sum_{j=0}^{k-1} \left\| \left( e^{\bar{A}_2 T} \right)^{k-j-1} \left[ - \int_{v=0}^T e^{\bar{A}_2(T-v)} \bar{B}_2 dv + T B_2 \right] \right\| \cdot r_{b,CT} \\
& + \|\bar{C}_2\| \cdot \sup_{0 \leq k < \infty} \sum_{j=0}^{k-1} \left\| \left( e^{\bar{A}_2 T} \right)^{k-j-1} \int_{v=0}^T e^{\bar{A}_2(T-v)} \bar{B}_2 \omega_{j,T}(v) dv \right\| \\
& + \|\Delta C_2\| \cdot \sum_{j=0}^{\infty} \left\| (T A_2 + I)^j \right\| \cdot \|B_2\| \cdot T \cdot r_{b,CT} \\
& + \|\bar{C}_2 + \Delta C_2\| \cdot \|B_2\| \cdot \Delta r_{b,T} \cdot \sup_{0 \leq k < \infty} \sum_{j=0}^{k-1} \left\| (T A_2 + I)^{k-j-1} \right\| T. \tag{A.39}
\end{aligned}$$

The bound can be further simplified as:

$$\begin{aligned}
& \sup_{0 \leq k < \infty} \left\| x_{G_T, k, T} - \hat{x}_{\bar{G}, k, T}(0) \right\| \\
\leq & \|\bar{C}_2\| \cdot \sup_{0 \leq k < \infty} \sum_{j=0}^{k-1} \left\| \left[ (T A_2 + I)^{k-j-1} - \left( e^{\bar{A}_2 T} \right)^{k-j-1} \right] \right\| T \|B_2\| \cdot r_{b,CT} \\
& + \|\bar{C}_2\| \cdot \sup_{0 \leq k < \infty} \sum_{j=0}^{k-1} \left\| \left( e^{\bar{A}_2 T} \right)^{k-j-1} \right\| T \cdot \left\| -\frac{1}{T} \int_{v=0}^T e^{\bar{A}_2(T-v)} \bar{B}_2 dv + B_2 \right\| \cdot r_{b,CT} \\
& + \|\bar{C}_2\| \cdot \sup_{0 \leq k < \infty} \sum_{j=0}^{k-1} \left\| \left( e^{\bar{A}_2 T} \right)^{k-j-1} \right\| T \cdot \frac{1}{T} \left\| \int_{v=0}^T e^{\bar{A}_2(T-v)} \bar{B}_2 \omega_{j,T}(v) dv \right\| \\
& + \sum_{j=0}^{\infty} \left\| (T A_2 + I)^j \right\| T \cdot \|B_2\| \cdot (\|\bar{C}_2 + \Delta C_2\| \cdot \Delta r_{b,T} + \|\Delta C_2\| \cdot r_{b,CT}). \tag{A.40}
\end{aligned}$$

It is clear that the bound can be made to go to zero as  $T \rightarrow 0$  since

$$\lim_{T \rightarrow 0} \sup_{0 \leq k < \infty} \sum_{j=0}^{k-1} \left\| \left[ (T A_2 + I)^{k-j-1} - \left( e^{\bar{A}_2 T} \right)^{k-j-1} \right] \right\| T = 0 \tag{A.41}$$

$$\lim_{T \rightarrow 0} \left\| -\frac{1}{T} \int_{v=0}^T e^{\bar{A}_2(T-v)} \bar{B}_2 dv + B_2 \right\| = 0 \tag{A.42}$$

$$\lim_{T \rightarrow 0} \frac{1}{T} \left\| \int_{v=0}^T e^{\bar{A}_2(T-v)} \bar{B}_2 \omega_{j,T}(v) dv \right\|$$

$$\leq \lim_{T \rightarrow 0} \frac{1}{T} \int_{v=0}^T \left\| e^{\bar{A}_2(T-v)} \bar{B}_2 \right\| dv \cdot \omega_{b,T}, \quad \forall j \quad (\text{A.43})$$

$$\lim_{T \rightarrow 0} \|\Delta C_2\| = 0 \quad (\text{A.44})$$

$$\lim_{T \rightarrow 0} \Delta r_{b,T} = 0 \quad (\text{A.45})$$

where  $\omega_{b,T} \rightarrow 0$  ( $T \rightarrow 0$ ) because of the assumption on the reference input to the continuous-time system. Then, given any  $\xi > 0$ , one can select a  $T < \kappa_1(\xi)$  such that  $f_{1,T} < \xi/3$  in (A.30).

For (A.31) and (A.32), part (i) of the proof implies that they can be made arbitrarily small. In (A.31), one can choose a  $T < \kappa_2(\xi)$  such that  $f_{2,T} < \xi/3$ . For (A.32), select a  $T < \kappa_3(\xi)$  such that  $f_{3,T} < \xi/3$ . Let  $\kappa = \min\{\kappa_1, \kappa_2, \kappa_3\}$ , and take  $T < \kappa(\xi)$ . Then  $\sup_{0 \leq k < \infty} \sup_{0 \leq \tau < T} \left| \widehat{y}_{k,T}(\tau) - \widehat{\bar{y}}_{k,T}(\tau) \right| \leq \xi$ .

### A.3 Proofs of Propositions 4.3.1, 4.3.2 and 4.3.3

#### Proposition 4.3.1

First, for the case when  $\bar{r}(t)$  is independent of  $T$ , is uniformly continuous, and has finite  $L^2$  norm, as  $t \rightarrow \infty$ ,  $|\bar{r}(t)|$  approaches zero [77]. Furthermore, the derivative of  $\bar{r}(t)$  with respect to time is limited and hence the ideal sampler is bounded in the sense that its output has finite  $l^2$  norm [4]. Second, with the staircase equivalent of  $\bar{r}(t)$  entering the ideal sampler, the output of the sampler can be written in operator form as  $SHS\bar{r}$ , where  $H$  is the ZOH,  $\bar{r}(t)$  is in  $\mathcal{S}_1$  and has finite  $L^2$  norm, and  $HS\bar{r}$  is the staircase equivalent of  $\bar{r}$ . With the convention adopted in this research about the ideal sampler and ZOH, as described in Section 1.2, the operator  $SH$  is the identity discrete-time operator; that is, the discrete-time output of  $SH$  equals to the discrete-time input. Therefore,  $SHS\bar{r} = S\bar{r}$  and the finiteness of the  $l^2$  norm of the sampler's output is guaranteed.

### Proposition 4.3.2

From Theorem 2.3.1,  $\sup_{\omega} |\bar{H}(j\omega)| < \infty$  and  $\sup_{\omega} |\bar{G}\bar{H}(j\omega)| < \infty$ , where  $j = \sqrt{-1}$ . With bounds  $\|\bar{u}(t)\|_{L^2}^2 \leq (\sup_{\omega} |\bar{H}(j\omega)|)^2 \cdot \|\bar{r}(t)\|_{L^2}^2$  and  $\|\bar{y}(t)\|_{L^2}^2 \leq (\sup_{\omega} |\bar{G}\bar{H}(j\omega)|)^2 \cdot \|\bar{r}(t)\|_{L^2}^2$  [59],  $\bar{u}(t)$  and  $\bar{y}(t)$  are in  $L^2$ .

### Proposition 4.3.3

The proof is divided into two parts: the control input and the controlled output.

(i) Control input.  $u_{k,T}$  has finite  $l^2$  norm since the sampled reference input has finite  $l^2$  norm, with the restriction on the type of input admitted, and the discrete-time PITF is stable, from Proposition 4.3.1 and [77]. The  $L^2$  norm of the output of the hold,  $u_T(t)$ , can then be bounded as:

$$\|u_T(t)\|_{L^2} \leq \left[ \sum_{k=0}^{\infty} |u_{k,T}|^2 T \right]^{1/2} \cdot \sup_{0 \leq \tau < T} |H(\tau)|. \quad (\text{A.46})$$

From the condition on the magnitude of the hold function, the control input is in  $L^2$ .

(ii) Controlled output. The following facts imply that the state of the discrete-time PITF is in  $l^2$ : closed-loop system stability and reference input in, or a staircase equivalent of a signal in,  $\mathcal{S}_1$  with finite  $L^2$  norm, and the control input in  $L^2$ . Using the representation in equations (4.4) to (4.6), where the state of the PITF is taken as the composite state, the finiteness of the terms multiplying the closed-loop discrete-time state and the sampled reference input, and the finite  $l^2$  norms of the discrete-time state and the sampled reference input make the  $L^2$  norm of the controlled output finite.

## A.4 Proof of Proposition 4.4.1

Proposition 4.4.1 provides the relationship between the solutions to the discrete-time and continuous-time Diophantine equations, obtained with the eliminant matrix method, when the sampling interval is reduced.

The difference between  $X$  and  $\bar{X}$  can be expressed as:

$$X - \bar{X} = \mathbf{A}^{-1}Y - \bar{\mathbf{A}}^{-1}\bar{Y} \quad (\text{A.47})$$

where the two inverses exist since  $\mathbf{A}$  and  $\bar{\mathbf{A}}$  have full rank. Since  $G_T(\varepsilon)$  and  $H_T(\varepsilon)$  are discrete-time models of  $\bar{G}(s)$  and  $\bar{H}(s)$  [13], respectively, and  $\bar{u}(s)$  and  $\bar{v}(s)$  have the same degrees as  $u(\varepsilon)$  and  $v(\varepsilon)$ , respectively, one can write

$$Y = \bar{Y} + \Delta Y \quad (\text{A.48})$$

$$\mathbf{A} = \bar{\mathbf{A}} + \Delta \mathbf{A} \quad (\text{A.49})$$

where  $\lim_{T \rightarrow 0} \Delta Y = 0_{(p+1) \times 1}$  and  $\lim_{T \rightarrow 0} \Delta \mathbf{A} = 0_{(p+1) \times (p+1)}$ . Then

$$\lim_{T \rightarrow 0} \|X - \bar{X}\| \leq \lim_{T \rightarrow 0} \left( \left\| (I + \bar{\mathbf{A}}^{-1} \Delta \mathbf{A})^{-1} - I \right\| \cdot \left\| \bar{\mathbf{A}}^{-1} \right\| + \|\mathbf{A}^{-1}\| \cdot \|\Delta Y\| \right) \quad (\text{A.50})$$

and  $X$  approaches  $\bar{X}$  as  $T \rightarrow 0$ .

## A.5 Proof of Proposition 4.4.2

For a given continuous-time control system, Proposition 4.4.2 relates the solution obtained with the eliminant matrix method to that obtained with the least-squares method.

To start the proof, let the continuous-time Diophantine equation of the given continuous-time control system be

$$(\bar{u}_f s^f + \dots + \bar{u}_0)(\bar{a}_n s^n + \dots + \bar{a}_0) + (\bar{v}_h s^h + \dots + \bar{v}_0)(\bar{b}_m s^m + \dots + \bar{b}_0) = \bar{d}_p s^p + \dots + \bar{d}_0 \quad (\text{A.51})$$

with the corresponding system of equations

$$\underbrace{\begin{bmatrix} \bar{a}_n & & & & & \\ \bar{a}_{n-1} & \ddots & & \bar{b}_m & & \\ \vdots & \ddots & \bar{a}_n & \bar{b}_{m-1} & \ddots & \\ \bar{a}_1 & & \bar{a}_{n-1} & \vdots & \ddots & \bar{b}_m \\ \bar{a}_0 & \ddots & \vdots & \bar{b}_0 & & \bar{b}_{m-1} \\ & \ddots & \bar{a}_1 & & \ddots & \vdots \\ & & \bar{a}_0 & & & \bar{b}_0 \end{bmatrix}}_{=\bar{\mathbf{A}}} \underbrace{\begin{bmatrix} \bar{u}_f \\ \vdots \\ \bar{u}_0 \\ \bar{v}_h \\ \vdots \\ \bar{v}_0 \end{bmatrix}}_{=\bar{\mathbf{X}}} = \underbrace{\begin{bmatrix} \bar{d}_p \\ \bar{d}_{p-1} \\ \vdots \\ \bar{d}_1 \\ \bar{d}_0 \end{bmatrix}}_{=\bar{\mathbf{Y}}} \quad (\text{A.52})$$

Before proceeding any further, it should be noted that (i)  $\bar{\mathbf{A}}_2 \bar{\mathbf{X}}_2 = \bar{\mathbf{A}} \bar{\mathbf{X}}$ ; (ii)  $\bar{u}(s)$  and  $\bar{u}_2(s)$  have the common degree  $p-n$ ; (iii) the system of equations  $\bar{\mathbf{A}} \bar{\mathbf{X}} = \bar{\mathbf{Y}}$  is consistent, i.e.  $\bar{\mathbf{Y}}$  is in the range space of  $\bar{\mathbf{A}}$ ; and (iv) by the assumption on the plant irreducibility and a theorem on unicity of solutions in [93],  $\bar{\mathbf{X}}$  is unique.

Partition the matrices as follows:

$$\bar{\mathbf{A}} = [\bar{\mathbf{A}}^1 \mid \bar{\mathbf{A}}^2 \mid \cdots \mid \bar{\mathbf{A}}^{f+h+2}], \quad \bar{\mathbf{A}}_2 = [\bar{\mathbf{A}}_2^1 \mid \bar{\mathbf{A}}_2^2 \mid \cdots \mid \bar{\mathbf{A}}_2^{p+1}] \quad (\text{A.53})$$

where  $\bar{\mathbf{A}}^j \in R^{(p+1) \times 1}$ , for  $j = 1, 2, \dots, f+h+2$ , and  $\bar{\mathbf{A}}_2^j \in R^{(p+1) \times 1}$ , for  $j = 1, 2, \dots, p+1$ , are the column vectors constituting the matrices  $\bar{\mathbf{A}}$  and  $\bar{\mathbf{A}}_2$ , respectively, and the superscript denotes the position of the vector in the matrix. Write the vectors  $\bar{\mathbf{X}}$  and  $\bar{\mathbf{X}}_2$  as follows:

$$\bar{\mathbf{X}} = [\bar{\mathbf{U}} \mid \bar{\mathbf{V}}]^T, \quad \bar{\mathbf{X}}_2 = [\bar{\mathbf{U}}_2 \mid \bar{\mathbf{V}}_2]^T \quad (\text{A.54})$$

where  $\bar{\mathbf{U}}$  and  $\bar{\mathbf{V}}$  are vectors of coefficients of the polynomials  $\bar{u}(s)$  and  $\bar{v}(s)$ , respectively, and  $\bar{\mathbf{U}}_2, \bar{\mathbf{V}}_2$  are vectors comprising the coefficients of  $\bar{u}_2(s)$  and  $\bar{v}_2(s)$ , respectively. Further expand the vectors as

$$\bar{\mathbf{U}} = [\bar{U}(1), \bar{U}(2), \dots, \bar{U}(p-n+1)]^T \quad (\text{A.55})$$

$$\bar{U}_2 = [\bar{U}_2(1), \bar{U}_2(2), \dots, \bar{U}_2(p-n+1)]^T \quad (\text{A.56})$$

$$\bar{V} = [\bar{V}(1), \bar{V}(2), \dots, \bar{V}(h+1)]^T \quad (\text{A.57})$$

$$\bar{V}_2 = [\bar{V}_2(1), \bar{V}_2(2), \dots, \bar{V}_2(n)]^T \quad (\text{A.58})$$

where  $\bar{U}(j)$  corresponds to the  $j$ th entry of the vector  $\bar{U}$ , and similarly for the other vectors. Use the fact that  $\bar{\mathbf{A}} \bar{X} = \bar{\mathbf{A}}_2 \bar{X}_2$  to write

$$[\bar{\mathbf{A}}^1 \mid \bar{\mathbf{A}}^2 \mid \dots \mid \bar{\mathbf{A}}^{f+h+2}] \bar{X} = [\bar{\mathbf{A}}_2^1 \mid \bar{\mathbf{A}}_2^2 \mid \dots \mid \bar{\mathbf{A}}_2^{p+1}] \bar{X}_2 \quad (\text{A.59})$$

or, in more details,

$$\begin{aligned} & \bar{\mathbf{A}}^1 \bar{U}(1) + \bar{\mathbf{A}}^2 \bar{U}(2) + \dots + \bar{\mathbf{A}}^{f+h+2} \bar{V}(h+1) \\ &= \bar{\mathbf{A}}_2^1 \bar{U}_2(1) + \bar{\mathbf{A}}_2^2 \bar{U}_2(2) + \dots + \bar{\mathbf{A}}_2^{p+1} \bar{V}_2(n). \end{aligned} \quad (\text{A.60})$$

The number of columns of  $\bar{\mathbf{A}}_2$  is greater than that in  $\bar{\mathbf{A}}$  since  $h < n - 1$ . In fact, the number of extra columns of  $\bar{\mathbf{A}}_2$  with respect to  $\bar{\mathbf{A}}$  equals  $n - h - 1$  (Note that if  $h = n - 1$ ,  $\bar{\mathbf{A}}_2 = \bar{\mathbf{A}}$  and  $\bar{X}_2 = \bar{X}$ ). Then, knowing  $\bar{\mathbf{A}}_2^j = \bar{\mathbf{A}}^j$  for  $j = 1, 2, \dots, p - n + 1$  and  $\bar{\mathbf{A}}_2^{p-h+j-1} = \bar{\mathbf{A}}^{p-n+j}$  for  $j = 2, 3, \dots, h + 2$ , equation (A.60) can be rewritten as:

$$\begin{aligned} & (\bar{U}(1) - \bar{U}_2(1)) \bar{\mathbf{A}}_2^1 + \dots + (\bar{U}(p-n+1) - \bar{U}_2(p-n+1)) \bar{\mathbf{A}}_2^{p-n+1} \\ & + \bar{V}_2(1) \bar{\mathbf{A}}_2^{p-n+2} + \dots + \bar{V}_2(n-h-1) \bar{\mathbf{A}}_2^{p-h} + (\bar{V}(1) - \bar{V}_2(n-h)) \bar{\mathbf{A}}_2^{p-h+1} \\ & + \dots + (\bar{V}(h+1) - \bar{V}_2(n)) \bar{\mathbf{A}}_2^{p+1} \\ &= 0. \end{aligned} \quad (\text{A.61})$$

Since  $\bar{\mathbf{A}}_2$  is a square matrix of rank  $(p+1)$ , the  $\bar{\mathbf{A}}_2^j$  are linearly independent vectors and the coefficients in front of them, in (A.61), are bound to be zero [94]. Therefore,

$$\begin{aligned} \bar{U}_2(1) &= \bar{U}(1) \\ &\vdots \end{aligned}$$

$$\begin{aligned}
\bar{U}_2(p-n+1) &= \bar{U}(p-n+1) \\
\bar{V}_2(1) &= 0 \\
&\vdots \\
\bar{V}_2(n-h-1) &= 0 \\
\bar{V}_2(n-h) &= \bar{V}(1) \\
&\vdots \\
\bar{V}_2(n) &= \bar{V}(h+1).
\end{aligned} \tag{A.62}$$

It follows readily that  $\bar{u}_2(s) = \bar{u}(s)$  and  $\bar{v}_2(s) = \bar{v}(s)$ .

## A.6 Proof of Proposition 4.4.3

Rewrite the Diophantine equation (4.33) as

$$\underbrace{(\bar{u}_{2,f_2}s^{f_2} + \dots + \bar{u}_{2,0})}_{=\bar{u}_2(s)} \bar{a}(s) + \underbrace{(\bar{v}_{2,h_2}s^{h_2} + \dots + \bar{v}_{2,0})}_{=\bar{v}_2(s)} \bar{b}(s) = \underbrace{\bar{d}_{2,p+c}s^{p+c} + \dots + \bar{d}_{2,0}}_{=\bar{d}_2(s)} \tag{A.63}$$

where  $\bar{u}_2(s)$  and  $\bar{v}_2(s)$  have degrees set to  $f_2 = f + c$  and  $h_2 = h + c$ , respectively, and  $\bar{d}_2(s) = \bar{\phi}(s) \cdot \bar{d}(s)$ . In the usual way, generate the linear system of equations (A.64).

$$\underbrace{\begin{bmatrix} \bar{a}_n & & & & & \\ \bar{a}_{n-1} & \ddots & & & \bar{b}_m & \\ \vdots & \ddots & \bar{a}_n & \bar{b}_{m-1} & \ddots & \\ \bar{a}_1 & & \bar{a}_{n-1} & \vdots & \ddots & \bar{b}_m \\ \bar{a}_0 & \ddots & \vdots & \bar{b}_0 & & \bar{b}_{m-1} \\ & \ddots & \bar{a}_1 & & \ddots & \vdots \\ & & \bar{a}_0 & & & \bar{b}_0 \end{bmatrix}}_{=\bar{A}_2} \underbrace{\begin{bmatrix} \bar{u}_{2,f_2} \\ \vdots \\ \bar{u}_{2,0} \\ \bar{v}_{2,h_2} \\ \vdots \\ \bar{v}_{2,0} \end{bmatrix}}_{=\bar{X}_2} = \underbrace{\begin{bmatrix} \bar{d}_{2,p+c} \\ \bar{d}_{2,p+c-1} \\ \vdots \\ \bar{d}_{2,1} \\ \bar{d}_{2,0} \end{bmatrix}}_{=\bar{Y}_2} \tag{A.64}$$

The polynomials  $\bar{u}_2(s) = \bar{\phi}(s) \cdot \bar{u}(s)$  and  $\bar{v}_2(s) = \bar{\phi}(s) \cdot \bar{v}(s)$  form a solution to (4.33) since substituting them in (4.33) satisfies the equality. Equivalently, the coefficients in front of the powers of  $s$  of the polynomials  $\bar{u}_2(s)$  and  $\bar{v}_2(s)$  which form the entries of the vector  $\bar{X}_2$  in (A.64) provide a solution to  $\bar{A}_2 \bar{X}_2 = \bar{Y}_2$ . In order to show that this solution to (A.64) is unique, it must be proved that, when  $\bar{a}(s)$  and  $\bar{b}(s)$  are coprime,  $\bar{A}_2$  in (A.64) has full column rank. To do so, one should first note that the value of  $c$  should lie within the range  $[2n - 1 - p, n - 1 - h]$  for reasons of unicity of solution (the upper limit  $n - 1 - h$  avoids obtaining an underdetermined system of equations) and properness of the controllers calculated with equations (3.12)-(3.15) from the solution vector  $\bar{X}_2$  (the lower limit  $2n - 1 - p$  in conjunction with the condition on  $h$  prevents improper controller transfer functions and assures  $p + c = 2n - 1$ ). In fact, multiplying  $\bar{d}(s)$  by  $\bar{\phi}(s)$  results in a vector  $\bar{Y}_2$  in (A.64) having a dimension greater than or equal to  $2n$ . From a continuous-time variant of the first part of the proof of Theorem 3.2.1, it results that, provided  $\bar{a}(s)$  and  $\bar{b}(s)$  are coprime,  $\bar{A}_2$  in (A.64) has full column rank. In more details, when  $p + c \geq 2n - 1$ , the coprimeness of  $\bar{a}(s)$  and  $\bar{b}(s)$  assures the full rank of a square matrix  $\bar{A}_2 \in R^{(p+c+1) \times (p+c+1)}$  in (A.64) provided  $f_2 = p + c - n$  and  $h_2 = n - 1$  from a continuous-time version of Theorem 3.1.1. Thus, with the degrees  $f_2 = p + c - n$  and  $h_2 \leq n - 1$ , as is the case here, the matrix  $\bar{A}_2 \in R^{(p+c+1) \times (f_2+h_2+2)}$  possesses  $f_2 + h_2 + 2$  linearly independent columns. For the non-square case ( $h_2 < n - 1$ ), the matrix  $\bar{A}_2 \in R^{(p+c+1) \times (f_2+h_2+2)}$  can be formed from the aforementioned square matrix by removing  $n - h_2 - 1$  columns.

Hence, the uniqueness of the solution polynomials  $\bar{u}_2(s)$  and  $\bar{v}_2(s)$  is achieved.

## A.7 Proof of Proposition 4.4.4

Sufficiency: Suppose one realization of  $W_T(\varepsilon)$  is  $[\bar{A} + \Delta A, \bar{B} + \Delta B, \bar{C} + \Delta C, \bar{D} + \Delta D]$ , where the  $\Delta \cdot$  terms satisfy (4.42). Then

$$W_T(\varepsilon) = \frac{(\bar{C} + \Delta C) \text{Adj}(\varepsilon I - (\bar{A} + \Delta A))(\bar{B} + \Delta B) + |\varepsilon I - (\bar{A} + \Delta A)| (\bar{D} + \Delta D)}{|\varepsilon I - (\bar{A} + \Delta A)|} \quad (\text{A.65})$$

whereas

$$\bar{W}(s) = \frac{\bar{C} \text{Adj}(sI - \bar{A})\bar{B} + |sI - \bar{A}| \bar{D}}{|sI - \bar{A}|}. \quad (\text{A.66})$$

It is clear that the coefficients of the powers of  $\varepsilon$  in the numerator and denominator parts of  $W_T(\varepsilon)$  approach those of the corresponding powers of  $s$  in  $\bar{W}(s)$  as  $T \rightarrow 0$  when the terms  $\Delta \cdot$  approach zero.

Necessity: From the knowledge of the transfer function coefficients, one can obtain a realization. If both realizations are for instance in the observable canonical form, then each element of the discrete-time realization will approach its corresponding continuous-time element, as  $T \rightarrow 0$ , provided the coefficients of the discrete-time transfer function given by (4.39) satisfy equation (4.41). In more details, let a realization of the discrete-

time system be given by

$$\begin{aligned}
 \delta x_{k,T} = & \underbrace{\begin{bmatrix} 0 & 0 & \cdots & 0 & -(\bar{b}_0 + \Delta b_0) \\ 1 & 0 & \cdots & 0 & -(\bar{b}_1 + \Delta b_1) \\ 0 & 1 & \cdots & 0 & -(\bar{b}_2 + \Delta b_2) \\ \vdots & \vdots & \vdots & \vdots & \vdots \\ 0 & 0 & \cdots & 1 & -(\bar{b}_{n-1} + \Delta b_{n-1}) \end{bmatrix}}_{=\bar{A}+\Delta A} x_{k,T} \\
 + & \underbrace{\begin{bmatrix} (\bar{a}_0 + \Delta a_0) - (\bar{b}_0 + \Delta b_0)(\bar{a}_n + \Delta a_n) \\ (\bar{a}_1 + \Delta a_1) - (\bar{b}_1 + \Delta b_1)(\bar{a}_n + \Delta a_n) \\ (\bar{a}_2 + \Delta a_2) - (\bar{b}_2 + \Delta b_2)(\bar{a}_n + \Delta a_n) \\ \vdots \\ (\bar{a}_{n-1} + \Delta a_{n-1}) - (\bar{b}_{n-1} + \Delta b_{n-1})(\bar{a}_n + \Delta a_n) \end{bmatrix}}_{=\bar{B}+\Delta B} r_{k,T} \\
 y_{k,T} = & \underbrace{\begin{bmatrix} 0 & \cdots & 0 & 1 \end{bmatrix}}_{=\bar{C}+\Delta C} x_{k,T} + \underbrace{(\bar{a}_n + \Delta a_n)}_{=\bar{D}+\Delta D} r_{k,T}
 \end{aligned} \tag{A.67}$$

where  $r_{k,T}$  is the input and  $y_{k,T}$ , the output of the system. The continuous-time system realization is

$$\begin{aligned}
 \frac{d\bar{x}(t)}{dt} = & \underbrace{\begin{bmatrix} 0 & 0 & \cdots & 0 & -\bar{b}_0 \\ 1 & 0 & \cdots & 0 & -\bar{b}_1 \\ 0 & 1 & \cdots & 0 & -\bar{b}_2 \\ \vdots & \vdots & \vdots & \vdots & \vdots \\ 0 & 0 & \cdots & 1 & -\bar{b}_{n-1} \end{bmatrix}}_{=\bar{A}} \bar{x}(t) + \underbrace{\begin{bmatrix} \bar{a}_0 - \bar{b}_0 \bar{a}_n \\ \bar{a}_1 - \bar{b}_1 \bar{a}_n \\ \bar{a}_2 - \bar{b}_2 \bar{a}_n \\ \vdots \\ \bar{a}_{n-1} - \bar{b}_{n-1} \bar{a}_n \end{bmatrix}}_{=\bar{B}} \bar{r}(t) \\
 \bar{y}(t) = & \underbrace{\begin{bmatrix} 0 & \cdots & 0 & 1 \end{bmatrix}}_{=\bar{C}} \bar{x}(t) + \underbrace{\bar{a}_n}_{=\bar{D}} \bar{r}(t)
 \end{aligned} \tag{A.68}$$

where  $\bar{r}(t)$  is the input and  $\bar{y}(t)$ , the output of the system.

## A.8 Proof of Theorem 4.6.2

The following proposition is used in the proof of Theorem 4.6.2.

**Proposition A.2** For a linear, time-invariant discrete-time system  $H_T$ , the ideal sampler  $S$  and the ZOH  $H$ ,

$$\|HH_T S\|_{L^\infty} = \|H_T\|_{l^\infty} \cdot \infty \quad (\text{A.69})$$

Proof: First, the induced norm of  $HH_T S$  can be bounded as follows

$$\begin{aligned} \|HH_T S\|_{L^\infty} &\leq \|H\|_{l^\infty \rightarrow L^\infty} \cdot \|H_T\|_{l^\infty} \cdot \|S\|_{L^\infty \rightarrow l^\infty} \\ &\leq \|H_T\|_{l^\infty} \end{aligned} \quad (\text{A.70})$$

since  $\|S\|_{L^\infty \rightarrow l^\infty} = 1$  and  $\|H\|_{l^\infty \rightarrow L^\infty} = 1$  [66], and the induced norms are submultiplicative for bounded, linear transformations [77].

Second,

$$\begin{aligned} \|H_T\|_{l^\infty} &= \|SHH_T SH\|_{l^\infty} \\ &\leq \|S\|_{L^\infty \rightarrow l^\infty} \cdot \|HH_T S\|_{L^\infty} \cdot \|H\|_{l^\infty \rightarrow L^\infty} \\ &\leq \|HH_T S\|_{L^\infty} \end{aligned} \quad (\text{A.71})$$

since  $SH = I$ , where  $I$  is the identity discrete-time system, with the conventions on the hold and ideal sampler adopted in this research. Then (A.69) follows.  $\square$

With the continuous-time lifting formalism, the induced norm of the continuous-time system can be rewritten as

$$\|\bar{H}\|_{L^\infty} = \sum_{k=0}^{\infty} \int_{\tau=0}^T \left| \hat{g}_{k,T}(\tau) \right| d\tau \quad (\text{A.72})$$

where  $\{\widehat{g}_{k,T}(\tau)\}_0^\infty$  is the lifted impulse response of  $\overline{H}$ . It is desired to show that

$$\lim_{T \rightarrow 0} \|HH_T S\|_{L^\infty} = \|\overline{H}\|_{L^\infty} \quad (\text{A.73})$$

or, equivalently, that given any  $\epsilon > 0$ , there exists a  $\gamma > 0$  such that

$$\left| \sum_{k=0}^{\infty} |g_{k,T}| \cdot T - \sum_{k=0}^{\infty} \int_{\tau=0}^T |\widehat{g}_{k,T}(\tau)| d\tau \right| < \epsilon \quad (\text{A.74})$$

whenever  $T < \gamma$ . With realizations given as  $[A, B, C, D]$  for  $H_T$  and as  $[\overline{A}, \overline{B}, \overline{C}, \overline{D}]$  for  $\overline{H}$ , a bound can be obtained as follows:

$$\begin{aligned} & \left| \sum_{k=0}^{\infty} |g_{k,T}| \cdot T - \sum_{k=0}^{\infty} \int_{\tau=0}^T |\widehat{g}_{k,T}(\tau)| d\tau \right| \\ & \leq \underbrace{(|\overline{D} + \Delta D| - |\overline{D}|)}_{\rightarrow 0 (T \rightarrow 0)} + \underbrace{\int_{\tau=0}^T |\overline{C} e^{\overline{A}\tau} \overline{B}| d\tau}_{\rightarrow 0 (T \rightarrow 0)} \\ & \quad + \left| \sum_{k=1}^{\infty} |(\overline{C} + \Delta C)(T(\overline{A} + \Delta A) + I)^{k-1}(\overline{B} + \Delta B)| \cdot T \right. \\ & \quad \left. - \sum_{k=1}^{\infty} \int_{\tau=0}^T |\overline{C}(e^{\overline{A}kT} e^{\overline{A}\tau} \overline{B})| d\tau \right|. \end{aligned} \quad (\text{A.75})$$

The first two terms on the right-hand side approach zero as  $T$  is reduced. The third term yields

$$\begin{aligned} & \left| \sum_{k=1}^{\infty} |(\overline{C} + \Delta C)(T(\overline{A} + \Delta A) + I)^{k-1}(\overline{B} + \Delta B)| \cdot T \right. \\ & \quad \left. - \sum_{k=1}^{\infty} \int_{\tau=0}^T |\overline{C}(e^{\overline{A}kT} e^{\overline{A}\tau} \overline{B})| d\tau \right| \\ & \leq \left| \sum_{k=1}^{\infty} |\overline{C}(T(\overline{A} + \Delta A) + I)^{k-1} \overline{B}| \cdot T - \sum_{k=1}^{\infty} \int_{\tau=0}^T |\overline{C}(e^{\overline{A}kT} e^{\overline{A}\tau} \overline{B})| d\tau \right| \end{aligned}$$

$$\begin{aligned}
& + \underbrace{\sum_{k=1}^{\infty} |\Delta C(T(\bar{A} + \Delta A) + I)^{k-1}(\bar{B} + \Delta B)| \cdot T}_{\rightarrow 0 (T \rightarrow 0)} \\
& + \underbrace{\sum_{k=1}^{\infty} |\bar{C}(T(\bar{A} + \Delta A) + I)^{k-1} \Delta B| \cdot T}_{\rightarrow 0 (T \rightarrow 0)}. \tag{A.76}
\end{aligned}$$

The internal stability at the sampling instants of the control systems renders the series in the first term of (A.76) finite [76] whereas the behavior of  $\Delta C$  and  $\Delta B$  make the last two terms on the right-hand side of (A.76) approach zero, as  $T \rightarrow 0$ . The first term of (A.76) can be bounded as:

$$\begin{aligned}
& \left| \sum_{k=1}^{\infty} |\bar{C}(T(\bar{A} + \Delta A) + I)^{k-1} \bar{B}| \cdot T - \sum_{k=1}^{\infty} \int_{\tau=0}^T |\bar{C}(e^{\bar{A}kT} e^{\bar{A}\tau} \bar{B})| d\tau \right| \\
& \leq \underbrace{\left| \sum_{k=0}^{\infty} |\bar{C}(T(\bar{A} + \Delta A) + I)^k \bar{B}| \cdot T - \sum_{k=0}^{\infty} |\bar{C}e^{\bar{A}kT} \bar{B}| \cdot T \right|}_{=f_{1,T}} + \underbrace{|\bar{C} \bar{B}| \cdot T}_{\rightarrow 0 (T \rightarrow 0)} \\
& \quad + \underbrace{\|\bar{C}\| \cdot \|\bar{B}\| \cdot \sum_{k=1}^{\infty} \|e^{\bar{A}kT}\| \cdot T \sup_{0 \leq \tau < T} \|e^{\bar{A}\tau} - I\|}_{\rightarrow 0 (T \rightarrow 0)}. \tag{A.77}
\end{aligned}$$

The first term on the right-hand side of the last inequality can be bounded as

$$f_{1,T} \leq \|\bar{C}\| \cdot \left| \sum_{k=0}^{\infty} \|(T(\bar{A} + \Delta A) + I)^k\| \cdot T - \sum_{k=0}^{\infty} \|e^{\bar{A}kT}\| \cdot T \right| \cdot \|\bar{B}\| \tag{A.78}$$

where the series are finite when  $T$  is sufficiently small and both are composed of terms which exhibit an exponentially decaying magnitude as  $k \rightarrow \infty$  [76]. As  $T \rightarrow 0$ , each series approaches the following integral

$$\int_{t=0}^{\infty} \|e^{\bar{A}t}\| dt \tag{A.79}$$

which has finite value from the internal stability of the continuous-time system [76]. The

bound on  $f_{1,T}$  can then be made arbitrarily close to zero with a sufficiently small sampling interval. Consequently, equation (4.60) follows.

## A.9 Proof of Theorem 4.6.3

The following propositions are used in the proof of Theorem 4.6.3.

**Proposition A.3** The induced norm of the ZOH  $H : l^2 \rightarrow L^2$  is unity.  $\square$

Proof: Suppose that the ZOH has period  $T$ , the input to the ZOH is  $u_{k,T}$ ,  $k \geq 0$ , and the output is  $u_T(t)$ . The  $L^2$  norm of  $u_T(t)$  is therefore given by

$$\begin{aligned}
 \|u_T(t)\|_{L^2} &= \left[ \int_{t=0}^{\infty} |u_T(t)|^2 dt \right]^{1/2} \\
 &= \left[ \sum_{k=0}^{\infty} \int_{\tau=0}^T |H(\tau)u_{k,T}|^2 d\tau \right]^{1/2} \\
 &= \left[ \sum_{k=0}^{\infty} \int_{\tau=0}^T |u_{k,T}|^2 d\tau \right]^{1/2} \\
 &= \left[ \sum_{k=0}^{\infty} |u_{k,T}|^2 \int_{\tau=0}^T d\tau \right]^{1/2} \\
 &= \left[ \sum_{k=0}^{\infty} |u_{k,T}|^2 T \right]^{1/2} = \|u_{k,T}\|_{l^2} \cdot \square
 \end{aligned} \tag{A.80}$$

**Proposition A.4** For a linear, time-invariant discrete-time system  $H_T$ , ideal sampler  $S$ , ZOH  $H$ , and reference input to the sampled-data system  $HH_T S$  lying in  $S_1$ , or being a staircase equivalent of a signal in,  $S_1$  and having a finite  $L^2$  norm,

$$\lim_{T \rightarrow 0} \|HH_T S\|_{L^2} = \lim_{T \rightarrow 0} \|H_T\|_{l^2} \cdot \infty \tag{A.81}$$

Proof: On the one hand, the induced norm of  $HH_T S$  can be bounded as follows

$$\begin{aligned} \lim_{T \rightarrow 0} \|HH_T S\|_{L^2} &\leq \lim_{T \rightarrow 0} \|H\|_{l^2 \rightarrow L^2} \cdot \|H_T\|_{l^2} \cdot \|S\|_{L^2 \rightarrow l^2} \\ &\leq \lim_{T \rightarrow 0} \|H_T\|_{l^2} \end{aligned} \quad (\text{A.82})$$

since  $\|H\|_{l^2 \rightarrow L^2} = 1$ , from Proposition A.3, and  $\lim_{T \rightarrow 0} \|S\|_{L^2 \rightarrow l^2} = 1$ . The norm of the ideal sampler necessitates some explanation. First of all, the finiteness of the sampler's induced norm comes from the fact the input is restricted to lie in  $\mathcal{S}_1$  and to have a finite  $L^2$  norm, or to be a staircase equivalent of a signal in  $\mathcal{S}_1$  with finite  $L^2$  norm. With such restriction, the ideal sampler is a bounded operator [4], and its output has a finite  $l^2$  norm. Second of all, concerning the fact  $\lim_{T \rightarrow 0} \|S\|_{L^2 \rightarrow l^2} = 1$ , the  $l^2$  norm of the sampler's output is given by

$$\|u_{k,T}\|_{l^2} = \left[ \sum_{k=0}^{\infty} |u_{k,T}|^2 T \right]^{1/2} \quad (\text{A.83})$$

whereas the  $L^2$  norm of the input to the sampler is

$$\|\bar{u}(t)\|_{L^2} = \left[ \int_{t=0}^{\infty} |\bar{u}(t)|^2 dt \right]^{1/2} \quad (\text{A.84})$$

where  $u_{k,T} = \bar{u}(t)|_{t=kT}$  for  $k \geq 0$ . Choose a fixed  $t^* \gg 0$ . Then, evaluate (A.84) over  $[0, t^*]$ , calculate the sum in (A.83) over the range  $[0, \text{int}\{t^*/T\}]$ , and let  $T \rightarrow 0$ , to obtain

$$\lim_{T \rightarrow 0} \left[ \sum_{k=0}^{\text{int}\{t^*/T\}} |u_{k,T}|^2 T \right]^{1/2} = \left[ \int_{t=0}^{t^*} |\bar{u}(t)|^2 dt \right]^{1/2}. \quad (\text{A.85})$$

Since  $\|\bar{u}(t)\|_{L^2} < \infty$ , one can let  $t^*$  be arbitrarily large and equation (A.85) still holds [92]. In fact, as  $t^* \rightarrow \infty$ ,

$$\lim_{t^* \rightarrow \infty} \left[ \int_{t=0}^{t^*} |\bar{u}(t)|^2 dt \right]^{1/2} = \left[ \int_{t=0}^{\infty} |\bar{u}(t)|^2 dt \right]^{1/2}. \quad (\text{A.86})$$

It results that  $\lim_{T \rightarrow 0} \|S\|_{L^2 \rightarrow L^2} = 1$ .

On the other hand,

$$\begin{aligned}
\lim_{T \rightarrow 0} \|H_T\|_{L^2} &= \lim_{T \rightarrow 0} \|SHH_TSH\|_{L^2} \\
&\leq \lim_{T \rightarrow 0} \|S\|_{L^2 \rightarrow L^2} \cdot \|HH_T S\|_{L^2} \cdot \|H\|_{L^2 \rightarrow L^2} \\
&\leq \lim_{T \rightarrow 0} \|HH_T S\|_{L^2}
\end{aligned} \tag{A.87}$$

where  $SH = I$ , the identity discrete-time system. Then (A.81) follows.  $\square$

With the preceding propositions, the aim of the proof is to show that, given any  $\epsilon > 0$ , there exists a  $\gamma > 0$  such that

$$|\|H_T\|_{L^2} - \|\bar{H}\|_{L^2}| < \epsilon \tag{A.88}$$

whenever  $T < \gamma$ . With  $H_T = [A, B, C, D]$  and  $\bar{H} = [\bar{A}, \bar{B}, \bar{C}, \bar{D}]$ , write

$$\begin{aligned}
&|\|H_T\|_{L^2} - \|\bar{H}\|_{L^2}| \\
&= \left| \sup_{-\pi/T \leq \omega \leq \pi/T} \left| C \left( \frac{e^{j\omega T} - 1}{T} I - A \right)^{-1} B + D \right| \right. \\
&\quad \left. - \sup_{-\infty < \omega < \infty} \left| \bar{C} (j\omega I - \bar{A})^{-1} \bar{B} + \bar{D} \right| \right|
\end{aligned} \tag{A.89}$$

It should be noted that the systems are internally stable and that their frequency responses obey  $|\bar{H}(j\omega)| = |\bar{H}(-j\omega)|$  and  $|H_T((e^{j\omega T} - 1)/T)| = |H_T((e^{-j\omega T} - 1)/T)|$  [40]. Hence, considering the positive frequency range is sufficient to obtain the supremum norm over the entire range of frequencies. As  $\omega \rightarrow \infty$ ,  $|\bar{H}(j\omega)|$  approaches a finite value: for a biproper system  $\bar{H}$  with realization elements  $[\bar{A}, \bar{B}, \bar{C}, \bar{D}]$ , it is  $\bar{D}$ , whereas for a strictly proper system, it is zero [5]. The frequency response magnitude  $|H_T((e^{j\omega T} - 1)/T)|$  is periodic with period  $2\pi$ ; that is, the frequency response magnitude for  $\omega \in [-\pi/T, \pi/T]$  is periodically repeated for the frequencies  $\omega > \pi/T$  and  $\omega < -\pi/T$  [40] (For frequencies  $\omega$  approaching to  $\pi/T$ , in the range  $[0, \pi/T]$ , the frequency response magnitude of  $H_T$  can

be made arbitrarily small by reducing the sampling period, when the transfer function is strictly proper.). Consequently, the supremum over all frequencies can be assessed over the interval  $[0, \pi/T]$ . In light of the aforementioned frequency response characteristics, it has to be shown that the supremum of the magnitude of the frequency response of the discrete-time system over the range of frequencies  $[0, \pi/T]$  can be as close as desired to that of the continuous-time system over frequencies in  $[0, \infty)$ , by employing sampling periods which are sufficiently small. A sufficient condition to the achievement of this behavior is to have the supremum of the magnitude of the difference in the frequency responses over  $[0, \pi/T]$  to be as small as desired. From the knowledge that  $A = \bar{A} + \Delta A$ ,  $B = \bar{B} + \Delta B$ ,  $C = \bar{C} + \Delta C$ , and  $D = \bar{D} + \Delta D$ , and Proposition 4.4.4, the supremum of the magnitude of the difference in frequency responses over  $[0, \pi/T]$  can be written as

$$\begin{aligned} & \sup_{0 \leq \omega \leq \pi/T} \left| \mathbf{H}_T((e^{j\omega T} - 1)/T) - \bar{\mathbf{H}}(j\omega) \right| \\ = & \sup_{0 \leq \omega \leq \pi/T} \left| \frac{(\bar{n}_q + \Delta_{n_q}) \frac{(e^{j\omega T} - 1)^q}{T^q} + \dots + (\bar{n}_0 + \Delta_{n_0})}{\frac{(e^{j\omega T} - 1)^p}{T^p} + (\bar{d}_{p-1} + \Delta_{d_{p-1}}) \frac{(e^{j\omega T} - 1)^{p-1}}{T^{p-1}} + \dots + (\bar{d}_0 + \Delta_{d_0})} \right. \\ & \left. - \frac{\bar{n}_q (j\omega)^q + \dots + \bar{n}_0}{(j\omega)^p + \bar{d}_{p-1} (j\omega)^{p-1} + \dots + \bar{d}_0} + \Delta D \right| \end{aligned} \quad (\text{A.90})$$

where  $q < p$ ,

$$\frac{(\bar{n}_q + \Delta_{n_q}) \frac{(e^{j\omega T} - 1)^q}{T^q} + \dots + (\bar{n}_0 + \Delta_{n_0})}{\frac{(e^{j\omega T} - 1)^p}{T^p} + \dots + (\bar{d}_0 + \Delta_{d_0})} = C \left( \frac{(e^{j\omega T} - 1)}{T} I - A \right)^{-1} B \quad (\text{A.91})$$

$$\frac{\bar{n}_q (j\omega)^q + \dots + \bar{n}_0}{(j\omega)^p + \dots + \bar{d}_0} = \bar{C} (j\omega I - \bar{A})^{-1} \bar{B} \quad (\text{A.92})$$

and

$$\lim_{T \rightarrow 0} \Delta_{d_j} = 0, \quad j = 0, \dots, p, \quad \lim_{T \rightarrow 0} \Delta_{n_j} = 0, \quad j = 0, \dots, q. \quad (\text{A.93})$$

With

$$\Sigma_{\omega, T} \triangleq \frac{e^{j\omega T} - 1}{j\omega T}, \quad (\text{A.94})$$

whose magnitude versus  $\omega T$  within  $[0, \pi]$  is shown in Figure A.2, one can write

$$\frac{e^{j\omega T} - 1}{T} = j\omega \cdot \Sigma_{\omega, T} \quad (\text{A.95})$$

and bound (A.90) as

$$\begin{aligned} & \sup_{0 \leq \omega \leq \pi/T} \left| H_T((e^{j\omega T} - 1)/T) - \bar{H}(j\omega) \right| \\ \leq & \sup_{0 \leq \omega \leq \pi/T} \left| \frac{\bar{n}_q \cdot (j\omega)^q \cdot (\Sigma_{\omega, T}^q - 1) + \dots + \bar{n}_1 \cdot (j\omega) \cdot (\Sigma_{\omega, T} - 1)}{(j\omega)^p \cdot \Sigma_{\omega, T}^p + d_{p-1}(j\omega)^{p-1} \cdot \Sigma_{\omega, T}^{p-1} + \dots + d_0} \right| \\ & + \sup_{0 \leq \omega \leq \pi/T} \left| \frac{\Delta_{n_q} \cdot (j\omega)^q \cdot \Sigma_{\omega, T}^q + \dots + \Delta_{n_1} \cdot (j\omega) \cdot \Sigma_{\omega, T} + \Delta_{n_0}}{(j\omega)^p \cdot \Sigma_{\omega, T}^p + d_{p-1}(j\omega)^{p-1} \cdot \Sigma_{\omega, T}^{p-1} + \dots + d_0} \right| \\ & + \sup_{0 \leq \omega \leq \pi/T} \left| \frac{\bar{n}_q(j\omega)^q + \bar{n}_{q-1}(j\omega)^{q-1} + \dots + \bar{n}_0}{(j\omega)^p + \bar{d}_{p-1}(j\omega)^{p-1} + \dots + \bar{d}_0} \right. \\ & \quad \left. \frac{(j\omega)^p \cdot (1 - \Sigma_{\omega, T}^p) + \dots + \bar{d}_1 \cdot (j\omega) \cdot (1 - \Sigma_{\omega, T})}{(j\omega)^p \cdot \Sigma_{\omega, T}^p + d_{p-1}(j\omega)^{p-1} \cdot \Sigma_{\omega, T}^{p-1} + \dots + d_0} \right| \\ & + \sup_{0 \leq \omega \leq \pi/T} \left| \frac{\bar{n}_q(j\omega)^q + \bar{n}_{q-1}(j\omega)^{q-1} + \dots + \bar{n}_0}{(j\omega)^p + \bar{d}_{p-1}(j\omega)^{p-1} + \dots + \bar{d}_0} \right. \\ & \quad \left. \frac{\Delta_{d_{p-1}} \cdot (j\omega)^{p-1} + \Delta_{d_{p-2}}(j\omega)^{p-2} + \dots + \Delta_{d_0}}{(j\omega)^p \cdot \Sigma_{\omega, T}^p + d_{p-1}(j\omega)^{p-1} \cdot \Sigma_{\omega, T}^{p-1} + \dots + d_0} \right| \\ & + |\Delta D|. \end{aligned} \quad (\text{A.96})$$

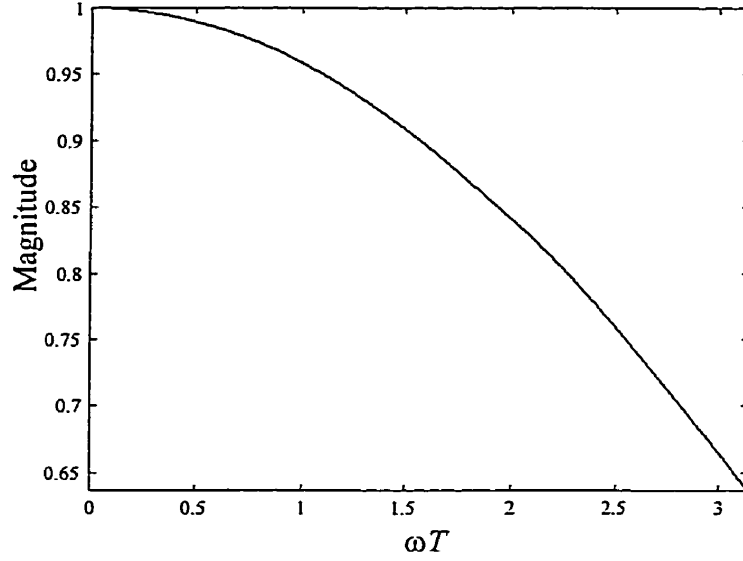


Figure A.2:  $|\Sigma_{\omega,T}|$  versus  $\omega T$

Each term of the bound in (A.96) can be made arbitrarily small by reducing  $T$ . This is seen as follows. Rewrite the first term as

$$\begin{aligned}
& \sup_{0 \leq \omega \leq \pi/T} \left| \frac{\bar{\pi}_q \cdot (j\omega)^q \cdot (\Sigma_{\omega,T}^q - 1) + \dots + \bar{\pi}_1 \cdot (j\omega) \cdot (\Sigma_{\omega,T} - 1)}{(j\omega)^p \cdot \Sigma_{\omega,T}^p + d_{p-1}(j\omega)^{p-1} \cdot \Sigma_{\omega,T}^{p-1} + \dots + d_0} \right| \\
\leq & \sup_{0 \leq \omega \leq \pi/T} \left| \frac{\bar{\pi}_q \cdot (j\omega)^q}{(j\omega)^p \cdot \Sigma_{\omega,T}^p + d_{p-1}(j\omega)^{p-1} \cdot \Sigma_{\omega,T}^{p-1} + \dots + d_0} \cdot (\Sigma_{\omega,T}^q - 1) \right| \\
& + \sup_{0 \leq \omega \leq \pi/T} \left| \frac{\bar{\pi}_{q-1} \cdot (j\omega)^{q-1}}{(j\omega)^p \cdot \Sigma_{\omega,T}^p + d_{p-1}(j\omega)^{p-1} \cdot \Sigma_{\omega,T}^{p-1} + \dots + d_0} \cdot (\Sigma_{\omega,T}^{q-1} - 1) \right| \\
& + \dots \\
& + \sup_{0 \leq \omega \leq \pi/T} \left| \frac{\bar{\pi}_1 \cdot (j\omega)}{(j\omega)^p \cdot \Sigma_{\omega,T}^p + d_{p-1}(j\omega)^{p-1} \cdot \Sigma_{\omega,T}^{p-1} + \dots + d_0} \cdot (\Sigma_{\omega,T} - 1) \right|. \quad (\text{A.97})
\end{aligned}$$

Each term on the right-hand side of (A.97) has close-to-zero magnitude in the low- and high-frequency (close to  $\pi/T$ ) ranges. For the low frequencies,  $(\Sigma_{\omega,T}^j - 1)$ ,  $j = 1, \dots, q$ , approaches zero for each fixed  $T$ . It should be noted that, as  $\omega \rightarrow \pi/T$ ,  $|\Sigma_{\omega,T}^j - 1| < 1$ ,  $j = 1, \dots, q$ . Furthermore, decreasing  $T$  results in  $(\Sigma_{\omega,T}^j - 1)$  becoming as small as required for a larger span of frequencies. For the high frequencies, these are filtered out by the

component

$$\frac{\bar{n}_j \cdot (j\omega)^j}{(j\omega)^p \cdot \Sigma_{\omega,T}^p + d_{p-1}(j\omega)^{p-1} \cdot \Sigma_{\omega,T}^{p-1} + \dots + d_0}, \quad j = 1, \dots, q$$

present in each term on the right-hand side of (A.97). Thus, one can always choose a  $T$  small enough such that the bound in (A.97) is as small as required. A similar development can be carried out for the third term of the bound in (A.96). Concerning the second term on the right-hand side of (A.96), a bound on this term is given by

$$\begin{aligned} & \sup_{0 \leq \omega \leq \pi/T} \left| \frac{\Delta_{n_q} \cdot (j\omega)^q \cdot \Sigma_{\omega,T}^q + \dots + \Delta_{n_1} \cdot (j\omega) \cdot \Sigma_{\omega,T} + \Delta_{n_0}}{(j\omega)^p \cdot \Sigma_{\omega,T}^p + d_{p-1}(j\omega)^{p-1} \cdot \Sigma_{\omega,T}^{p-1} + \dots + d_0} \right| \\ \leq & \sup_{0 \leq \omega \leq \pi/T} \left| \frac{(j\omega)^q \cdot \Sigma_{\omega,T}^q}{(j\omega)^p \cdot \Sigma_{\omega,T}^p + d_{p-1}(j\omega)^{p-1} \cdot \Sigma_{\omega,T}^{p-1} + \dots + d_0} \right| \cdot |\Delta_{n_q}| \\ & + \sup_{0 \leq \omega \leq \pi/T} \left| \frac{(j\omega)^{q-1} \cdot \Sigma_{\omega,T}^{q-1}}{(j\omega)^p \cdot \Sigma_{\omega,T}^p + d_{p-1}(j\omega)^{p-1} \cdot \Sigma_{\omega,T}^{p-1} + \dots + d_0} \right| \cdot |\Delta_{n_{q-1}}| \\ & + \dots \\ & + \sup_{0 \leq \omega \leq \pi/T} \left| \frac{1}{(j\omega)^p \cdot \Sigma_{\omega,T}^p + d_{p-1}(j\omega)^{p-1} \cdot \Sigma_{\omega,T}^{p-1} + \dots + d_0} \right| \cdot |\Delta_{n_0}| \quad (\text{A.98}) \end{aligned}$$

In the low-frequencies, each term on the right-hand side of (A.98) can be made arbitrarily close to zero by reducing  $T$ , whereas the higher frequencies are filtered out by the first component of each term. Therefore, there exists a  $T$  small enough such that the bound in (A.98) can be made as small as needed. A variant of the above development can be applied to the fourth term of the bound in (A.96). Finally, the last term of the upper bound in (A.96),  $|\Delta D|$ , can be made arbitrarily small by letting  $T \rightarrow 0$ .

It is clear that a sampling period can be selected such that the magnitude of the discrete-time frequency response of the discrete-time system can be made arbitrarily close to the magnitude of the continuous-time frequency response of the continuous-time system for frequencies in  $[0, \pi/T]$ . Then the theorem is proved.

## Appendix B

# Matched Pole-Zero Discrete-Time Model as a Hold-Equivalent Structure

This appendix proposes a state-space formulation for the matched pole-zero discrete-time model of a continuous-time system. The concepts of generalized hold functions [53, 95] and continuous-time lifting are used in order to express the discrete-time system as a hold-equivalent model of the continuous-time system, as shown in Figure B.1. The main advantage of using this structure is that it directly relates the state-space parameters of a matched pole-zero discrete-time model, such as the discrete-time PITF of a PIM-based sampled-data control system or the discrete-time plant model, with those of the continuous-time system.

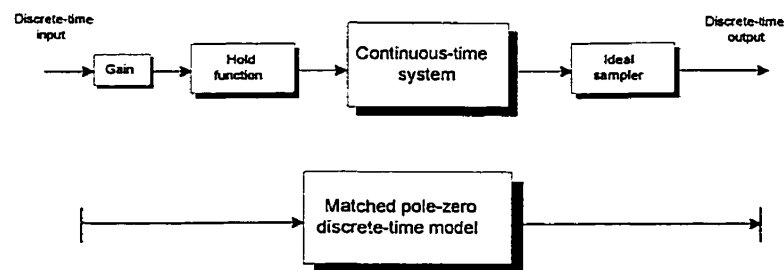


Figure B.1: Matched pole-zero model as a hold-equivalent discrete-time system

Consider a general causal continuous-time linear, time-invariant system  $\overline{G}$ . Its realization is given by the set  $[\overline{A}, \overline{B}, \overline{C}, \overline{D}]$ , where  $\overline{A} \in R^{n \times n}$ ,  $\overline{B} \in R^{n \times 1}$ ,  $\overline{C} \in R^{1 \times n}$  and  $\overline{D} \in R$ . Suppose that this system is preceded by a gain  $K$ , in cascade with a generalized hold, and followed by an ideal sampler, as shown in Figure B.2. In the type I structure of Fig. B.2(a), the discrete-time system, denoted as  $G_{T,I}$ , has the following state and output equations:

$$\begin{aligned} \delta x_{k,T} &= \underbrace{\left( \frac{e^{\overline{A}T} - I}{T} \right)}_{=A} x_{k,T} + \underbrace{\frac{1}{T} \left( \int_{v=0}^T e^{\overline{A}(T-v)} \overline{B} H_I(v) dv \right)}_{=B_I} \cdot K r_{k,T}, \quad x_{0,T} = 0_{n \times 1}, \\ \phi_{k,T} &= \underbrace{\overline{C}}_{=C} x_{k,T} + \underbrace{\overline{D} \cdot K}_{=D} r_{k,T}, \end{aligned} \quad (\text{B.1})$$

where  $r_{k,T} = \overline{r}(t)|_{t=kT}$ . The type II structure of Fig. B.2(b) comprises a generalized hold which is assumed to satisfy  $H_{II}(\tau)|_{\tau=0} = 1$ . The resulting discrete-time system,  $G_{T,II}$ , has a state equation as given in (B.2) and an output equation identical to that provided in (B.1).

$$\delta x_{k,T} = \underbrace{\left( \frac{e^{\overline{A}T} - I}{T} \right)}_{=A} x_{k,T} + \underbrace{\frac{1}{T} \left( \int_{v=0}^T e^{\overline{A}(T-v)} \overline{B} H_{II}(v) dv \right)}_{=B_{II}} \cdot K r_{k,T}, \quad x_{0,T} = 0_{n \times 1} \quad (\text{B.2})$$

In the above two equations,  $x_{k,T} = \overline{x}(kT)$  for each  $k$ ,  $K \neq 0$  is a function of  $T$ , and  $H_I$  and  $H_{II}$  correspond to the generalized holds of types I and II, respectively. Two structures are considered in order to allow more freedom to the engineer in the choice of a hold function. For the realizations in (B.1) and (B.2) to correspond to a matched pole-zero discrete-time model of the system  $\overline{G}$ , the zeros must be adjusted through the generalized hold, and the DC, or low-frequency, gain must match that of its continuous-time system counterpart, for each fixed  $T$ , by properly selecting the gain  $K$ .

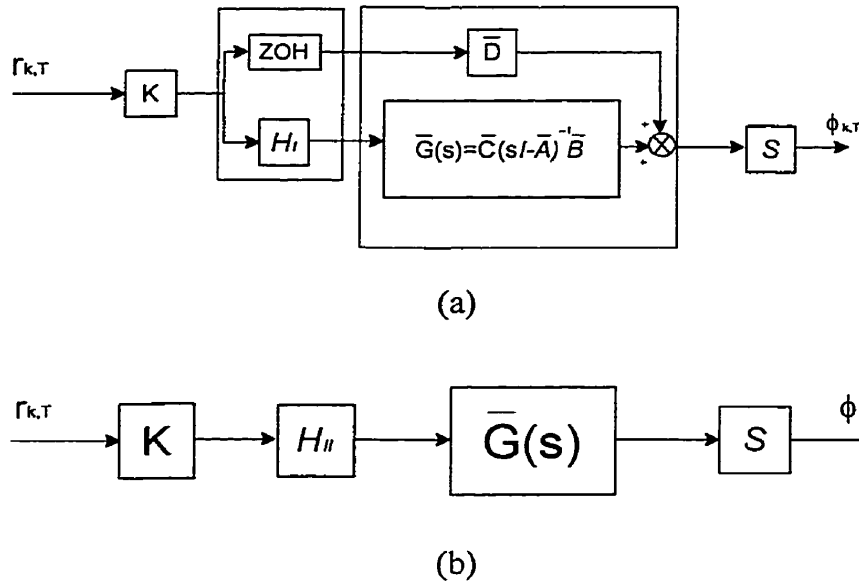


Figure B.2: Hold-equivalent structures

## B.1 Determination of Hold Functions

A generalized hold cascaded in front of a controllable and observable continuous-time system realization can be designed for arbitrary placement of the zeros of the discrete-time system [95]. However, if the continuous-time system realization is non-minimal, the system should be decomposed into minimal and non-minimal subsystems and the hold function calculated only for the minimal part. The following theorem establishes this fact.

**Theorem B.1** A pole-zero cancellation associated with the transfer function of a non-minimal continuous-time system realization is preserved in the conversion to a discrete-time system, having the structures of Figure B.2, provided  $T$  is selected as non-pathological.  $\square$

**Proof:** Consider the conversion to discrete-time according to the structures of Figure B.2 and assume  $T$  is non-pathological in order to prevent the occurrence of extra discrete-time pole-zero cancellations which are not present in the continuous-time system. A continuous-time realization  $[\bar{A}, \bar{B}, \bar{C}, \bar{D}]$  can be decomposed into minimal and non-

minimal subsystems via a Lyapunov transformation [96] to yield  $[\widehat{A}, \widehat{B}, \widehat{C}, \widehat{D}]$ . Then, the discrete-time system can be written as

$$\begin{aligned}\widehat{A} &= \frac{e^{\widehat{A}T} - I}{T} \\ &= \frac{1}{T} \exp \left\{ \begin{bmatrix} \overline{A}_{c,o} & 0 & \overline{A}_{1,3} & 0 \\ \overline{A}_{2,1} & \overline{A}_{c,\bar{o}} & \overline{A}_{2,3} & \overline{A}_{2,4} \\ 0 & 0 & \overline{A}_{\bar{c},o} & 0 \\ 0 & 0 & \overline{A}_{4,3} & \overline{A}_{\bar{c},\bar{o}} \end{bmatrix} T \right\} - I \\ &= \begin{bmatrix} \frac{e^{\overline{A}_{c,o}T} - I}{T} & 0 & & \\ A_1 & \frac{e^{\overline{A}_{c,\bar{o}}T} - I}{T} & & A_2 \\ & 0 & \frac{e^{\overline{A}_{\bar{c},o}T} - I}{T} & 0 \\ & & A_3 & \frac{e^{\overline{A}_{\bar{c},\bar{o}}T} - I}{T} \end{bmatrix},\end{aligned}\tag{B.3}$$

$$\widehat{B} = \frac{1}{T} \int_{v=0}^T \begin{bmatrix} e^{\overline{A}_{c,o}(T-v)} \overline{B}_{c,o} \\ \widehat{A} \overline{B}_2 \\ 0 \end{bmatrix} H(v) dv \cdot K,\tag{B.4}$$

$$\widehat{C} = \overline{C} = \begin{bmatrix} \overline{C}_{c,o} & 0 & \overline{C}_{\bar{c},o} & 0 \end{bmatrix}, \quad \widehat{D} = \overline{D} \cdot K\tag{B.5}$$

where the subscripts  $c$  and  $o$  correspond to controllable and observable portions, respectively, and  $H$  represents either  $H_I$  or  $H_{II}$ . The minimal realization is given by

$$\begin{aligned}\delta x_{\min,k,T} &= \left( \frac{e^{\overline{A}_{c,o}T} - I}{T} \right) x_{\min,k,T} + \frac{1}{T} \left( \int_{v=0}^T e^{\overline{A}_{c,o}(T-v)} \overline{B}_{c,o} H(v) dv \right) \cdot K r_{k,T}, \\ \phi_{k,T} &= \overline{C}_{c,o} x_{\min,k,T} + \overline{D} \cdot K r_{k,T},\end{aligned}\tag{B.6}$$

and the transfer function, by

$$\overline{C}_{c,o} \left( \varepsilon I - \left( \frac{e^{\overline{A}_{c,o}T} - I}{T} \right) \right)^{-1} \left( \frac{1}{T} \int_{v=0}^T e^{\overline{A}_{c,o}(T-v)} \overline{B}_{c,o} H(v) dv \right) K + \overline{D} \cdot K.\tag{B.7}$$

Since the transfer function can be written in terms of the elements of the discrete-time

minimal realization, the zeros in extra to those associated with the transfer function of the minimal realization are mapped in the same manner as the poles, and this ensures that the pole-zero cancellations take place in discrete-time.  $\square$

### B.1.1 Discrete-time Vectors $B_{I,c,o}$ and $B_{II,c,o}$

The entries of the vectors  $B_{I,c,o}$  and  $B_{II,c,o}$  are calculated. Since  $B_{I,c,o} = B_{II,c,o}$ , for fixed zero locations, from now on  $B_{c,o}$  will denote either vector. The procedure to calculate  $B_{c,o}$  is as follows:

*Step 1:* Obtain each finite zero location as  $z_i = (e^{\bar{z}_i T} - 1)/T$ , where  $\bar{z}_i$  is the  $i$ th zero associated with the minimal realization of  $\bar{G}(s)$ , and  $T$  is chosen to be non-pathological with respect to  $\bar{G}$ . When there are  $m^* \geq 1$  zeros, write the polynomial  $p^*(\varepsilon)$  as

$$\begin{aligned} p^*(\varepsilon) &= (\varepsilon - z_1)(\varepsilon - z_2)\dots(\varepsilon - z_m) \\ &= \varepsilon^{m^*} + p_{m^*-1}^* \varepsilon^{m^*-1} + \dots + p_1^* \varepsilon + p_0^* \end{aligned} \quad (\text{B.8})$$

for  $m^* \leq n_{c,o}$ , where  $1 \leq n_{c,o} \leq n$  is the order of the minimal realization of the continuous-time system. When  $m^* = 0$ , set  $p^*(\varepsilon) = 1$ .

*Step 2:* When  $n_{c,o} \geq 2$ , define the polynomial  $v^*(\varepsilon)$  as

$$\begin{aligned} v^*(\varepsilon) &= \bar{C}_{c,o} \text{Adj} \left( \varepsilon I - \frac{e^{\bar{A}_{c,o} T} - I}{T} \right) B'_{c,o} + \bar{D} \det \left( \varepsilon I - \frac{e^{\bar{A}_{c,o} T} - I}{T} \right) \\ &= v_{m^*}^* \varepsilon^{m^*} + v_{m^*-1}^* \varepsilon^{m^*-1} + \dots + v_1^* \varepsilon + v_0^* \end{aligned} \quad (\text{B.9})$$

where  $B'_{c,o} = B_{c,o}/K$ , otherwise  $v(\varepsilon) = \bar{C}_{c,o} B'_{c,o} + \bar{D}(\varepsilon - (e^{\bar{A}_{c,o} T} - 1)/T)$ . Set  $l(\varepsilon) = v^*(\varepsilon)/v_{m^*}^*$  when  $m^* = n_{c,o}$ , and  $l(\varepsilon) = v^*(\varepsilon)$  when  $0 \leq m^* < n_{c,o}$ .

*Step 3:* Equate like powers of  $\varepsilon$  in  $p^*(\varepsilon)$  and  $l(\varepsilon)$ , and solve for the entries of  $B'_{c,o}$ .

*Step 4:* The gain  $K$  is established from the minimal part of the systems and is given by:

$$K = \frac{\overline{C}_{c,o} (s_o I - \overline{A}_{c,o})^{-1} \overline{B}_{c,o} + \overline{D}}{\overline{C}_{c,o} \left( \varepsilon_o I - \frac{e^{\overline{A}_{c,o} T} - I}{T} \right)^{-1} B'_{c,o} + \overline{D}} \quad (\text{B.10})$$

where  $s_o$  is real and  $0 \leq s_o \ll 1$ , and  $\varepsilon_o = (e^{s_o T} - 1)/T$ .

With  $B'_{c,o}$  known, one can solve for the response functions of the generalized holds of types I and II.

### B.1.2 Response Function of Generalized Hold of Type I

One candidate for generalized hold of type I is the minimum-energy hold [97], with response function defined as

$$H_{\min}(\tau) = \overline{B}_{c,o}^T e^{\overline{A}_{c,o}^T (T-\tau)} \left( \frac{W}{T} \right)^{-1} B'_{c,o}, \quad \tau \in [0, T], \quad (\text{B.11})$$

where  $W$  is the controllability Gramian given by

$$W = \int_{v=0}^T e^{\overline{A}_{c,o} (T-v)} \overline{B}_{c,o} \overline{B}_{c,o}^T e^{\overline{A}_{c,o}^T (T-v)} dv. \quad (\text{B.12})$$

Another hold of type I can be defined as having  $n_{c,o}$  uniform, piecewise-constant functions of time within each period  $T$ ; that is,

$$H_I(\tau) = \begin{cases} \alpha_0, & \text{for } \tau \in [0, T/n_{c,o}) \\ \alpha_1, & \text{for } \tau \in [T/n_{c,o}, 2T/n_{c,o}) \\ \vdots & \\ \alpha_{n_{c,o}-1}, & \text{for } \tau \in [(n_{c,o} - 1)T/n_{c,o}, T) \end{cases} \quad (\text{B.13})$$

where the  $\alpha_i$ s are finite, real numbers. Therefore, an expression equivalent to  $B_{c,o}$  is given by

$$\left[ \sum_{j=0}^{n_{c,o}-1} \alpha_j e^{\frac{-\bar{A}_{c,o} T}{n_{c,o}} j} \right] \frac{1}{T} \int_{v=0}^{T/n_{c,o}} e^{\bar{A}_{c,o}(T-v)} \bar{B}_{c,o} dv \cdot K. \quad (\text{B.14})$$

To solve for the  $\alpha_j$ s, the following lemma and theorem are invoked.

**Lemma B.1** If  $T$  is non-pathological, so is  $T/N$ , where  $N$  is any positive integer.  $\blacktriangleleft$

**Theorem B.2** For the pair  $(\bar{A}_{c,o}, \bar{B}_{c,o})$ , if  $T \in (0, \infty)$  is non-pathological, the  $n_{c,o} \times n_{c,o}$  matrix  $\Psi$  given by (B.15), where  $\Gamma = \int_{v=0}^{T/n_{c,o}} e^{\bar{A}_{c,o}(T-v)} \bar{B}_{c,o} dv$ , is non-singular.  $\blacktriangleleft$

$$\Psi = \left[ \Gamma, e^{-\bar{A}_{c,o} T/n_{c,o}} \Gamma, \dots, e^{-\bar{A}_{c,o} T(n_{c,o}-1)/n_{c,o}} \Gamma \right] \quad (\text{B.15})$$

Proof: Let  $\Upsilon = T/n_{c,o}$  and  $\Gamma = A_{SIM}^{(n_{c,o}-1)} B_{SIM}$  where

$$A_{SIM} = e^{\bar{A}_{c,o} \Upsilon}, \quad B_{SIM} = \int_{v=0}^{\Upsilon} e^{\bar{A}_{c,o}(\Upsilon-v)} \bar{B}_{c,o} dv \quad (\text{B.16})$$

are state-space elements associated with a step invariant model (SIM) of the continuous-time system, in the shift form, for a sampling period of  $\Upsilon$ , as given by

$$x_{k+1, \Upsilon} = A_{SIM} x_{k, \Upsilon} + B_{SIM} r_{k, \Upsilon}. \quad (\text{B.17})$$

Then  $\Psi$  can be expressed as

$$\Psi = \left[ A_{SIM}^{n_{c,o}-1} B_{SIM}, A_{SIM}^{n_{c,o}-2} B_{SIM}, \dots, A_{SIM} B_{SIM}, B_{SIM} \right]. \quad (\text{B.18})$$

The controllability matrix for the SIM in (B.17) is known to be [36]

$$\mathcal{C} = \left[ B_{SIM}, A_{SIM} B_{SIM}, \dots, A_{SIM}^{n_{c,o}-2} B_{SIM}, A_{SIM}^{n_{c,o}-1} B_{SIM} \right]. \quad (\text{B.19})$$

The full rank of  $\mathcal{C}$ , which is guaranteed by the facts  $(\bar{A}_{c,o}, \bar{B}_{c,o})$  is controllable and  $\Upsilon$  is

non-pathological [4], implies invertibility of  $\Psi$ .  $\square$

Then

$$\begin{bmatrix} \alpha_0 \\ \vdots \\ \alpha_{n_{c,o}-1} \end{bmatrix} = \Psi^{-1} T B'_{c,o}. \quad (\text{B.20})$$

### B.1.3 Response Function of Generalized Hold of Type II

One possible hold of this type is defined as having  $n_{c,o} + 1$  uniform, piecewise-constant functions of time within each period  $T$ ; that is,

$$H_{II}(\tau) = \begin{cases} 1, & \text{for } \tau \in [0, T/(n_{c,o} + 1)) \\ \beta_1, & \text{for } \tau \in [T/(n_{c,o} + 1), 2T/(n_{c,o} + 1)) \\ \vdots \\ \beta_{n_{c,o}}, & \text{for } \tau \in [n_{c,o}T/(n_{c,o} + 1), T) \end{cases} \quad (\text{B.21})$$

where the  $\beta_i$ s are finite, real numbers. An expression for the vector  $B_{c,o}$  is then given by

$$\left[ I + \sum_{j=1}^{n_{c,o}} \beta_j e^{\frac{-\bar{A}_{c,o} T}{n_{c,o}+1} j} \right] \frac{1}{T} \underbrace{\int_{v=0}^{T/(n_{c,o}+1)} e^{\bar{A}_{c,o}(T-v)} \bar{B}_{c,o} dv}_{=\Omega} \cdot K. \quad (\text{B.22})$$

The coefficients of the hold can be solved as

$$\begin{bmatrix} \beta_1 \\ \vdots \\ \beta_{n_{c,o}} \end{bmatrix} = \Phi^{-1} \left[ T B'_{c,o} - \Omega \right] \quad (\text{B.23})$$

where

$$\Phi = \left[ e^{\frac{-\bar{A}_{c,o} T}{n_{c,o}+1} \Omega}, \quad \dots, \quad e^{\frac{-\bar{A}_{c,o} T}{n_{c,o}+1} n_{c,o} \Omega} \right] \quad (\text{B.24})$$

since  $T/(n_{c,o} + 1)$  is non-pathological, from Lemma B.1, and  $\Phi$  is invertible, from a variant of Theorem B.2.

## B.2 Properties of the Matched Pole-Zero Discrete-Time Model

Controllability and observability of the matched pole-zero discrete-time model, and stability of the newly established structures are addressed. The limiting form of the state-space elements, as  $T \rightarrow 0$ , is provided and connections with classical invariant discrete-time models are established.

### B.2.1 Stability, Controllability and Observability

**Theorem B.3** A necessary and sufficient condition for the discrete-time systems  $G_{T,I}$  and  $G_{T,II}$ , given by equations (B.1) and (B.2), to be exponentially stable, i.e. the eigenvalues  $\lambda_i$  of  $A$  lie in the region  $|T\lambda_i + 1| < 1$  for  $i = 1, 2, \dots, n$ , is that the continuous-time system  $\bar{G}$  be exponentially stable, i.e. all eigenvalues  $\bar{\lambda}_i$  of  $\bar{A}$  have strictly negative real parts.  $\square$

Proof: (i) Sufficiency. Let  $\bar{\lambda}_i = \bar{\sigma}_i \pm j \cdot \bar{\omega}_i$  for  $i = 1, \dots, n$ . Suppose the continuous-time system  $\bar{G}$  is exponentially stable:  $\bar{\sigma}_i < 0$ . The eigenvalues  $\lambda_i$  of  $A$  are given by

$$\lambda_i = \frac{e^{\bar{\lambda}_i T} - 1}{T} \text{ for } i = 1, 2, \dots, n \quad (\text{B.25})$$

where  $T > 0$ . Then  $|T\lambda_i + 1| = e^{\bar{\sigma}_i T} < 1$ .

(ii) Necessity. The discrete-time systems  $G_{T,I}$  and  $G_{T,II}$  are assumed exponentially stable:  $|T\lambda_i + 1| < 1$ . Suppose that one eigenvalue of  $\bar{G}$ ,  $\bar{\lambda}_j$ , has non-negative real part:  $\bar{\sigma}_j \geq 0$ ,  $j \in [0, n]$ . Then  $e^{\bar{\sigma}_j T} \geq 1$ , which violates the initial assumption for the discrete-time systems.  $\square$

**Theorem B.4** If the pair  $(\bar{C}, \bar{A})$  is observable and  $T$  is non-pathological, then the pair  $(\bar{C}, \frac{e^{\bar{A}T} - I}{T})$  is observable in a discrete-time sense.  $\square$

Proof: To demonstrate observability of the discrete-time realization, it must be shown

that [4]

$$\text{rank} \begin{bmatrix} \frac{e^{\bar{A}T} - I}{T} - \frac{e^{\bar{\lambda}_i T} - 1}{T} I \\ \bar{C} \end{bmatrix} = n \text{ for } i = 1, 2, \dots, n \quad (\text{B.26})$$

knowing that, in the continuous-time domain,

$$\text{rank} \begin{bmatrix} \bar{A} - \bar{\lambda}_i I \\ \bar{C} \end{bmatrix} = n \text{ for } i = 1, 2, \dots, n. \quad (\text{B.27})$$

In a procedure reminiscent of the proof of Theorem 3.2.1 in [4], assume  $(\bar{C}, \bar{A})$  is observable and  $T$  is non-pathological. Define

$$g(s) = \frac{\left(\frac{e^{Ts} - 1}{T}\right) - \left(\frac{e^{T\bar{\lambda}_i} - 1}{T}\right)}{s - \bar{\lambda}_i} \text{ for } i = 1, 2, \dots, n \quad (\text{B.28})$$

which is analytic for all  $s$  and which satisfies  $\lim_{T \rightarrow 0} g(s) = 1$ , for all  $s$ . The zeros of  $g(s)$  are given by the set  $\{s : s = \bar{\lambda}_i \pm j \cdot 2\pi j/T, j = 1, 2, \dots \text{ and } i = 1, 2, \dots, n\}$ . The fact that  $T$  is non-pathological assures that no zero of  $g(s)$  equals to an eigenvalue  $\bar{\lambda}_i$ . From the spectral mapping theorem, the eigenvalues of  $g(\bar{A})$  correspond to the values of  $g$  at the eigenvalues of  $\bar{A}$ . Since 0 is not an eigenvalue of  $g(\bar{A})$ , even if it belongs to the set of eigenvalues of  $\bar{A}$ ,  $g(\bar{A})$  is non-singular. Therefore, one can write

$$\begin{bmatrix} \frac{e^{\bar{A}T} - I}{T} - \frac{e^{\bar{\lambda}_i T} - 1}{T} I \\ \bar{C} \end{bmatrix} = \begin{bmatrix} g(\bar{A}) & 0 \\ 0 & 1 \end{bmatrix} \begin{bmatrix} \bar{A} - \bar{\lambda}_i I \\ \bar{C} \end{bmatrix}. \quad (\text{B.29})$$

The right-most term on the right-hand side of (B.29) is invertible from the observability of the continuous-time realization, whereas the matrix

$$\begin{bmatrix} g(\bar{A}) & 0 \\ 0 & 1 \end{bmatrix} \quad (\text{B.30})$$

is non-singular since  $g(\bar{A})$  is so.  $\square$

**Theorem B.5** If the pair  $(\bar{A}, \bar{B})$  is controllable and  $T$  is non-pathological, then the pair  $(\frac{e^{\bar{A}T} - I}{T}, \frac{1}{T} \int_{v=0}^T e^{\bar{A}(T-v)} \bar{B} H(v) dv \cdot K)$ , where  $H(v)$  is either  $H_I(v)$  or  $H_{II}(v)$ , depending on the case, is controllable in a discrete-time sense.  $\blacktriangleright$

Proof: The continuous-time realization is either (i) minimal, or (ii) controllable and unobservable. The first case is proven in Theorem B.6. For the second case, the transfer function associated with  $[\bar{A}, \bar{B}, \bar{C}, \bar{D}]$  has pole/zero cancellations corresponding to the unobservable modes. Knowing how the poles and zeros are mapped with the matched pole-zero model and using a  $T$  which is non-pathological in the transformation, the discrete-time poles which cancel zeros correspond to unobservable, and not to uncontrollable, discrete-time modes. Therefore, the realization  $[\frac{e^{\bar{A}T} - I}{T}, \frac{1}{T} \int_{v=0}^T e^{\bar{A}(T-v)} \bar{B} H(v) dv \cdot K, \bar{C}, \bar{D} \cdot K]$  is controllable.  $\square$

**Theorem B.6** If the realization of the continuous-time system  $\bar{G}$ , with elements  $[\bar{A}, \bar{B}, \bar{C}, \bar{D}]$ , is minimal and  $T$  is non-pathological, then so are the discrete-time realizations with elements  $[A, B, C, D]$ , as given by equations (B.1) and (B.2).  $\blacktriangleright$

Proof: The minimality of the realization of the continuous-time system corresponds to an irreducible transfer function  $\bar{G}(s)$ . The state-space element  $B$  is selected in such a way that the zeros of  $G_{T,I}$  and  $G_{T,II}$  are  $z_i = (e^{\bar{z}_i T} - 1)/T$ , where the  $\bar{z}_i$ s are the finite zeros of the continuous-time system. The poles of  $G_{T,I}$  and  $G_{T,II}$  are given by  $\lambda_i = (e^{\bar{\lambda}_i T} - 1)/T$ . The non-pathologicity of  $T$  assures that the poles of  $G_{T,I}$  and  $G_{T,II}$  are disjoint from their zeros. Hence, minimality of the realization of  $\bar{G}$  implies that of  $G_{T,I}$  and  $G_{T,II}$  given by (B.1) and (B.2).  $\square$

## B.2.2 Behavior as the Sampling Period Approaches Zero

The behavior of the matched pole-zero model, in the transfer function format, is well known [9]: the coefficients in front of the powers of  $\varepsilon$  at numerator and denominator of the discrete-time transfer function approach the corresponding coefficients of  $\bar{G}(s)$ , as  $T \rightarrow 0$ . With the structures introduced in this appendix, the elements of the realizations

have limits, as  $T \rightarrow 0$ , given by

$$\lim_{T \rightarrow 0} A = \bar{A}, \quad \lim_{T \rightarrow 0} B = \bar{B}, \quad \lim_{T \rightarrow 0} K = 1, \quad \lim_{T \rightarrow 0} C = \bar{C}, \quad \lim_{T \rightarrow 0} D = \bar{D}. \quad (\text{B.31})$$

In turn, the limiting behavior of  $B$  results in the elements of the hold functions satisfying (B.32), as  $T \rightarrow 0$ :

$$\lim_{T \rightarrow 0} \left( \sum_{j=0}^{n-1} \alpha_j \right) = n, \quad \lim_{T \rightarrow 0} \left( \sum_{j=1}^n \beta_j \right) = n. \quad (\text{B.32})$$

**Remark B.1** The method presented in this appendix to solve for the hold coefficients requires inversion of the matrices  $\Psi$  and  $\Phi$ . One should be aware that, when the values of  $T$  are approaching zero, although the linear independence of the column vectors making up  $\Psi$  and  $\Phi$  is preserved, numerical problems may arise since the matrix entries become close to zero.

### B.2.3 Similarities and Differences with the Invariant Models

Relations between matched pole-zero and invariant models can be simply established from the knowledge of the hold device and gain  $K$ . For instance, the first order, strictly proper matched pole-zero model is known to correspond to the step invariant model for the same continuous-time system. With the structural interpretation of the matched pole-zero model introduced in this appendix, this correspondence is explained by the use of a ZOH and unit gain  $K$ . More generally, if a continuous-time realization is converted to step invariant and matched pole-zero discrete-time models, the discrete-time realizations will possess the same  $A$  and  $C$  elements, yet different  $B$  and  $D$  matrices for each fixed sampling period. Thus, one could state that the observability of one discrete-time model implies that of the other. Contrary to a SIM which has its output agreeing with that of the continuous-time system, at the sampling instants, given a step or piecewise-constant signal is applied, the matched pole-zero model never match the output of its continuous-time counterpart at the sampling instants, for finite  $T$ . The outputs would agree at

the sampling instants if  $K$  could be set to unity and the input to the continuous-time system would be a periodic extension of  $H(\tau)$ , for  $0 \leq \tau < T$ , i.e.  $\bar{r}(t) = \sum_{k=0}^{\infty} H(t - kT)$  for  $t \geq 0$ , where  $H(\tau)$  denotes  $H_I(\tau)$  or  $H_{II}(\tau)$ , depending on the structure. Whilst the hold-equivalent structures associated with the matched pole-zero model and that of the invariant models are similar, the philosophies behind their developments are quite disparate. For the step, ramp and impulse invariant models, the hold functions are independent of the system parameters whereas for the matched pole-zero model the discrete zero assignment requires a hold which depends on the knowledge of the continuous-time system.

# Appendix C

## Alternative Digital Redesign Methods Based on the Classical Discretization of a Closed-Loop System

The two techniques presented in Section 3.3 are explained in more details.

### C.1 Digital Redesign Based on Discretization of System Relating Reference Input to Control Input Using Numerical Integration and Hold-Equivalent Techniques

In addition to the matched pole-zero method, the numerical integration and hold-equivalent techniques can be used to discretize the system relating the reference input to the control input. However, a modification to the calculated discrete-time PITF must be brought in

order to implement the discrete-time controllers under the structure of Figure 1.4(b).

The steps in obtaining the sampled-data control system are the following:

*Step 1:* Having the knowledge of an internally stable continuous-time control system, as shown in Figure 1.4(a), calculate  $\bar{H}(s)$ .

*Step 2:* Discretize  $\bar{H}(s)$  to  $H_T^*(\varepsilon)$  with any numerical integration or hold-equivalent technique for a sampling period yielding a discrete-time PITF having all its poles inside the stability boundary of the  $\varepsilon$ -plane. Write  $H_T^*(\varepsilon) = n^*(\varepsilon)/d^*(\varepsilon)$ .

*Step 3:* Discretize  $\bar{G}(s)$  as a hold-equivalent discrete-time model, which depends on the hold placed at the control input of the sampled-data control system, to obtain  $G_T(\varepsilon) = b(\varepsilon)/a(\varepsilon)$ .

*Step 4:* (a) For step 2 performed with a numerical integration technique: Multiply  $H_T^*(\varepsilon)$  by the correcting factor  $Ka(\varepsilon)/a^*(\varepsilon)$ , which yields  $H_T(\varepsilon) = Km(\varepsilon)a(\varepsilon)/d^*(\varepsilon)$ , where  $K$  is the gain adjusted to match that of  $\bar{H}(s)$  at a desired frequency,  $a^*(\varepsilon)$  is the monic polynomial obtained by mapping the poles of  $\bar{G}(s)$  with the discretization method used in step 2, and  $m(\varepsilon)$  comes from the numerator of  $H_T^*(\varepsilon)$  which can be written as  $n^*(\varepsilon) = m(\varepsilon)a^*(\varepsilon)$ .

(b) For step 2 carried out with a hold-equivalent technique: Multiply  $H_T^*(\varepsilon)$  by the correcting factor  $\beta a(\varepsilon)/a^*(\varepsilon)$  to obtain  $H_T(\varepsilon) = \beta m(\varepsilon)a(\varepsilon)/d^*(\varepsilon)$ , where  $\beta$  serves the same purpose as  $K$  in part (a),  $a^*(\varepsilon)$  is the monic denominator polynomial of the hold-equivalent discretization of  $\bar{G}(s)$  as carried out with the discretization method used in step 2, and  $m(\varepsilon)$  is as defined in part (a).

*Step 5:* Solve the Diophantine equation

$$u(\varepsilon)a(\varepsilon) + v(\varepsilon)b(\varepsilon) = d^*(\varepsilon) \quad (\text{C.1})$$

for  $u(\varepsilon)$  and  $v(\varepsilon)$ .

*Step 6:* To realize the discrete-time controllers under a structure as shown in Figure 1.4(b), utilize any applicable equation among (3.12) to (3.15).

## C.2 Digital Redesign Based on Discretization of System Relating Reference Input to Controlled Output

This section shows that a plant output mapping digital redesign can be carried out provided that the hold at control input is an integral part of the process. However, such an approach has limitations in the sense that a possible detrimental intersample behavior can take place depending on the hold at control input.

The continuous-time control system of Figure 1.4(a) is digitally redesigned with the plant output mapping method and results in the sampled-data control system of Figure 1.4(b) once the following steps are carried out:

*Step 1:* Calculate the transfer function of the continuous-time closed-loop system from reference input to controlled output. Denote it as  $\bar{M}(s)$ .

*Step 2:* Discretize  $\bar{M}(s)$  with the matched pole-zero discretization method to obtain  $M_T(\varepsilon) = n(\varepsilon)/d(\varepsilon)$ , where  $n(\varepsilon)$  and  $d(\varepsilon)$  have degrees  $w$  and  $p$ , respectively.

*Step 3:* Obtain the matched pole-zero model of the plant  $\bar{G}(s)$ ,  $G_T(\varepsilon) = b(\varepsilon)/a(\varepsilon)$ , where  $b(\varepsilon)$  and  $a(\varepsilon)$  have degrees  $m$  and  $n$ , respectively.

*Step 4:* In order to implement  $M_T(\varepsilon)$  with a structure as on Figure 1.4(b), solve the following discrete-time Diophantine equation:

$$v(\varepsilon)b(\varepsilon) + u(\varepsilon)a(\varepsilon) = d(\varepsilon) \tag{C.2}$$

for the polynomials  $v(\varepsilon)$  of degree  $r$  and  $u(\varepsilon)$  of degree  $l$ . Also, from the structure of the systems in Figure 1.4 and the fact  $M_T(\varepsilon)$  and  $G_T(\varepsilon)$  are matched pole-zero models of  $\bar{M}(s)$  and  $\bar{G}(s)$ , respectively, one can write  $M_T(\varepsilon) = m(\varepsilon)b(\varepsilon)/d(\varepsilon)$ , where  $m(\varepsilon)$  is of degree  $(w-m)$ . Once  $u(\varepsilon)$  and  $v(\varepsilon)$  have been found, the transfer functions of the discrete-time controllers can be obtained with one of the following:

1. Let  $w(\varepsilon)$  be an arbitrary stable polynomial of degree  $l$ . If  $r \leq l$  and  $(w-m) \leq l$ , set

$$\Pi_T(\varepsilon) = \frac{m(\varepsilon)}{w(\varepsilon)}, \quad \Omega_T(\varepsilon) = \frac{w(\varepsilon)}{u(\varepsilon)}, \quad \Gamma_T(\varepsilon) = \frac{v(\varepsilon)}{w(\varepsilon)}. \quad (\text{C.3})$$

2. If  $u(\varepsilon)$  is stable,  $r \leq l$  and  $(w-m) \leq l$ , set

$$\Pi_T(\varepsilon) = \frac{m(\varepsilon)}{u(\varepsilon)}, \quad \Omega_T(\varepsilon) = 1, \quad \Gamma_T(\varepsilon) = \frac{v(\varepsilon)}{u(\varepsilon)}. \quad (\text{C.4})$$

3. If  $m(\varepsilon)$  is stable and  $r \leq (w-m) \leq l$ , set

$$\Pi_T(\varepsilon) = 1, \quad \Omega_T(\varepsilon) = \frac{m(\varepsilon)}{u(\varepsilon)}, \quad \Gamma_T(\varepsilon) = \frac{v(\varepsilon)}{m(\varepsilon)}. \quad (\text{C.5})$$

4. If  $v(\varepsilon)$  is stable and  $(w-m) \leq r \leq l$ , set

$$\Pi_T(\varepsilon) = \frac{m(\varepsilon)}{v(\varepsilon)}, \quad \Omega_T(\varepsilon) = \frac{v(\varepsilon)}{u(\varepsilon)}, \quad \Gamma_T(\varepsilon) = 1. \quad (\text{C.6})$$

The plant output mapping method is made possible from the introduction of a hold-equivalent structure for the matched pole-zero discrete-time model, as first presented in [11] and thoroughly discussed in Appendix B. Any hold which results in the matched pole-zero model of the plant can be placed at control input. However, for a satisfactory intersample behavior at control input and controlled output, i.e. exempt from large ripples, when the plant model is a first order transfer function, one should place a

minimum-energy hold given by

$$H_{\min}(\tau) = \bar{b}e^{\bar{a}(T-\tau)} \left(\frac{W}{T}\right)^{-1} b, \quad \tau \in [0, T), \quad (\text{C.7})$$

where  $\bar{G} = [\bar{a}, \bar{b}, \bar{c}, \bar{d}]$ ,  $b$  is the vector coupling the input with the state in the state equation of the discrete-time plant model, and  $W$  is the controllability Gramian of  $\bar{G}$  [76] given by  $W = (e^{2\bar{a}T} - 1)\bar{b}^2/2\bar{a}$  when  $\bar{a} \neq 0$ . In the case  $\bar{a} = 0$ ,  $W = T\bar{b}^2$ . The controllability Gramian is calculated with equation (B.12). For higher-order plant models, no hold function was found to guarantee a tolerable intersample behavior by making  $T$  sufficiently small. The intersample problems associated with generalized holds have been reported in [98] and [99], although not with a digital redesign strategy in mind. A possible solution to the intersample problem would be to design a hold with a quadratic performance criterion set for a desired intersample behavior, as discussed in [100], with a  $T$ -dependent index.

Given that the continuous-time control system is internally stable, the sampled-data control system obtained with the plant output mapping method is internally stable at the sampling instants for any non-pathological  $T$ . However, the hold at control input, in addition to being the cause of possible intersample oscillations, is physically impractical. Indeed, it is, if not impossible, very costly to generate a hold function which depends on the value of  $T$  and the plant dynamics and can take on arbitrary waveform.

Connections with PIM-based systems can be established. First, suppose that a continuous-time control system has been digitally redesigned with the PIM and the plant output mapping methods for a given  $T$ . The two control systems have the same set of discrete-time controllers when (i) their holds at control input are identical, (ii) the Diophantine equations have been solved with the same method, and (iii) the controllers have been calculated with the same equations. Second, the same methodology as that used in obtaining modified PIM methods can be applied to obtain modified plant output mapping methods.

## Appendix D

# Laplace Transforms of Control Input and Controlled Output

The Laplace transforms of the control input and controlled output of digitally redesigned control systems are investigated. For the control input  $u_T(t)$  of the sampled-data control system of Figure 1.4(b), the Laplace transform is

$$U_T(s) = \beta_T(s) \cdot \mathcal{D} \{u_{k,T}\}_{\epsilon = \frac{e^{sT}-1}{T}} \quad (\text{D.1})$$

where  $u_{k,T}$  is the discrete-time control input, and the transfer function of the hold with response function  $H(\tau)$  is defined as

$$\beta_T(s) = \frac{1}{T} \int_{\tau=0}^T H(\tau) e^{-s\tau} d\tau. \quad (\text{D.2})$$

For instance, the transfer function of the ZOH is  $\beta_T(s) = (1 - e^{-sT})/(sT)$ . For a hold with transfer function  $\beta_T(s)$ , the *hold condition in the complex domain* is defined as

$$\lim_{T \rightarrow 0} \beta_T(s) = 1, \text{ pointwise in } s. \quad (\text{D.3})$$

To satisfy this condition, it is sufficient that the hold function satisfies the hold condition in the time domain, as given in Section 4.1. The following theorem establishes the convergence  $U_T(s) \rightarrow \bar{U}(s)$  as  $T \rightarrow 0$ , where  $\bar{U}(s)$  is the Laplace transform of  $\bar{u}(t)$ .

**Theorem D.1** Consider the systems in Fig. 1.4, where the hold  $H$  has a transfer function which satisfies the hold condition in the complex domain. If the limit on the discrete-time PITF satisfies  $\lim_{T \rightarrow 0} H_T(\varepsilon)|_{\varepsilon=(e^{sT}-1)/T} = \bar{H}(s)$ , pointwise in  $s$ , then  $U_T(s)$  converges to  $\bar{U}(s)$ , pointwise in  $s$ .  $\square$

Proof: For each fixed  $s$  in the region of convergence of the Laplace transforms,

$$\begin{aligned} |U_T(s) - \bar{U}(s)| &\leq \left| \beta_T(s) (H_T(\varepsilon) R_T(\varepsilon)|_{\varepsilon=\frac{e^{sT}-1}{T}} - \bar{H}(s) \bar{R}(s)) \right| \\ &\quad + |(\beta_T(s) - 1) \bar{H}(s) \bar{R}(s)| \end{aligned} \quad (\text{D.4})$$

where  $R_T(\varepsilon)$  is the Delta transform of the sampled reference input  $r_{k,T}$ ; i.e.

$$\begin{aligned} R_T(\varepsilon)|_{\varepsilon=\frac{e^{sT}-1}{T}} &= \sum_{k=0}^{\infty} r_{k,T} (T\varepsilon + 1)^{-k} \cdot T \Big|_{\varepsilon=\frac{e^{sT}-1}{T}} \\ &= \bar{R}(s) + \varphi_T(s). \end{aligned} \quad (\text{D.5})$$

In equation (D.5),  $|\varphi_T(s)| \rightarrow 0$ , as  $T \rightarrow 0$ , for any  $s$  in the region of convergence. Therefore,

$$\begin{aligned} &|U_T(s) - \bar{U}(s)| \\ &\leq \underbrace{\left| H_T(\varepsilon)|_{\varepsilon=\frac{e^{sT}-1}{T}} - \bar{H}(s) \right| \cdot |\bar{R}(s)| \cdot |\beta_T(s)|}_{=F_1(s,T)} \\ &\quad + \underbrace{\left| H_T(\varepsilon)|_{\varepsilon=\frac{e^{sT}-1}{T}} \right| \cdot |\varphi_T(s)| \cdot |\beta_T(s)|}_{=F_2(s,T)} \\ &\quad + \underbrace{|\bar{H}(s) \bar{R}(s)| \cdot |\beta_T(s) - 1|}_{=F_3(s,T)}. \end{aligned} \quad (\text{D.6})$$

Given any  $\xi > 0$ , select  $T_1$  such that  $F_1(s, T) < \xi/3$ ,  $T_2$  such that  $F_2(s, T) < \xi/3$

and  $T_3$  such that  $F_3(s, T) < \xi/3$  for any  $s$  in the region of convergence. Let  $\kappa = \min\{T_1, T_2, T_3\}$ , then  $T < \kappa$  implies  $|U_T(s) - \bar{U}(s)| < \xi/3 + \xi/3 + \xi/3 = \xi$ .  $\square$

The theorem emphasizes the fact that no matter which digital redesign method is used, the transfer function of the hold and the discrete-time PITF determine the convergence of the transform of the control input, when the sampled-data and continuous-time control systems are subjected to the same reference input. The theorem also applies to the case when the Delta transform of the sampled reference input to the sampled-data control system, with the substitution  $\varepsilon = (e^{sT} - 1)/T$ , approaches pointwise in  $s$  the Laplace transform of the reference input to the continuous-time control system. Furthermore, the theorem can be expanded to include MIMO systems in the following manner: replace the absolute values in the proof and in the hold condition in the complex domain by vector or matrix norms, depending on the case, and substitute the identity matrix in place of the unity scalar. For the sake of completeness, it should be mentioned that when convergence in transfer function, as defined in Definition 4.4.1, is achieved with a discrete-time system, so is pointwise convergence in  $s$ .

Given the knowledge of the transform of the control input as  $T \rightarrow 0$ , the convergence of the transform of the controlled output can be deduced as follows.

**Corollary D.1**  $Y_T(s) = \bar{G}(s)U_T(s)$  converges, pointwise in  $s$ , to  $\bar{Y}(s) = \bar{G}(s)\bar{U}(s)$ .  $\bowtie$

In terms of the controllers in Fig. 1.4, if  $\lim_{T \rightarrow 0} \Phi_T(\varepsilon)|_{\varepsilon=(e^{sT}-1)/T} = \bar{\Phi}(s)$ , pointwise in  $s$ , where  $\Phi_T(\varepsilon)$  denotes  $\Pi_T(\varepsilon)$ ,  $\Gamma_T(\varepsilon)$  and  $\Omega_T(\varepsilon)$ , and  $\bar{\Phi}(s)$  denotes  $\bar{\Pi}(s)$ ,  $\bar{\Gamma}(s)$ , and  $\bar{\Omega}(s)$ , respectively, then  $Y_T(s)$  converges, pointwise in  $s$ , to  $\bar{Y}(s)$ . This is so since the convergence of each discrete-time block to its continuous-time counterpart, when it exists, warrants that of the PITF [71].

# Appendix E

## Gas-Turbine Engine Speed Control

Figures E.1, E.2 and E.3 present the responses obtained with several gain-scheduled sampled-data control systems subjected to the test input shown in Figure 5.41(a).

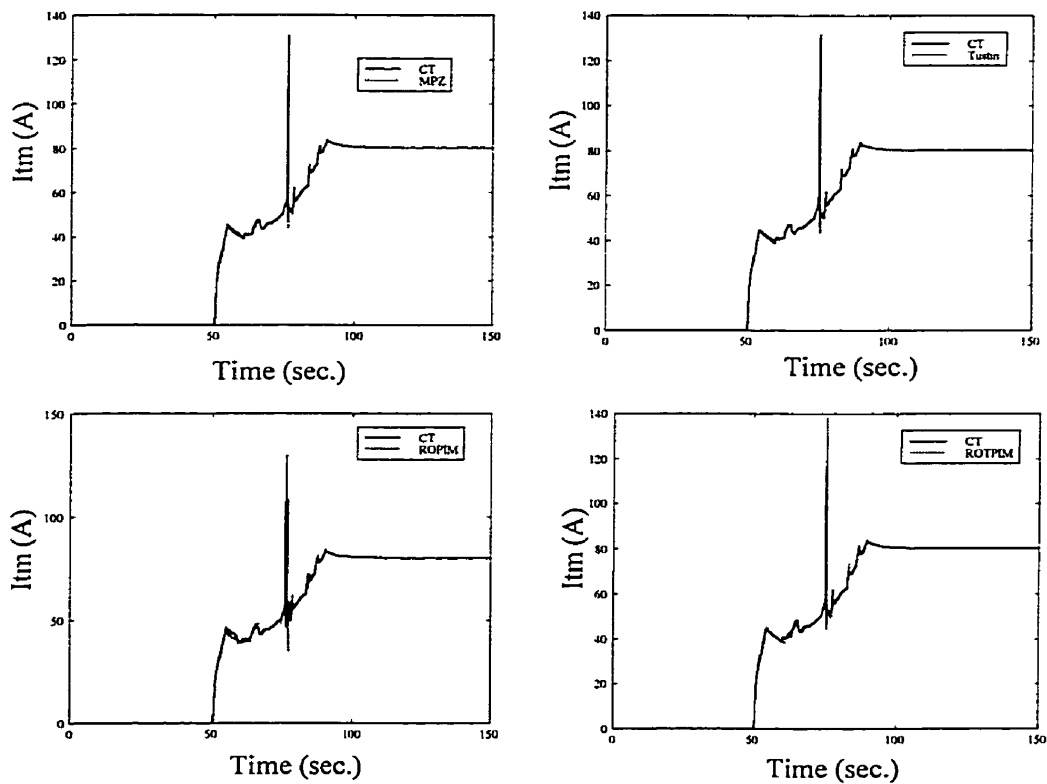


Figure E.1: Control inputs for  $T = 0.0208$  second

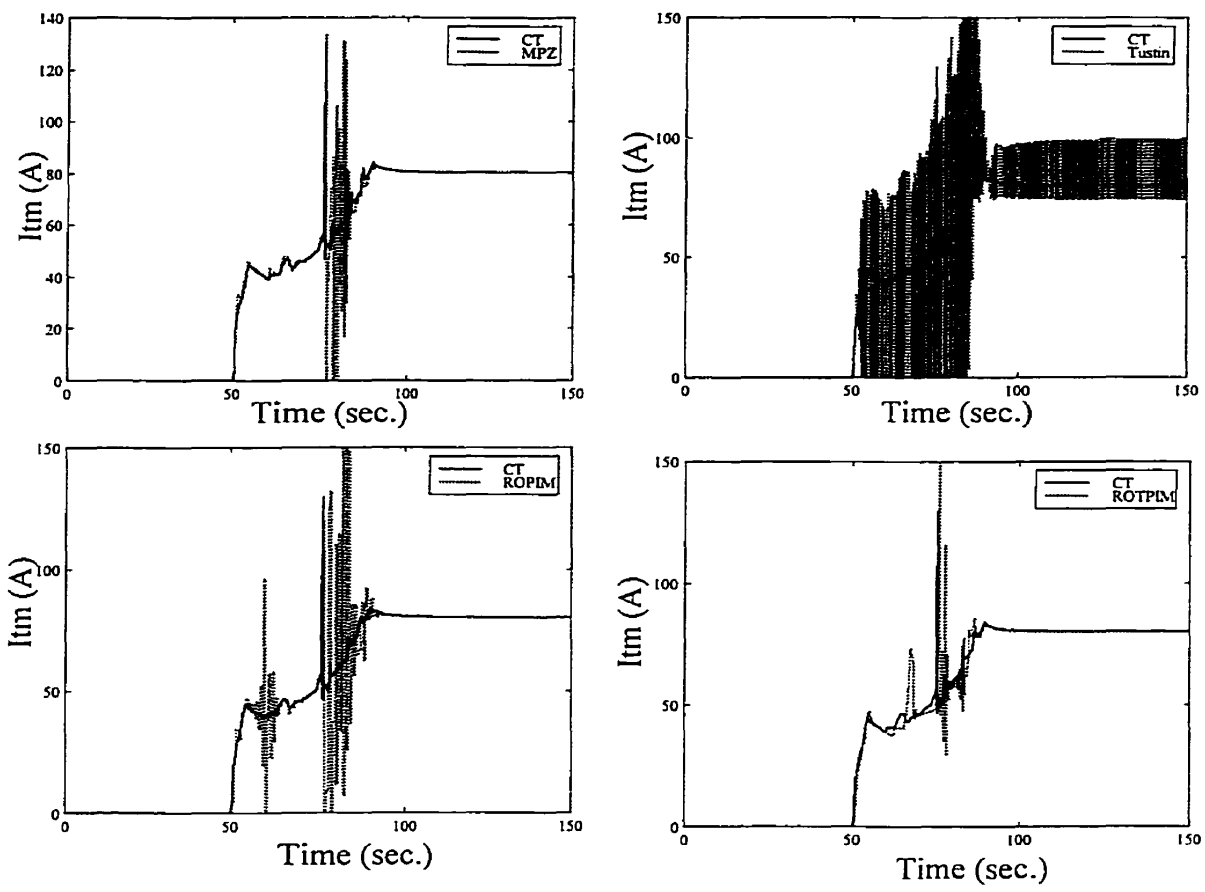


Figure E.2: Control inputs for  $T = 0.35$  second

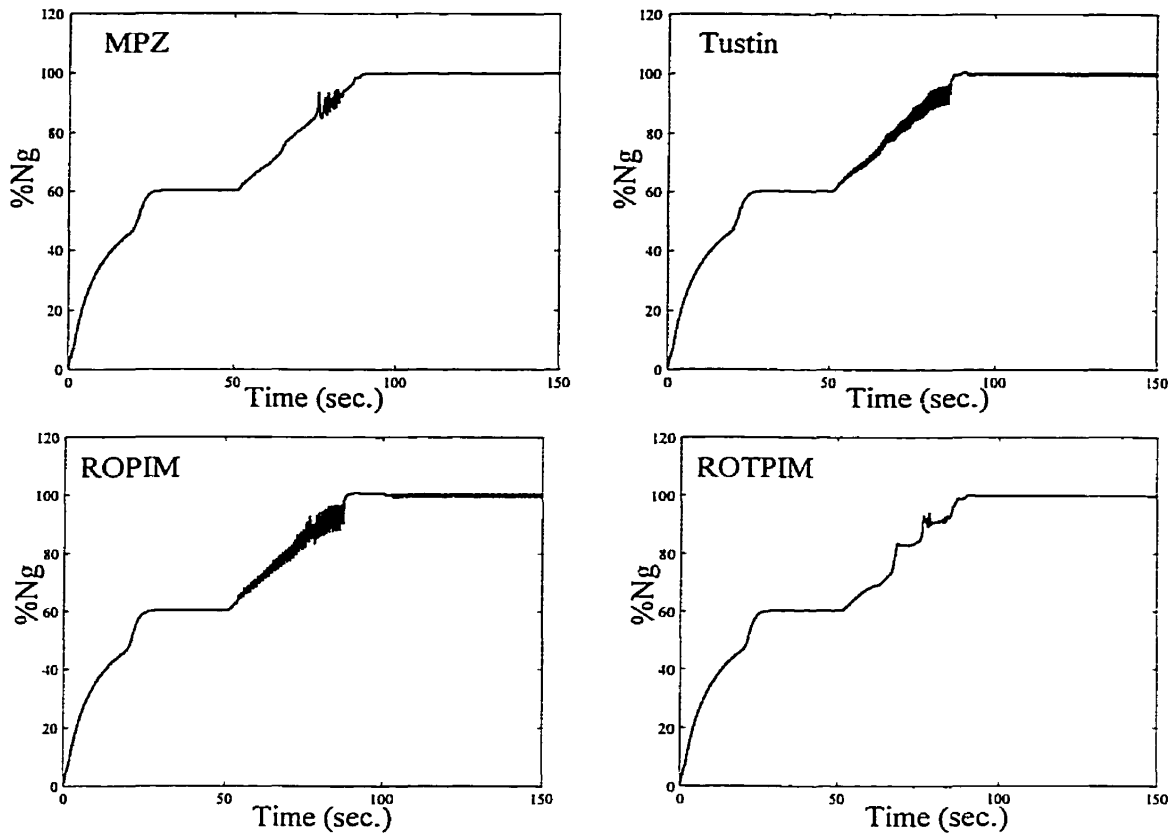


Figure E.3: Controlled outputs for  $T = 0.35$  second

Table E.1 presents the continuous-time controller parameters associated with each operating point. The continuous-time gain-scheduled control system relies on these values.

$\%N_g$	$K_p$	$K_I$	$1/\omega_1$	$1/\omega_2$	$\%N_g$	$K_p$	$K_I$	$1/\omega_1$	$1/\omega_2$
60	25.82	16.13	0.1147	0.0250	86	14.08	11.90	0.0962	0.0250
62	43.13	29.93	0.1280	0.0250	88	13.32	35.71	0.1105	0.0250
64	39.56	28.27	0.1187	0.0250	92	13.13	12.31	0.0969	0.0250
69	22.41	2.95	0.1046	0.0250	93	15.79	14.78	0.0959	0.0250
72	18.19	2.24	0.1040	0.0250	94	11.17	15.29	0.0998	0.0250
77	16.69	7.10	0.0978	0.0250	96	10.97	14.39	0.1059	0.0250
78	14.46	6.87	0.0973	0.0250	98	10.81	18.95	0.1183	0.0250
80	15.00	8.43	0.0984	0.0250	100	8.66	17.04	0.1249	0.0250
82	13.75	8.59	0.0983	0.0250	102	9.92	18.81	0.1251	0.0250
84	17.75	8.62	0.0956	0.0250					

Table E.1: Continuous-time controller parameters